Universidade de Aveiro Departamento de Química
2011

Ana Gisela Guedes Nunes da Cunha

Preparação de Novos Materiais por Modificação Heterogénea de Celulose

Preparation of New Materials by Heterogeneous Modification of Cellulose

Universidade de Aveiro Departamento de Química
2011

Ana Gisela Guedes Nunes da Cunha

Preparação de Novos Materiais por Modificação Heterogénea de Celulose

Preparation of New Materials by Heterogeneous Modification of Cellulose

Dissertação apresentada à Universidade de Aveiro para cumprimento dos requisitos necessários à obtenção do grau de Doutor em Química, realizada sob a orientação científica da Doutora Carmen Freire, Investigadora Auxiliar do CICECO e do Departamento de Química da Universidade de Aveiro e do Doutor Armando Silvestre, Professor Associado com Agregação do Departamento de Química da Universidade de Aveiro.

Apoio financeiro do projecto de I&D da FCT (PTDC/QUI/68472/2006) no âmbito do III Quadro Comunitário de Apoio.

Apoio financeiro da FCT e do POPH/FSE (SFRH/BD/31124/2006) no âmbito do III Quadro Comunitário de Apoio.

Aos meus pais, irmãs, sobrinhas e, muito em especial, à minha avó Célia por ter enriquecido a minha vida muito para além do amor mortal de palavras.

"Ó gotinhas, lindas gotinhas
porque não espalham?

Já tentámos, mas foi impossível!
Impossível? Não gostam da superfície?
Gostávamos, mas ela tornou-se
hiper-hidrófoba, por encanto!

A Carmen, a Gisela e um misterioso italiano
utilizaram uma poção fluorada mágica
e tudo mudou: já não vemos
nossos queridos OH celulósicos!

Coitadinhas, devem estar tão tristes!
Não!!! Adoramos que as nossas moléculas
fiquem abraçadas num
namoro coesivo, e além disso
podemos voltear à vontade e rolar
sob a mínima inclinação.

Ó papel, branca celulose,
não tens saudades da suave molhagem?
Não!!! Nunca fiquei tão satisfeito com a minha nova pele,
formidável barreira aos insuportáveis
e húmidos beijos de anónimas gotinhas."

Alessandro Gandini

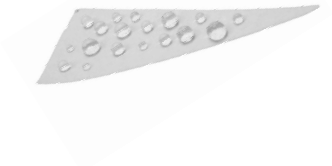

o júri

presidente

Doutor Manuel João Senos Matias
professor catedrático da Universidade de Aveiro

Doutor Mohamed Naceur Belgacem
professor catedrático do Institut National Polytechnique de Grenoble - França

Doutora Maria Helena Mendes Gil
professora catedrática da Faculdade de Ciências e Tecnologia da Universidade de Coimbra

Doutor Armando Jorge Domingues Silvestre
professor associado com agregação da Universidade de Aveiro

Doutor Alessandro Gandini
investigador coordenador do CICECO – Centro de Investigação em Materiais Cerâmicos e Compósitos da Universidade de Aveiro

Doutor João Filipe Colardelle da Luz Mano
professor auxiliar da Universidade do Minho

Doutora Carmen Sofia da Rocha Freire Barros
investigadora auxiliar da Universidade de Aveiro

agradecimentos

Gostaria de expressar os meus agradecimentos primeiramente aos meus orientadores, Doutora Carmen Freire e Prof. Doutor Armando Silvestre, por me terem proporcionado a oportunidade de desenvolver este trabalho e por terem acreditado e confiado nas minhas capacidades. Agradeço ainda a sua preciosa orientação científica, o apoio e a disponibilidade constante.

Gostaria de agradecer também ao Prof. Doutor Alessandro Gandini por toda a ajuda prestada, pela presença constante, pelas discussões científicas que me ajudaram a evoluir ao longo destes anos, e por confiar em mim e nas minhas capacidades.

Ao Prof. Doutor Carlos Pascoal Neto por me ter recebido no seu grupo de investigação de Materiais Macromoleculares e Lenhocelulósicos, mais conhecido por LignoMacro, e por ter prestado a sua ajuda e conhecimentos científicos sempre que foram necessários.

Ao Prof. Doutor Naceur Belgacem por me ter acolhido no seu laboratório em Grenoble, ter proporcionado todo o auxílio necessário e ter acompanhado de perto o meu trabalho durante o período que lá estive. Agradeço ainda a partilha de conhecimentos científicos e as suas palavras de apoio e incentivo.

Ao Dr. Davide Beneventi e ao Prof. Doutor Didier Chaussy por terem acompanhado e contribuído para o trabalho desenvolvido em Grenoble, pela sua amizade e apoio.

À Universidade de Aveiro, CICECO e PAGORA por terem reunido as condições necessárias à realização da parte experimental desta dissertação, e à FCT pela bolsa de doutoramento (SFRH/BD/31124/2006).

A todos os técnicos superiores que contribuíram para esta dissertação através da sua prestação de serviços, permitindo a caracterização das minhas amostras. Em especial, gostaria de agradecer à Celeste Azevedo pelas análises de TGA; Dulce Helena Teixeira pelos ensinamentos de FTIR-ATR; Marta Assunção pelos ensinamentos de SEM e por ter acompanhado parte das minhas sessões; Rosário Soares pelas análises de Raios-X; Isabel Martins pelas análises de RMN no estado sólido e Elina Orblin pelas análises de XPS e ToF-SIMS.

Ao grupo LignoMacro, no qual encontrei verdadeiros amigos para além de vários colegas, agradeço a convivência saudável, o bom-humor, a partilha e a confiança, que representaram, ao longo destes anos todos, um grande incentivo e estímulo para mim, mesmo naqueles dias mais cinzentos. O meu muito obrigada a todos vós!

Às pessoas fantásticas e multi-culturais que fui conhecendo por Grenoble e pela PAGORA, que enriqueceram a minha vida a vários níveis, e que me ajudaram a suportar a distância física que me separava da minha terra natal.

A todos os meus queridos amigos, tanto aos de longa data como aos mais

recentes, que me foram acompanhando ao longo deste meu percurso, que me souberam levantar sempre que tropeçava, e que metaforicamente podem ser descritos como raios de sol a espreitar por entre densas nuvens negras em dias mais cinzentos. Agradeço também por terem celebrado comigo as minhas “vitórias” e terem chorado as minhas “derrotas”, e mais importante que tudo, por terem estado sempre lá. Vocês fazem parte do tesouro que levarei sempre comigo. MUITO OBRIGADA!

A todas aquelas pessoas que tive oportunidade de ir conhecendo “por aí” ao longo destes anos, sendo que muitas delas provavelmente nunca mais verei ou terei contacto, mas que no entanto, de uma forma ou de outra, deixaram a sua marca na minha vida, contribuindo para o meu crescimento e para a estruturação da pessoa que sou hoje.

Ao João Paulo por me ter ensinado que muitas vezes somos nós que estabelecemos os nossos próprios obstáculos e que com muita força de vontade e coragem, os obstáculos *reais* são passíveis de serem ultrapassados com sucesso.

À Joan pela ajuda preciosa e leitura atenta de todos os manuscritos que lhe foram passando pelas mãos, pela sua amizade, carinho, e por ser a pessoa maravilhosa que é.

Agradeço ao meu mano e querido amigo Vi por toda a sua amizade, ajuda, compreensão, partilha, carinho, e todos os momentos passados juntos, que nos fizeram crescer como pessoas ao longo destes anos.

Um agradecimento especial ao meu amigo Sandro por toda a força, incentivo e amizade, pelas diversas conversas sobre temas vários, pela boa disposição, pela troca de ideias e partilha, e, mais importante que tudo, por acreditar em mim. MUITO OBRIGADA!

Por fim, gostaria de expressar os meus sinceros agradecimentos às pessoas mais importantes da minha vida. Aos meus pais, irmãs e sobrinhas, agradeço todo o amor, carinho, paciência, compreensão, dedicação, apoio e incentivo que me têm prestado, não só ao longo deste percurso, mas ao longo de toda a minha vida. Muito em especial, gostaria de agradecer à minha querida avó Célia pela maravilhosa pessoa que era, por me ter apoiado incondicionalmente enquanto viva (e acredito que ainda continue, esteja onde estiver...), por todo o seu amor, carinho e por todas as lições de vida, que me tornaram numa pessoa melhor. Todos vós são a outra parte do meu tesouro e, por tudo isto e muito mais, o meu sincero MUITO OBRIGADA!

palavras-chave

fibras de celulose, modificação química heterogénea, reagentes perfluorados, siloxanos, híbridos orgânico-inorgânico classe-II, clorossilanos, hidroficidade, lipofobicidade, omnifobicidade

resumo

O presente trabalho teve como principal objectivo estudar a modificação química heterogénea controlada de fibras de celulose com diferentes reagentes de modo a alterar as suas propriedades de superfície, em especial em termos da criação de um carácter hidrofóbico e lipofóbico, preservando, sempre que possível, as suas propriedades mecânicas e, consequentemente, abrindo novas perspectivas de aplicação. O desenvolvimento do trabalho envolveu três abordagens principais, envolvendo, em cada caso, o estudo de diferentes condições reaccionais.

Na primeira abordagem foram utilizados como reagentes de modificação compostos perfluorados, nomeadamente o anidrido trifluoroacético (TFAA), o cloreto de 2,3,4,5,6-pentafluorobenzoílo (PFBz) e o cloreto de 3,3,3-trifluoropropanoílo (TFP), para promover a acilação heterogénea da superfície das fibras.
A segunda estratégia usada consistiu na preparação de híbridos de celulose do tipo orgânico-inorgânico classe-II, através da modificação das fibras de celulose com o (3-isocianatopropil)trietoxissilano (ICPTEOS), um reagente organossilano bifuncional. A ligação às fibras de celulose foi efectuada através das funções isocianato e, posteriormente, os grupos etoxissilano foram sujeitos a tratamentos de hidrólise ácida, como tal ou na presença de outros siloxanos, nomeadamente o tetraetoxissilano (TEOS) e o *1H,1H,2H,2H*-perfluorodeciltrietoxissilano (PFDTEOS).
Finalmente, a última abordagem foi baseada na modificação das fibras com triclorometilssilano (TCMS), através de uma reacção gás-sólido, que dispensou assim o uso de solventes orgânicos.

A ocorrência de modificação química foi em cada caso confirmada por Espectroscopia de Infravermelho com Transformada de Fourier e Reflectância Total Atenuada (FTIR-ATR), Análise Elementar (EA) e determinação de ângulos de contacto. Adicionalmente, e dependendo de cada caso específico, diversas outras técnicas foram empregues na caracterização aprofundada dos materiais preparados, nomeadamente Ressonância Magnética Nuclear CP-MAS no Estado Sólido (RMN), Espectroscopia de Difracção de Raios-X (XRD), Análise Termogravimétrica (TGA), Espectrometria de Massa de Iões Secundários com Análise de Tempo de Vôo (ToF-SIMS), Espectroscopia Fotoelectrónica de Raios-X (XPS) e Microscopia Electrónica de Varrimento (SEM).

Relativamente à acilação das fibras de celulose com reagentes perfluorados, o sucesso da reacção foi comprovado por FTIR-ATR, EA, XPS e ToF-SIMS. Neste contexto, obtiveram-se fibras modificadas possuindo graus de

substituição (DS) compreendidos entre 0.006 e 0.39. Verificou-se por XRD que, em geral, mesmo para os valores de DS mais elevados, a cristalinidade das fibras não foi afectada, indicando que a modificação foi limitada às camadas mais superficiais das mesmas ou a regiões amorfas das suas camadas mais internas. Adicionalmente, observou-se por ToF-SIMS que a distribuição dos grupos perfluorados à superfície das fibras foi, de facto, bastante heterogénea.
Todos os derivados de celulose perfluorados apresentaram elevada hidrofobicidade e lipofobicidade, tendo-se atingido ângulos de contacto com água e diiodometano de 126º e 104º, respectivamente. Um aspecto interessante relativo a estes materiais é que a elevada omnifobicidade foi observada mesmo para valores de DS muito reduzidos, não se mostrando significativamente afectada pelo aumento dos mesmos. Em consonância, verificou-se por XPS que a cobertura da superfície das fibras de celulose com grupos perfluorados aumentou apenas ligeiramente com o aumento do DS, apontando para a esterificação de camadas mais internas das fibras, associada, neste caso, predominantemente aos seus domínios amorfos.
No que diz respeito à estabilidade hidrolítica destes derivados, obtiveram-se dois tipos distintos de comportamento. Por um lado, as fibras de celulose trifluoroacetiladas são facilmente hidrolisáveis em meio neutro, e, por outro, as fibras pentafluorobenzoiladas e trifluoropropanoiladas mostram-se bastante resistentes face a condições de hidrólise em meio neutro e ácido (pH 4), podendo, contudo, ser facilmente hidrolisadas em meio alcalino (pH 9 e 12, para derivados do PFBz e do TFP, respectivamente).

Na segunda abordagem verificou-se a ocorrência de reacção por FTIR-ATR e EA. Em geral, a modificação química com ICPTEOS ocorre predominantemente nas zonas mais superficiais das fibras de celulose ou em regiões amorfas. Contudo, em condições reaccionais mais severas (maior quantidade de reagente e tempo de reacção), esta atingiu também regiões cristalinas, afectando, consequentemente, a estrutura cristalina das fibras, como verificado por XRD. Por RMN de ^{29}Si observou-se que após reacção com o ICPTEOS já existiam indícios de alguma hidrólise dos grupos etoxissilano, e que a sua subsequente condensação parcial tinha levado à formação de uma película inorgânica em redor das fibras (verificado por SEM), constituída maioritariamente por estruturas lineares, com uma contribuição mais modesta de estruturas “diméricas” e outras mais ramificadas. Consequentemente, este revestimento inorgânico transformou as fibras de celulose em materiais híbridos com elevada hidrofobicidade (ângulos de contacto com água entre 103-129º).
A hidrólise ácida dos restantes grupos etoxissilano, como tal ou na presença de TEOS, originou híbridos de celulose com elevada hidrofilicidade, sendo impossível medirem-se os ângulos de contacto com água dos produtos finais, devido à presença maioritária de grupos silanol (Si-OH) e ligações Si-O-Si à superfície, os quais contribuíram para o consequente aumento de energia de superfície. No entanto, quando a hidrólise foi realizada na presença de PFDTEOS, obtiveram-se materiais híbridos com elevada hidrofobicidade e lipofobicidade (ângulos de contacto com água e diiodometano de 140º e 134º, respectivamente), devido à combinação da presença de grupos perfluorados e micro- e nano-rugosidades na superfície das fibras de celulose, conforme confirmado por SEM.

Finalmente, a última abordagem permitiu preparar materiais derivados de celulose altamente hidrofóbicos e lipofóbicos (ângulos de contacto com água e diiodometano de 136º e 109º, respectivamente) por um processo simples, envolvendo tempos de tratamento tão curtos como 0.5 min. Este comportamento omnifóbico foi gerado pelo efeito sinergético entre a diminuição de energia de superfície das fibras, devido à presença de grupos metilo dos resíduos de TCMS ligados a estas, e a condensação dos resíduos de TCMS na forma de micro- e nano-partículas inorgânicas, que levou à criação de um revestimento rugoso à superfície das fibras, conforme observado por RMN de ^{29}Si e SEM, respectivamente.
A pré-humidificação das fibras de celulose demonstrou desempenhar um importante papel de “acelerador” dos processos de hidrólise e condensação das moléculas de TCMS. Nestas condições, o tempo de tratamento foi um dos parâmetros mais relevantes, pois para tempos de tratamento muito curtos (0.5

min) os materiais resultantes não apresentaram quaisquer diferenças a nível de propriedades físico-químicas em relação ao substrato de partida (a humidade em excesso consumiu todo o TCMS antes que este conseguisse reagir com os grupos hidroxilo das fibras de celulose), possuindo, por exemplo, valores de ângulos de contacto com água idênticos. Para tempos de tratamento mais longos, como 30 min, os materiais finais apresentaram a maior quantidade de componentes inorgânicos, tal como verificado por EA e TGA. Assim, o controlo da humidade das fibras é imperativo para se poder moldar as propriedades finais dos produtos.
Esta última abordagem é particularmente promissora uma vez que tem como base um sistema simples e "verde" que pode ser facilmente implementado.

Em conclusão, este trabalho permitiu demonstrar que a modificação química heterogénea controlada das fibras de celulose representa uma iniciativa promissora para a preparação de novos materiais obtidos a partir de recursos renováveis, com propriedades interessantes e passíveis de ser potencialmente aplicados em diferentes áreas. Para além do mais, as estratégias de modificação estudadas podem também ser precursoras de novos estudos que possam vir a ser desenvolvidos dentro do mesmo âmbito.

keywords

cellulose fibers, heterogeneous chemical modification, perfluorinated reagents, siloxanes, class-II organic-inorganic hybrids, chlorosilanes, hydrophobicity, lipophobicity, omniphobicity

abstract

The main objective of the present work was to study the controlled heterogeneous chemical modification of cellulose fibers with different reagents in order to change their surface features, especially in terms of creating a hydrophobic and lipophobic character, while preserving, as far as possible, their mechanical properties and, consequently, opening new perspectives of potential applications. The work was developed following three main approaches, involving, in each case, the study of different reaction conditions.

In the first approach, perfluorinated compounds, namely trifluoroacetic anhydride (TFAA), 2,3,4,5,6-pentafluorobenzoyl choride (PFBz) and 3,3,3-trifluoropropanoyl chloride (TFP), were used as modification reagents in order to promote the heterogeneous acylation of the fibers' surface.
The second approach consisted in the preparation of class-II organic-inorganic cellulose hybrids, through the modification of the cellulose fibers with (3-isocyanatepropyl)triethoxysilane (ICPTEOS), a bifunctional organosilane reagent. The attachment to the cellulose fibers was ensured by the isocyanate function and, subsequently, the ethoxysilane groups were submitted to acid hydrolysis treatments, as such, or in the presence of other siloxanes, namely tetraethoxysilane (TEOS) and *1H,1H,2H,2H*-perfluorodecyltriethoxysilane (PFDTEOS).
Finally, the last approach was based on the modification of the fibers with trichloromethylsilane (TCMS), through a gas-solid reaction, thus avoiding the use of organic solvents.

The occurrence of chemical modification was in each case confirmed by Attenuated Total Reflectance - Fourier Transform Infrared Spectroscopy (FTIR-ATR), Elemental Analysis (EA) and contact angle measurements. Additionally, and depending on each specific case, several other techniques were employed in the thorough characterization of the materials prepared, namely Solid State Cross-Polarization Magic-Angle Spinning Nuclear Magnetic Resonance (CP-MAS NMR), X-Ray Diffraction Spectroscopy (XRD), Thermogravimetric Analysis (TGA), Time of Flight Secondary Ion Mass Spectrometry (ToF-SIMS), X-Ray Photoelectron Spectroscopy (XPS) and Scanning Electron Microscopy (SEM).

Regarding the acylation of the cellulose fibers with the perfluorinated reagents, the success of the reaction was proved by FTIR-ATR, EA, XPS and ToF-SIMS. In this context, modified fibers possessing degrees of substitution (DS) in the range 0.006-0.39 were obtained. It was verified by XRD that, on the whole, even for the highest DS values, the crystallinity of the fibers was not affected,

which indicated that the modification was limited to their outermost layers or to the amorphous regions of their inner layers. Additionally, it was observed by ToF-SIMS that the distribution of the perfluorinated groups at the fibers' surface was, indeed, quite heterogeneous.
All the perfluorinated cellulose derivatives exhibited a high hydrophobicity and lipophobicity, attaining contact angles with water and diiodomethane of 126º and 104º, respectively. Interestingly, the highly omniphobic behavior was observed even for very low DS values, and did not seem affected by their increase. Accordingly, it was verified by XPS that the surface coverage of the cellulose fibers with the perfluorinated groups presented only a slight increase with increasing DS, pointing to an in-depth esterification of the fibers, associated, in this case, only to their amorphous domains.
Concerning the hydrolytic stability of these derivatives, two distinct features were observed. On the one hand, the trifluoroacetylated cellulose fibers showed to be easily hydrolyzable in a neutral medium, and, on the other, the pentafluorobenzoylated and trifluoropropanoylated fibers showed to be very stable towards neutral and acid (pH 4) hydrolysis conditions, but could, however, be hydrolyzed under alkaline medium (pH 9 and 12, for PFBz and TFP derivatives, respectively).

In the second approach, the occurrence of reaction was verified by FTIR-ATR and EA. On the whole, the chemical modification with ICPTEOS took place within the outermost layers of the cellulose fibers or in their amorphous regions. However, in the case of the most severe reaction conditions (higher ICPTEOS amount and reaction time), this modification also occurred in the crystalline domains, affecting, consequently, the crystalline structure of the fibers, as verified by XRD. ^{29}Si CP-MAS NMR spectroscopy showed that after the reaction with ICPTEOS there was already an indication of some hydrolysis of the ethoxysilane groups, and that their subsequent partial condensation led to the formation of an inorganic "sleeve" around the fibers (verified by SEM), mainly constituted by linear structures, with smaller contributions from "dimeric" counterparts and more branched networks. Consequently, this inorganic coating transformed the cellulose fibers into highly hydrophobic hybrid materials (contact angles with water in the range 103-129º).
The acid hydrolysis of the remaining ethoxysilane groups, as such or in the presence of TEOS, gave rise to cellulose hybrids bearing a high hydrophilicity, as shown by the impossibility to measure the water contact angles of the final products, due to the dominant presence of silanol (Si-OH) groups and Si-O-Si bridges at their surface, which contributed to the consequent increase of the surface energy. Nonetheless, when the hydrolysis was carried out in the presence of PFDTEOS, hybrid materials with both high hydrophobicity and lipophobicity were attained (contact angles with water and diiodomethane of 140º and 134º, respectively), due to the combination of the presence of perfluorinated groups and micro- and nano-rugosities at the surface of the cellulose fibers, as confirmed by SEM.

Finally, the last approach permitted to prepare highly hydrophobic and lipophobic materials derived from cellulose (contact angles with water and diiodomethane of 136º and 109º, respectively) by a simple process, involving treatment times, which could be as low as 0.5 min. This omniphobic behavior was generated by the synergetic effect between the decrease in the fibers surface energy, due to the presence of methyl groups of the TCMS residues attached to them, and the condensation of the TCMS moieties in the form of inorganic micro- and nano-particles, which led to the creation of a rough coating onto the surface of the fibers, as confirmed by ^{29}Si CP-MAS NMR and SEM, respectively.
The pre-humidification of the cellulose fibers showed to play an important accelerating role in the processes of hydrolysis and condensation of the TCMS molecules. In these conditions, the treatment time demonstrated to be quite relevant, since, for shorter treatment times (0.5 min), the ensuing materials did not exhibit any difference in terms of physicochemical properties, compared with the pristine substrate (the excess humidity consumed all the TCMS before it could react with the hydroxyl groups of the cellulose fibers), possessing, for example, similar water contact angles. For longer times, such as 30 min, the final materials presented the highest amounts of inorganic components, as verified by EA and TGA. Thus, it is imperative to control the moisture content of

the fibers in order to tailor the desired final properties of the products.
This third approach is particularly promising because it is based on a straightforward and “green” system, which could be readily implemented.

In conclusion, this work permitted to demonstrate that the controlled heterogeneous chemical modification of the cellulose fibers represents a promising strategy for the preparation of novel materials obtained from renewable resources, with interesting properties and capable of being potentially applied in different areas. Furthermore, the modification strategies studied in this thesis can also be precursors of new studies that may be developed within the same general scope.

Contents

List of Abbreviations

AFM	Atomic Force Microscopy
AKD	Alkyl Ketene Dimers
APS	γ-Aminopropyltriethoxysilane
Ar	Aromatic Ring
ASA	Alkenyl Succinic Anhydrides
Cadoxen	Cadmium Ethylenediamine
CP-MAS	Cross-Polarization Magic-Angle Spinning
DBTL	Dibutyltin Dilaurate
DMAc	*N,N*-Dimethylacetamide
DMF	*N,N*-Dimethylformamide
DMSO	Dimethyl Sulfoxide
DP	Degree of Polymerization
DS	Degree of Substitution
EA	Elemental Analysis
ECF	Elemental Chlorine Free
ESCA	Electron Spectroscopy for Chemical Analysis
FA	Fatty Acids
FTIR-ATR	Fourier Transform Infrared – Attenuated Total Reflectance
HDS	Hexadecyltrimethoxysilane
ICPTEOS	(3-Isocyanatepropyl)triethoxysilane
IR	Infrared
LA	L-Lactide
LbL	Layer-by-Layer
MPS	γ-Methacryloxypropyltrimethoxysilane
NMR	Nuclear Magnetic Resonance
PA	Pyromellitic Anhydride
PCL	Polycaprolactone
PFBz	2,3,4,5,6-Pentafluorobenzoyl Chloride
PFDTEOS	*1H,1H,2H,2H*-Perfluorodecyltriethoxysilane
PLA	Poly(Lactic Acid)

PLLA	Poly-L-Lactic Acid
PVA	Polyvinyl Alcohol
RT	Room Temperature
SEM	Scanning Electron Microscopy
t/a	Tons per Year
TCMS	Trichloromethylsilane
T_d	Temperature of Maximum Decomposition Rate
T_{di}	Temperature of Initial Decomposition
TEOS	Tetraethoxysilane
TFAA	Trifluoroacetic Anhydride
TFP	3,3,3-Trifluoropropanoyl Chloride
TGA	Thermogravimetric Analysis
ToF-SIMS	Time-of-Flight Secondary Ion Mass Spectrometry
TPS	Thermoplastic Starch
XPS	X-Ray Photoelectron Spectroscopy
XRD	X-Ray Diffraction
α	Sliding Angle
ε-CL	ε-Caprolactone
γ^d_l	Dispersive Component of the Surface Tension
γ^d_s	Dispersive Component of the Surface Free Energy
γ_l	Surface Tension
γ_{lv}	Liquid/Vapor Interfacial Tension
γ^p_l	Polar Component of the Surface Tension
γ^p_s	Polar Component of the Surface Free Energy
γ_s	Surface Free Energy
γ_{sl}	Solid/Liquid Interfacial Tension
γ_{sv}	Solid/Vapor Interfacial Tension
θ	Contact Angle
θ_w	Water Contact Angle

Introduction

The progressive increase in the global population during the last two centuries, as well as the development of modern society, were conducted under an excessive consumption of fossil resources, namely petroleum, natural gas and coal. As a consequence, currently, worldwide experts predict that within one-to-three generations, the availability of these non-renewable resources, at least at a useful time scale, will dwindle and/or their exploitation become too costly [1].

Additionally, environmental problems, such as water, air and soil pollution, are becoming topic of serious concern, and, nowadays, a rising consciousness of both academic and industrial circles on the importance of preserving the ecological systems has been strongly encouraging the search for sustainable alternatives.

Thus, worldwide researchers are motivated to take advantage of renewable and low-polluting raw material sources, *i.e.*, biomass, instead of the fossil resources, and also to develop "greener" chemical processes and produce easily degradable, or at least easily recyclable, materials. Nonetheless, the exploitation of the alternative sources should be controlled, in order to permit the actual regeneration of their natural stock, in order to avoid the loss of their availability.

Research initiatives to this effect are being implemented ubiquitously with a sense of rising urgency, which, moreover, are being accompanied by a remarkable increase in scientific publications, patents and international conferences covering the topic of the rational exploitation of renewable resources to produce chemicals and novel materials, either in partial substitution of counterparts derived from fossil resources, or as materials with original properties [1].

Within this new context, among the copious alternative investigations carried out in recent years, the resurgent interest in the utilization of polysaccharides as raw materials for the preparation of new derivatives is quite inspiring, considering that some of these natural polymers were the first source of “plastics” about 150 years ago, in the form of cellulose esters, well before the dawn of petrochemistry. Indeed, these materials never lost their industrial and economical impact, as proved by the current rise in cellulose acetate production [2-4].

The research activities associated with the utilization of polysaccharides are nowadays crossing many new paths related with the development of novel materials to be applied in several domains, such as food, packaging, cosmetics and pharmaceuticals.

Polysaccharides are important naturally occurring polymers that possess an ubiquitous character, being present in plant, animal, or microbial (including fungi and algae) realms, where they perform different functions and roles, such as structural features, energy storage and gel formation, all relying on their specific chemical structure, composition, molecular weight, and possible ionic character [5].

Among the existing specimens of this class of biopolymers, cellulose, chitin and starch are the major representatives in terms of abundance, possessing different properties, e.g., crystallinity, mechanical properties and aptitude to chemical modification, despite the similarity on their basic building blocks (Figure 1) [6].

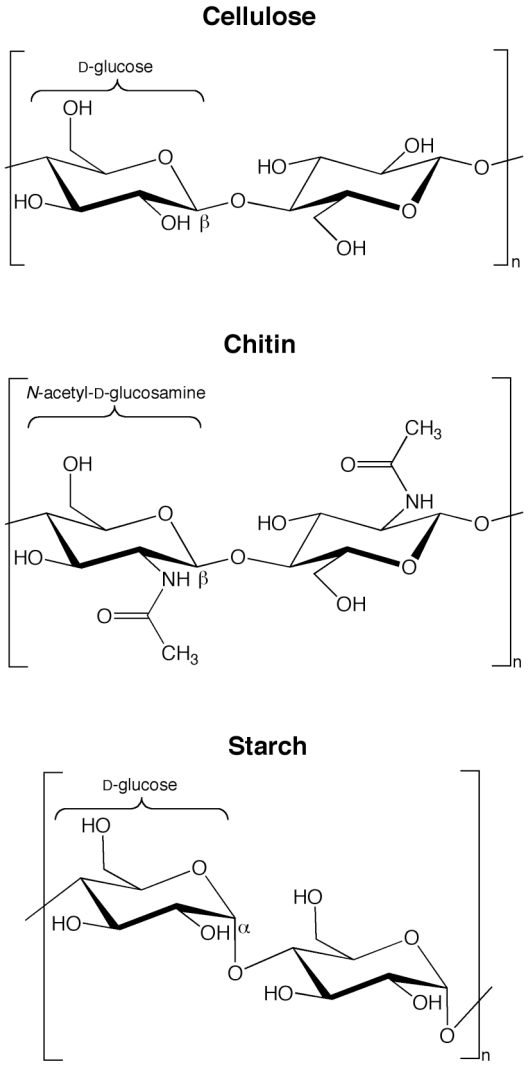

Figure 1. Structural representation of cellulose, chitin and one of the starch components, amylose.

Given this state of affairs, the purpose of this dissertation was to develop new materials based on the most abundant polysaccharide, *viz.* cellulose, which, apart from the mentioned ecological reasons, had been introduced into our research group several years prior to this work [7, 8], not only because of the recognized importance and magnitude of the agroforestry sector in Portugal, but also because of the existence of close collaborations between our group and Portuguese pulp and paper entities, including industries. In general, our group has been concentrating its attention on the conscientious use of renewable resources, some of them considered as peddling industrial residues and by-products, as precursors or aids to novel macromolecular materials, always aiming at updating their value.

One of the approaches involving this promising natural resource consisted in the controlled heterogeneous modification of cellulose fibers from *Eucalyptus globulus* with fatty acids (FA) [7], which led to the preparation of new cellulose-based materials that could be used either as reinforcing elements in polymer matrix composites, when low degrees of substitution (DS) were attained and the esterification occurred essentially at the fiber surface, or for the preparation of co-continuous composites, when higher DS were achieved and the esterification extended to the inner layers of the fibers. The other approach, comprising cellulose fibers from the same source, consisted in the preparation of cellulose/silica hybrid materials without covalent attachments [8], which displayed higher thermal stability than native cellulose and some hydrophobicity.

The former approach, *i.e.*, the controlled heterogeneous modification of cellulose, is particularly interesting, because it offers the possibility of overcoming some of the natural drawbacks of cellulose, particularly its high hydrophilicity, which is associated with poor dimensional stability.

Moreover, a major driving force for this kind of approach is precisely the rising interest in cellulose-based composite materials observed in the last decades. Cellulose fibers present in general a great potential as alternative to the traditional synthetic materials (*e.g.* aramide and glass fibers) used to reinforce the common non-polar polymeric matrices, such as polyolefins, in composite materials. Furthermore, the utilization of these lightweight and low-cost natural fibers as fillers in composites offers the possibility of replacing and, at the same time, decreasing large portion of synthetic and non-biodegradable polymers.

Following the initial and motivating initiatives developed in our group, this thesis deals with a fundamental study of the controlled heterogeneous modification of cellulose fibers by means of different strategies, in view of the preparation of novel materials, mainly having in common valuable properties such as highly hydrophobic and lipophobic character, which could ensure them promising applications in different areas, as for example packaging and textiles.

This dissertation is arranged in four different chapters. The *first chapter* consists in a bibliographic survey concentrating upon the relevant topics related to the aim of this work. The *second chapter* relates to the experimental part, in which all the procedures employed in the conduct of the work are specified, as well as the comprehensive list of

equipments and techniques used to thoroughly characterize the materials obtained. In the *third chapter*, which is subdivided into three main sections corresponding to the different approaches developed for the controlled heterogeneous modification of cellulose, the relevant results are expounded and discussed with the associated conclusions. Finally, the *fourth chapter* covers the concluding remarks about all the work developed, followed by some suggestions for further work.

Chapter 1

Bibliographic Review

Chapter 1 – Bibliographic Review

1. Cellulose

As referred in the *Introduction*, cellulose is the most abundant natural polymer on earth, with an annual production reaching about 1.5 x 10^{12} tons [2, 9]. Part of this cellulose is produced in a rather pure form, as in cotton, in which its content is usually higher than 95%, but predominantly combined with lignin and hemicelluloses in the cell walls of woody plants, as depicted in Figure 2, *viz.* softwoods and hardwoods and also the stalks of some annual plants, in which its content is variable but typically in the range of 35 to 50% of the plant dry weight [10]. Vegetable cellulose is therefore an intra-cellular component that plays a vital structural role in the plant cell walls, being particularly more abundant in the secondary cell wall layer S2 (Figure 2).

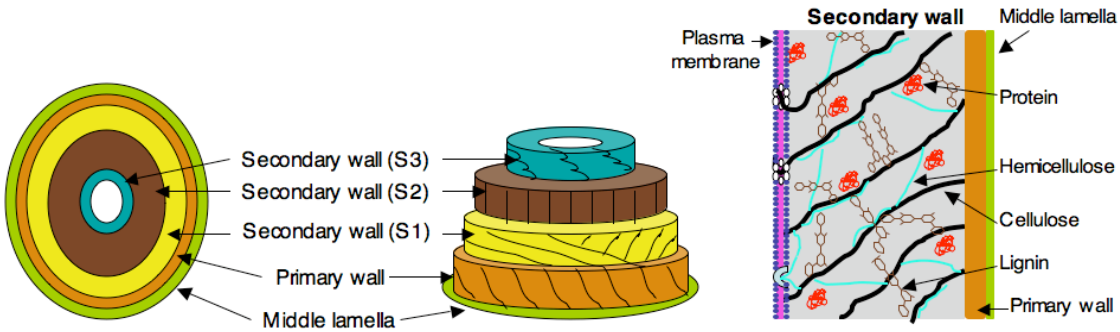

Figure 2. Schematic representation of the different structured layers of a plant cell wall (on the left) and close-up of the secondary cell wall and its constituents (on the right).

Apart from its vegetable origin, cellulose is also synthesized extracellularly by algae, fungi, and some bacteria [2], *e.g.*, *Gluconacetobacter xylinus*. In the latter case, it is denominated as bacterial cellulose, and is produced with both high degree of purity and crystallinity, among other unique properties [2].

Throughout human history, cellulose has been used in various forms, from clothing to housing, and has formed a significant part of human culture since the Egyptian papyri, however, at that time, in an uninformed way [3].

It was just in the first half of the 19th century that cellulose was first discovered, isolated and named by Anselme Payen [2, 3, 10, 11]. Since then, multiple physical and chemical aspects about it have been thoroughly studied, and discoveries are constantly being made regarding its biosynthesis, assembly, and structural features. Indeed, the state of knowledge regarding this remarkable natural polymer has been updated through the years, as shown by the copious number of books, chapters and reviews devoted to it [2-4, 9-16]. This fact clearly indicates that cellulose still is of the upmost importance, inspiring new paths of valorization, especially in the area of materials science and technology.

1.1.1. Biosynthesis of Cellulose

Cellulose can be biosynthesized by two different pathways, depending on its origin, *i.e.*, from plants or microorganisms [2]. In plants, the cellulose biosynthesis process is intimately associated with the photosynthesis [17, 18], thus the cellulose precursors in this case are carbon dioxide and water, which pave the way to the production of glucose and, subsequently, of cellulose. On the other hand, in microorganisms devoid of photosynthetic capacity, sugars or other carbon-sources, typically glucose, are required for the production of cellulose [19, 20]. The dominant pathway, however, is by far the cellulose biosynthesis from plants, which, comparatively to the other pathways, requires further steps of isolation and purification, because, as previously mentioned, cellulose forms a native composite material with lignin and hemicelluloses in plant cell walls.

1.1.2. Molecular Structure of Cellulose

Cellulose can be generally described as a high molecular weight homopolymer of β-1,4-linked anhydro-D-glucose units, which are rotated 180° with respect to one another (Figure 1). Consequently, its repeating unit is, in fact, a glucose dimer, known as cellobiose (Figure 1). It is admitted that, depending on the origin, cellulose chains are constituted by 300 to 10000 glucose units [2].

In the cellulose structure, each anhydro-D-glucose unit bears three hydroxyl groups (one primary and two secondary), with the exception of the terminal ones, of which one possesses a chemically reducing functionality, namely a hemi-acetal unit, known as the reducing end, and the other, termed the non-reducing end, bears four hydroxyl groups. Additionally, technical celluloses, such as bleached wood pulp, may also contain some carbonyl and carboxyl groups arising from their isolation and purification processes [3, 21].

The β-D-glucopyranose rings in the cellulose chains assume a $^4C_1$ chair conformation, with the hydroxyl groups in an equatorial position and the hydrogen atoms in an axial position.

In nature, vegetable cellulose occurs as assemblies of cellulose chains, which are stabilized through intra- and inter-molecular hydrogen bonds, specifically intramolecular hydrogen-bonding between C2-OH and C6-OH (*i*) and C3-OH with endocyclic oxygen (*ii*) (Figure 3a) and intermolecular hydrogen-bonding between C3-OH and C6-OH (*iii*) (Figure 3b). During its biosynthesis, individual cellulose chains are brought together into larger units known as elementary fibrils or protofibrils (1.5-3.5 nm in width), which aggregate into larger units called microfibrils (10-30 nm in width), the latter finally assembling into the familiar cellulose fibers (about 20 μm in width) [2, 22]. Celluloses from different sources may however aggregate in different ways, as dictated by their biosynthetic conditions [3]. Thus, for example, bacterial cellulose consists in a three-dimensional network of fibrils, which possess 1/100 of the vegetable cellulose fibers width, as can be seen in Figure 4.

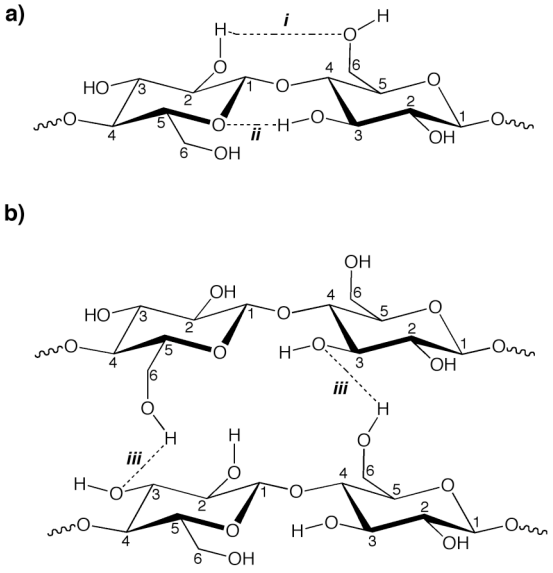

Figure 3. Cellulose intra- and inter-molecular hydrogen-bonding system.

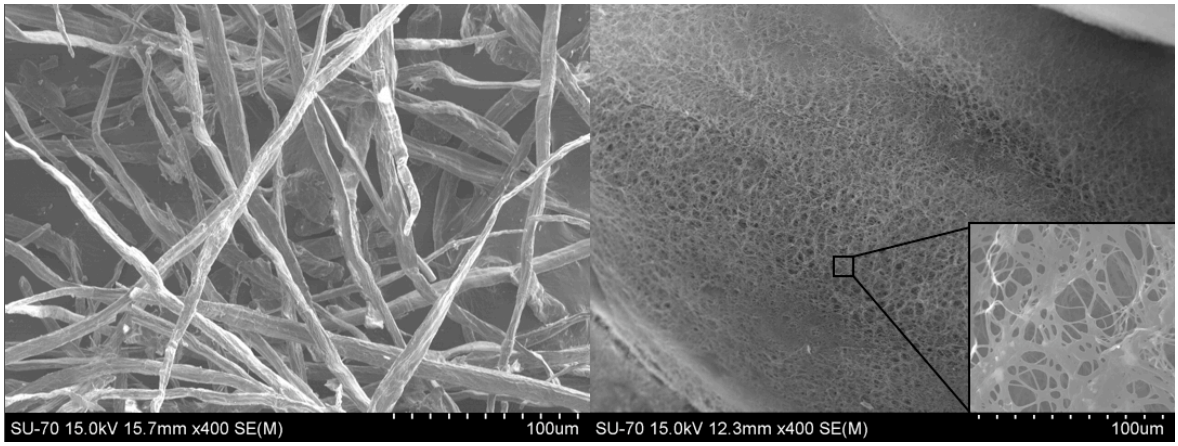

Figure 4. Scanning electron micrographs of vegetable (on the right) and bacterial (on the left) cellulose fibers, at 400x magnification (in the case of the bacterial cellulose, it is also showed a higher magnification of the fibers at the bottom right corner).

Due to its fibrous supramolecular arrangements, vegetable cellulose possesses unique properties, such as high mechanical resistance and insolubility in most solvents, including water [2, 3]. The same is true for bacterial cellulose, which is moreover known to possess even better mechanical properties than its vegetable counterpart and a very large water retention capacity, up to about one hundred times its weight [20].

As opposed to the remarkably high degree of crystallinity of bacterial cellulose (65-80%) [23], vegetable cellulose displays a less uniform macromolecular ordering, and hence exhibits both highly ordered crystalline regions, the main responsible for its toughness, density and resistance to traction, accompanied by amorphous or less ordered regions, in which the chemical accessibility (reactivity) to the hydroxyl groups is higher.

1.1.3. Polymorphism of cellulose

According to the source, and depending on the method of cellulose extraction or treatment, the hydrogen-bonding network and molecular orientation in vegetable cellulose supramolecular structure are variable, affecting its degree of crystallinity, which is usually in the range 40-60% [10]. This variability in cellulose structural arrangement gives rise to six cellulose polymorphs, namely, I, II, III_I, III_{II}, IV_I, and IV_{II}, as illustrated in Figure 5 [24], which differ in unit cell dimensions, whose values are given in Table 1 [9, 10].

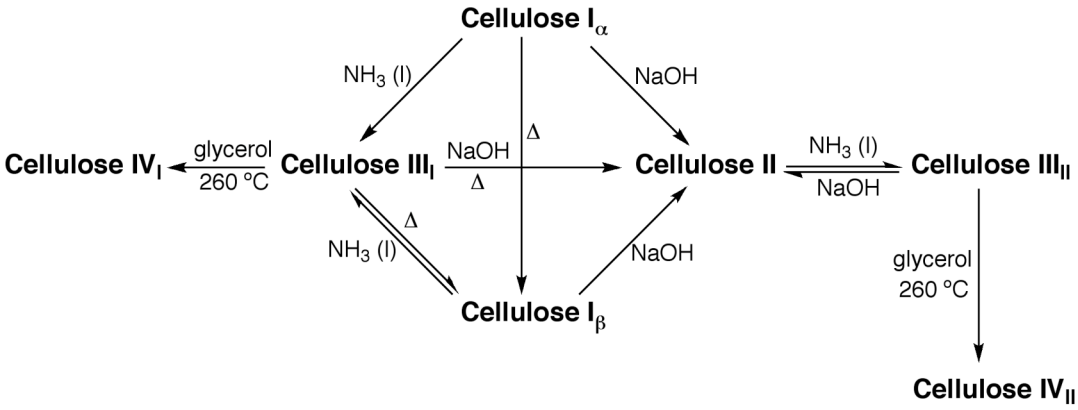

Figure 5. Schematic representation of cellulose transformation into its several polymorphs [10].

Table 1. Unit cell dimensions of the four main types of cellulose polymorphs, as published by Krässig [11].

Unit cell	a-axis (Å)	b-axis (Å)	c-axis (Å)	γ (°)	Polymorph
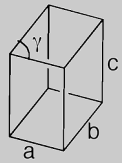	7.85	8.17	10.34	96.4	Cellulose I
	9.08	7.92	10.34	117.3	Cellulose II
	9.9	7.74	10.3	122	Cellulose III
	7.9	8.11	10.3	90	Cellulose IV

More recently, it was found that cellulose I, which is the form of cellulose found in nature (*native cellulose*), is indeed a mixture of two polymorphs, *viz.* I_α and I_β [25, 26]. Depending on the origin of cellulose, these two polymorphs exist in different ratios. While in celluloses from algae and bacteria it is well-known that I_α prevails, in cellulose from higher plants, this topic is not totally clarified, albeit with studies pointing to the dominance of the I_β sub-class [3, 24]. In both the I_α and I_β structures, cellulose chains adopt parallel configurations, differing, however, in their hydrogen-bonding patterns [24]. The meta-stable phase I_α can be converted to the more thermodynamically stable I_β phase by high-temperature annealing in various media (Figure 5) [27].

Cellulose II (regenerated cellulose), the second most extensively studied polymorph, due to its high stability and technical relevance, can be obtained by two different processes, namely (i) alkaline treatment with an aqueous solution of sodium hydroxide (mercerization) or (ii) dissolution and subsequent precipitation/regeneration, both starting from cellulose I (Figure 5) [2]. Cellulose III results from the treatment of

cellulose I or II with liquid or gaseous ammonia, or organic amines (Figure 5) [28]. Finally, polymorph IV can be obtained by heating cellulose III up to 260 ºC in glycerol (Figure 5) [29].

As previously mentioned, the supramolecular arrangement of cellulose, in terms of crystallinity or fibrillar architecture, strongly influences its properties. In addition to the mechanical strength and solubility, this structural aspect plays a decisive role in determining the rate and often also the course of a chemical reaction, especially in the case of heterogeneous systems, thus influencing the extent and distribution of substitution and the product solubility. For instance, a high supramolecular order of the cellulose chains, synonymous of lower accessibility of the hydroxyl groups due to the large amount of interfibrillar hydrogen-bonding, generally hinders the progress of chemical reactions [3]. This problem can be easily overcome however, and thus the reaction rate enhance, by changing the nature of the medium, *i.e.*, from heterogeneous to homogeneous [3].

2. Chemical Modification of Cellulose

From a technological and commercial point of view, cellulose derivatives constitute a very important and promising domain, representing value-added products derived from the chemical modification of a low-cost naturally available raw material.

The chemical modification of cellulose is a common approach whose actors are its hydroxyl groups. Accordingly, it is typically carried out under the well-known classical reactions of these moieties, specifically esterification, etherification and oxidation reactions, as depicted in Figure 6.

Esterification is usually accomplished by reacting cellulose with an appropriate acid, anhydride or acyl chloride [3, 4].

Cellulose etherification can be carried out by three main routes, namely i) by the Williamson ether synthesis with alkyl halides in the presence of a strong base, ii) with alkylene oxides in a weakly basic medium, or iii) by Michael addition of acrylic or related unsaturated compounds, such as acrylonitrile [3, 4].

Both reactions, *i.e.*, esterification and etherification, can also serve as starting point for other more elaborated strategies, such as crosslinking and grafting polymerization. The former is usually carried out employing bifunctional modification reagents [3, 4]. The latter can consist, on the one hand, of the grafting of short side chains *onto* the cellulose backbone, performed, for example, during etherification with alkylene oxides *via* addition of more than one alkylene oxide unit or, on the other hand, of a grafting-from process, for instance, by radical polymerization of vinyl compounds after the creation of a radical site at the cellulose chain [3, 4].

The oxidation of the cellulose hydroxyl groups can occur at the C-6 position first to give an aldheyde group and then the corresponding carboxylic counterpart (Figure 6, A and B). If this reaction takes places at C-2 and/or C-3 positions, it generates ketones (Figure 6, C to E) or, in the case of bond scission between C-2 and C-3, the corresponding dialdehyde (Figure 6, F), oxidizable in turn to the diacid moieties (Figure 6, G) [3]. The preference towards a certain type of oxidation depends substantially on the nature of the oxidants, but usually both carbonyl and carboxylic functions are produced in varying proportions [4].

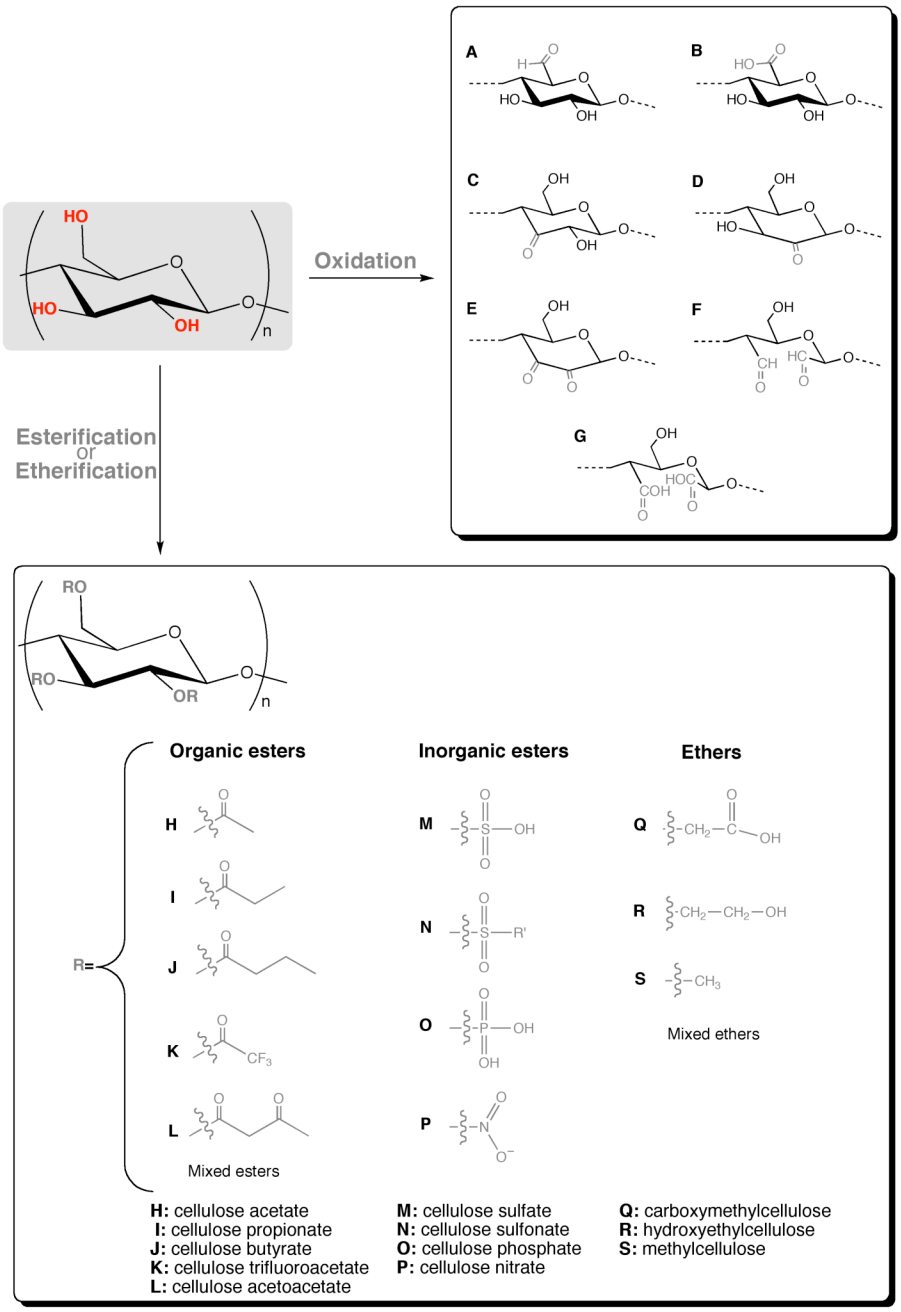

Figure 6. Schematic representation of the main types of cellulose chemical modification and some of the typical ensuing products [3].

Besides these three main types of cellulose functionalization, the formation of cellulose carbamates [-O-C(O)-NH-] by reaction with isocyanate functions (O=C=N-) is also well established [3, 4].

In contrast with the cellulose applications as a natural product for the production of high volume commodities like textiles and paper, the use of this polysaccharide as a

chemical raw material only started about 150 years ago. The first synthesized cellulose derivative was cellulose nitrate (Figure 6, P), an inorganic ester also designated "nitrocellulose", a thermoplastic material accidentally discovered in 1846 by Christian Friedrich Schönbein, who soon verified the explosive properties of this derivative. "Nitrocellulose" was first used as flexible films produced by Eastman Kodak, in 1889. However, as these films were highly inflammable, brittle and unstable, they were replaced, in 1934, by safer films based on cellulose acetate (Figure 6, H).

Cellulose acetate (Figure 6, H) was the second synthesized cellulose derivative, but the first of its organic esters, prepared in 1865 by Schützenberger. Apart from its primary use in photographic films, it found many other applications through the years, such as in textile fibers, adhesives and coatings, which are still produced nowadays [2-4] at an annual rate of about 900.000 tons (Table 2). Its industrial manufacture is usually performed using acetic anhydride as the esterifying agent and sulfuric acid (or in special cases perchloric acid) as the catalyst, and the raw materials typically used are cotton linters and refined wood pulp [4]. The term cellulose acetate reflects in fact a family of compounds with varying properties and applications as a function of the degree of esterification, which can vary from 1 to 3 (Table 2).

Since the end of the 19th century, numerous other cellulose derivatives have been developed (Table 2), possessing different properties and, consequently, diverse applications, such as in coatings, controlled release systems, paint and food additives and varnishes, among others [2-4].

The properties of cellulose derivatives are mainly determined by the nature of the appended moiety, but they can also be adjusted by the extent of the substitution, defined as the degree of substitution (DS), *i.e.*, the average number of functionalized hydroxyl groups per anhydroglucose unit, which varies from 0 to 3. Of course, the product degree of polymerization (DP) also plays an important role in this context. Table 2 provides some examples of the dependence of the solubility of some of these derivatives on their DS, together with their yearly production, some properties and applications.

Ethers and esters are still today the major commercial derivatives prepared from cellulose (Table 2).

Table 2. Commercially important cellulose esters and ethers: their worldwide production, examples of solubility regarding the degree of substitution (DS), some properties and common applications [2-4, 30, 31].

Product	Worldwide production (t/a)	DS	Solubility	Properties	Applications
Cellulose acetate	900.000	0.6-0.9	Water	White, odorless and non toxic	Textile fibers, cigarette filters, photographic films, plastics, coatings, adhesives and membranes
		1.2-1.8	2-Methoxyethanol		
		2.2-2.7	Acetone		
		2.8-3.0	Chloroform		
Cellulose acetate butyrate	—[a]	0.2/2.7	Acetone, 2,6-dimethyl-4-heptanone	Thermoplastic	Coatings, adhesives and plastics
		1.1/1.6	Acetone		
Cellulose nitrate	200.000	1.8-2.0	Ethanol	Unstable and explosive	Explosives, membranes, plastics and adhesives
		2.0-2.3	Methanol, acetone, 2-butanone		
		2.2-2.8	Acetone		
Carboxymethyl cellulose	300.000	0.5-2.9	Water	Non toxic, non allergenic and high viscosity	Food, beverages, coatings, paints, adhesives and pharmaceuticals
Methylcellulose	150.000	0.4-0.6	4% NaOH aqueous solution	White powder, high aptitude to gel formation and non toxic	Food, cosmetics, pharmaceuticals, paints, films, textiles and construction materials
		1.3-2.6	Cold water		
		2.5-3.0	Organic solvents		
Ethylcellulose	4.000	0.5-0.7	4% NaOH aqueous solution	Thermoplastic	Coatings, paints and pharmaceuticals
		0.8-1.7	Cold water		
		2.3-2.6	Organic solvents		
Hydroxyethyl cellulose	50.000	0.1-0.5	4% NaOH aqueous solution	High capacity of water retention	Coatings, paints, cosmetics and construction materials
		0.6-1.5	Water		

[a] Not available.

Carboxymethylcellulose (Figure 6, Q), for example, with an annual production of about 300.000 tons worldwide (Table 2), constitutes the most commercially significant cellulose ether derivative, which has, moreover, attracted much attention because of its polyelectrolyte character and its associated water solubility [3]. The carboxymethylation of cellulose is usually carried out by the Williamson etherification of alkali cellulose with sodium monochloroacetic acid in an aqueous or aqueous-alcoholic medium [3, 4]. This cellulose derivative find applications in diverse areas, like food industry, where it can be used as thickening agent or emulsion stabilizer, and in pharmaceuticals, where it can be employed in the production of laxatives and diet pills (Table 2) [3].

Methylcellulose (Figure 6, S), is the most representative of cellulose alkyl ethers, and is also largely produced worldwide (Table 2). The corresponding commercial products are obtained by a the Williamson reaction of alkali cellulose with gaseous or liquid methyl chloride [4], which gives rise to white non toxic solids, exhibiting a graded solubility in various media, both water and organic solvents (*e.g.*, ethanol [4]), as a function of the DS (Table 2). They possess furthermore a high aptitude to form gels in contact with water [4]. Their main application sectors are in the building, paints and cosmetic industries (Table 2) [4].

Apart from the different types of cellulose functionalizations, the concept of chemical modification can be subdivided into two main categories: (i) homogeneous and (ii) heterogeneous modifications. These categories are roughly associated with transformations starting from dissolved cellulose and solid cellulose in a non- or weakly-swollen state, respectively [3].

2.1. Homogeneous Modification of Cellulose

In homogeneous reaction conditions, cellulose is dissolved in an appropriate medium, and, consequently, all the OH moieties are equally available for reaction, thus leading to a bulk modification [3, 32].

This kind of modification implies the destruction of the microfibrillar integrity of the cellulose fibers, *i.e.*, the hydrogen-bonding between the cellulose microfibrils, which deeply affects their supramolecular structure. As a consequence, the products obtained generally possess properties totally different from those of the pristine cellulose fibers,

including physical and mechanical properties, constituting materials with thoroughly novel features [3].

Homogeneous modifications have represented an important aspect of cellulose research for many years, because more uniform products can be obtained, compared to working in heterogeneous conditions [3].

Cellulose dissolution can be attained by (i) physical interactions with the solvent or (ii) chemical reaction with the solvent leading to covalent bond formation [3, 33]. At present, cellulose solvents can be subdivided into derivatizing and non-derivatizing, and both categories include aqueous and non-aqueous media [3, 30, 32, 34]. The term "derivatizing solvents" refers to all solvents and solvent systems in which the dissolution of cellulose occurs together with the formation of a labile ether, ester, or acetal derivative, called intermediate. This means that the intermediates should be easily decomposed to regenerate cellulose by changing the medium (e.g., non-aqueous to aqueous) or its pH. *N,N*-dimethylformamide (DMF)/N_2O_4 is an example of a derivatizing system, whose intermediate is cellulose nitrite [3].

On the other hand, the non-derivatizing category comprises solvents or solvent systems, such as cadoxen (common denomination for cadmium ethylenediamine) and *N,N*-dimethylacetamide (DMAc)/LiCl system, which are able to dissolve cellulose only by intermolecular interactions [3]. Additionally, more recently, much attention has been focused on a new class of solvents, the ionic liquids, also known as "green solvents" due to their intrinsic features, such as negligible volatility, *i.e.*, the absence of one of the main problems associated with the use of common organic solvents [35].

The representative cellulose derivatives obtained by means of homogeneous reaction conditions consist of pure or mixed cellulose organic and inorganic esters and cellulose ethers, illustrated in Figure 6 by the derivatives H to S, which include the already mentioned cellulose nitrate, acetate, carboxymethylcellulose and methylcellulose (Table 2) [36-38]. Although nowadays, the industrial trend is moving toward heterogeneous reaction conditions, at least at the beginning of the conversion, because of the cost and ecological drawbacks of many solvents, the use of homogeneous reaction conditions still continues to be widely explored, particularly in laboratory experiments [33].

In this sense, for example, several aliphatic cellulose esters, from C6 to C18, were prepared in a homogeneous medium based on the DMAc/LiCl system, using the respective acyl chlorides as esterification reagents and either pyridine or triethylamine as catalyst [39, 40].

In another vein, Rahn and co-workers [41] prepared cellulose *p*-toluenesulfonates (tosylates) by reacting cellulose dissolved in the DMAc/LiCl system with tosylchloride in the presence of triethylamine.

2.2. Heterogeneous Modification of Cellulose

The heterogeneous modification of cellulose is usually carried out in a medium where the polysaccharide is insoluble, though the reaction products could dissolve gradually into it [2]. Contrary to the homogeneous modifications, with these types of conditions, the supramolecular order and fibrillar architecture of the cellulose substrate largely determine the extent and rate of the chemical transformation. Thus, depending on the type of reaction, the medium (swelling or non-swelling), the degree of steric hindrance with the reagent, the sample morphology and reaction parameters, heterogeneous cellulose modifications can proceed within a wide spectrum of situations, from a surface-limited transformation to a in-depth or quasi-homogeneous bulk reaction [3].

The non-uniform character of the macromolecular ordering in native cellulose, due to the presence of the crystalline and amorphous regions, frequently leads to reactions that, depending on the conditions, can be limited to the latter regions or at least can proceed much faster in these disordered domains as compared with those of high order, as already mentioned. As a result, frequently the modification extent of cellulose in heterogeneous conditions can be significantly increased by lowering the supramolecular order and/or by loosening the interfibrillar bonding *via* an appropriate pretreatment. This pretreatment can either consist in the complete destruction of the supramolecular order by dissolution and subsequent reprecipitation of the sample in a more amorphous form (only suitable for laboratory-scale studies), or in cellulose activation using liquids of high swelling power, such as water, aqueous alkali or dimethyl sulfoxide (DMSO), which may also be employed as the reaction medium [3]. These liquids promote a loosening of the cellulose supramolecular structure, while usually preserving the original solid state of the sample [3].

This kind of cellulose modification has been progressively attracting the attention of researchers all over the world [14, 42], especially due to the possibility, under specific conditions, of limiting the functionalization to the surface layers of the fibers, changing

their surface features, whilst maintaining their ultrastructure and bulk properties, *i.e.*, their integrity and, consequently, their mechanical properties.

2.2.1. Controlled Heterogeneous Modification of Cellulose

Recently, increasing interest has been devoted to the controlled heterogeneous chemical modification of cellulose fibers, especially at their outermost layers, essentially aiming at reducing the polar contribution to their surface energy, and thus make them suitable as reinforcing elements in composites or as sources of highly hydrophobic materials [43].

As mentioned in the *Introduction*, regarding the former aspect, this kind of modification fulfills two fundamental requisites that help to overcome the drawbacks related to the naturally high polarity and hydrophilicity of cellulose fibers: (i) improve their interfacial adhesion with non-polar matrices and (ii) reduce their moisture uptake capacity [44]. Chemically modified cellulose fibers were first used to prepare composite materials with common polymer matrices, such as polyethylene and polypropylene [45-49]. Nonetheless, due to the already mentioned upsurge in environmental concerns in the last decades, composites exclusively made of biodegradable components have started to emerge [43, 47, 50-58]. These completely biodegradable composites, also called green composites, comprise either biocomposites containing vegetable fibers and biodegradable matrices, such as poly(lactic acid) (PLA) and polycaprolactone (PCL) [43, 50-58], or else the so-called co-continuous or self-reinforced composites, obtained by partial oxypropylation or other controlled modifications of cellulose-based fibers, which can lead to their partial thermoplasticization [7, 14, 43, 59-70].

On the other hand, nowadays, highly hydrophobic and superhydrophobic surfaces based on cellulose constitute hot-topics [71-77], whose high relevance in this doctoral research justifies that *Section 3* of this bibliographic review be devoted to this issue.

The controlled heterogeneous modification of cellulose can be attained following different approaches, for example by using (i) slightly- or non-swelling solvents, (ii) solid-gas reactions, including (iii) chemical vapor deposition, and also (iv) plasma induced grafting [14].

The literature of the last few decades is rich in publications dealing with the controlled heterogeneous chemical modification of cellulose following numerous

strategies, which in this bibliographic review will be divided into two main categories: (i) modification by single-phase approaches and (ii) modification by multi-phase approaches. The former strategy is here associated with the employment of monofunctional reagents, and thus the products obtained constitute by themselves the final cellulose derivatives. The latter strategy, consists of more elaborated approaches, involving either the use of polyfunctional reagents, containing at least two functional groups, which could act as bridges between cellulose and other compounds, or grafting and polymerization *onto* or *from* the surface of the fibers, thus permitting further tailoring of their surface properties.

2.2.1.1. Controlled Heterogeneous Modification by Single-Phase Approaches

Similarly to the case of the homogeneous reaction conditions, the most common and oldest approach within this type of heterogeneous modification is by far the esterification of the cellulose fibers with acids, acyl chlorides or anhydrides [7, 61, 73, 78-90]. Table 3 shows some of the reagents already employed within this strategy.

Accordingly, Jandura *et al.* [83] studied the modification of cellulose fibers, under controlled heterogeneous conditions in a pyridine/toluene sulfonyl chloride system, with both saturated and unsaturated fatty acids (FA), namely undecanoic and undecylenic acids and oleic and stearic acids, respectively (Table 3). These authors were able to prepare cellulose esters possessing different degrees of substitution, which retained their fibrous structure. More recently, and as already mentioned in the *Introduction*, the acylation of cellulose fibers with fatty acids was also carried out in our group [7], but using a wider range of FA, namely hexanoic, dodecanoic, octadecanoic and docosanoic acids (Table 3). Furthermore, this work involved a thorough study of the effect of some parameters, such as the reaction time and type of solvent, on the final properties of the fibers.

Table 3. Examples of monofunctional reagents commonly used to esterify the surface of cellulose fibers.

Name	Structure	Reference
Acetic acid	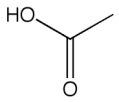	[86]
Acetic anhydride	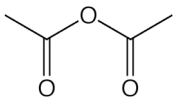	[78, 85, 86]
Alkenyl succinic anhydrides (ASA)	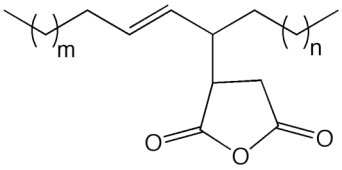 m + n = 10-12	[79]
Alkyl ketene dimers (AKD)	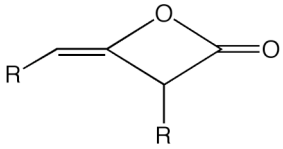 R = long aliphatic chains	[79]
Fatty acids or acid chlorides (C6-C22)	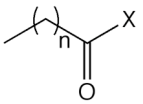 X = OH or Cl n = 4-20	[7, 61, 79, 81, 82]
Pentadecafluorooctanoyl chloride	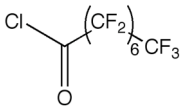	[73]
Trifluoroethoxyacetic acid	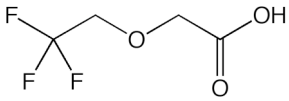	[81]
Trifluoroacetic anhydride (TFAA)	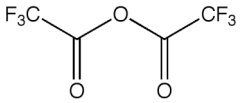	[86-88]

The heterogeneous acetylation of cellulose fibers using acetic anhydride (Table 3) was carried out by Frisoni *et al.* [85], who tested the effect of different amounts of sulfuric acid and time of reaction on the progress of the acetylation. The same authors studied the extent of biodegradation of the acetylated cellulose fibers as well, having verified that this aptitude decreased with increasing acetylation degree, which is understandable given the

lower accessibility of the degrading medium associated with the correspondingly lower surface hydrophilicity (fiber wettability).

Quillin *et al.* [79] treated cellulose fibers with alkyl ketene dimers (AKD), alkenyl succinic anhydrides (ASA), and stearic acid (Table 3), studying the effect of the different treatments on the surface energy of the fibers. In this way, they succeeded in decreasing the hydrophilicity of the fibers, though that behavior was partially attributed to the presence of unreacted species deposited on their surface, which could have been removed by an adequate extraction procedure subsequent to the treatments.

In another vein, Yuan *et al.* [86] reported the esterification of cellulose fibers with mixed TFAA/acetic acid or TFAA/acetic anhydride vapors (Table 3), which introduced acetyl and, to a lesser extent, trifluoroacetyl groups onto the fibers' surface, responsible for the hydrophobic character acquired by the fibers. Moreover, the authors claimed that this could be a promising procedure to produce water-repellent papers and fabrics.

Apart from the conventional esterification reactions, cellulose esters were also prepared by transesterification reactions [91, 92]. In this context, Antova *et al.* [92] prepared cellulose stearate with DS values up to 1.04, by transesterification of methylstearate with cellulose under microwave heating. In this study, the authors established the influence of different parameters on the extent of the cellulose modification, concluding that microwave heating was a promising method for synthesizing cellulose esters by transesterification under mild conditions and in the absence of solvents, thus providing several advantages in relation to the conventional methods.

2.2.1.2. Controlled Heterogeneous Modification by Multi-Phase Approaches

The controlled heterogeneous modification of cellulose fibers by multi-phase approaches has been essentially developed along the last decade by employing numerous types of polyfunctional reagents, including bifunctional anhydrides [84, 93, 94] or isocyanates [93, 95-98] and silane-coupling agents [71, 95, 98-108]. The latter strategy was also applied within the scope of this thesis.

The use of these kinds of reagents to modify cellulose fibers can, for example, pave the way to their application in composite materials, since it can promote the creation

of covalent bridges between the fibers and the matrix, which ensures the best mechanical properties for the composite.

Additionally, other approaches are included in this sort of heterogeneous modification, namely cellulose modification with chlorosilanes [109, 110], also employed in this thesis, or polymerization techniques such as grafting-from, either via free-radical initiation [73, 98, 111-122] or ring-opening polymerization [65, 123, 124], grafting by electrical discharges and irradiation techniques [125-130], and also by admicelle-based processes [90, 131-135]. These approaches enable the preparation of cellulose graft-copolymers possessing tailored surface properties. Apart from their possible application as reinforcing agents in composite materials [136], as well as for the preparations of co-continuous composites [65], the ensuing cellulose graft-copolymers can have other multiple applications, for instance in the production of antibacterial surfaces [122], temperature-responsive smart materials [137], ion-exchange materials [138], sorption agents for removal of heavy metals [139] and hydrophobic or superhydrophobic surfaces [109], the latter, as previously mentioned, being of particular interest to this thesis.

Within this type of cellulose modification, Gandini *et al.* [93] performed an interesting study which called upon the heterogeneous grafting of bifunctional molecules possessing either isocyanate or anhydride functions, namely 1,4-phenyl diisocyanate, 4,4'-methylenebis(phenyl isocyanate) and 1,2,4,5-benzenetetracarboxylic anhydride (pyromellitic anhydride, PA) (Figure 7, A to C), onto the surface of several cellulose substrates. The covalent binding of such reagents gave rise to the surface functionalization of the cellulose substrates, which retained an active function available for further exploitation. Indeed, the same authors tested the polycondensation of the PA-modified fibers with 1,4-butanediol and succeeded in preparing the corresponding fiber-bound polyester.

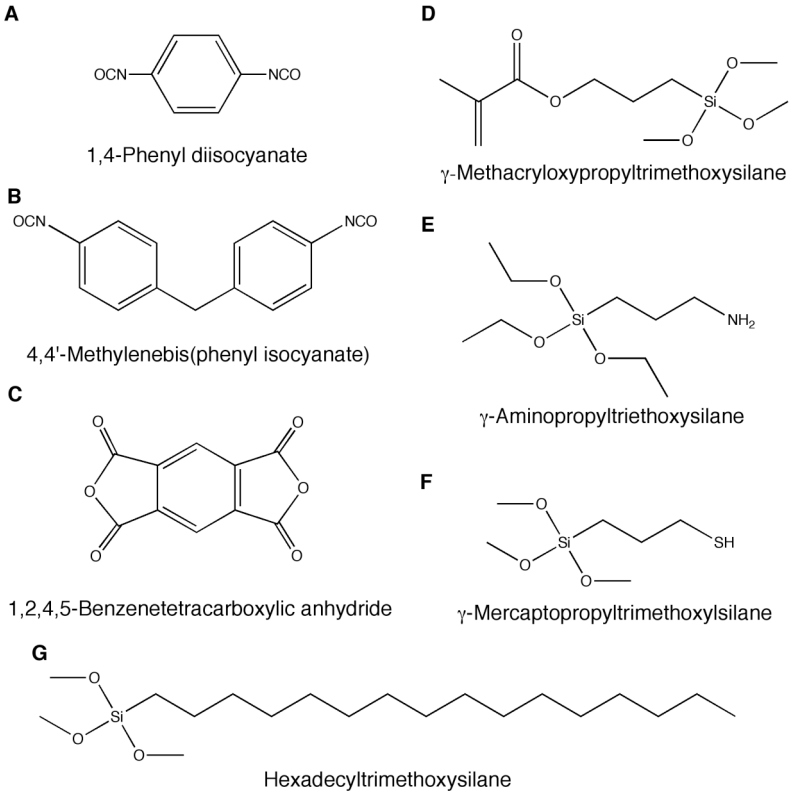

Figure 7. Polyfunctional reagents used to modify cellulose [93, 102].

The other kinds of polyfunctional reagents, namely silane-coupling agents, are compounds that can enable the formation of covalent bonds between organic and inorganic components, leading to the preparation of the so-called class-II organic-inorganic hybrid materials (Figure 8). In general, the relevant hybrid materials do not simply reflect the mere sum of the features of their precursors, but rather display broad synergy effects resulting from specific morphological interactions between the two phases at the micro- or nano-scale [140]. This class of materials are not only academic alternatives to more traditional counterparts, since instead, their original properties lead frequently to the development of innovative industrial applications, as in electronics, optics, medicine, sensors, smart coatings and polymer composites [140].

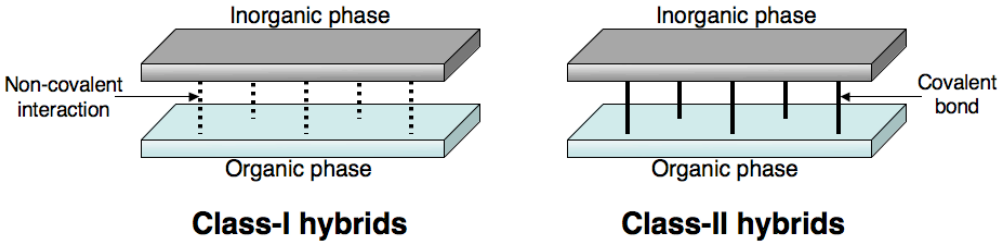

Figure 8. Schematic representation of class-I and class-II organic-inorganic hybrids.

The preparation of organic-inorganic hybrid materials combining cellulose with silicon compounds has been reported mainly within the last decade, and, although some were only class-I combinations [8, 141-147], *i.e.*, without covalent attachments between the organic and inorganic phases (Figure 8), several studies have already been published dealing with class-II hybrid materials [95, 98-105, 148].

In this context, Abdelmouleh *et al.* [102] employed four organofunctional silane-coupling agents, specifically γ-methacryloxypropyltrimethoxysilane (MPS), γ-aminopropyltriethoxysilane (APS), γ-mercaptopropyltrimethoxysilane and hexadecyltrimethoxysilane (HDS) (Figure 7, D to G), for the surface modification of cellulose fibers. These reagents were successfully appended onto the fibers' surface through both condensation reactions with the cellulose hydroxyl groups and self-condensation couplings between silanol groups, giving rise to significant changes of the surface properties, especially a strong decrease in its hydrophilic character. Furthermore, MPS-treated cellulose fibers were used to prepare co-continuous matrix-fiber composites, employing styrene or methylmethacrylate as monomers, whereas an epoxy formulation based on *bis*-phenol-A-diglycidylether was used to graft APS- and HDS-treated fibers.

The atom transfer radical polymerization of methyl acrylate from the surface of cellulose fibers, previously functionalized with tertiary bromoester groups by reaction with 2-bromoisobutyrylbromide, was reported by Carlmark and Malmström [115] (Figure 9). The ensuing polymer-grafted cellulose fibers presented a pronounced hydrophobic character.

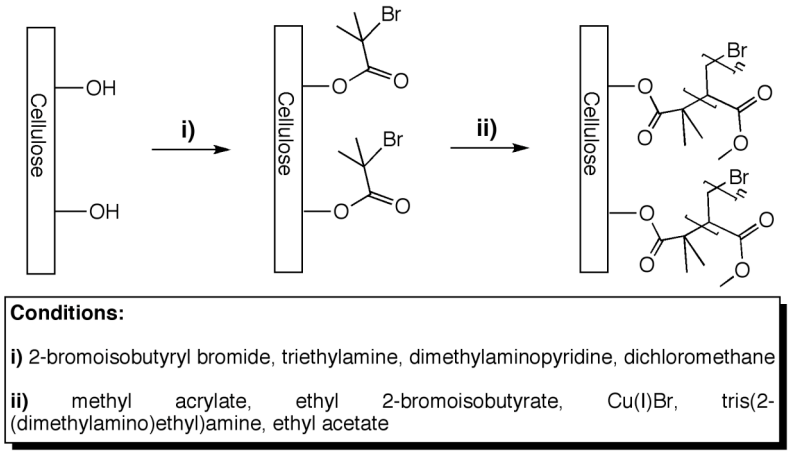

Figure 9. Grafting-from polymerization procedure adopted by Carlmark and Malmström [115].

Similarly, Lönnberg *et al.* [124] studied the ring-opening polymerization of ε-caprolactone (ε-CL) and L-lactide (LA) from cellulose fibers (Figure 10). Both unmodified fibers and those previously activated with xyloglucan-bis(methylol)-2-methylpropanamide and 2,2-bis(methylol)propionic acid, for the case of ε-CL and LA, respectively, were employed in this study. The purpose of the pretreatments was to introduce more available hydroxyl groups on the surface of the fibers, and thereby obtain a higher grafting efficiency. With these approaches, the authors succeeded in bind covalently PCL and poly-L-lactic acid (PLLA) to the surface of the cellulose fibers, and thus reduced their hydrophilicity.

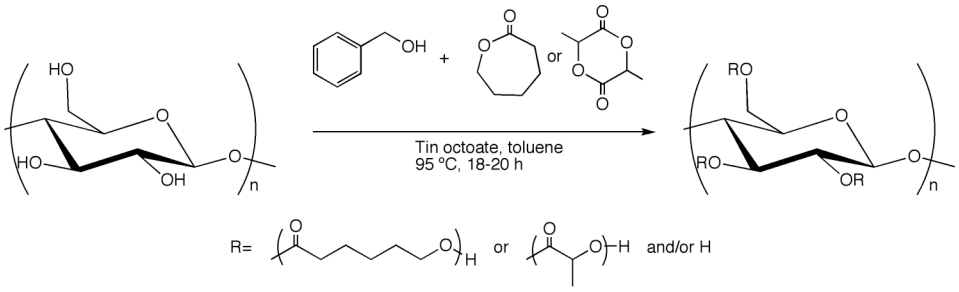

Figure 10. Ring-opening polymerization procedure of ε-CL or L-LA from unmodified cellulose fibers adopted by Lönnberg *et al.* [124].

3. Surface Free Energy and Hydrophobicity

The determination of the surface free energy (γ_s) of a solid is of great importance in applied materials science, and as it is impossible to measure directly this parameter with most materials, indirect approaches have been developed through the years [149]. The measurement of the contact angles of liquids onto a solid surface constitutes the simplest and the most frequently used method for the estimation of γ_s. The contact angle (θ) of a liquid drop on a solid surface is usually defined by the mechanical equilibrium of the drop under the action of three interfacial tensions, namely solid/vapor (γ_{sv}), solid/liquid (γ_{sl}) and liquid/vapor (γ_{lv}). It can be seen as a measure of the competing tendencies of the liquid drop onto the solid surface, determining whether the former spreads over the solid surface or recedes to minimize its own surface area [149]. For a given solid surface, the final shape of the drop depends on the relative magnitudes of the molecular forces that exist within the liquid (cohesive) and between liquid and solid (adhesive) [149].

Most often, the contact angle concept is illustrated with a small liquid droplet resting on a flat horizontal solid surface, as depicted in Figure 11 [149].

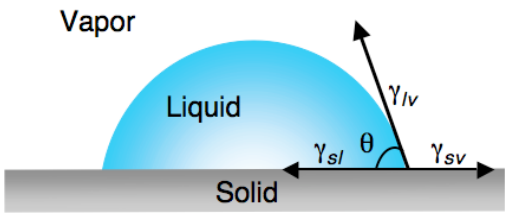

Figure 11. Schematic representation of the contact angle of a liquid drop resting on a flat solid surface.

By definition, γ_s is the work required to increase the surface area of a solid substance by unit area, being highly dependent on the type of interactions of the molecules making up the solid surface [149].

The determination of γ_s of solids from contact angles is based on an equilibrium relation proposed by Young at the beginning of the 19th century, thus known as Young's equation (although Young never postulated this equation), which describes the equilibrium of forces between the three surface tensions presented in Figure 11:

$$\gamma_{sv} - \gamma_{sl} = \gamma_{lv}.\cos\theta \quad \textbf{(Equation 1)}$$

Different methods, based on this equation, either graphical or numerical, are available in the literature for the determination of γ_s. None of these approaches is scientifically rigorous because the *Equation 1* contains two unknowns, *viz.* γ_{sv} and γ_{sl}, and therefore some reasonable but unverifiable assumptions must be introduced to solve the problem. The most often used method is by far that proposed by Owens-Wendt-Rable-Kaeble, often kwown as Owens-Wendt method, which considers γ_s as the sum of two contributions, namely the dispersive (γ^d_s) and polar (γ^p_s) components:

$$(1+\cos\theta).\gamma_l = 2.(\sqrt{\gamma_s^d.\gamma_l^d} + \sqrt{\gamma_s^p.\gamma_l^p}) \qquad (\textbf{Equation 2})$$

where γ_l stands for the surface tension of the liquid, and γ^d_l and γ^p_l for its respective dispersive and polar components, parameters that are available in the literature [149]. The assumptions here arise from considering that, on the one hand, these contributions are the only parameters intervening to define the solid-liquid interface and, on the other, from postulating that the polar interactions can be expressed as a geometric mean, which is strictly valid only for dispersive contributions. Notwithstanding these approximations, the method has proved a very useful tool for the determination of the surface energy of solids, of course by measuring the contact angle of droplets of at least two different liquids, but preferably several ones. The absolute values might not be strictly correct but comparisons, variations and tendencies can be obtained with a satisfactory degree of reliability. Given these considerations, it was decided to adopt Owens-Wendt method in the work carried out in this thesis.

The hydrophobicity of a solid surface is strongly related to the extent of the polar contribution to its surface energy for the obvious reason that water is among the most polar liquids. It follows that the lower the γ^p_s of a solid surface the higher will be the contact angle of a water droplet deposited onto it, or in other words water will not wet the solid, and conversely, spontaneous water spreading will occur on a solid surface displaying a high value of γ^p_s. As for non-polar liquids like alkanes, the behavior of one such drop on a solid surface will be highly dependent on γ^d_s, with low values favoring again high contact angles and hence lack of spreading and wetting, and *vice-versa* for solids possessing a high dispersive contribution. Different situations can therefore occur on a solid surface, including spontaneous wetting by all types of liquids (omniphilic surface), wetting limited to non-polar liquids (hydrophobic and lipophilic surface) and lack of spreading from different types of liquids (omniphobic surface). Among these situations the most interesting version

within the scope of this thesis is at least the intermediate one and in certain cases better still the latter feature of omniphobicity.

It has been conventionally proposed that a solid surface is defined as hydrophobic when the contact angle formed by a drop of water (θ_w) deposited onto it is higher than 90º and that this property becomes superhydrophobic when the angle exceeds 150º [150-154]. Additionally, a "completely superhydrophobic" surface should also exhibit a low sliding angle (α), which is the minimum tilt angle that makes the water drop roll off the surface, as illustrated in Figure 12 [150, 151, 153, 155].

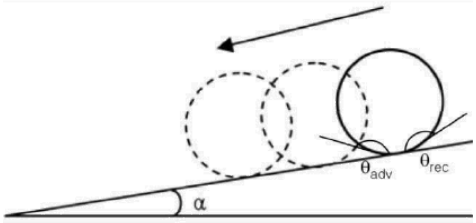

Figure 12. Schematic representation of the sliding angle α [156].

Nature provides several examples of superhydrophobic surfaces, with the lotus leaf being the most quoted example, with θ_w and α of about 160º and 2º, respectively [150]. The amazing ability of this plant, as well as other natural surfaces, to promote water repellency and self-cleaning by inducing water drops to roll off them carrying undesirable particles, *i.e.*, the so-called "lotus effect" [154, 157-159], has been inspiring numerous researchers engaged in preparing synthetic superhydrophobic analogues by mimicking them (biomimetics) [150, 152, 154, 158, 160-182]. Figure 13 is an illustration of the "lotus effect", where it is possible to observe (a) the high water-repellent character of a lotus leaf, *i.e.*, water droplets with very high contact angle rolling on its surface, and (b) the self-cleaning ability of a superhydrophobic biomimetic surface covered with dirt particles, *i.e.*, water drops rolling off the surface, while dragging them away [158, 174].

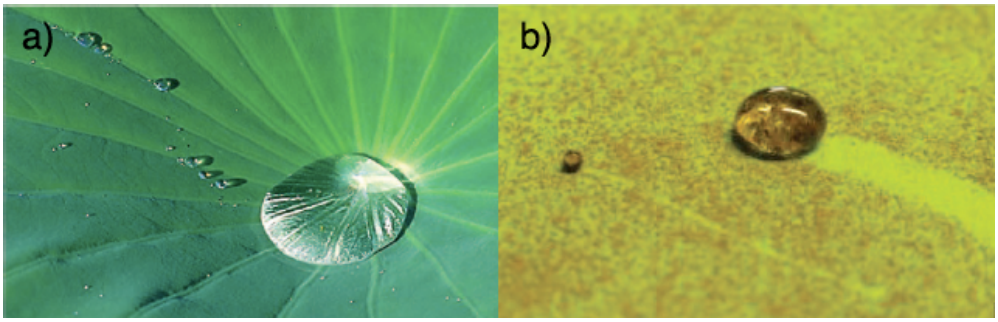

Figure 13. Schematic illustration of the "lotus effect" on (a) a lotus leaf and (b) a water-repellent biomimetic surface [158, 174].

Together with the concept of superhydrophobicity many other new concepts started to emerge, like superhydrophilicity, *i.e.*, a very high affinity towards water wetting ($\theta_w < 5^o$), superoleophobicity or superlipophobicity, concerning a very low affinity towards non-polar liquids, among others [161, 183-196]. Furthermore, many studies have been devoted to attain tunable and switchable surface wetting (*e.g.*, reversibility of the superhydrophobic condition to superhydrophilic, and *vice versa*) by thermochemical, photochemical or other processes [161, 192, 194, 197-203].

The water wetting of solid surfaces constitutes more and more a feature of major concern in materials science [160, 161, 163, 204]. The adhesion of water to a solid surface is ruled by both its chemical composition and its morphology/topography. In this sense, it can be easily rationalized that hydrophobicity can be achieved, on the one hand, by lowering the surface energy of the solid surface, as previously mentioned, more specifically its polar contribution, and/or, on the other, by creating adequate surface micro- and/or nano-morphologies on the solid surface, which hinder water spreading [151, 152].

3.1. Chemical Features Influencing Hydrophobicity

Conventionally, hydrophilic materials may be rendered hydrophobic by appropriate modifications involving either physical treatments or chemical reactions applied to the surface of the concerned substrate. Nonetheless, since only chemical modifications are relevant to the context of the present thesis, the physical treatments will not be reviewed.

In this sense, hydrophobic and superhydrophobic surfaces can be obtained by chemical reaction with compounds that can induce a substantial lowering of γ_s to those surfaces [202, 203, 205-213], such as aliphatic or fluorinated compounds.

Compounds containing methyl (-CH_3) and methylene (-CH_2-) functions at their surface are usually associated with γ_s values of about 20 and 30 mJ.m^{-2}, respectively, whereas those possessing trifluorinated methyl (-CF_3) and difluorinated methylene (-CF_2-) groups are frequently associated with γ_s values of about 6 and 18 mJ.m^{-2}, respectively [149].

The very low surface energies associated with fluorine-containing compounds is intimately related to the specific properties of this element. Atomic fluorine is one of the less polarizable elements, associating very high chemical reactivity and electronegativity. Fluorine atoms are known to bind tightly to carbon atoms in organic molecules (C-F bond energy is *ca.* 450 kJ.mol^{-1}) and modest fluorination of a given molecular structure leads to large changes in its physical and chemical properties [214]. Among the several new functionalities imparted by fluorine in fluoro-organic compounds, one of the most prominent is the enhanced hydrophobicity, and in the case of perfluorinated moieties also lipophobicity [149, 214], as discussed in *Chapter 3*.

In this sense, Jeong *et al.* [205] prepared transparent coating films with smooth surface on glass substrates by a sol-gel process using different alkoxide solutions containing variable molar ratios of a perfluoroalkylsilane and tetraethoxysilane (TEOS). With this procedure, the authors obtained hydrophobic glass surfaces with θ_w as high as 118º.

Anodically oxidized aluminum surfaces, highly wettable by water as such, were treated with *1H,1H,2H,2H*-perfluorooctyltrichlorosilane by Shibuichi and co-workers [209]. After the treatment, the aluminum surfaces became water super repellent, showing θ_w up to160º.

Although, synthetic materials have been the most explored in the field of hydrophobization and superhydrophobization of surfaces, an increasing interest has emerged on the use of natural raw materials to prepare hydrophobic or superhydrophobic surfaces, including polysaccharides [215, 216].

For example, Carvalho *et al.* [213] treated thermoplastic starch (TPS) films with several non-perfluorinated reagents, specifically phenyl isocyanate, a phenol blocked polyisocyanate of trimethylol propane and toluene diisocyanate, a styrene-*co*-glycidyl methacrylate co-polymer and stearoyl chloride. In all instances, the authors verified that the γ^p_s of the TPS films was strongly decreased, indicating that the surfaces had become more hydrophobic, with θ_w in the range of 90-107º.

Several studies related to the hydrophobization and superhydrophobization of cellulose by chemical means were also carried out, as discussed in the *section 3.3*.

3.2. Surface Morphology Influencing Hydrophobicity

Regarding the morphological aspects, it is known that a hydrophobic surface possessing a flat topography favors a better adhesion of a water drop, *i.e.*, a lower water repellency than a hydrophobic surface containing micro- or nano-structured topographies (Figure 14). Furthermore, the presence of a hierarchical topography, *i.e.*, roughness at both a micro- and nano-scale, leads to an even lower water adhesion (high θ_w) and, consequently, a higher water repellent behavior (Figure 14) [161, 183, 184, 204, 217-225].

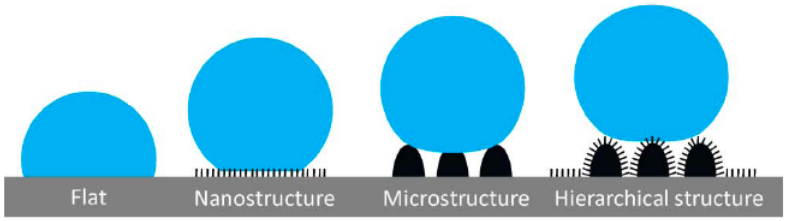

Figure 14. Wettability of four hydrophobic surfaces with different morphologies [156].

Thus, a superhydrophobic surface usually results from the synergetic effect between its chemistry and its morphology/topography. Therefore, this kind of surface can be prepared mainly by two approaches, *viz.* (i) by creating a rough topography on a hydrophobic surface or (ii) by modifying a rough surface with functions capable to induce a low γ_s, such as those mentioned above [149, 151, 152, 154].

Although rough surfaces are typically attained by applying appropriate physical treatments, such as lithography and etching [156], some chemical modifications can also ensure the creation of micro- and nano-asperities, which enhance the air trapping capability of that surface, and at the same time changing its chemistry [226, 227]. Chlorosilanes, for instance, are a class of reagents extensively applied in this context [110, 228]. Their molecules readily couple with the OH-bearing substrates through condensation reactions [110, 228], with the additional advantage of their possible exploitation in gas-solid systems, given the volatility of some of their homologous [110,

229]. Furthermore, chlorosilanes promptly react with water to give self-condensation hydrolysis products, leading to the construction of micro- and nano-morphologies. Specifically, organic chlorosilanes are commonly used as coatings for silicon [160, 224] and glass surfaces [206, 207], as well as in the production of silicone polymers (polysiloxanes) [110, 228-230].

Table 4 gives some examples of studies that produced the hydrophobization and superhydrophobization of the surface of various solid materials, both synthetic and natural, by changing the topography of their surfaces through chemical reactions, which not always implied covalent attachments.

Table 4. Examples of different substrates hydrophobized by chemical reactions that changed their surface topography and thus increased the corresponding θ_w.

Substrate	Strategy	θ_w (º)	Reference
Glass	Perfluoroalkyltrichlorosilanes $CF_3(CF_2)_n(CH_2)_2SiCl_3$ (n=0, 3 and 7)	108-123	[206, 207]
	Amino- and epoxy-functionalized silicas and 2-perfluorohexylethyl-4-formylthiobenzoate	113-154	[208]
Copper (oxidized)	*n*-Alkanoic acids (C3-C18)	90-160	[210]
Silicon substrates	Poly(*N*-isopropylacrylamide)	93-149[a]	[202]
Poly(tetrafluoroethylene)	Carboxyl-terminated poly(styrene-*co*-2,3,4,5,6-pentafluorostyrene) and poly(2-vinylpyridine)	118-160[b]	[203]
PLA	Silica particles possessing vinyl functions	150	[211]
Chitosan	*tert*-Butyldimethylsilyl chloride	104-153	[212]

[a]Temperature dependent (T=40 ºC)
[b]Solvent-treatment dependent (toluene-treatment)

For example, Amigoni and co-workers [208] prepared organic-inorganic hybrid glass surfaces by a covalent layer-by-layer (LbL) assembly made of layers of amino-

functionalized silica nanoparticles of 300 nm diameter (Figure 15, i) and smaller epoxy-functionalized silica nanoparticles of 20 nm diameter (Figure 15, ii), which were alternated (Figure 15, iii). Subsequent to the LbL treatment, which ended with the deposition of a layer of the former type of silica nanoparticles, the ensuing surfaces were grafted with 2-perfluorohexylethyl-4-formylthiobenzoate, creating a perfluorinated monomolecular layer *via* the formation of an imine function (Figure 15, iv). With this multi-step treatment, superhydrophobic glass surfaces, with θ_w as high as 154º, were obtained due to the combination of the hierarchical topography ensured by the silica nanoparticles and the decrease in the γ_s promoted by the modification with the perfluorinated reagent.

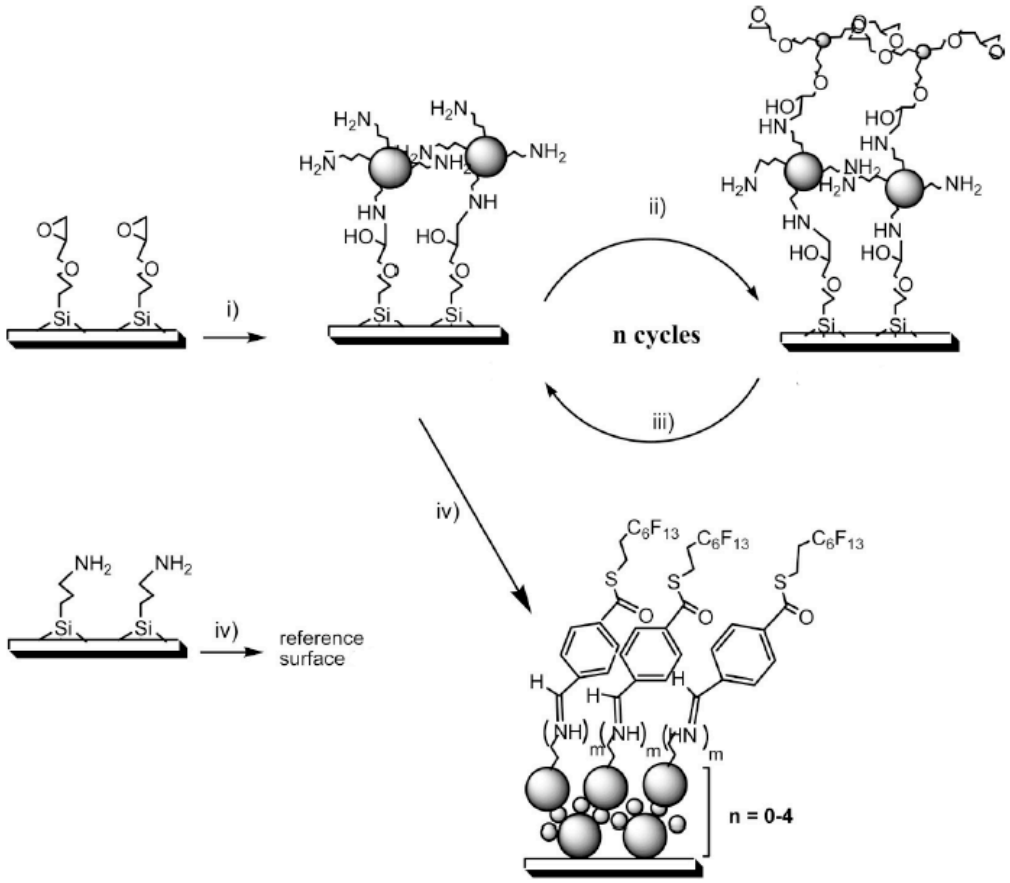

Figure 15. Multi-step procedure adopted by Amigoni *et al.* to prepare superhydrophobic glass surfaces [208].

Another approach was developed by Song et al. [212], who synthesized a silylated chitosan derivative, namely 3,6-*O*-di-tertbutyldimethylsilyl chitosan, and subsequently prepared highly water-repellent smooth and rough films. The rough films were obtained by using a phase-separation method that gave rise to a topography characterized by a three-

level hierarchical roughness organization, as can be observed in the scanning electron microscopy (SEM) and atomic force microscopy (AFM) images in Figure 16 (B to E). The θ_w values clearly showed the strong enhancement in hydrophobicity related with this chemical modification and at the same time the important additional role of surface roughness. Thus, the latter aspect was associated with an increase in θ_w from 104º for a smooth surface to 145º for its rough counterpart (Figure 16, A and B).

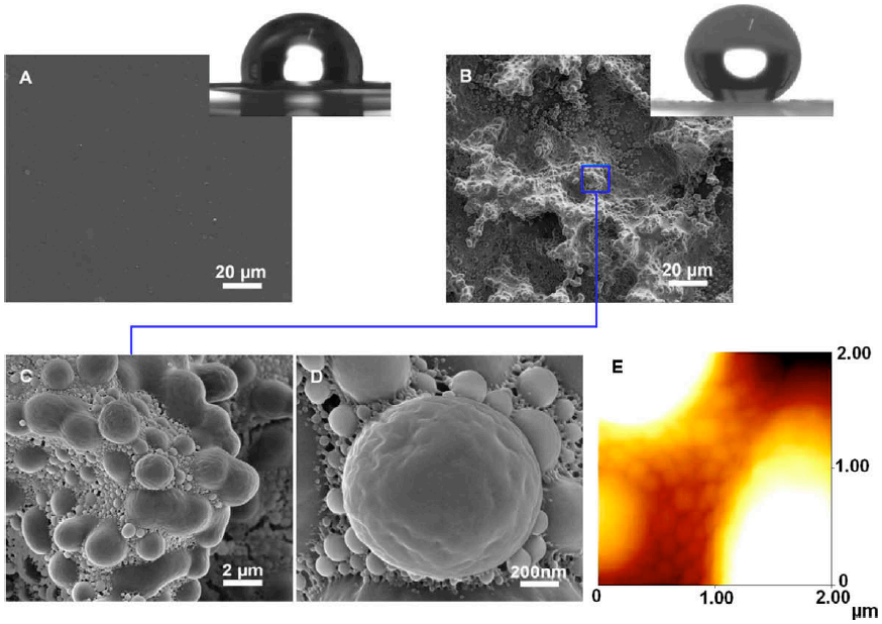

Figure 16. SEM (A to D) and AFM (E) images of the smooth (A) and rough (B to E) chitosan films prepared by Song *et al.* [212].

3.3. Cellulose-Based Hydrophobic and Superhydrophobic Materials

The preparation of highly hydrophobic cellulose-based materials is in part a consequence of the upsurge in activities associated with renewable resources. Although this topic has stimulated an impressive number of studies in the last decades [7, 71, 76, 77, 82, 86, 87, 89-91, 102, 105-108, 127, 128, 141, 142, 231-248], and is still hot, the necessity to confer hydrophobic characteristics to such a hydrophilic biopolymer as cellulose does not constitute necessarily an absolute novelty. In fact, the hydrophobization of cellulose fibers, or at least an effort to turn them less hydrophilic, has always been part of the history of papermaking, particularly in what concerns the sizing operation [249].

Cellulose-based hydrophobic materials can find potential applications in such important areas as textile and packaging [2], where they can play the role of a barrier to water and moisture, a feat, thus far, mainly performed by synthetic polymers and their derivatives. Additionally, the self-cleaning performance in superhydrophobic cellulose-based materials can also constitute a most valuable property, particularly in the textile domain.

Similarly to what was described above, the hydrophobization or superhydrophobization of cellulose may be carried out by applying suitable modifications, either by physical treatments or chemical reactions. However, once again, only the chemical treatments will be considered here.

3.3.1. Hydrophobization and Superhydrophobization of Cellulose by Chemical Treatments

The first attempts to turn cellulose fibers less hydrophilic were related with the sizing process in the papermaking sector, as mentioned above [249]. Sizing is generally conducted at the wet-end section of the papermaking process in order to reduce the paper tendency to absorb liquids, *e.g.*, to ensure the drying of an ink without smudging or excessive in-depth penetration, or to retain the mechanical strength of cardboard in a dump atmosphere [249]. The most common sizing agents used in papermaking are ASA, AKD and rosin [249-251]. The development of new sizing methods is witnessing renewed attention [75, 252, 253], not only within the traditional area of papermaking, but more broadly within the context of cellulose hydrophobization.

Other studies on the hydrophobization of cellulose started in the late ‘70s with the elaboration of cellulose esters, of both alkyl and aryl carboxylic acids, for enzyme immobilization tests [254-256]. In the last few decades, long chain cellulose esters have still been prepared by grafting FA and their derivatives onto cellulose, as already discussed, either by surface or bulk reactions, employing various methods, or else by transesterification reaction with triglycerides from several plant oils [7, 82, 89-91, 243-245]. These cellulose derivatives, which were elaborated with different substrates and purposes, showed a lower hydrophilic character, with θ_w exceeding 90º in some intances.

Apart from esterification, various other approaches have been developed to confer water repellent properties to cellulose, such as the modification with (i) perfluorinated reagents [86, 87], (ii) silane-coupling agents [71, 98, 99, 102, 105-108], (iii) natural products like terpenes [246], among others [247, 248].

Table 5 summarizes some approaches employed in the chemical hydrophobization of cellulose, as well as the maximum θ_w achieved in each study.

Table 5. Examples of approaches used for the chemical hydrophobization of cellulose and the maximum θ_w achieved in each one.

Modification type	Reagent	Maximum θ_w (º)	Reference
Fatty acids (FA) and derivatives	C6-22 chain length FA	93	[7]
	C12-C18 chain length FA	109	[245]
Perfluorinated reagents	Trifluoroacetic anhydride	98	[86]
	Pentadecafluorooctanoyl chloride (+ glycidyl methacrylate)	154	[73]
Silane-coupling agents	Hexadecyltrimethoxysilane	118	[102]
	3,3,3-Trifluoropropyltrimethoxysilane and *1H,1H,2H,2H*-perfluorooctyltrimethoxysilane	129	[107]
	1H,1H,2H,2H-perfluorooctyl triethoxysilane	155	[71]
Terpenes	Myrcene and Limonene	107	[246]
Other	Olygoether chains	113	[247]
	PCL	95	[248]

Nyström *et al.* [73] prepared highly hydrophobic cellulose substrates by their surface modification with pentadecafluorooctanoyl chloride and superhydrophobic cellulose surfaces with micro-nano-binary surface structure by performing a surface-confined grafting of glycidyl methacrylate from the cellulose substrates, using a branched

"graft-on-graft" architecture, prior to their modification with the perfluorinated acyl chloride. The ensuing superhydrophobic cellulose surfaces attained θ_w as high as 154º.

Cotton fabrics were treated with *1H,1H,2H,2H*-perfluorooctyl triethoxysilane in a study by Erasmus and Barkhuysen [71]. The perfluorinated moieties appended onto the surface of the cellulose substrates produced a strong hydrophobic effect, as revealed by the high θ_w, which exceeded 150º under specific experimental conditions.

Terpenes, *viz.* myrcene and limonene, *i.e.*, naturally available and cheap molecules, were also employed in the surface modification of cellulose fibers by means of a cold plasma treatment [246]. Both compounds conferred a hydrophobic character to the fibers, with θ_w as high as 107º, consequence of the large decrease in the γ^p_s, which was practically zero after the treatment.

4. Aims of the Work

As mentioned in the *Introduction*, due to the environmental concerns associated with the production and use of fossil-based products, nowadays researchers all over the world are encouraged to find alternatives. Thus, the exploitation of raw materials from natural renewable resources for the development of novel products is becoming a recurrent activity.

Accordingly, in the present thesis, *cellulose*, the most abundant natural polymer on earth, was used as raw material with the following main objectives:

(i) Develop new approaches for the controlled heterogeneous chemical modification of cellulose fibers with different reagents;

(ii) Evaluate the impact of the chemical modifications on the physicochemical properties of the cellulose fibers in terms of their surface and bulk features;

(iii) Prepare novel materials based on a natural renewable resource.

In this sense, three novel approaches for the controlled heterogeneous modification of cellulose fibers were developed, specifically:

(a) esterification with perfluorinated reagents, namely trifluoroacetic anhydride (TFAA), 2,3,4,5,6-pentafluorobenzoyl chloride (PFBz) and 3,3,3-trifluoropropanoyl chloride (TFP);

(b) preparation of class-II organic-inorganic cellulose hybrids by a multi-phase approach comprising the modification of the cellulose fibers with (3-isocyanatepropyl)triethoxysilane (ICPTEOS) and a subsequent acid hydrolysis treatment, either alone, or in the presence of other siloxanes, namely tetraethoxysilane (TEOS) and *1H,1H,2H,2H*-perfluorodecyltriethoxysilane (PFDTEOS);

(c) modification with a chlorosilane, *viz.* trichloromethylsilane (TCMS), *via* a gas-solid reaction.

The following chapter, *Chapter 2*, describes the experimental conditions used to achieve these objectives, and *Chapter 3* provides the obtained results, their discussion and some conclusions, arranged into three main sections that correspond to the three strategies enumerated above.

Chapter 2

Experimental

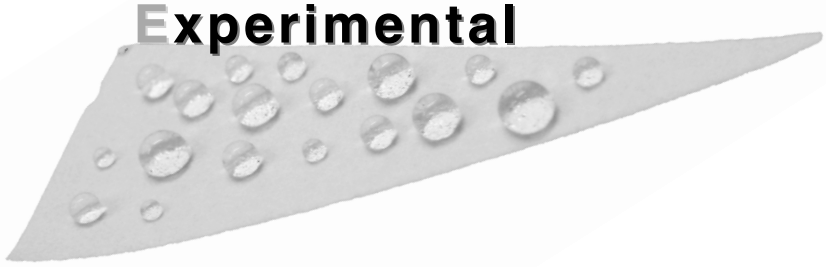

Chapter 2 – Experimental

This chapter describes the cellulose substrates that were employed in the studies presented in *Chapter 3*, the methods applied for their chemical modification, as well as the analytical techniques used to evaluate the physicochemical properties of the ensuing cellulose derivatives.

1. Materials and Reagents

1.1. Materials

The cellulose substrates used here came from three distinct origins, namely, vegetable fibers in the form of i) ECF (Elemental Chlorine Free) *Eucalyptus globulus* (DEDED) industrial bleached kraft pulp and ii) Schleicher & Schuell Microscience and Whatman pure cellulose filter papers, and iii) bacterial cellulose produced by *Gluconacetobacter xylinus* in the form of a wet (about 95% humidity) three-dimensional network of ribbon-like nanofibril structures (50-100 nm width), which was freeze-dried prior to use.

Before the modification reactions, all the vegetable cellulose samples were dried in a vacuum oven at 60 ºC, in the presence of phosphorus pentoxide, during about 24 h, and subsequently kept in a desiccator.

1.2. Solvents and reagents

All the solvents employed were analytically pure or purified by distillation. All other reagents were used as received.

Toluene, dichloromethane and acetone were purchased from Fisher Scientific, being the former dried over sodium wire. Hydrochloric acid (HCl) was supplied by Riedel-de Haën. Ethanol, sodium hydroxide (NaOH), trifluoroacetic anhydride (TFAA), 2,3,4,5,6-pentafluorobenzoyl chloride (PFBz), (3-isocyanatepropyl)triethoxysilane (ICPTEOS), tetraethoxysilane (TEOS), anhydrous *N,N*-dimethylformamide (DMF), dibutyltin dilaurate (DBTL) and trichloromethylsilane (TCMS) were supplied by Sigma-Aldrich. 3,3,3-

trifluoropropionic acid and *1H,1H,2H,2H*-perfluorodecyltriethoxysilane (PFDTEOS) were purchased from Apollo Scientific Ltd. and Fluorochem, respectively. Thionyl chloride and pyridine were supplied by Fluka, being the latter purified and dried by distillation over sodium hydroxide pellets.

2. Methodology

2.1. Preparation of Perfluorinated Cellulose Derivatives

Vegetable cellulose fibers were modified with three perfluorinated reagents, *viz.* TFAA, PFBz and 3,3,3-trifluoropropanoyl chloride (TFP), the latter being obtained from its acid counterpart. Moreover, PFBz was also used to modify bacterial cellulose fibers, in order to evaluate the influence of the cellulose morphology, according to the different origin, on the properties of the final products.

The heterogeneous esterification reactions of the fibers with these three compounds were carried out following the same procedure, which is discussed below, only varying reaction time and temperature.

Additionally, the hydrolytic stability of the perfluorinated samples was assessed following the general procedure detailed below.

2.1.1. Preparation of 3,3,3-Trifluoropropanoyl Chloride

3,3,3-Trifluoropropanoyl chloride (TFP) was prepared by the reaction of the 3,3,3-trifluoropropionic acid with thionyl chloride. Thus, 3,3,3-trifluoropropionic acid was placed in a round-bottom flask and then 1.1 equiv. of thionyl chloride was added dropwise under magnetic stirring. The mixture was subsequently refluxed at 100 °C for 3 h. The condenser was connected to a washing bottle filled with a concentrated aqueous sodium hydroxide solution, through a glass tube packed with activated silica gel. At the end of the reaction, the excess of thionyl chloride was removed by vacuum evaporation.

2.1.2. Controlled Heterogeneous Esterification of the Cellulose Fibers with Perfluorinated Reagents

A quantity of 1 equiv. (relative to the total cellulose OH functions) of the perfluorinated reagent, *viz.* TFAA, PFBz or TFP, was placed in a round-bottom flask, to which dry toluene (about 50 mL/g of cellulose), pyridine (1 equiv.), and finally cellulose fibers were added in a nitrogen atmosphere. The esterification reactions were conducted under magnetic stirring at different temperatures and times, which are listed in Table 6 for each perfluorinating reagent. The use of variable reaction times and temperatures was intended for establishing the effect of these reaction parameters on the extent of esterification and hence on the properties of the modified fibers.

Table 6. Reaction conditions (time and temperature) used for each perfluorinated reagent employed in the heterogeneous modification of the cellulose fibers.

	Reaction conditions	
Perfluorinated reagent	**Temperature / ºC**	**Time / h**
TFAA	RT[a]	1
	50	5
	80	20
PFBz	RT[a]	1
	50	5[b]
	65[b]	20
	80	
TFP	RT[a]	2
	50	15
	65	
	80	
	100	

[a]RT – room temperature
[b]Conditions applied to modify the bacterial cellulose fibers.

At the end of the reactions, the esterified fibers were filtered and sequentially washed with dichloromethane, acetone and ethanol, and again with acetone and dichloromethane, before being submitted to a Soxhlet extraction with dichloromethane for 12 h before drying them in an oven at 60 ºC for 24 h.

2.1.3. Evaluation of the Hydrolytic Stability of the Perfluorinated Cellulose Fibers

Aliquots of *ca.* 50 mg of the modified fibers were placed in an Erlenmeyer flask containing 20 mL of distilled water, and the ensuing suspension stirred at room temperature (about 20 ºC) for different times, depending on the perfluorinated derivative (Table 7). These experiments were also carried out without stirring with all the perfluorinated derivatives (Table 7). Regarding the pentafluorobenzoylated derivatives, both modified pulp fibers and filter paper were used for comparative reasons.

Table 7. Hydrolytic conditions tested for each perfluorinated cellulose sample.

Sample	Hydrolytic conditions			
	pH	Stirring	Temperature (ºC)	Time
TFAA	7	Yes	RT	17 h
(1 h 50 ºC)[a]	7	No	RT	1-7 days
	4	Yes	RT	5 h
PFBz	7	Yes	RT	1-7 h
(5 h 65 ºC)[a]	7	No	RT	1-30 days
	9	Yes	RT	5 h
	7	Yes	RT	1-96 h
TFP	7	No	RT	1-8 days
(2 h 80 ºC)[a]	9	Yes	RT	2-96 h
	12	Yes	RT	2-96 h

[a]Time and temperature conditions used to esterify the cellulose sample.

In the case of PFBz- and TFP-derivatives, alkaline conditions were tested as well, namely pH 9 for both derivatives, and also pH 12 for TFP-modified samples (Table 7). Additionally, for PFBz-modified cellulose fibers, acidic conditions were applied using a pH 4 water medium (Table 7).

The progress of the hydrolysis was followed by Fourier-transform infrared – attenuated total reflectance (FTIR-ATR) spectroscopy, and for the PFBz- and TFP-derivatives also by water contact angle measurements.

2.1.3.1. Hydrolysis Under Controlled Relative Humidity

Hydrolysis experiments were also carried out under controlled relative humidity (RH) with the TFAA cellulose derivatives. For that, the modified cellulose fibers were placed in a closed container (Figure 17) that was maintained at constant RH through the use of appropriate saturated salt aqueous solutions ($CaCl_2$ and $NaHSO_4$ for 30 and 52% RH, respectively) or pure distilled water (100% RH), and left for 1-17 days at 25 ºC.

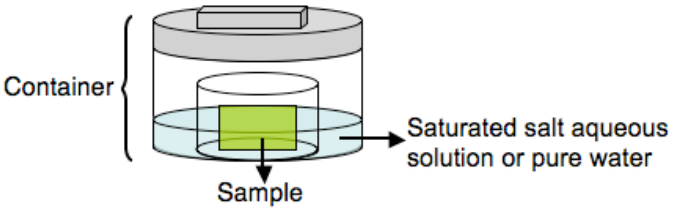

Figure 17. Setup used to perform the hydrolysis studies under controlled relative humidity conditions.

The progress of the hydrolysis was followed by FTIR-ATR spectroscopy and water contact angle measurements.

2.2. Preparation of Class-II Organic-Inorganic Hybrid Cellulose Derivatives

The preparation of class-II organic-inorganic hybrid cellulose derivatives was carried out following a two-step procedure. In the first stage, the cellulose fibers were modified with ICPTEOS under heterogeneous conditions, and subsequently the ensuing modified fibers submitted to acid hydrolysis treatments, which in some cases were performed in the presence of other silicon-containing reagents, namely TEOS and PFDTEOS.

2.2.1. Controlled Heterogeneous Modification of Cellulose with (3-Isocyanatepropyl)triethoxysilane

For the modification of the cellulose fibers with ICPTEOS, 0.4, 0.6 or 1 equiv. (relative to the total cellulose OH functions) of this reagent were placed in a round-bottom flask, to which anhydrous DMF (*ca.* 25 mL/g of cellulose), DBTL (0.05 equiv.) and the dried cellulose fibers were added while the system was kept under a nitrogen atmosphere.

The reactions were conducted under magnetic stirring at 60 ºC, for 5 h, when 0.4 or 0.6 equiv. of ICPTEOS were used, or for 24 h, with 1 equiv. of ICPTEOS. The latter reaction gave rise to a gel, which was dispersed in 1.5 L of acetone with continuous stirring for 30 min, before leaving the ensuing suspension to rest overnight in order to enable the modified fibers to sediment. After the subsequent filtration, the fibers were sequentially washed with acetone and ethanol, and again with acetone, and then dried in an oven at 40 ºC for 24 h.

2.2.2. Acid Hydrolysis Treatments

The modified cellulose fibers with 0.4, 0.6 and 1 equiv. of ICPTEOS were suspended in a 1/3.2/0.13 (v/v/v) water/etanol/HCl mixture (*ca.* 70 mL/g of cellulose), in a round-bottom flask and stirred for 24 h at room temperature.

Two other samples of each group of modified cellulose fibers were submitted to a similar treatment, but in the presence of TEOS (840 μL) or PFDTEOS (840 μL).

2.3. Vapor-Phase Modification of Cellulose with Chlorosilanes

A simple system was developed for the vapor-phase silanization of cellulose fibers, in the form of filter paper, with TCMS, as represented in Figure 18.

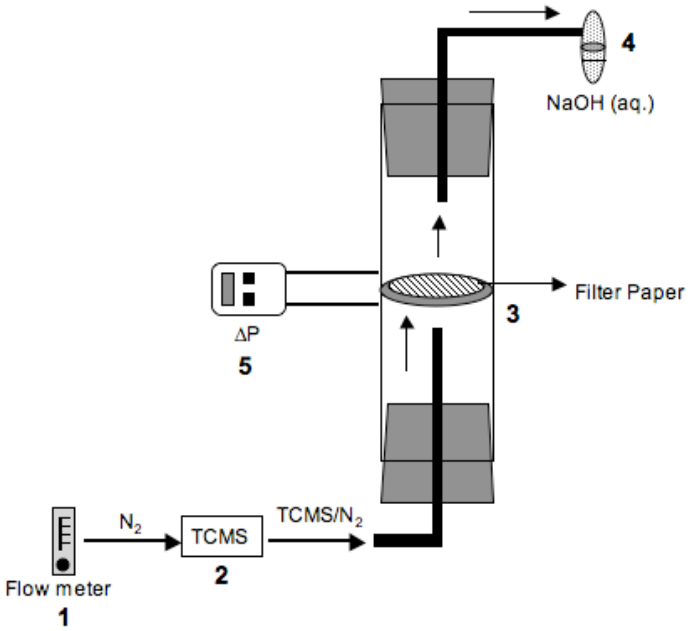

Figure 18. Schematic representation of the system used for the gas-solid reaction of cellulose with TCMS.

2.3.1. Controlled Heterogeneous Modification of Cellulose with Vapor-Phase Trichloromethylsilane

For the controlled heterogeneous modification of cellulose with TCMS in the vapor-phase system, both distilled water pre-humidified or ‘‘dry” filter papers were placed inside the reactor shown in Figure 18 onto the gas-tight holder **3**.

The humidification step consisted in depositing a drop of water (*ca.* 20 μL) on the substrate and allowing it to spread and penetrate by capillarity into the paper, whereas the term ‘‘dry” is to be understood here as paper in equilibrium with the atmospheric moisture at room temperature.

The liquid TCMS was kept in a flat-bottom flask (**2**) through which was passed the nitrogen stream that served as the carrier gas (controlled with flow meter **1**) (Figure 18). The reaction was conducted at room temperature (*ca.* 20 ºC) by streaming the N_2/TCMS mixture (0.1-0.5 L/min) through the filter paper for a given period of time (0.5-30 min).

The HCl formed as the by-product was removed by bubbling the gaseous waste through an outlet trap **4** containing a NaOH aqueous solution (Figure 18).

Although nitrogen was used here as the carrier gas, tests with air were also performed, showing no significant differences.

At the end of the reaction, the modified cellulose samples were washed with ethanol, before being submitted to a Soxhlet extraction also with ethanol for 7 h, and air-dried overnight in the laboratory hood.

3. Equipments and General Procedures

All the cellulose derivatives prepared were thoroughly characterized by means of numerous techniques, comprising both bulk and surface analyses, which are described below.

3.1. Bulk Characterization Techniques

3.1.1. Elemental Analysis and Determination of the Degree of Substitution

The elemental analysis (EA) of all the cellulose derivatives was performed at the CNRS "Service Central d'Analyze" in Vernaison - France, and each elemental content was obtained in duplicate.

In the case of the perfluorinated cellulose derivatives, their fluorine content (%F) as determined by this method, was used to determine their degree of substitution (DS), *i.e.*, the number of perfluorinated groups per cellulose monosaccharide unit, using the following equation:

$$DS = \frac{M_W(\text{anhydroglucose unit}).(\%F)}{n.100.M_W(F) - [(M_W(\text{perfluorinated moiety}) - M_W(H)).(\%F)]} \quad (\textbf{Equation 3})$$

where *n* stands for the number of fluorine atoms per perfluorinated moiety. As the perfluorinated moieties are CF_3CO and CF_3CH_2CO for the TFAA- and TFP-derivatives, *n* is equal to 3 in these cases. For the PFBz-derivatives, as the perfluorinated moiety is C_6F_5CO, *n* is equal to 5.

3.1.2. Solid-State Cross-Polarization Magic-Angle Spinning Nuclear Magnetic Resonance Spectroscopy

Solid-state ^{29}Si cross-polarization magic–angle spinning nuclear magnetic resonance (^{29}Si CP-MAS NMR) spectra were recorded on a *Bruker Avance 400* spectrometer.

The samples were packed into a zirconia rotor sealed with Kel-F caps and spun at 5 kHz.

The acquisition parameters were 4 μs 90º-pulse width, 37 ms contact time and 5 s dead-time delay.

3.1.3. X-Ray Diffraction Spectroscopy

The X-ray diffraction (XRD) measurements were performed in a *Phillips X'pert MPD* diffractometer using Cu Kα radiation. For these analyses the cellulose fibers, both unmodified and modified, were pressed into small pellets using a laboratory press.

3.1.4. Thermogravimetric Analysis

The thermogravimetric assays were carried out with a *Shimadzu TGA 50* analyzer equipped with a platinum cell. Samples were heated at a constant rate of 10 °C/min from room temperature (*ca.* 20 °C) to 800 °C, under a nitrogen flow of 20 mL/min, except in the study related to the preparation of the cellulose hybrid materials, where samples were heated in air from room temperature to 900 ºC.

3.2. Surface Characterization Techniques

Several techniques were employed to inspect the surface of the modified fibers. It is worth noting that each surface characterization technique analyzes the surface of the materials down to a certain depth, as shown in Figure 19.

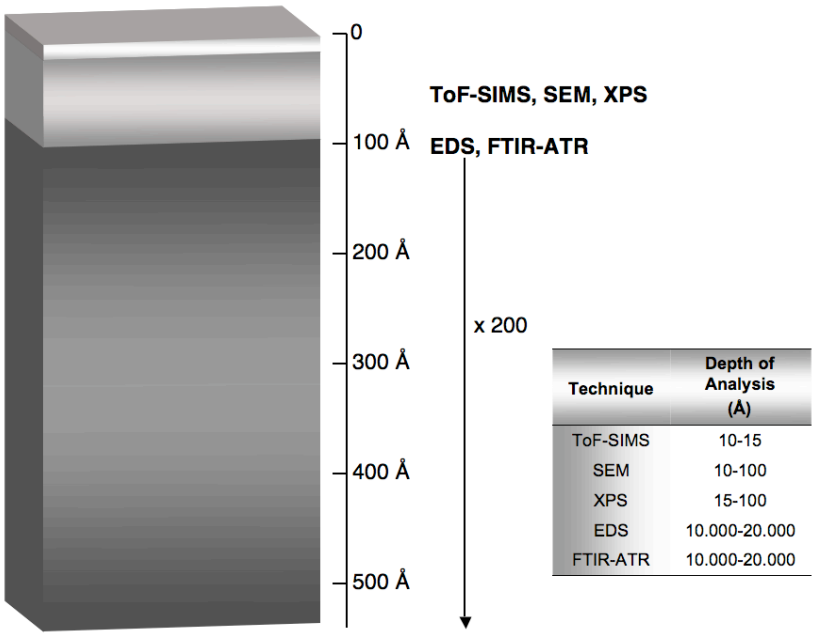

Technique	Depth of Analysis (Å)
ToF-SIMS	10-15
SEM	10-100
XPS	15-100
EDS	10.000-20.000
FTIR-ATR	10.000-20.000

Figure 19. Measurement depth of some major surface characterization techniques (adapted from [257]).

3.2.1. Fourier Transform Infrared – Attenuated Total Reflectance Spectroscopy

FTIR-ATR spectra of the unmodified and perfluorinated cellulose samples were recorded with a Brücker IFS FTIR spectrometer equipped with a single horizontal Golden Gate ATR cell. The acquisition conditions were 128 scans and 8 cm^{-1} resolution.

In the study dealing with the preparation of the cellulose hybrid materials, the FTIR-ATR spectra were obtained with 4 cm^{-1} resolution after 8 scans in a *Perkin-Elmer FTIR BX* spectrophotometer equipped with a single horizontal Golden Gate ATR cell.

Finally, the FTIR-ATR spectra of the cellulose samples obtained in the study of gas-solid reaction with TCMS were acquired in a *PARAGON 1000 Perkin-Elmer FTIR* spectrometer equipped with a single horizontal Golden Gate ATR cell, with 8 cm^{-1} resolution after 128 scans.

3.2.2. Contact Angle Measurements and Determination of the Surface Energy

Contact angles with liquids possessing different polarities and surface tensions (listed in Table 8) were measured on the surface of the unmodified and modified cellulose samples using a ''*Surface Energy Evaluation System*" commercialized by Brno University (Czech Republic), except in the case of the TCMS-treated cellulose samples, where a *Dataphysics* device equipped with a *Pulnix* camera was used. The measurement of the contact angle was performed 5 s after the deposition of the liquid drop to ensure the attainment of equilibrium. For the more hydrophilic samples, including the pristine cellulose substrates, the contact angle was the first captured by the instrument following the drop deposition. Each reported contact angle value was the average of at least five determinations.

Table 8. Values of the surface tension (γ_l) of the testing liquids used for the contact angle measurements, and its polar (γ^p_l) and dispersive (γ^d_l) components [149].

Testing liquid	Surface tension (mJ.m^{-2})		
	γ^p_l	γ^d_l	γ_l
Water	51.0	21.8	72.8
Glycerol	30.0	34.0	64.0
Formamide	19.0	39.0	58.0
Ethylene glycol	19.0	29.0	48.0
Diiodomethane	0	50.8	50.8
1-Bromonaphthalene	0	44.4	44.4

In the study related to the preparation of the cellulose hybrids, prior to the contact angle measurements, the pristine fibers and the hybrid materials were pressed (6 tons) into small pellets (10 mm diameter and 1 mm thick) using a laboratory press, in order to work on flat surfaces, which were insured by the polished steal surfaces of the press. In the other studies, filter paper was used as substrate to provide the flat surfaces.

The contact angle values were then used to calculate the dispersive (γ^d_s) and polar (γ^p_s) contributions to the surface energy (γ_s) of the cellulose substrates, using Owens-Wendt's approach discussed in *Chapter 1* (Equation 2).

3.2.3. X-Ray Photoelectron Spectroscopy

The X-ray photoelectron spectroscopy (XPS), also known as electron spectroscopy for chemical analysis (ESCA), is a technique based on the photoelectric effect. This means that the XPS principle consists in the irradiation of a material with an X-ray beam at a fixed wavelength, provoking the emission of electrons from its surface, either from the outer shells or core levels of the elements there present [258, 259]. One of the most valuable features of this technique is its ability to distinguish different chemical bonding configurations, as well as different elements (except hydrogen). The identification of the elemental composition of a sample by XPS is possible due to the unique binding energy of each element, which is intimately related with the atom's chemical environment [260]. Thus, in this thesis, this technique was used to examine the surface elemental composition of the cellulose fibers before and after modification.

The XPS spectra of the unmodified and perfluorinated cellulose fibers' surfaces were obtained with a *Physical Electronics PHI Quantum 2000 ESCA* instrument equipped with a monochromatic AlKα X-ray source and operated at 25 W, with a combination of an electron flood gun and ion bombarding for charge compensation. The take-off angle was 45º in relation to the sample surface. The analyzed area was 500 × 400 μm^2 in the TFAA derivatives and 100 x 100 μm^2 in the PFBz and TFP derivatives. At least three different spots were analyzed on each sample and a Gaussian curve-fitting program was used to treat the C*1s* signal.

In relation to the TCMS-modified cellulose samples, the XPS experiments were performed using a *XR3E2* apparatus (Vacuum Generators, UK) equipped with a monochromated MgKα X-ray source (1253.6 eV) and operated at 15 kV under a current of 20 mA. Samples were placed in an ultrahigh vacuum chamber (10^{-8} mbar) with the electrons captured by a hemispherical analyzer at an angle of 90º. Signal decomposition was carried out using a *Spectrum NT*, with the C–H signal as the reference peak at 285.0 kV.

3.2.4. Time-of-Flight Secondary Ion Mass Spectrometry

Time-of-flight secondary ion mass spectrometry (ToF-SIMS) is a surface-sensitive analytical technique, which uses a pulsed primary ion beam to desorb and ionize chemical species from the very outermost surface of a sample (atomic monolayers on the surface). The resulting secondary ions are then accelerated into a mass spectrometer, where they are analyzed by measuring the exact time at which they reach the detector, *i.e.*, their time-of-flight from the sample surface to the detector [261, 262].

This technique was conducted here in two different operational modes, namely surface spectroscopy and surface imaging. The former mode consisted in the acquisition of the mass spectra and determination of the elemental and molecular species on the surface, while in the latter mode, images were acquired to visualize the distribution of selected surface individual species, which were $C_6F_5^+$ and $C_6F_5CO^+$ ions and $CF_3CH_2CO^+$ ions in the case of the pentafluorobenzoylated and trifluoropropanoylated cellulose samples, respectively [261, 262].

ToF-SIMS spectra of the unmodified and perfluorinated cellulose fibers were obtained using a *Physical Electronics ToF-SIMS TRIFT II* spectrometer. A primary ion beam of $^{69}Ga^+$ liquid metal ion source (LMIS) with 15 kV applied voltage, 600 pA aperture current and a bunched pulse width of 20 ns, was used in both positive and negative modes.

A raster size of 200 × 200 µm was scanned and at least three different spots were analyzed.

The surface distribution of the perfluorinated moieties mentioned above was obtained with the best spatial resolution using the ion gun operating at 25 kV, 600 pA aperture current and an unbunched pulse width of 20 ns.

The spectra were acquired for 6 min with a fluency of ~1012 ions/cm^2, ensuring static conditions. Charge compensation was attained with an electron flood gun pulsed out of phase with respect to the ion gun.

3.2.5. Scanning Electron Microscopy

The scanning electron microscopy (SEM) images obtained in this investigation were collected with a *Hitachi SU-70* operating at 4 kV in the case of the hybrid cellulose materials, and a *FEI QUANTA 200* microscope operating at 15 and 10 kV in the case of the TCMS-modified cellulose derivatives.

Samples were deposited on an aluminum plate and coated with a carbon layer, approximately 15–50 nm thick, by evaporation of carbon rods (outgas time: 30 s, evaporating time: 1000 ms).

3.2.6. Mapping of Atomic Elements

C and Si mapping of the unmodified and modified cellulose substrates with TCMS was conducted with a *FEG-SEM Zeiss Ultra 55* device operating at 15 kV.

Samples were deposited on an aluminum plate and coated with a carbon layer, approximately 15–50 nm thick, by evaporation of carbon rods (outgas time: 30 s, evaporating time: 1000 ms).

Chapter 3

Results and Discussion

Chapter 3 – Results and Discussion

The aim of this dissertation was the development of new materials from the controlled heterogeneous modification of cellulose. Accordingly, novel cellulose derivatives, the majority with both highly hydrophobic and lipophobic behavior, and also remarkably low surface energies, were prepared by means of three main different procedures.

The first approach consisted in the heterogeneous modification of cellulose fibers with perfluorinated reagents. The second study, dealt with the preparation of class-II organic-inorganic cellulose hybrid materials by the controlled heterogeneous modification of cellulose fibers with a silane-coupling agent, and subsequent acid hydrolysis (and condensation) of the appended siloxane moieties as such, or in the presence of two different alkoxysilanes. Finally, the third approach, called upon a gas-solid type reaction, thus avoiding the use of solvents, for the surface modification of the cellulose fibers with a chlorosilane.

Depending on each specific case, the cellulose derivatives prepared were thoroughly characterized using a wide number of analytical tools, specifically FTIR-ATR, contact angle measurements, EA, CP-MAS NMR, SEM, TGA, ToF-SIMS and XPS. Hence, the details of the studies, comprising the results, their discussion, and some conclusions are presented in the following sections.

1. Preparation of Perfluorinated Cellulose Derivatives

As previously referred in *Chapter 1*, fluorinated organic compounds are known to display remarkable hydrophobic and lipophobic properties [214], which depend on the nature of the fluorine-containing moiety and its fluorine content. The controlled heterogeneous modification of cellulose fibers with fluorinated reagents represents therefore a promising strategy for the development of materials with novel properties. Although the preparation of fluorine-containing cellulose derivatives does not constitute a pioneering approach [263], thus far, the number of published studies dealing with the chemical modification of cellulose with fluorine-containing compounds is limited [71, 73, 74, 81, 86, 88, 107, 108, 127, 128, 240, 264-275], and some of them comprise studies carried out under homogeneous conditions.

Here, the cellulose modification with the different perfluorinated reagents were conducted in toluene, a non-swelling solvent, in order to avoid the swelling of the cellulose fibers and thus to limit the modification, as much as possible, to their outermost layers, enabling the intended controlled heterogeneous esterification of the fibers to take place.

Furthermore, as mentioned in *Chapter 2*, several reaction times and temperatures were tested in order to determine the effect of these reaction parameters on the extent of esterification and hence on the properties of the modified fibers.

1.1. Controlled Heterogeneous Esterification of Cellulose with Perfluorinated Reagents

The controlled heterogeneous modification of cellulose fibers with TFAA, PFBz and TFP was performed by means of an esterification reaction between the cellulose hydroxyl groups and the carboxyl functions of the perfluorinated reagents. An illustrative scheme of these reactions is presented in Figure 20.

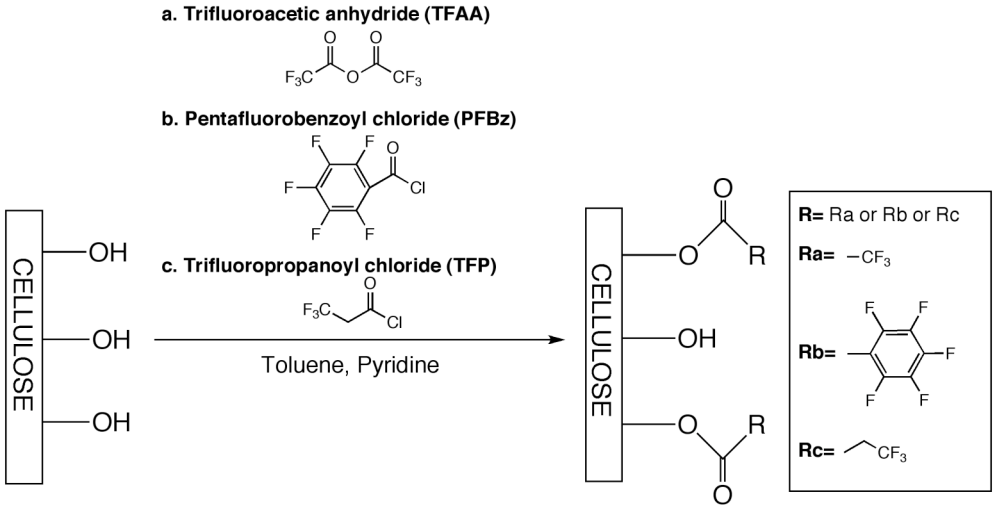

Figure 20. Schematic representation of the modification of cellulose fibers with the perfluorinated reagents.

1.1.1. FTIR-ATR Spectroscopic Analysis

The FTIR-ATR spectrum of the unmodified cellulose fibers (Figure 21, A) displayed the typical cellulose bands, which are summarized in Table 9.

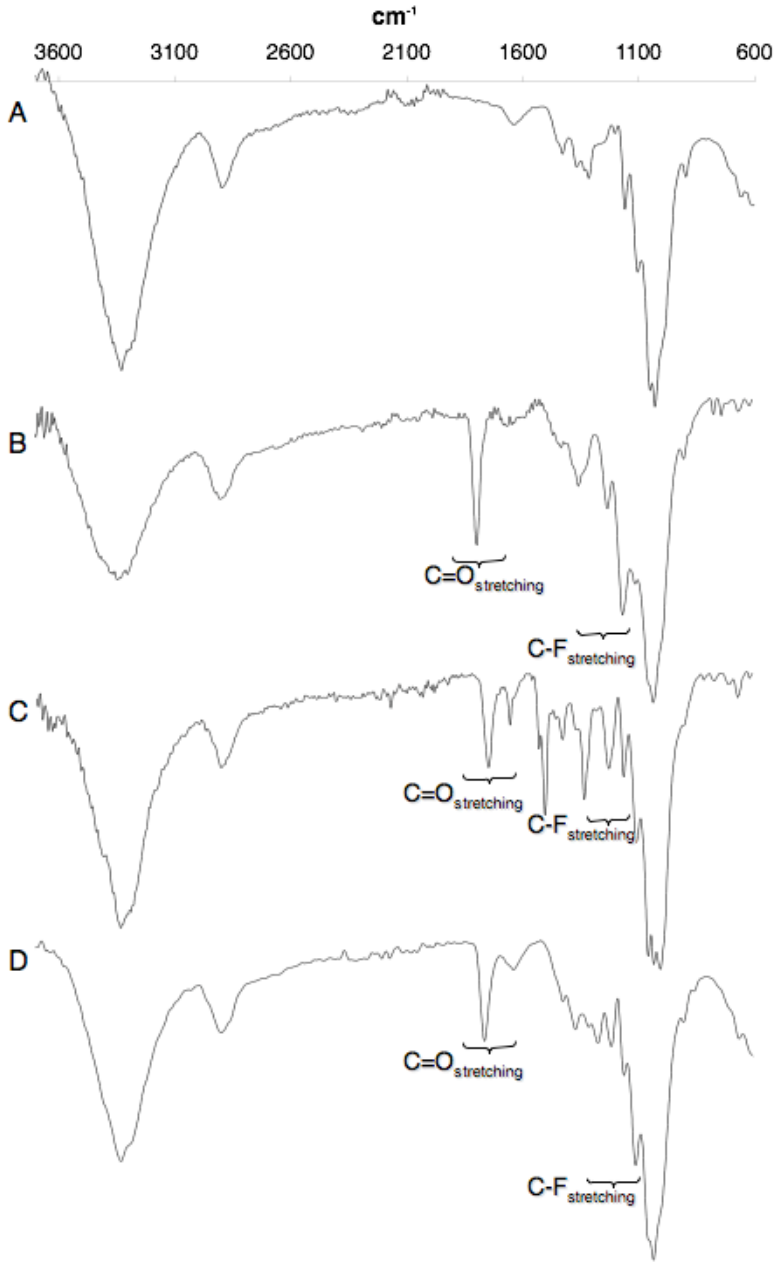

Figure 21. FTIR-ATR spectra of (A) unmodified, (B) trifluoroacetylated, (C) pentafluorobenzoylated and (D) trifluoropropanoylated cellulose fibers.

Table 9. Typical IR-absorption bands of cellulose [3, 276].

Assignment		Vibration frequency (cm^{-1})
Function	**Type of contribution**	
O-H (free)	stretching	3500-3600
O-H (bonded – intramolecular bonds)	stretching	3400-3500
O-H (bonded – intermolecular bonds)	streching	3000-3400
C-H (from CH_2)	stretching (antisymmetric)	2960
C-H (from CH)	stretching	2850-2970
O-H (absorbed H_2O)	bending	1635-1670
O-H	in-plane bending	1440-1450
C-H (from CH_2)	bending	1425-1430
C-H (from CH)	bending	1365-1370
O-H	in-plane bending	1330-1340
CH_2	wagging	1315-1320
C-H (from CH)	bending	1240-1250
O-H	in-plane bending	1170-1180
C-O-C (bridge O)	stretching (antisymmetric)	1160
ring	in-phase stretching (antisymmetric)	1110
O-H	bending	1050-1100
C-O	stretching	1025-1050
ring	out-of-phase stretching (antisymmetric)	890

After comparison between the FTIR-ATR spectra of unmodified and modified cellulose fibers, the success of the esterification with the perfluorinated reagents was clearly confirmed by the emergence of new carbonyl ester bands around 1800 cm^{-1} (Figure 21, B), 1740 cm^{-1} (Figure 21, C) and 1760 cm^{-1} (Figure 21, D), assigned to trifluoroacetate, pentafluorobenzoate and trifluoropropanoate groups stretching modes, respectively [276]. Moreover, the occurrence of new absorptions in the range of 1000-1300 cm^{-1} (Figure 21, B to D), typical of C-F groups vibrations in the stretching mode [276], gave additional confirmation of the presence of fluorine-containing moieties. Likewise, the decrease in the intensity of the broad band centered at ~3300 cm^{-1},

attributed to the cellulose hydroxyl groups' vibrations [276], constituted further evidence of the functionalization of the OH functions by the perfluorinated moieties.

Additionally, in the case of the pentafluorobenzoylated cellulose fibers new peaks emerged at about 1330 cm^{-1} and in the range 760-1000 cm^{-1} (Figure 21, C), which were associated with stretching and bending vibrations typical of the aromatic ring (Ar). Besides, the increment in the peaks related to C-H bending and CH_2 wagging (Table 9), at *ca.* 1365 cm^{-1} and 1265 cm^{-1}, respectively, in the spectra of the trifluoropropanoylated samples (Figure 21, D), assigned to the new methylene group, corroborated the actual occurrence of the esterification reaction.

It is worth recalling that all the modified samples had been submitted to appropriate extraction procedures before being characterized, which excludes any spectroscopic artifact associated with the presence of residual reagents or side products.

The progress of esterification according to the different reaction conditions tested (Table 6) was also assessed by FTIR-ATR spectroscopy, through the monitoring of the intensity of the bands mentioned above (O-H, C=O and C-F), as illustrated in Figure 22 for the case of the trifluoroacetylated samples. Thus, the preliminary studies on the effect of the reaction temperature and time on the extent of the OH groups' functionalization showed that it was very sensitive to the former parameter (Figure 22, Annexes), particularly above a certain temperature, which was 50 ºC in the case of TFAA- and PFBz-derivatives and 65 ºC for the TFP-derivatives, whereas it did not increase significantly beyond a 2 and 5 h period, for the TFP-derivatives and TFAA- and PFBz-derivatives, respectively. Nonetheless, the trifluoroacetylated samples obtained with the highest temperature, *i.e.* 80 ºC, seemed slightly degraded, displaying a fairly brownish color and being quite fragile.

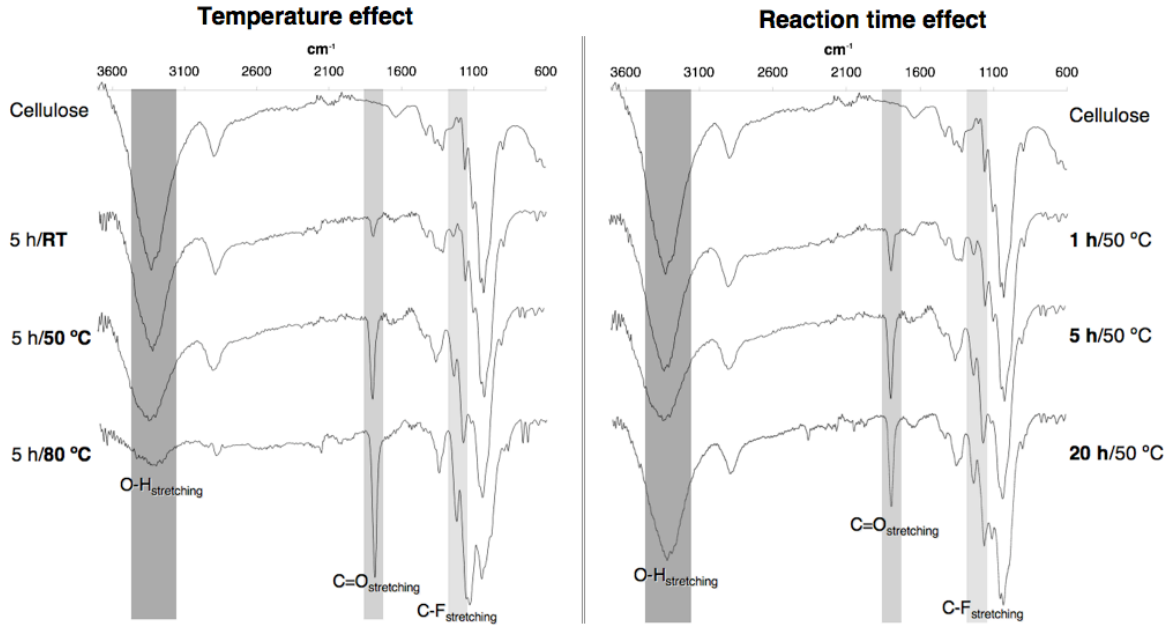

Figure 22. Progress of the trifluoroacetylation with temperature and reaction time as followed by FTIR-ATR.

As referred in *Chapter 2*, a sample of bacterial cellulose was also modified with pentafluorobenzoyl chloride for 5 h at 65 °C (BCPFBz). The FTIR-ATR spectrum of the ensuing product (BCPFBz) is presented in Figure 23, together with the spectrum of the unmodified bacterial cellulose. As can be easily perceived, this latter spectrum showed, as expected, the same bands as those of the vegetable counterpart (Figure 21), albeit with slightly different relative intensities. Similarly to the vegetable cellulose fibers, the occurrence of reaction in BCPFBz was readily confirmed by the emergence of the new carbonyl ester band at about 1740 cm^{-1}, and the additional new absorptions in the range 760-1330 cm^{-1}, typical of C-F stretching modes and of the aromatic ring (Ar) stretching and bending vibrations (Figure 23) [276].

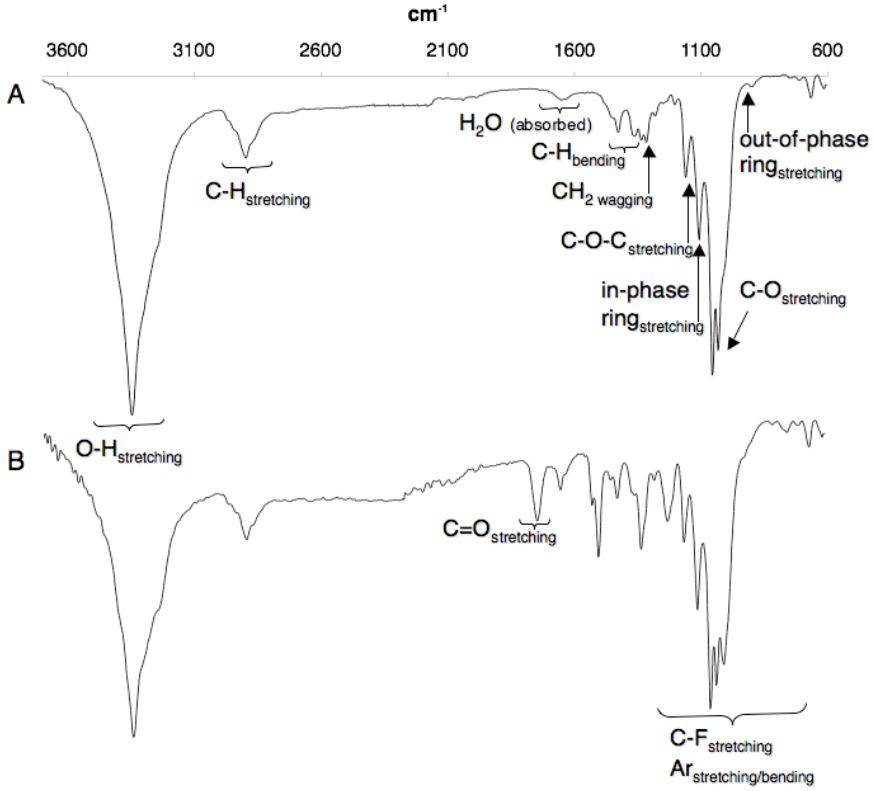

Figure 23. FTIR-ATR spectra of (A) unmodified and (B) pentafluorobenzoylated bacterial cellulose fibers.

For further characterization studies, together with the pristine vegetable and bacterial cellulose fibers, some samples from each type of perfluorinated derivatives were selected, which are listed in Table 10.

Table 10. Identification of the perfluorinated cellulose samples selected for further characterization studies.

Sample identification	Reaction conditions	
	Time / h	Temperature / ºC
TFAA1	1	50
TFAA2	5	50
TFAA3	5	80
PFBz1	5	50
PFBz2	5	65
PFBz3	5	80
BCPFBz	5	65
TFP1	2	RT
TFP2	2	65
TFP3	2	100
TFP4[a]	2	80

[a]Used in the study of hydrolytic stability.

1.1.2. Elemental Analysis and Determination of the Degree of Substitution

The elemental composition of the unmodified and esterified cellulose fibers was determined and the results are presented in Table 11. As can be observed, after chemical modification, beyond carbon and hydrogen (oxygen was not determined) also present in unmodified cellulose fibers, the perfluorinated samples contained fluorine, which corroborated the success of the cellulose functionalizations.

Table 11. Elemental composition and DS of the unmodified and perfluorinated cellulose samples.

Sample	%C	%H	%F	DS
Vegetable Cellulose	42.8	6.3	—	—
TFAA1	42.1	6.1	1.4	0.04
TFAA2	40.8	5.8	4.5	0.14
TFAA3	38.2	4.9	9.0	0.30
PFBz1	41.0	6.1	0.79	0.014
PFBz2	40.0	5.1	10.4	0.23
PFBz3	39.2	4.9	15.7	0.39
TFP1	41.9	6.1	<0.20	<0.006
TFP2	42.0	5.9	1.0	0.03
TFP3	41.0	5.2	8.8	0.30
TFP4	41.6	5.9	2.4	0.07
Bacterial Cellulose	40.6	5.9	—	—
BCPFBz	39.8	5.3	7.8	0.16

The degree of substitution (DS) of the modified samples (Table 11) was calculated from their fluorine content (%F), using the Equation 3 (*Chapter 2*) and gave values ranging from <0.006 to 0.39. Since these values were calculated on the basis of all the glucose units present in the cellulose samples, and considering that the proportion of surface to bulk OH groups in the vegetable fibers used was about 2-4% [136], it seems likely that for DS values higher than 0.20, representing more than 6% of the OH groups, the surface esterification had reached a very high yield. Moreover, this can be an indication that the OH functionalization in the TFAA3, PFBz2, PFBz3 and TFP3 samples may have occurred further than just in the cellulose fibers' surface layers.

Taking into account the extensive surface area (high availability of OH groups) usually attributed to bacterial cellulose [24], due to the nanometric scale of its fibrils and their specific 3D-arrangement, the somewhat lower DS value of the BCPFBz sample (DS=0.16) comparatively to PBFz2 (DS=0.23), which was obtained in the same conditions, was here attributed to a correspondingly lower accessibility of this cellulose substrate to the reagent due to the more compact matlike morphology, compared with that of the loose vegetable fibers.

1.1.3. X-Ray Diffraction Analysis

In order to determine if the modification reactions affected the crystallinity of the cellulose fibers, XRD experiments were performed. Figure 24 displays the diffractograms obtained for the unmodified and trifluoroacetylated cellulose fibers.

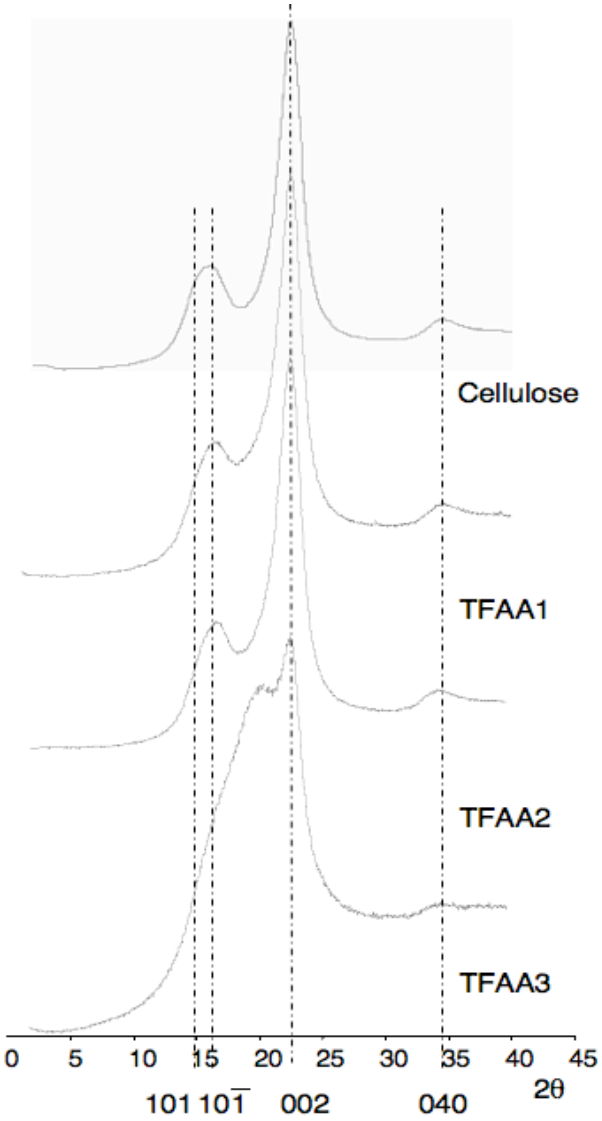

Figure 24. X-ray diffractograms of the unmodified and trifluoroacetylated cellulose fibers.

Vegetable cellulose fibers are known to display XRD patterns typical of cellulose I, with the main diffraction signals at 2θ values of 14.9º, 16.3º, 22.5º, and 34.6º, usually assigned to the diffraction planes 101, 10$\bar{1}$, 002, and 040, respectively [277]. As can be

observed in Figure 24, the trifluoroacetylated cellulose samples TFAA1 and TFAA2 preserved the essential XRD features of cellulose I displayed by the pristine fibers, suggesting that the reaction occurred essentially on the amorphous regions of the outer layers of the fibers' cell wall, without affecting to any substantial extent their crystallinity and ultrastructure. However, as previously suggested by the DS values, an extensive OH functionalization occurred in the TFAA3 sample, which led to a large decline in the crystallinity of the corresponding cellulose fibers, as illustrated by the increase in the intensity of the diffraction signal at $2\theta = 18^{o}$, normally assigned to the less ordered regions of the cellulose chains, and the accompanying decrease in the diffraction intensities of the crystalline planes of cellulose I. These observations suggest that in this case, the reaction also involved hydroxyl groups belonging to the crystalline regions situated in deep layers of the fibers' wall.

Regarding the PFBz- and TFP-derivatives, all the samples preserved the cellulose I XRD pattern (Figure 25), which means that, in the case of PFBz2 (DS=0.23), PFBz3 (DS=0.39) and TFP3 (DS=0.30) samples, the probable in-depth esterification, indicated by the DS values, must have involved also the hydroxyl groups of the amorphous regions of the inner layers, without affecting the crystalline domains.

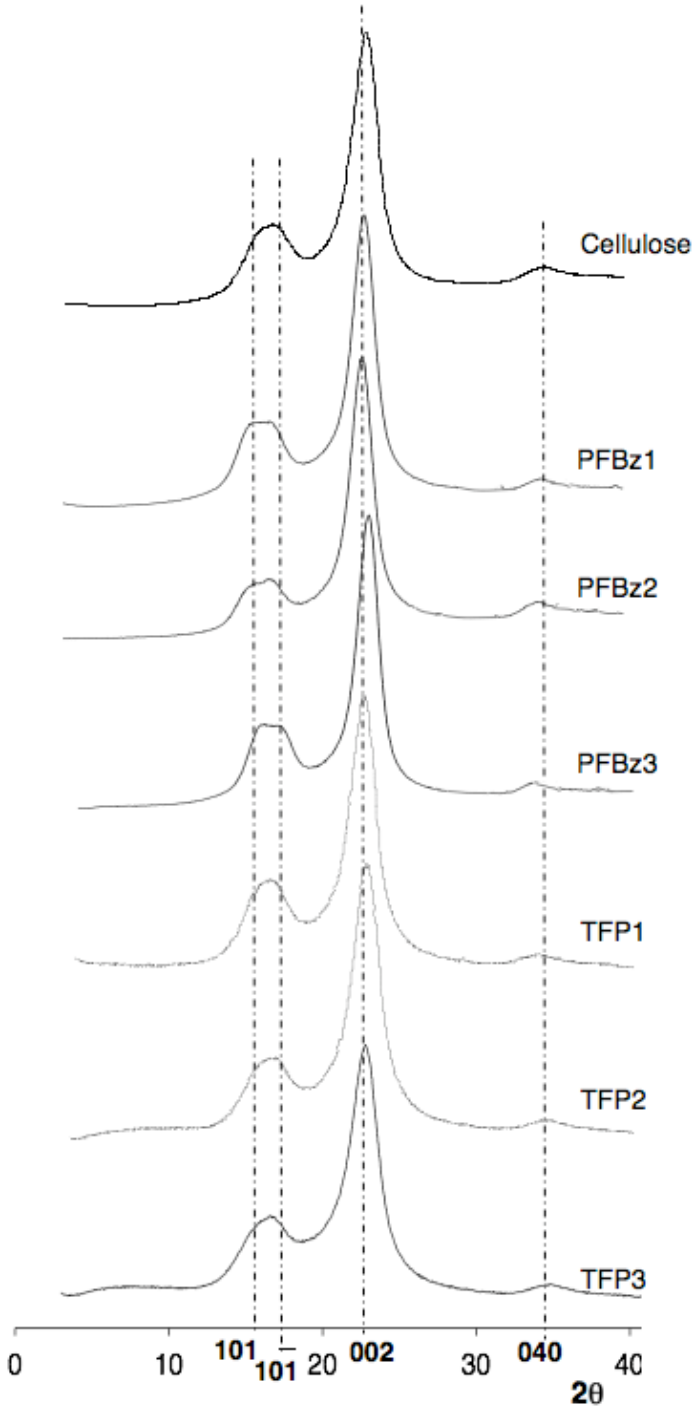

Figure 25. X-ray diffractograms of the PFBz- and TFP-derivatives.

The bacterial cellulose also displayed the typical XRD pattern of cellulose I (Figure 26). However, in its diffractogram the peaks at about 2θ=14.7 and 17.1°, attributed to the 101 and $10\bar{1}$ planes, are better resolved than in the vegetable cellulose diffractogram (Figure 24), which is related to the higher crystallinity associated to the former fibers [23].

Furthermore, the BCPFBz sample maintained this pattern, which once again suggests that the esterification did not affect significantly the crystallinity of the sample.

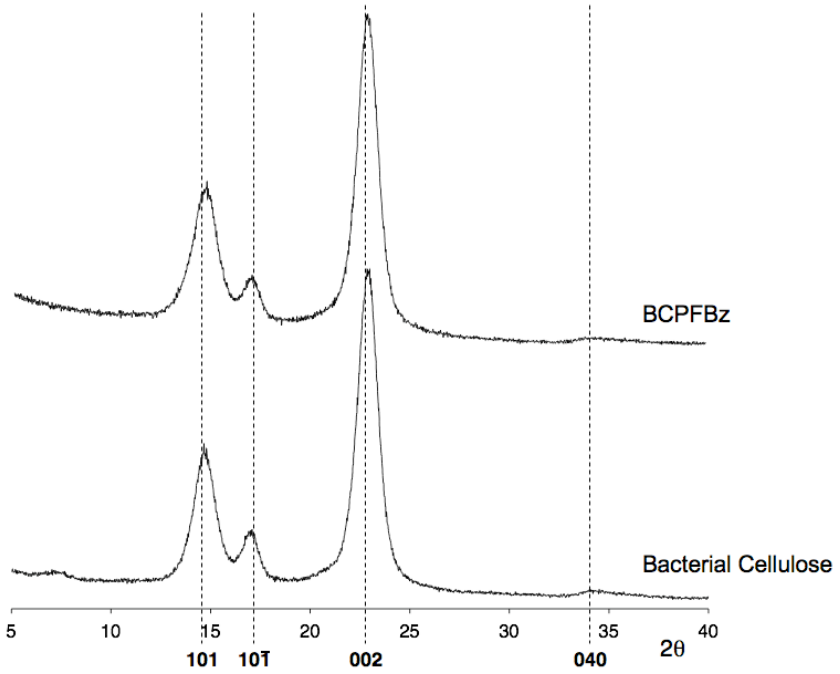

Figure 26. XRD patterns of unmodified and pentafluorobenzoylated bacterial cellulose fibers.

1.1.4. Thermogravimetric Analysis

The thermal stability of the unmodified and perfluorinated cellulose fibers was evaluated by thermogravimetric analysis (TGA). The thermograms obtained are exemplified in Figure 27 for the pristine vegetable and bacterial cellulose fibers together with the TFAA1 and BCPFBz samples. The thermogravimetric parameters attained for the different samples are summarized in Table 12.

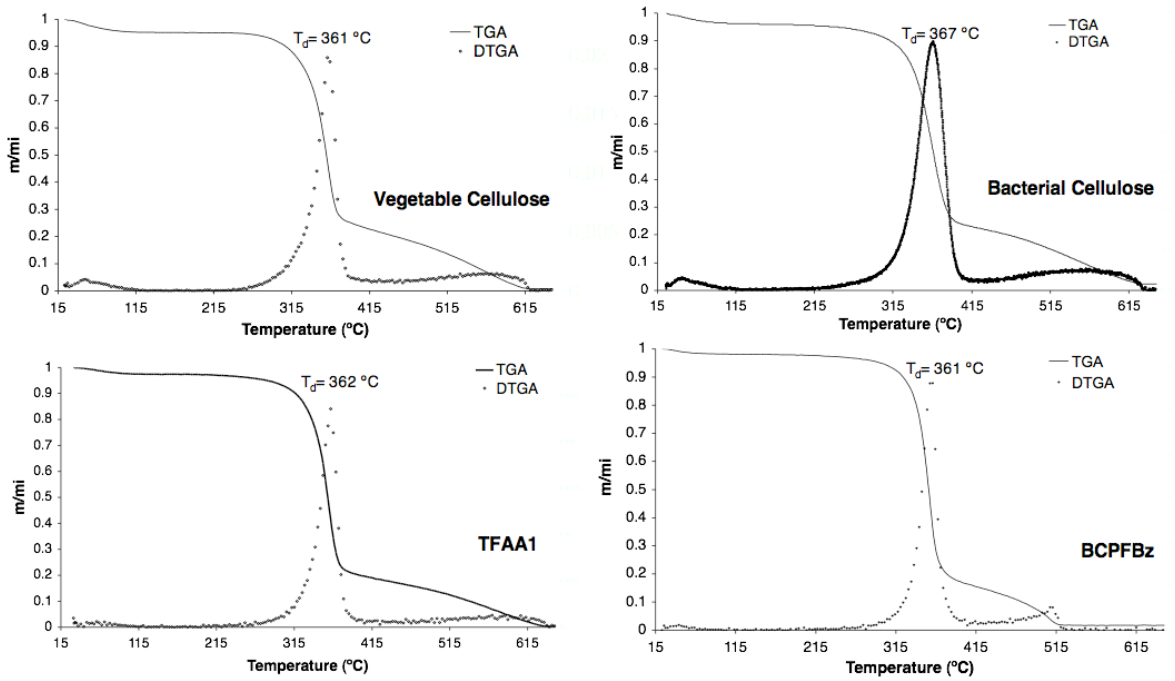

Figure 27. Thermograms of unmodified vegetable and bacterial cellulose fibers and TFAA1 and BCPFBz samples.

Table 12. Thermogravimetric data of unmodified and perfluorinated cellulose fibers.

Sample	DS	Weight loss at 100 °C (%)	T_{di} (°C)	T_d (°C)
Vegetable Cellulose	—	4.5	240	361
TFAA1	0.04	2.4	238	362
TFAA2	0.14	2.2	235	357
TFAA3	0.30	2.3	241	360
PFBz1	0.014	2.7	242	359
PFBz2	0.23	3.2	245	354
PFBz3	0.39	3.5	244	357
TFP1	<0.006	5.6	237	370
TFP2	0.03	6.2	246	353
TFP3	0.30	2.3	276	370
Bacterial Cellulose	—	3.6	228	367
BCPFBz	0.16	1.8	247	361

As can be observed in Figure 27, the thermograms of both unmodified vegetable and bacterial fibers exhibited the typical thermal degradation behavior of pristine cellulose fibers, with a double weight-loss, at temperatures of initial decomposition (T_{di}) of about 240 and 228 ºC and temperatures of maximum decomposition rate (T_d) around 360 and 367 ºC, respectively. The two weight-loss steps observed are related to different phenomena, namely (i) dehydratation and occasional depolymerization of cellulose, and (ii) its decomposition into a number of gaseous products and residual char [3, 278].

The TGA profiles of all the other perfluorinated fibers, were very similar to those of the pristine substrates, as depicted in Figure 27 for TFAA1 and BCPFBz samples, with T_{di} and T_d values varying in the range 237-276 ºC and 353-370 ºC (Table 12), respectively.

Considering that the thermal stability is evaluated taking into account T_{di} values, the expected increase in thermal stability, usually associated with fluorination [214], was not observed here, except for the TFP3 and BCPFBz samples, which exhibited T_{di} values higher than those of the corresponding pristine fibers (36 and 19 ºC higher, respectively) (Table 12). Furthermore, in the former sample, T_d was also higher than in the unmodified cellulose fibers (Table 12), indicating that the appended trifluoropropanoyl groups (DS=0.30) provided a fair thermal barrier.

Nevertheless, on the whole, these perfluorinated derivatives showed to be more thermally stable than other organic cellulose esters, such as those derived from fatty acids, which are known to start decomposing at temperatures much lower than that of pristine cellulose fibers [7].

Moreover, it can be verified in Table 12 that some samples presented lower weight loss at 100 ºC, ascribed to moisture loss, when compared with the pristine cellulose fibers, which suggested a correspondingly lower water adsorption, associated with the hydrophobic character attained after modification, as discussed below.

Additionally, in general, the DS did not seem to play a significant role on the thermal degradation profile of the perfluorinated cellulose samples, at least within the range of DS values attained, since they displayed similar thermogravimetric results.

1.1.5. Surface Characterization by Time-of-Flight Secondary Ion Mass Spectrometry and X-Ray Photoelectron Spectroscopy

The ToF-SIMS spectrum of cellulose fibers from *Eucalyptus globulus* ECF bleached kraft pulp usually shows characteristic fragments at *m/z* 127 and 145, assigned to $C_6H_7O_3^+$ and $C_6H_9O_4^+$ ions, respectively, inherent to the cellulose structure [61, 279], as well as secondary ions at *m/z* 115 and 133, assigned to $C_5H_7O_3^+$ and $C_5H_9O_4^+$ ions, respectively, usually associated to hemicelluloses, specifically to xylans [61, 279]. The mass spectrum of the pristine bacterial cellulose fibers exhibited the same fragments at *m/z* 127 and 145, as can be observed in Figure 28.

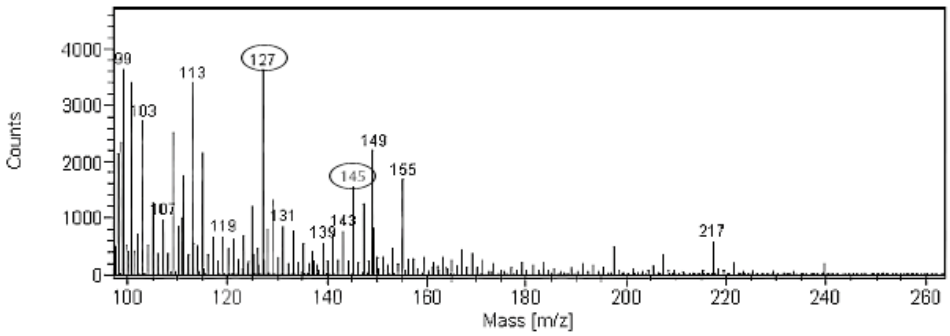

Figure 28. Partial positive ToF-SIMS spectrum of pristine bacterial cellulose.

The ToF-SIMS spectra of the modified cellulose fibers corroborated the presence of perfluorinated moieties covalently bound to the fibers' surface. In the case of the trifluoroacetylated samples, it was observed the predominance of the secondary ion CF_3^+ at m/z = 69 (Figure 29), which is generated by the cleavage of the CF_3CO moieties of trifluoroacetate group and their subsequent fragmentation into CO and trifluoromethyl cations.

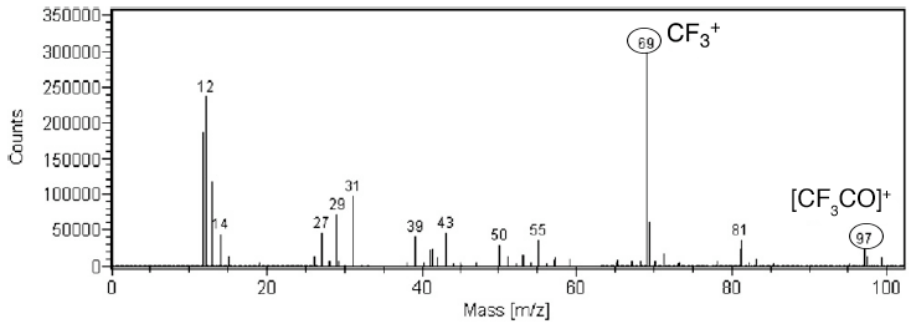

Figure 29. Partial positive ToF-SIMS mass spectrum of TFAA2.

In addition, a secondary ion CF_3CO^+ at *m/z* = 97 (Figure 29), was also verified, but since this *m/z* value could also arise from the fragmentation of the cellulose backbone [61], it did not constitute, on its own, an unambiguous indication of the occurrence of the esterification reaction. The absence of the quasimolecular ion $[CF_3COOCOCF_3 + H]^+$ at *m/z* = 211 indicated moreover that the removal of residual unbound trifluoroacetic anhydride during the washing and extraction steps had been quite efficient. However, the absence of sporadic adsorbed amounts of trifluoroacetic acid could not be excluded, because of the presence of an ion at *m/z* = 115, that could be assigned to the corresponding quasimolecular ion $[CF_3COOH + H]^+$, but which also coincides with the $C_5H_7O_3^+$ ion typically present on the spectra of the unmodified cellulose fibers, as already mentioned above [61, 279].

In the case of the PFBz- and TFP-derivatives, the presence of perfluorinated moieties covalently bound to the surface of the cellulose fibers was confirmed by this technique due to the occurrence of the secondary ions $C_6F_5^+$ and $C_6F_5CO^+$ at *m/z* 167 and 195, respectively, in the former (Figure 30, A), and $CF_3CH_2^+$ and $CF_3CH_2CO^+$ at *m/z* 83 and 111, respectively, in the latter (Figure 30, B), generated by the cleavage of the corresponding ester groups. Moreover, once again, it was verified that the washing and extraction stages had been highly efficient, due to the absence of unbound pentafluorobenzoyl and trifluoropropanoyl chlorides in the mass spectra of the PFBz- and TFP-derivatives, respectively, as well as of their corresponding acid and ethyl esters (the quasimolecular ions $[C_6F_5COCl + H]^+$ at *m/z* 230, $[C_6F_5CO_2H + H]^+$ at *m/z* 213, and $[C_6F_5CO_2CH_2CH_3 + H]^+$ at *m/z* 213, for the PFBz-derivatives, and $[CF_3CH_2COCl+H]^+$ at *m/z* 147, $[CF_3CH_2CO_2H +H]^+$ at *m/z* 129 and $[CF_3CH_2CO_2CH_2CH_3 +H]^+$ at *m/z* 157, for the TFP-derivatives, respectively).

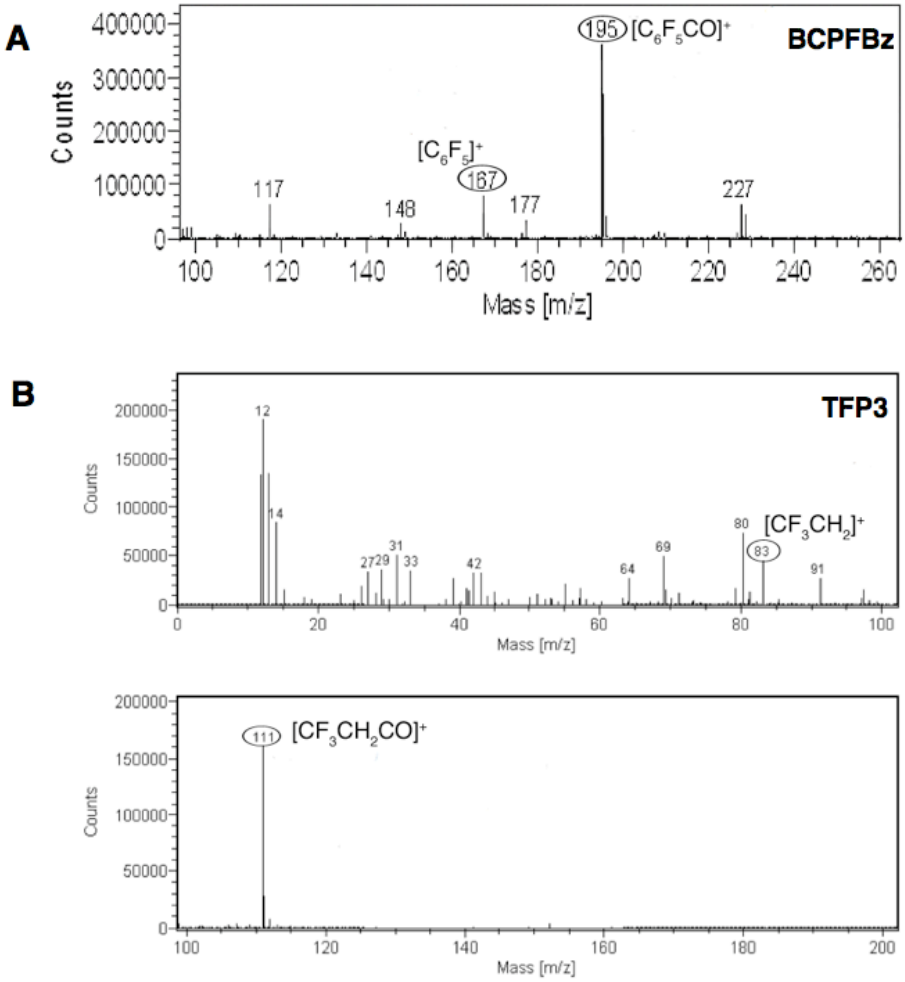

Figure 30. Partial positive ToF-SIMS mass spectra of the (A) BCPFBz and (B) TFP3 samples.

Furthermore, ToF-SIMS imaging was used to study qualitatively the distribution (in terms of both homogeneity and extent of coverage) of pentafluorobenzoyl and trifluoropropanoyl moieties attached to the fibers' surface, in the case of the PFBz- and TFP-derivatives, respectively, by monitoring the $C_6F_5^+$ and $C_6F_5CO^+$ ions, in the former (Figure 31) and the $CF_3CH_2CO^+$ ions, in the latter (Figure 32). As displayed in Figure 31 and Figure 32 the distribution of the pentafluorobenzoyl and trifluoropropanoyl moieties in the PFBz- and TFP-derivatives, respectively, was, on the whole, quite heterogeneous, a feature related with the different reactivity resulting from the degree of order of the cellulose macromolecules near the surface. Moreover, it was perceived that the extent of surface esterification was highly dependent on the reaction temperature (especially above 50 and 65 ºC, for the PFBz and TFP-derivatives, respectively), depicted in Figure 31 and Figure 32 by the large increment of the amount of $C_6F_5^+$ and $C_6F_5CO^+$ ions from PFBz1 to

PFBz2 and $CF_3CH_2CO^+$ ions from TFP1 to TFP2 and to TFP3, respectively. These results came to support what was already inferred from the FTIR-ATR analysis.

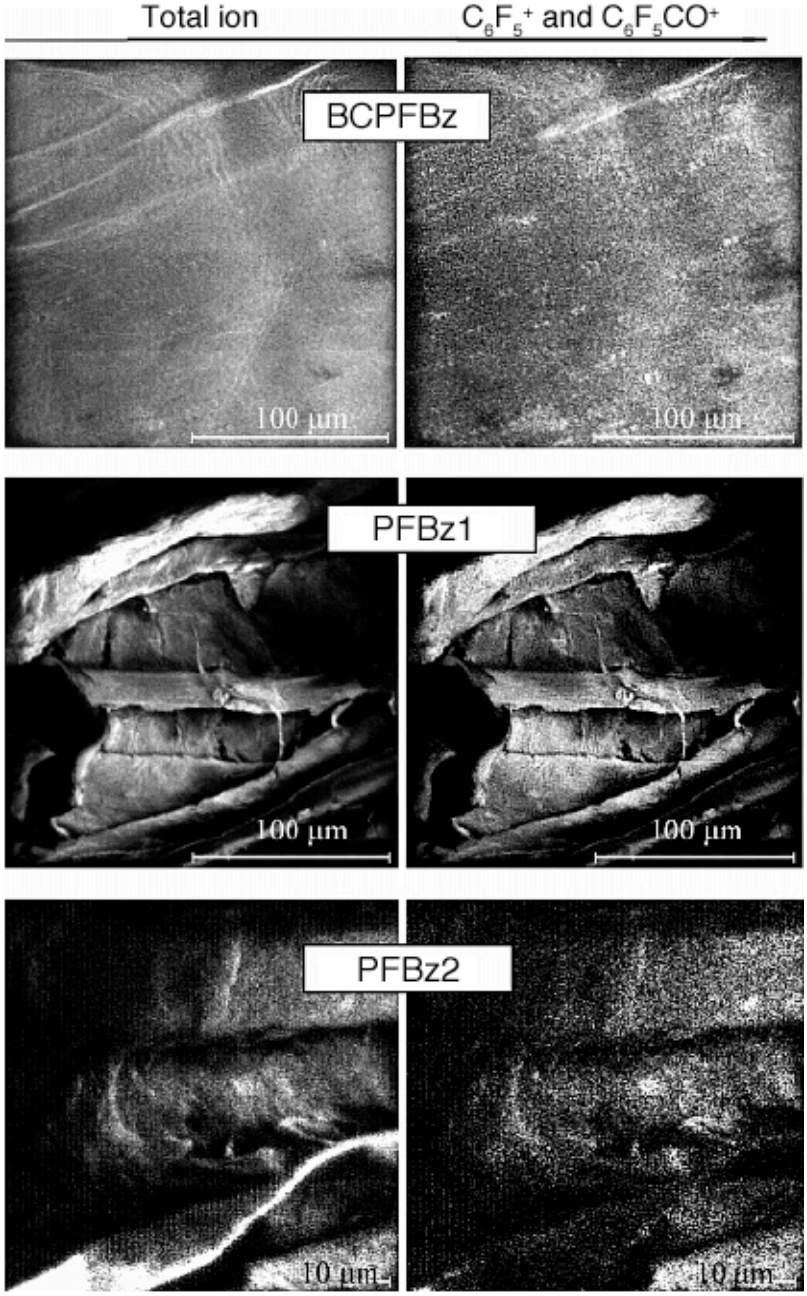

Figure 31. Total ion images and surface distribution of pentafluorobenzoyl moieties ($C_6F_5^+$ and $C_6F_5CO^+$) appended to the cellulose fibers' surface in the PFBz-derivatives.

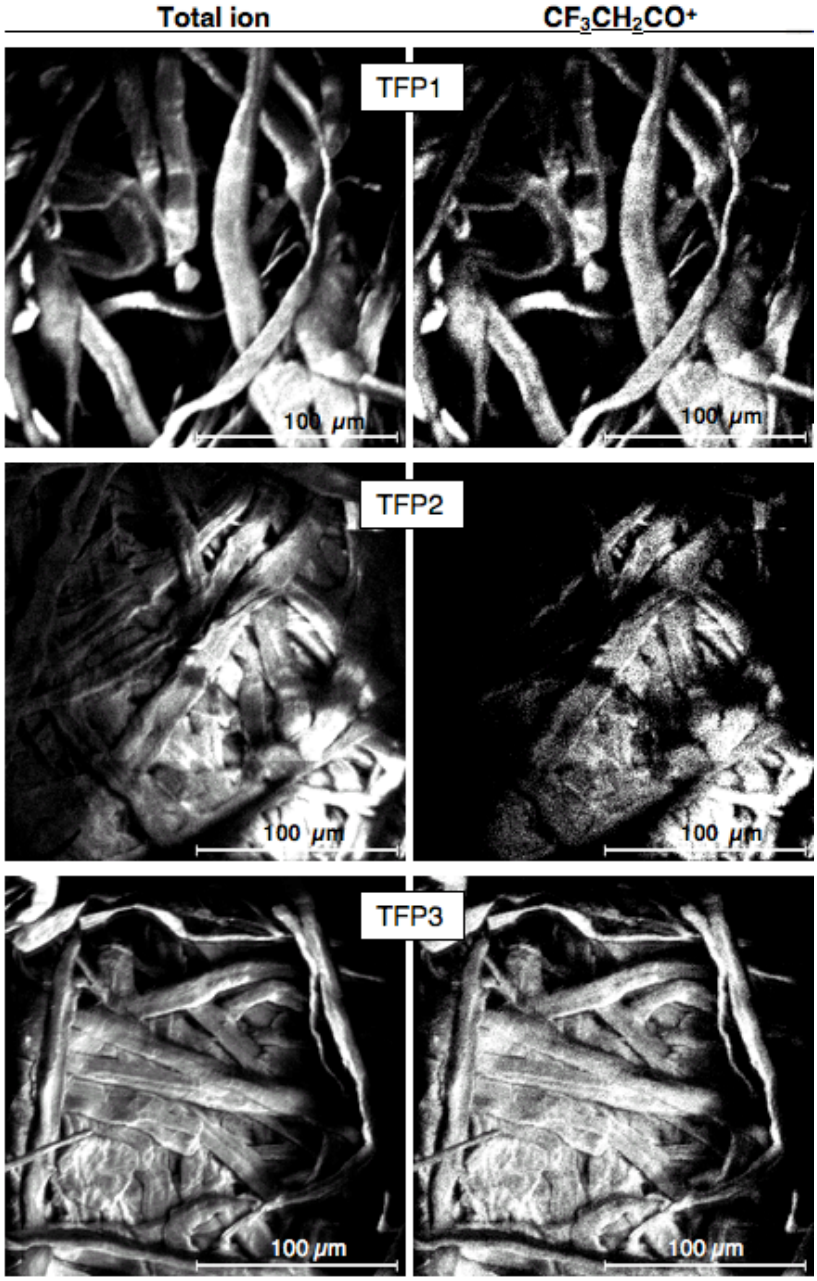

Figure 32. Total ion images and surface distribution of trifluoropropanoyl moieties ($CF_3CH_2CO^+$) appended to the cellulose fibers' surface in the TFP-derivatives.

The surface elemental composition of the fibers before and after modification was also inspected by XPS analysis.

The low resolution XPS spectrum of native cellulose, presented in Figure 33, displayed the predictable peaks related to carbon (C*1s*) and oxygen (O*1s*) at *ca.* 290 eV and 535 eV, respectively. In addition to these two peaks, the low resolution XPS spectra of the perfluorinated cellulose fibers showed the presence of fluorine, giving further

evidence of the occurrence of esterification, as illustrated in Figure 33 for the TFAA2 sample, in which the new peaks appeared at about 690 eV and 40 eV, corresponding to F*1s* and F*2s*, respectively.

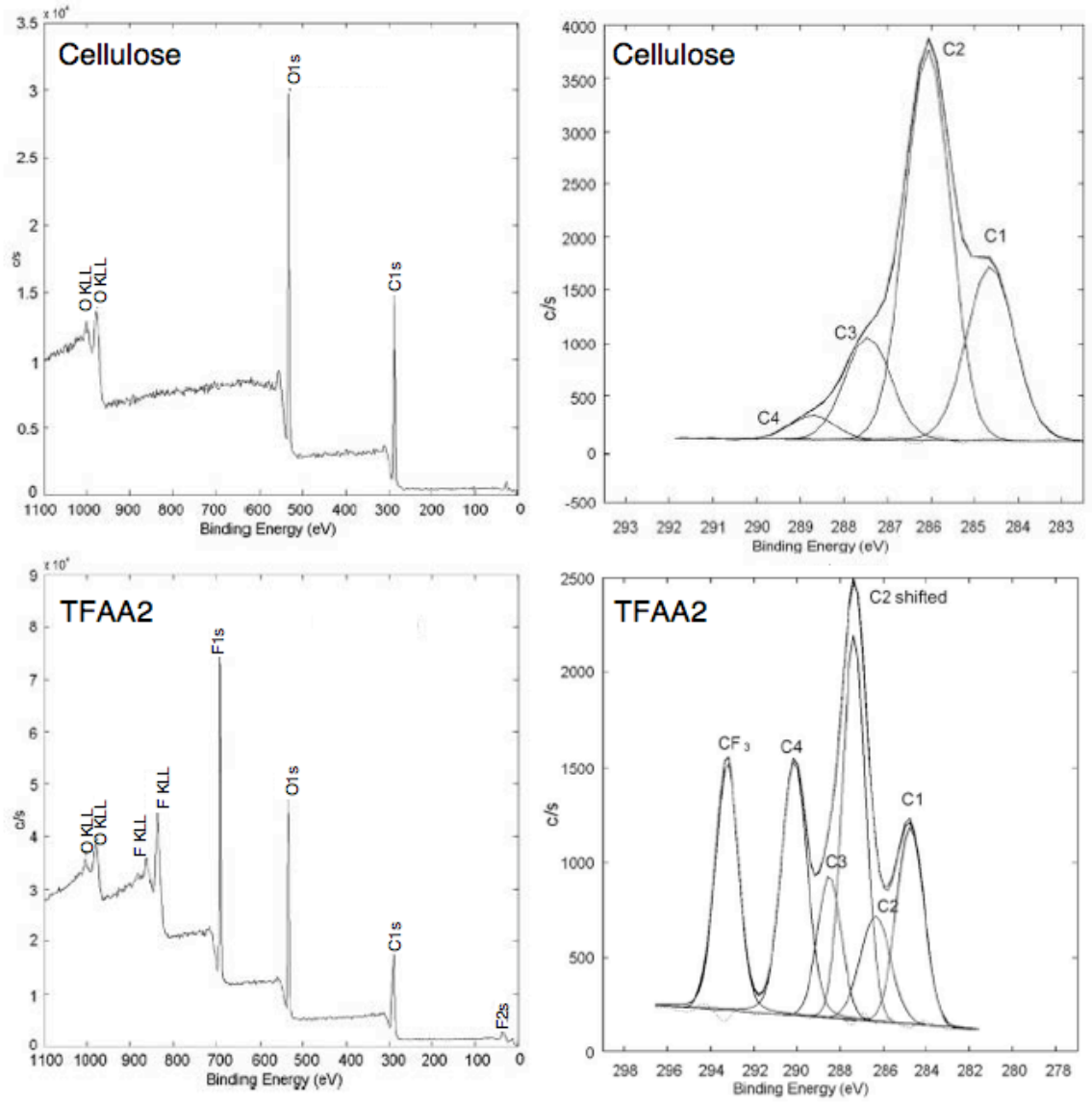

Figure 33. Left-hand side: Low resolution XPS spectra of pristine cellulose fibers and the TFAA2 sample. Right-hand side: C*1s* curve fitting of pristine cellulose and TFAA2 sample.

Table 13 summarizes the surface elemental composition of the pristine cellulose fibers and PFBz- and TFP-derivatives. As can be perceived, after modification, the O/C ratio decreased, as the F/C ratio increased, due to the corresponding increase of fluorine concentration at the surface of the samples, according to the increasing DS values. However, the very fact that this increase was not proportional, *i.e.* a DS=0.014 (PFBz1)

corresponded to a surface fluorine concentration of about 16% and a DS=0.23 (PFBz2), almost 20 times higher, corresponded only to a fluorine concentration of about 22% (less than the double of the first), corroborated the hypothesis of esterification of the amorphous regions in the inner layers of the cellulose fibers.

Furthermore, it was verified that BCPFBz sample possessed a lower amount of fluorine at the surface than its counterpart from vegetable fibers, PFBz2, which should be related to the specific morphology of the bacterial cellulose substrate used here, as previously discussed, and what is coherent with the equally lower DS of this sample compared to that of PFBz2.

Table 13. Low-resolution XPS results of pristine cellulose fibers and PFBz- and TFP-derivatives.

Sample	DS	Low-resolution XPS				
		[O]/%	[C]/%	[F]/%	O/C	F/C
Vegetable Cellulose	—	42.1	57.9	—	0.73	—
PFBz1	0.014	28.4	55.7	15.5	0.51	0.28
PFBz2	0.23	22.9	53.4	21.7	0.4	0.41
PFBz3	0.39	19.0	52.9	26.4	0.36	0.50
TFP1	<0.006	35.6	50.4	14.0	0.71	0.28
TFP2	0.03	29.6	48.6	20.7	0.60	0.42
TFP3	0.30	28.5	49.4	21.6	0.58	0.44
Bacterial Cellulose	—	44.3	55.4	—	0.80	—
BCPFBz	0.16	34.1	48.7	12.5	0.70	0.26

A further analysis on the high-resolution deconvolution of the C*1s* peak (Table 14, Figure 33, and Table 15) revealed the increment of the contribution of C4 carbons (O–C=O) and the appearance of a new carbon environment (CF), assigned to the C–F bonds, as illustrated in Figure 33 for TFAA2. In this figure, the shift of an important fraction of C2 carbons to higher binding energies was due to the presence of the C*–O–C=O ester linkage directly bound to them [280].

Table 14. Correspondence between C1s signals and the type of C environments.

C *1s* signals	**C environment**
C1	C-H, C-C
C2	C-O
C3	O-C-O or C=O
C4	O-C=O
CF	C-F

Table 15. High-resolution deconvolution of C*1s* signals of pristine cellulose fibers and PFBz- and TFP-derivatives.

		High-resolution XPS (Area/%)				
Sample	**DS**	C1	C2	C3	C4	CF
Vegetable Cellulose	—	22.3	58.5	16.0	3.2	—
PFBz1	0.014	16.8	47.1	20.0	5.0	11.1
PFBz2	0.23	7.8	45.4	24.3	8.9	13.6
PFBz3	0.39	6.2	42.4	21.4	11.6	18.4
TFP1	<0.006	6.9	57.0	12.7	7.4	4.8
TFP2	0.03	4.2	44.1	12.6	13.1	10.4
TFP3	0.30	2.1	35.3	12.1	15.4	11.2
Bacterial Cellulose	—	19.9	61.3	15.9	2.8	—
BCPFBz	0.16	10.1	54.7	18.5	4.6	12.1

The CF carbon contributions reflected the extent of surface coverage by the perfluorinated groups. However, it was verified again that the increment was not totally proportional to the DS values, giving additional evidence in favor of in-depth esterification, following the consumption of the more accessible surface OH groups associated with the amorphous cellulose domains.

The presence of C4 carbons in native vegetable cellulose could be related to the presence of partially oxidized hydroxyl groups or hemicelluloses, such as xylans, a fact

that would be coherent with some fragments observed by ToF-SIMS, as already discussed.

1.1.6. Contact Angle Measurements and Determination of the Surface Energy

The contact angles of liquids possessing different surface tensions (Table 8) were measured onto the unmodified and modified cellulose fibers' surface. The liquids used were water, glycerol, formamide, ethylene glycol and diiodomethane, depending on the type of perfluorinated derivative. The average contact angle values measured are registered in Table 16, and it is worth mentioning that the somewhat higher value of glycerol contact angle compared with that of water onto the bacterial cellulose fibers' surface was probably related to the high viscosity of the former, which made its measurements difficult.

Table 16. Contact angles on the pristine and perfluorinated cellulose fibers.

Sample	DS	Contact angles (°)				
		Water	Glycerol	Formamide	Ethylene glycol	Diiodomethane
Vegetable Cellulose	—	56±1	—	33±2	50±1	37±2
TFAA1	0.04	126±2	—	115±2	112±1	104±2
TFAA2	0.14	126±3	—	115±1	109±3	103±3
TFAA3	0.30	119±2	—	100±4	80[a]	94±3
PFBz1	0.014	120±1	105±2	96±5	—	71±6
PFBz2	0.23	124±2	108±3	95±6	—	73±1
PFBz3	0.39	128±1	111±6	107±2	—	82±2
TFP1	<0.006	113±2	—	—	—	84±2
TFP2	0.03	117±1	—	—	—	86±2
TFP3	0.30	122±2	—	—	—	91±4
Bacterial Cellulose	—	46±0.1	63	36±0.1	—	40±3
BCPFBz	0.16	103±2	90±3	78±4	—	64±3

[a]Unreliable values: the drops were rapidly adsorbed onto the sample's surface.

The significant increase in the hydrophobic character of the fibers after chemical modification was evidenced by the high contact angle values, not only with water, but also with the other polar liquids, namely glycerol (PFBz-derivatives), formamide and ethylene glycol (TFAA-derivatives) (Table 8). Interestingly, even for very low DS values, as in the case of the TFAA1 (DS= 0.04), PFBz1 (0.014) and TFP1 (<0.006) samples, the surface showed to be highly hydrophobic, which suggested that an extensive surface coverage of the cellulose fibers with the perfluorinated moieties is not necessary to attain a highly hydrophobic character. Indeed, the contact angle of polar liquids did not vary significantly for higher DS values, which is in good agreement with the XPS results, giving evidence for in-depth esterification. For the TFAA3 sample, which was the trifluoroacetylated derivative that possessed the highest DS value (DS= 0.30), the possibility of partial degradation previously mentioned, could constitute an explanation for the slightly lower contact angle values with the polar liquids.

On the other hand, the equally high contact angle values with the non-polar diiodomethane (Table 8), indicated that the modified cellulose fibers had also acquired a lipophobic behavior. This bi-phobic character is typical of perfluorinated materials [214], such as poly(tetrafluoroethylene), and confirms here the strong role of the perfluorinated moieties at the surface of the modified samples.

By means of the Owens-Wendt equation (Equation 2), using the values of the testing liquids' surface tension and their contact angles (Table 8 and Table 16, respectively), it was possible to estimate the surface free energy of the unmodified and modified cellulose fibers, as well as its polar and dispersive components.

After modification, the cellulose fibers attained very low surface energy values, varying in the range 6.7-26.7 $mJ.m^{-2}$, comparatively to about 50 $mJ.m^{-2}$ typical for the pristine cellulose fibers, as depicted in Figure 34. Moreover, it is very important to emphasize the particularly accentuated decrease in the polar component, in some instances a value close to 0 (Figure 34), caused by the functionalization of the OH functions by the perfluorinated moieties, which explains the high water repellency, *i.e.* the cohesive forces in water became higher than its adhesion ability to the samples' surfaces. The dispersive contribution to the surface energy also decreased, albeit to a minor degree (Figure 34). Furthermore, the low surface energy values attained are in excellent

agreement with those obtained in a similar study using perfluoro oligoethers as grafted moieties [268].

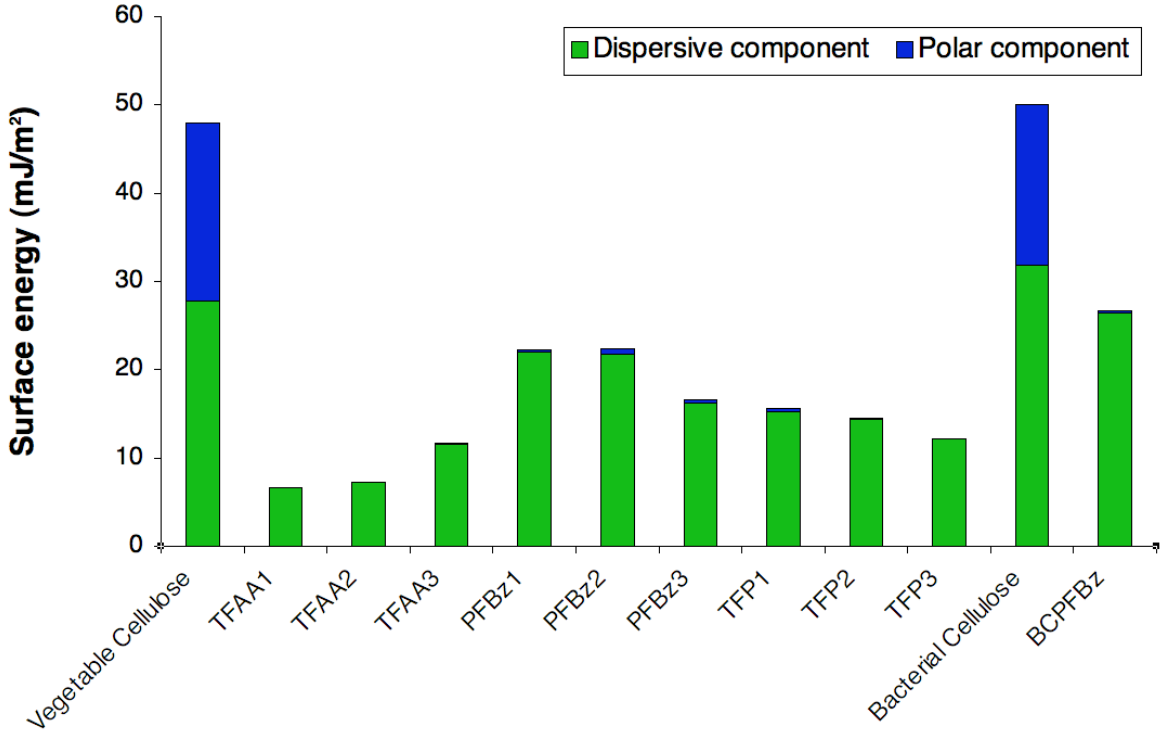

Figure 34. Surface energy, and its respective dispersive and polar components, of cellulose fibers before and after modification with the perfluorinated reagents.

Thus, as desired, it was verified that the chemical modification succeeded in lowering the surface energy of the cellulose fibers, conferring them new interesting properties, namely a dual-phobic character.

Additionally, it is worth noting that despite the fact that the trifluoropropanoylated cellulose derivatives exhibited slightly lower amounts of fluorine at their surface than the pentafluorobenzoylated counterparts, as assessed by XPS, they possessed lower surface energies as well. This observation is related with the specific nature of the perfluorinated moiety appended to the surface of the fibers, since CF_3 moieties are known to display lower surface energies than C_6F_5 functions, as already shown in previous studies [281].

1.1.7. Hydrolytic Stability of the Perfluorinated Cellulose Derivatives

Trifluoroacetates are known to be much more sensitive to hydrolysis than the corresponding acetates, even under very mild conditions [282]. In particular cellulose trifluoroacetates were also shown to undergo prompt hydrolysis [36], as illustrated by their total hydrolysis with neutral water within few minutes when dissolved in DMF [265].

In order to verify this property, reversibility essays were performed, specifically with the TFAA1 sample, testing two different parameters, *viz.* (i) floating or stirring in liquid water and (ii) exposure of the solid fibers to variable percentages of relative humidity (RH) in the surround atmosphere. The extent of hydrolysis was followed by FTIR-ATR analysis, through the decrease in the intensity of the carbonyl ester band at about 1800 cm^{-1}, and was also evaluated by water contact angle, through the observation of its decrease against time.

Aiming to test the importance of stirring, samples were suspended in water (pH 7), at room temperature, with and without stirring, during a certain period of time. As it is possible to verify in Figure 35, when the sample was just suspended in neutral water without stirring, the cleavage of the trifluoroacetyl moieties was completed within one week at room temperature, as proved by the total disappearance of the carbonyl ester band. Although after 3 days of contact with water, over 90% of the ester groups had been removed, the sample was still floating, indicating once again that the presence of a small amount of perfluorinated groups at the surface of the cellulose fibers was enough to provide them with a hydrophobic character.

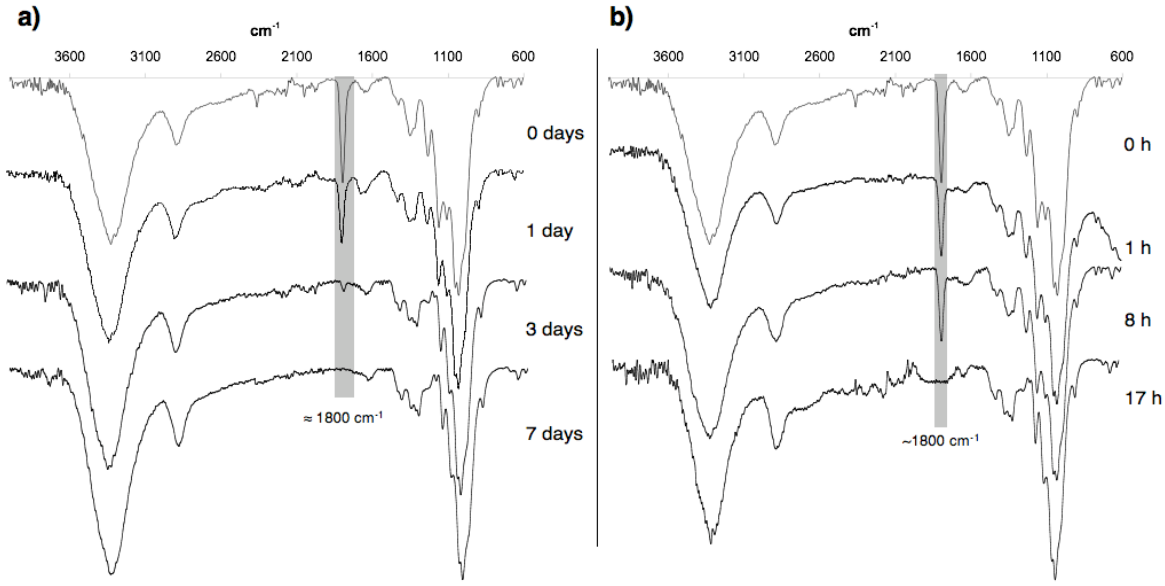

Figure 35. Hydrolysis progress of the trifluoroacetyl groups in the TFAA1 samples suspended in neutral water (a) without and (b) with stirring.

However, as expected, when the sample remained in contact with water under stirring, it was verified that the total hydrolysis was attained more rapidly, as can be seen in Figure 35, where the complete disappearance of the carbonyl ester group band at 1800 cm^{-1} took only about 17 h, indicating that, as consequence of stirring, a more frequent contact of water molecules was attained.

In another experiment, a drop of water was deposited onto the surface of the TFAA1 sample (Figure 36), which gave rise to a progressive decrease in the contact angle with time, and this phenomenon culminated in the absorption of the drop after about 100 min, suggesting that a sufficient number of OH groups had been regenerated, thus facilitating its capillary penetration.

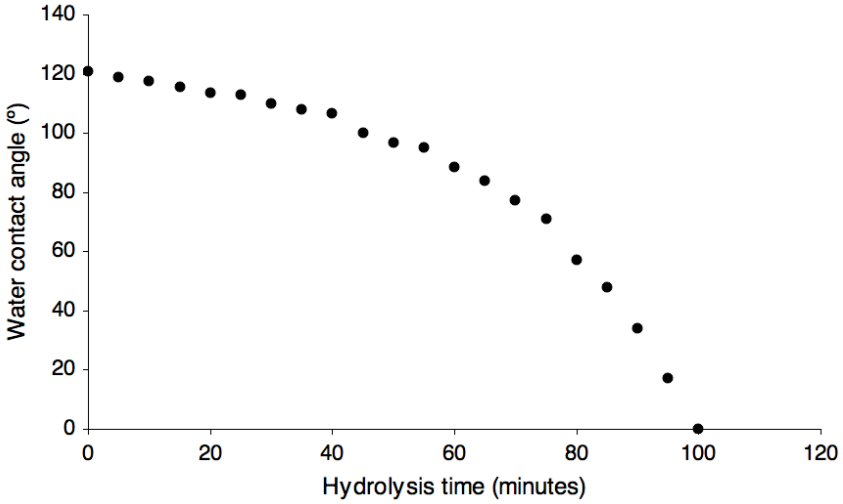

Figure 36. Time evolution of the water contact angle onto the TFAA1 sample.

For the relative humidity (RH) study, three systems were tested, namely surrounding atmospheres containing 30, 52 and 100% RH, and it was verified, as expected, that the progress of the trifluoroacetylated cellulose fibers' hydrolysis was strongly influenced by this parameter (Figure 37). Figure 37a displays the progress of trifluoroacetyl groups' hydrolysis in the TFAA1 sample with time and RH, as followed by FTIR-ATR, which, in this case, was expressed by the decrease in the ratio between the absorbance intensity of the peak related to the carbonyl ester group at 1800 cm^{-1} and the intensity of the C-O stretching peak, inherent to the cellulose structure, at about 1026 cm^{-1} (Table 9). As it is possible to verify, in the system with 100% RH, the peak related to the carbonyl function had totally disappeared within 4 days, which means that the sample's trifluoroacetyl groups were completely hydrolyzed within that period of time, as compared with 7 days with the still liquid water experiment mentioned above. It was thus possible to conclude that the penetration of water molecules from a moisture-saturated atmosphere into the modified fibers was more effective than that of liquid water into the same floating sample. This fact is probably associated with the physical state in which water was present in each case, since in the gaseous state its intermolecular interactions were weaker and thus its molecules possessed more mobility, which could promote a more intimate interaction with the sample, and hence with the trifluoroacetylated groups at its surface. It is moreover possible that the trifluoroacetic acid generated on the fibers in the moisture experiment accelerated catalytically the pursuit of the hydrolysis, whereas in the liquid water experiment this effect would not have occurred because of the rapid diffusion of the acid into the liquid medium. Furthermore, the water contact angle measurements

onto the sample surface (Figure 37b) corroborated the FTIR-ATR results, since within 4 days the initially high water contact angle (*ca.* 120º) dropped to the typical values for untreated cellulose (~50º), indicating that virtually all the CF_3CO groups had been removed.

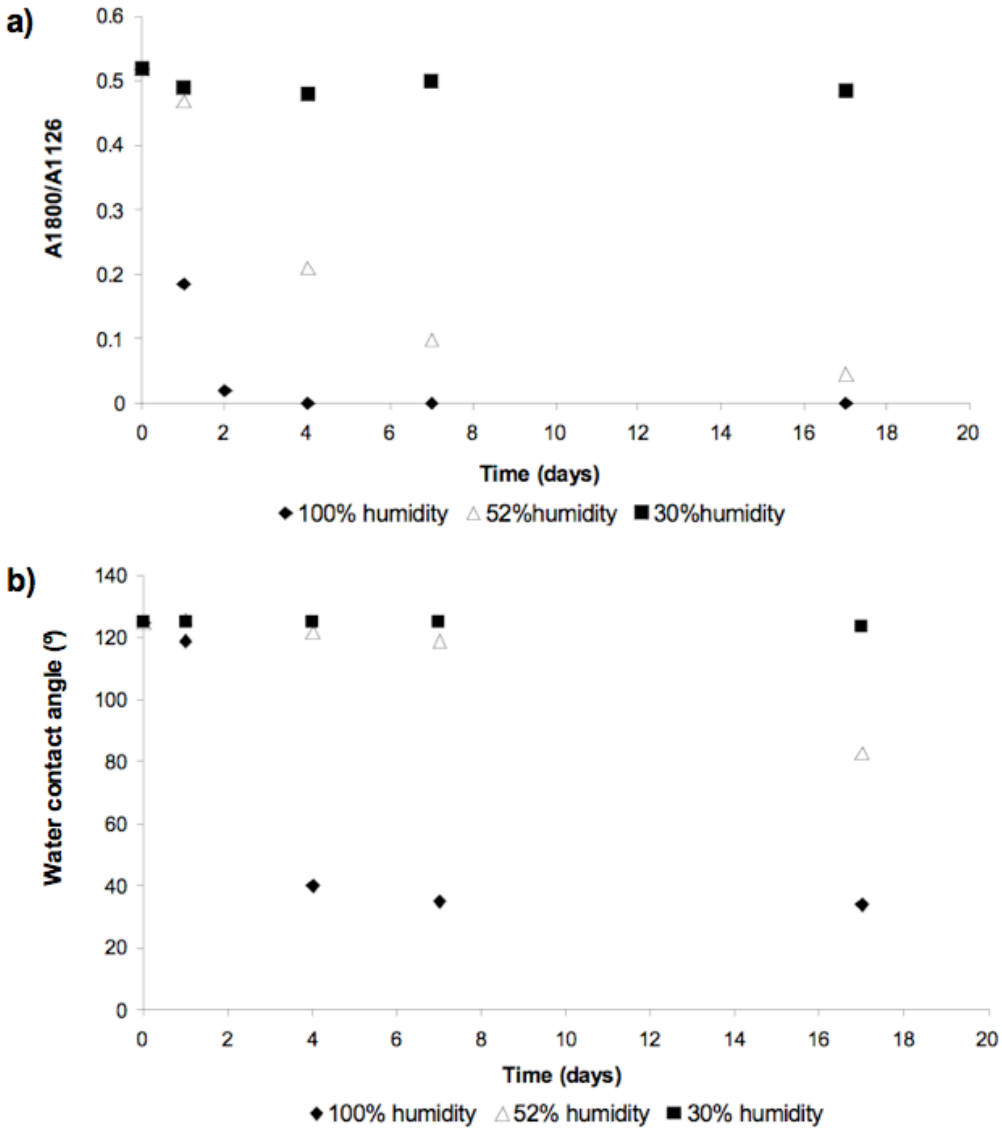

Figure 37. Progress of TFAA1 trifluoroacetylated groups' hydrolysis with time and RH (30, 52 and 100%), as followed by a) FTIR-ATR and b) water contact angle measurements.

Conversely, with only 30% RH, the modified fibers were very stable, since less than 20% of the trifluoroacetyl groups were hydrolyzed within 17 days (Figure 37a), a feature which was confirmed by the water contact angle results that did not vary significantly within that period of time (Figure 37b). Finally, at 52% humidity, an intermediate situation was observed, with about 50 and 90% of the ester groups

hydrolyzed within 4 and 17 days, respectively (Figure 37a). Interestingly, the water contact angle remained close to 120º after 50% of the trifluoroacetylated groups have been removed, and even when 90% of the ester groups were hydrolyzed, the sample's surface was still slightly "hydrophobic", with a water contact angle of about 80º (Figure 37b). These observations confirm, once more, that an extensive coverage of the fibers by perfluoro-moieties is not indispensable to attain their highly hydrophobic character.

Moreover, these reversibility essays permitted to verify that, if desired, the hydrophobic character of the trifluoroacetylated cellulose fibers can be modulated in time by adequately controlling the atmospheric RH.

Regarding the hydrolytic stability of the pentafluorobenzoylated and trifluoropropanoylated cellulose fibers, both were also suspended in water at room temperature (*ca.* 21 ºC), with and without stirring, and the extent of their hydrolysis followed by FTIR-ATR through the decrease in the intensity of the carbonyl ester bands at about 1740 and 1760 cm^{-1}, respectively, and, additionally, by measuring the water contact angle. In the case of the PFBz-derivatives both modified pulp fibers and filter paper were studied, in order to establish the effect of the fibers morphology on the hydrolysis of the pentafluorobenzoyl moieties.

These two types of cellulose perfluorinated derivatives were in general very stable towards hydrolysis when suspended in distilled water, with or without stirring, as illustrated in Figure 38 for the PFBz-derivatives. In the same figure it is possible to perceive that the cellulose pulp fibers were moderately more sensitive to hydrolysis than the filter paper, particularly under vigorous stirring, where about 40% of the pentafluorobenzoyl groups were hydrolyzed within 4 days. This difference was attributed to a topochemical feature related to the lower accessibility of the hydrolysable moieties in the case of the more compact morphology of the filter paper, compared with that of the pulp fibers.

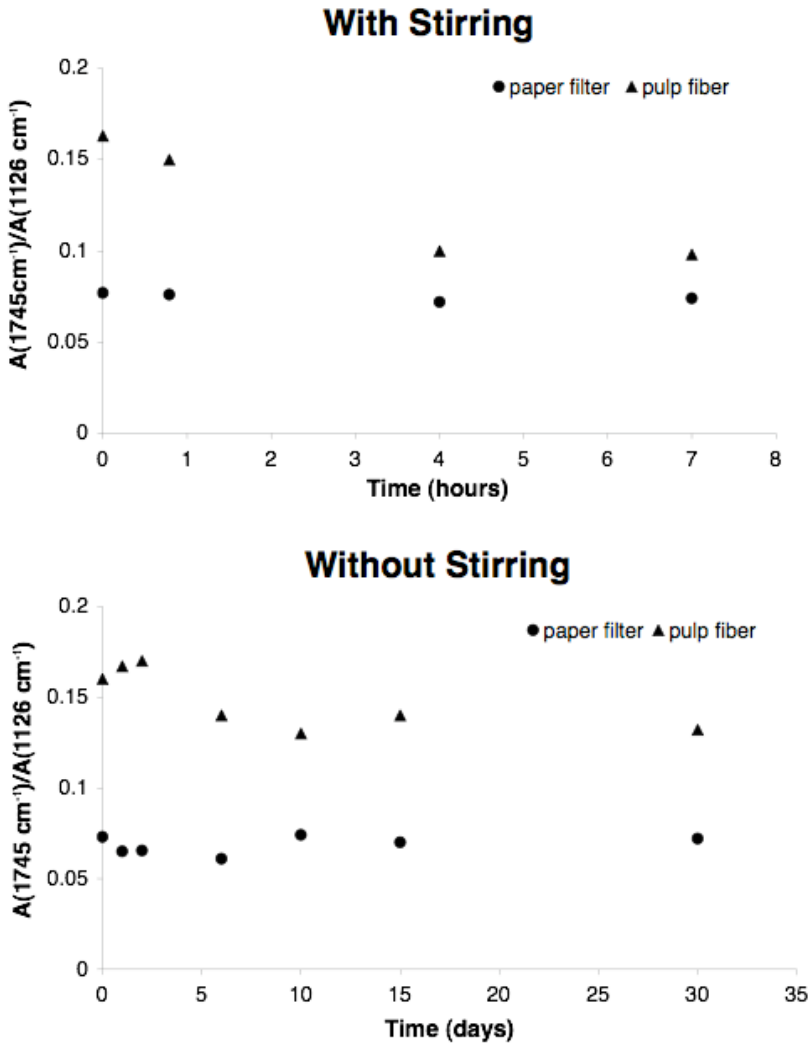

Figure 38. Variation of the extent of hydrolysis of the pentafluorobenzoyl moieties as a function of time, stirring, and cellulose substrate.

The high stability towards hydrolysis of the PFBz- and TFP-derivatives was also confirmed by water contact angle measurements. As shown in Figure 39, for the case of PFBz-derivatives, both hydrolysis with and without stirring did not affect significantly the water contact angle of the modified samples, since they did not vary appreciably with time (θ_w=102-123º).

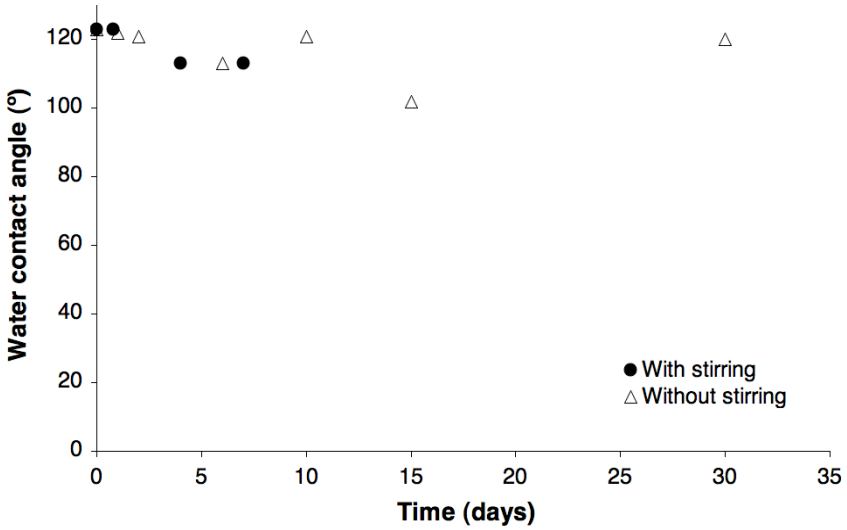

Figure 39. Variation of the water contact angle as a function of hydrolysis time and stirring for PFBz2 (filter paper).

The increased stability of these fluorinated cellulose derivatives, compared with that of their trifluoroacetylated counterparts, is attributed to the fact that the fluorine atoms are not bound to the carbon atom directly linked to the carbonyl ester group [283], thus permitting a higher stability of the ester function. In other words, these situations were approaching that of common carboxylic esters.

Following the hydrolytic stability under neutral conditions, similar hydrolysis experiments in acidic (pH 4) (for PFBz-derivatives) and alkaline (pH 9 and pH 12, the latter only for TFP-derivatives) media, under stirring and at room temperature, were carried out. In the former conditions, no hydrolysis was detected after 5 h (Figure 40), whereas in the alkaline conditions, *ca.* 25% of the pentafluorobenzoylated groups were removed after 5 h (Figure 40) and 40% of trifluoropropanoylated groups after 96 h, at pH 9 (Figure 41). Moreover, within the same period of time (96 h), at pH 12 all the trifluoropropanoylated groups were removed (Figure 41).

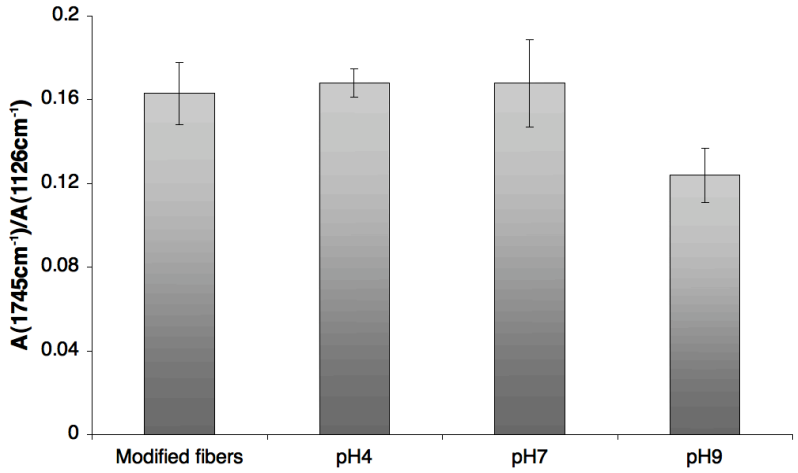

Figure 40. Hydrolysis, at room temperature and under stirring for 5 h, of the pentafluorobenzoyl moieties as a function of pH, as determined by FTIR-ATR, for PFBz2.

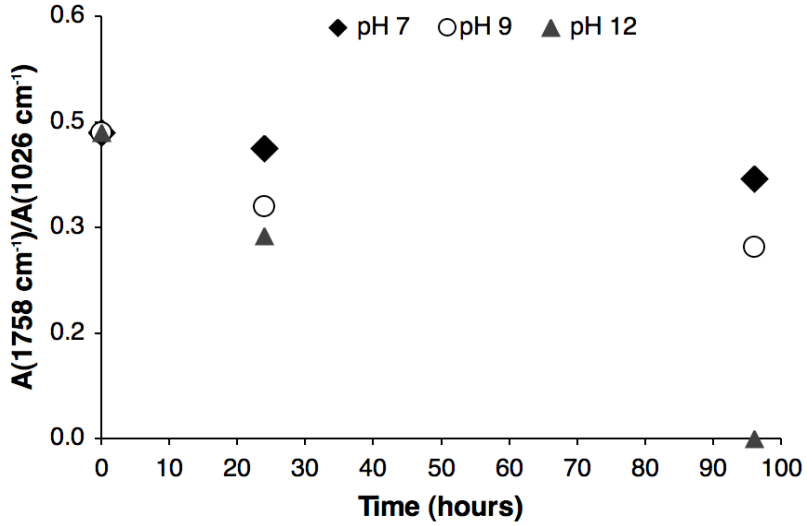

Figure 41. Hydrolysis, at room temperature and under stirring, of the trifluoropropanoyl groups as a function of pH and time, as determined by FTIR-ATR, for TFP4.

The total removal of the perfluorinated moieties by base-catalyzed hydrolysis is therefore feasible, as previously reported in the case of cellulose fatty acid esters [284].

Interestingly, the different hydrolytic stability of the various perfluorinated cellulose fibers constitutes a promising context in which different practical requirements in terms of time-scale of the return of hydrophilicity would be satisfied by choosing the appropriate derivative.

1.2. Conclusions

Cellulose fibers were readily converted into highly hydrophobic and lipophobic materials (DS= <0.006-0.39) by their simple esterification with three perfluorinated reagents, specifically TFAA, PFBz and TFP, as evidenced by the high contact angles obtained with both polar and non-polar liquids, respectively.

The prominent change in the surface properties of these cellulose derivatives, was attributed to the very low surface energies attained, especially the polar component, comparatively to the pristine cellulose fibers, as a result of the introduction of the perfluorinated moieties.

Trifluoropropanoylated samples possessing low percentage of fluorine at their surface, displayed lower surface energy than the pentafluorobenzoylated counterparts bearing higher amounts of fluorine at that location, due to the specific nature of the CF_3- and C_6F_5- moieties, since the former are known to display correspondingly lower surface energy than the latter [281].

The surface coverage of the cellulose fibers by the perfluorinated groups, as assessed by XPS, apart from being quite heterogeneous (ToF-SIMS imaging), did not follow the increase in the DS values, which is in conformity with the values observed for the contact angles and surface energies, giving evidence of in-depth esterification, associated with the amorphous cellulose domains.

Indeed, the omniphobic character was exhibited even by samples with very low DS values, and was not significantly affected by increasing them, which demonstrated that a high surface coverage of the cellulose fibers with the perfluorinated moieties was not necessary for its manifestation. This observation can constitute a key factor for potential applications of these cellulose perfluorinated derivatives. In actual fact, in comparison with the perfluorinated counterparts derived from homogeneous or uncontrolled heterogeneous reaction conditions found in the literature [265-267, 273, 275], the derivatives prepared here possess the advantage of new surface features that were acquired without the need of cellulose dissolution and/or total functionalization of the OH groups, a fact that, moreover, ensures the preservation of the cellulose bulk features, including its good mechanical properties.

Regarding the hydrolytic stability of these novel perfluorinated cellulose derivatives, they exhibited two different behaviors. On the one hand, the trifluoroacetylated cellulose fibers showed to be very labile, being readily hydrolyzed even in a neutral

medium. On the other hand, the pentafluorobenzoylated and trifluoropropanoylated derivatives demonstrated to be more stable towards hydrolysis in neutral, and even acid (pH 4), media, but could, however, be hydrolyzed in a highly alkaline suspension (pH 9 and pH 12, respectively). The different hydrolytic behaviors were attributed to the presence of a carbon-spacer between the carbonyl ester group and the fluorocarbon moieties in the latter derivatives, which ensured a higher stability of the ester function towards hydrolysis, and could be exploited for the preparation of bi-phobic materials that require different stability kinetic profiles.

On the one hand, TFAA-derived fibers might be useful for applications where the hydrophobic character is just required for a short period of time. Thus, for instance, certain operations in papermaking or paper and cardboard processing would be improved by such temporary low-energy surface of the cellulose fibers, whereas the final materials would recover the “normal” properties of cellulose. Another realm in which this specific behavior would be useful concerns the elaboration of containers for young nursery plants, which must retain water for days, before being transferred into the soil. The use of these cellulose derivatives would insure water tightness and, after hydrolysis, they would biodegrade in the soil and allow the roots to propagate. It is moreover well known that the released trifluoroacetic acid would not interfere with plant growth [285]. The reverse situation can also be envisaged, where the container would act as a barrier to water penetration during an initial stage and then become progressively more hydrophilic. Other specific packaging situations seem conducive to the use of these materials, *e.g.*, when a wrapping should initially be impenetrable to both aqueous and oily or greasy substances and the package is then stored in subfreezing conditions (absence of hydrolysis). Its subsequent commercialization would imply its return to room temperature and a short time delay (during which the barrier properties of the envelope are maintained) before its contents are removed, as in the case of frozen foods. It is important to underline that even in the case of high surface modification, the quantities of trifluoroacetic acid released during hydrolysis in these applications would be minimal and harmless, once rapidly converted into one of its salts [286].

On the other hand, when long-term stability of the modified fibers in contact with moisture is necessary, PFBz- and TFP-derived fibers can be used. These perfluorinated derivatives could be potentially employed in the preparation of composite materials with adequate apolar matrices, as well as in packaging and textiles. Nevertheless, in any case, at the end of their useful life-cycle, these perfluorinated cellulose materials will always be

readily recycled/degraded by restoring the characteristic hydrophilic behavior of pristine cellulose fibers through alkaline hydrolysis. The perfluorinated acids or corresponding salts released in this process are certainly subject of concern, but, within the conditions discussed here, their amount would be so low that it would not constitute a serious problem.

In this sense, the controlled heterogeneous modification of cellulose fibers with the perfluorinated reagents prepared in this work, despite its more fundamental connotation, seems to constitute a promising approach for the development of new functional biopolymeric materials.

2. Preparation of Class-II Organic-Inorganic Hybrid Cellulose Derivatives

The possibility of combining the properties of organic and inorganic substances into just one material constitutes the main driving force for the preparation of organic-inorganic hybrid materials.

Here cellulose was used as the organic component, which was covalently linked to an inorganic phase by means of the silane-coupling agent (3-isocyanatepropyl)triethoxysilane (ICPTEOS), giving rise to class-II organic-inorganic hybrid materials.

The modification with ICPTEOS had already been applied to chitosan for the preparation of class-II organic-inorganic hybrid materials [287]. Additionally, it has also been employed for the preparation of cellulose carbamate-silica hybrids with potential of being applied as chiral stationary phases in chromatography, although with different cellulose substrates and preparation procedures [288].

2.1. Controlled Heterogeneous Modification of Cellulose with (3-Isocyanatepropyl)triethoxysilane

The system investigated for the preparation of class-II organic-inorganic hybrid cellulose derivatives called upon the heterogeneous modification of cellulose fibers with ICPTEOS as illustrated in Figure 42, followed by the acid hydrolysis of the ethoxy groups of the siloxane moieties, in some cases in the presence of other siloxanes bearing specific side chains (Figure 42). This last step aimed, on the one hand, at generating the adequate surface morphology of the siloxanes, and, on the other, at promoting the insertion of specific side chains, allowing tailoring of the final properties of the hybrid materials in terms of the desired applications. Thus, the hydrolysis in the presence of tetraethoxysilane (TEOS) was aimed at building a three-dimensional inorganic coating onto the fibers, based on the formation of additional multiple Si-O-Si bonds. Alternatively, the hydrolysis in the presence of *1H,1H,2H,2H*-perfluorodecyltriethoxysilane (PFDTEOS) was performed in order to induce an omniphobic character at the surface of the ensuing fibers, based on the

well-known features associated with perfluorinated moieties [214], already discussed in the previous section.

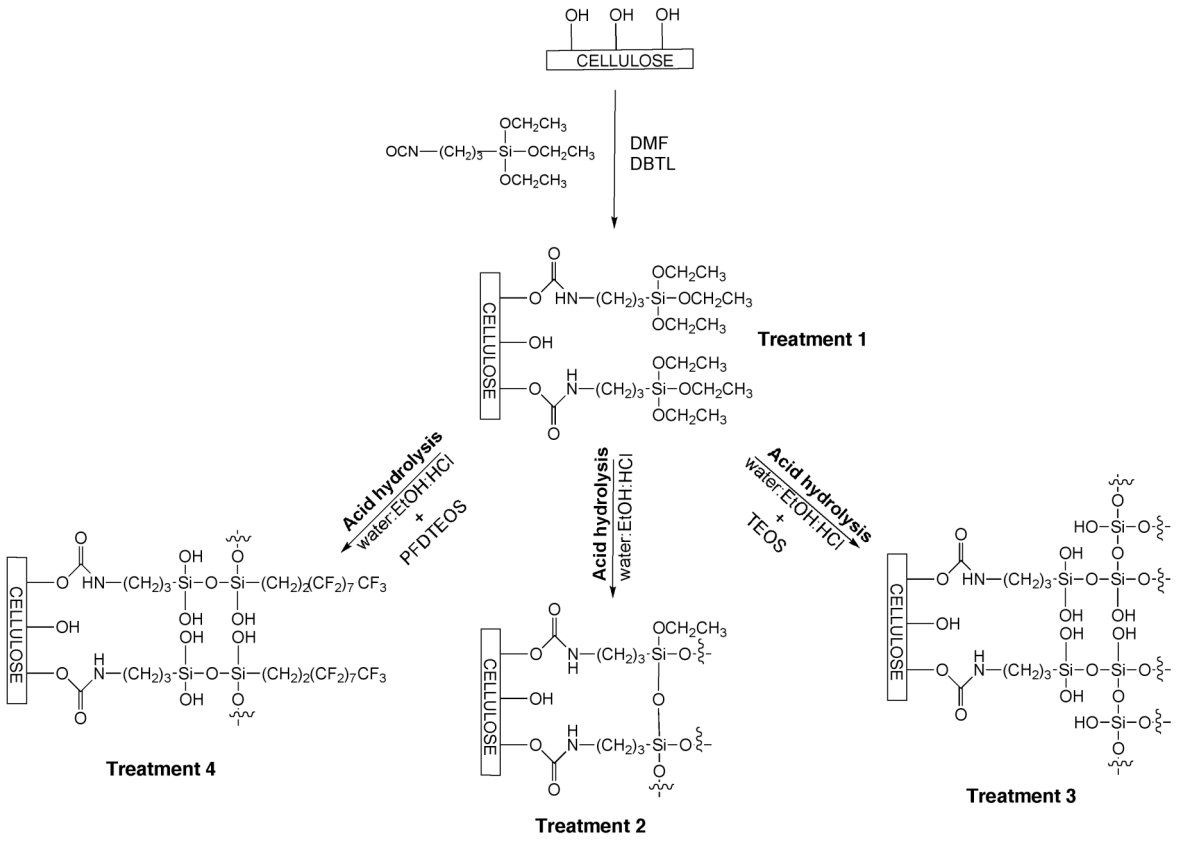

Figure 42. Schematic representation of the chemical modification of cellulose fibers with ICPTEOS and subsequent acid hydrolysis treatments of the ensuing cellulose fibers.

Within this approach, different OH:ICPTEOS ratios were tested, namely 0.4, 0.6 and 1 equiv. relative to the total cellulose OH functions, in order to evaluate the effect of this parameter on the extent of the reaction and on the properties of the ensuing cellulose derivatives. The organic-inorganic hybrid cellulose derivatives prepared according to the reaction conditions tested are listed in Table 17.

Table 17. Identification of the organic-inorganic hybrid cellulose derivatives prepared in this study.

Sample	[OH]:[ICPTEOS] ratio	Reaction time (h)	Subsequent treatment
Cel	—	—	—
A1	1:0.4	5	—
A2			Acid hydrolysis
A3			Acid hydrolysis in the presence of TEOS
A4			Acid hydrolysis in the presence of PFDTEOS
B1	1:0.6	5	—
B2			Acid hydrolysis
B3			Acid hydrolysis in the presence of TEOS
B4			Acid hydrolysis in the presence of PFDTEOS
C1	1:1	24	—
C2			Acid hydrolysis
C3			Acid hydrolysis in the presence of TEOS
C4			Acid hydrolysis in the presence of PFDTEOS

2.1.1. FTIR-ATR Spectroscopic Analysis

The progress of the reaction of the cellulose fibers with ICPTEOS, as well as the subsequent hydrolysis of the siloxane groups, were followed by FTIR-ATR spectroscopy. The success of the modification was clearly confirmed, mainly on the basis of the appearance of a new band at *ca.* 1700 cm^{-1} (Figure 43), attributed to the free C=O stretching mode of the urethane moieties. Moreover, in the case of C1 (Table 17), another band appeared at 1650 cm^{-1}, which is typical of the hydrogen-bonded C=O stretching mode of urethanes (Figure 43) [276]. Additionally, the emergence of a new peak at about 1530 cm^{-1}, associated with the C–N vibrations, gave further evidence of the success of these reactions. Furthermore, the appearance of a new peak around 2960 cm^{-1}, typical of C–H bond stretching vibrations in CH_3, indicated the presence of methyl groups from the ethoxysilane moieties. The intensity of this peak was very modest in the case of C1, as a result of the partial hydrolysis of the ethoxy groups provoked by residual moisture, as

suggested by the ^{29}Si CP-MAS NMR results presented below. Finally, the occurrence of new absorptions at 1250 and 760 cm^{-1}, typical of methylene symmetric deformation and rocking vibrations from the Si–CH_2 groups, respectively, gave further confirmation of the presence of silane-containing moieties. The results shown in Figure 43 also indicated that the extent of the modification increased with increasing amounts of ICPTEOS (from sample A1 to sample B1), as well as with the simultaneous increase in the amount of ICPTEOS and in the reaction time (from sample B1 to sample C1), as monitored by the peak at *ca.* 1700 cm^{-1}.

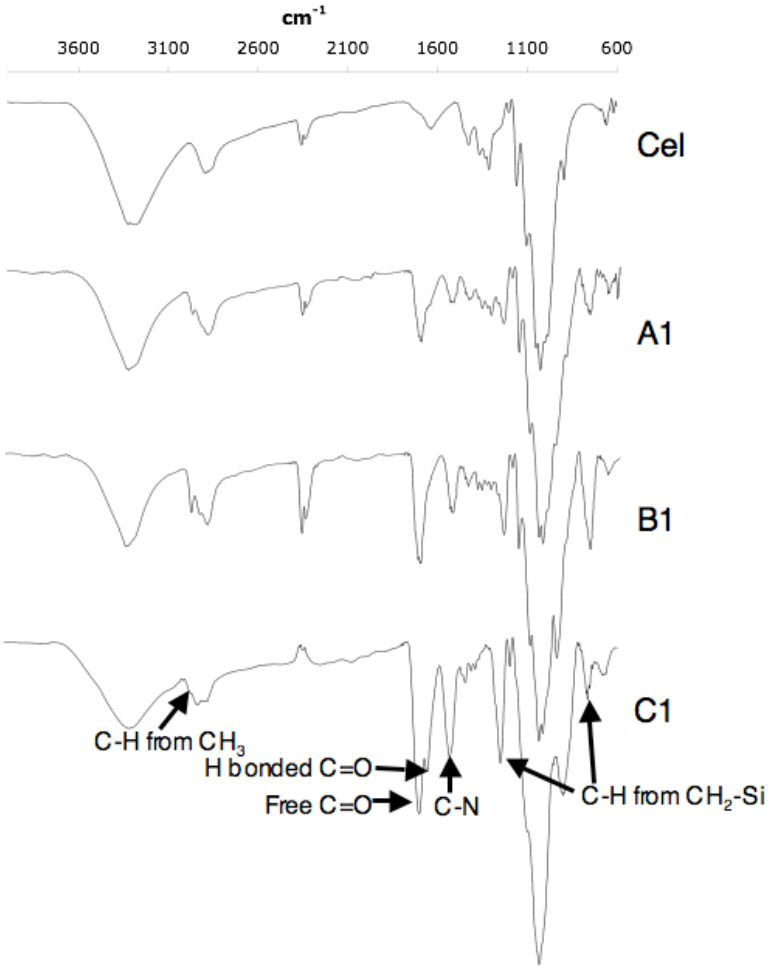

Figure 43. FTIR-ATR spectra of cellulose fibers before and after modification with ICPTEOS at different ratios (Treatment 1).

After the acid hydrolysis, it was observed that, for the samples prepared by the reaction with the 1:1 ratio and 24 h reaction time (series C), the doublet of the urethane bands in the C1 FTIR-ATR spectrum had converged into a single peak at *ca.* 1700 cm^{-1},

revealing that this treatment had ‘‘broken” the hydrogen bonds established by the C=O of some urethane groups (Figure 44), possibly because of the formation of new Si–O–Si bridges. This treatment also induced the complete loss of the peak related to the CH_3 groups, which indicated its effectiveness, *i.e.*, the near-complete hydrolysis of the ethoxysilane groups. These observations are in good agreement with the evolution of the ^{29}Si CP-MAS NMR results discussed below, which clearly demonstrated the increase in the content of Si–O–Si bridges, with the corresponding decrease in Si–OCH_2CH_3 moieties. The presence of Si–OH or Si–O–Si bridges is not easily detected by FTIR-ATR, since the typical vibration frequencies of these groups around 950 and 1100 cm^{-1}, respectively, are masked by the large and intense cellulose C–O stretching band centered at 1026 cm^{-1} (Figure 44).

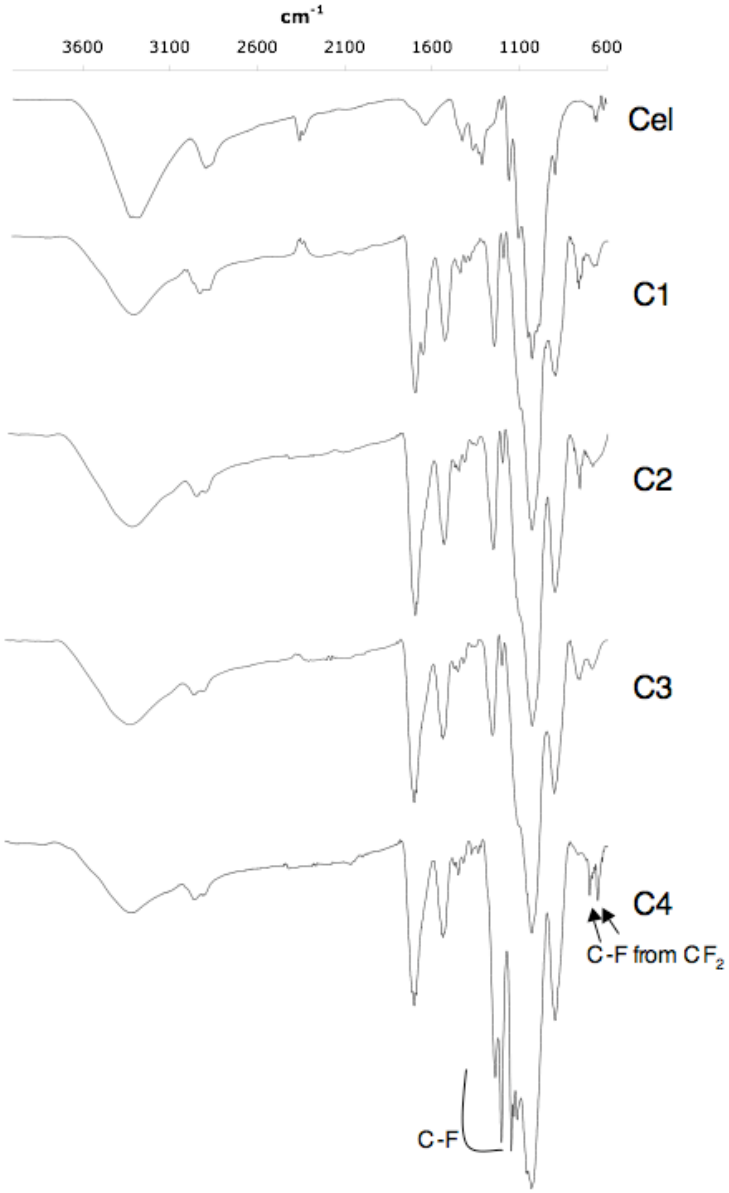

Figure 44. FTIR-ATR spectra of cellulose fibers before and after modification with 1 equiv. of ICPTEOS and subsequent acid hydrolysis treatments (Series C).

The FTIR-ATR spectra of the samples obtained after acid hydrolysis in the presence of TEOS (A3, B3 and C3), represented by C3 in Figure 44, were identical to those of the samples obtained by the simple acid hydrolysis (A2, B2 and C2), and thus no further information could be retrieved.

The spectra of the samples obtained after acid hydrolysis in the presence of PFDTEOS (A4, B4 and C4) showed new intense absorptions in the range 1100–1235 cm^{-1} (Figure 44), characteristic of C–F stretching modes [276]. Moreover, two new peaks at *ca.* 650 and 705 cm^{-1} were also present in these spectra, which were attributed to the

combination of CF_2 group rocking and wagging modes [289]. These observations clearly demonstrated the insertion of perfluorinated moieties into the inorganic network at the fiber surface.

2.1.2. Elemental Analysis

The elemental analysis (EA) results of all the cellulose hybrid materials are given in Table 18. Apart from carbon and hydrogen present in the unmodified cellulose fibers, the cellulose hybrid materials also contained a further contribution of silicon and nitrogen, due to the incorporation of the ICPTEOS moieties, and the former element being also derived from the other siloxanes used during the acid hydrolysis treatments, namely TEOS and PFDTEOS. Furthermore, when the hydrolysis treatment was conducted in the presence of PFDTEOS, fluorine was also detected in the EA of the respective derivatives (A4, B4 and C4), which gave further evidence of the occurrence of the actual condensation of the perfluorinated siloxane molecules with the silane-moieties appended at the cellulose fibers in the initial treatment.

Table 18. Elemental composition of unmodified cellulose and all the hybrid materials.

Sample	C (%)	H (%)	Si (%)	N (%)	F (%)	Si/C	Si/N	F/C	F/N
Cellulose	42.8	6.3	—	—	—	—	—	—	—
A1	39.9	6.4	3.0	1.8	—	0.08	1.70	—	—
A2	39.7	6.2	3.1	1.6	—	0.08	1.87	—	—
A3	37.4	6.0	4.4	1.5	—	0.12	2.88	—	—
A4	30.5	3.4	4.3	0.5	40.3	0.14	8.19	1.32	77.5
B1	39.2	6.2	5.0	2.6	—	0.13	1.95	—	—
B2	37.8	6.0	5.0	2.7	—	0.13	1.86	—	—
B3	34.9	5.8	6.8	2.6	—	0.20	2.62	—	—
B4	28.9	2.9	5.2	0.8	42.3	0.18	6.99	1.47	56.4
C1	35.4	6.2	9.4	5.2	—	0.26	1.79	—	—
C2	33.5	5.7	10.0	5.2	—	0.30	1.92	—	—
C3	32.1	5.5	11.6	4.9	—	0.36	2.38	—	—
C4	28.7	3.6	7.9	2.9	24.8	0.27	2.75	0.86	8.7

The increase in silicon content depended on several parameters. When comparing samples from different series, *e.g.*, A1 with B1 or with C1, it depended on the amount of ICPTEOS used to perform the modification reaction, *viz.* 0.4, 0.6 or 1 equiv., giving an idea of the extent of that modification, namely A1<B1<C1. This trend was also verified in the other samples derived from the different subsequent treatments applied to these three precursors (Table 18 and Figure 45), which is in very good accordance with the FTIR-ATR results.

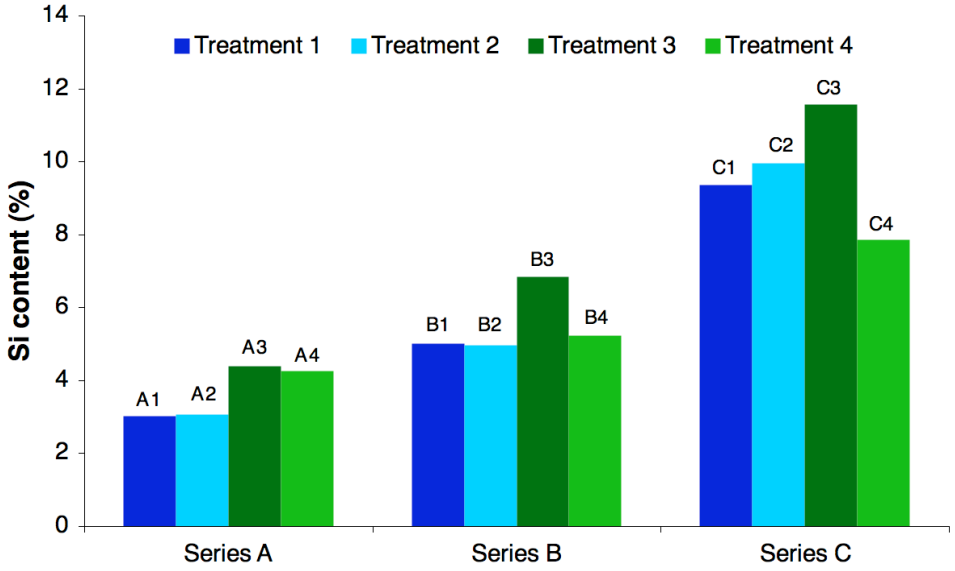

Figure 45. Comparison of Si content in the different cellulose hybrids.

On the other hand, when comparing samples from the same series (A, B or C), *e.g.*, A1 with A2 or with A3, the treatment type was the crucial factor affecting the ensuing Si content. Thus, for the same series, the amount of silicon was similar for samples that were only modified with ICPTEOS (treatment 1) and that suffered a subsequent simple acid hydrolysis treatment (treatment 2) (Table 18 and Figure 45), because in this second step no further silicon source was added to the reaction medium. When the acid hydrolysis was conducted in the presence of TEOS (treatment 3), the Si amount increased comparatively to the latter two groups of samples (Table 18 and Figure 45), due to the additional source of silicon. Nevertheless, this increase in Si content showed to be more pronounced in series A, where it increased by about 47% from the precursor (A1) to A3, followed by series B with an increase of about 36% (from B1 to B3), and finally series C with 28% of rise in Si content (from C1 to C3) (Table 18). However, this fact does not mean that in the A3 sample more TEOS moieties were attached to the cellulose fibers compared to the B3 and C3 counterparts. Instead, it is related to the proportion of silane moieties present in the initial materials (A1, B1 and C1) and the TEOS molecules added to react during the acid hydrolysis. Thus, as the amount of TEOS introduced in the reaction media was always the same, *viz.* 0.004 mol, its contribution to the overall Si content was less prominent in the samples where the extent of modification with ICPTEOS was higher (higher Si and N content).

Finally, when PFDTEOS was used (about 0.002 mol) instead of TEOS (A4, B4 and C4) during the acid hydrolysis (treatment 4), the silicon values showed a similar trend than

that displayed in the latter case (from A1 to A4, an increase of 43%; from B1 to B4, an increase of 4%; from C1 to C4, an decrease of 16%) (Table 18), being moreover aggravated by the presence of a new element in the samples, *viz.* fluorine, which played an important role in terms of its contribution to molecular weight of the relevant moiety. Therefore, as the elemental percentage is relative to the total weight of the samples, the presence of fluorine (17 fluorine atoms per PFDTEOS moiety with Ar=19) attenuated the contribution of the supplementary silicon (1 silicon atom per PFDTEOS moiety with Ar=28) (Table 18 and Figure 45).

Regarding the Si/C ratio, as it is possible to verify in Figure 46 and Table 18, it was similar for samples derived from treatments 1 and 2 in all the sample series, which suggested that during the treatment 1 some hydrolysis of the ethoxysilane groups from the ICPTEOS moieties linked to the cellulose fibers had already occurred, as confirmed by the low intensity of CH_3 peaks in the FTIR-ATR spectra and ^{29}Si CP-MAS NMR results presented below. Furthermore, this ratio increased for samples obtained from treatment 3 in all the series, due to the addition of other silicon-source in the reaction medium, *viz.* TEOS, as already discussed. Finally, as PFDTEOS moieties possess ten carbon and just one silicon atom, the Si/C ratio tended to decrease in samples derived from treatment 4, comparatively to those derived from treatment 3, except in the sample series A. Once again, this ratio increased from series A to series C.

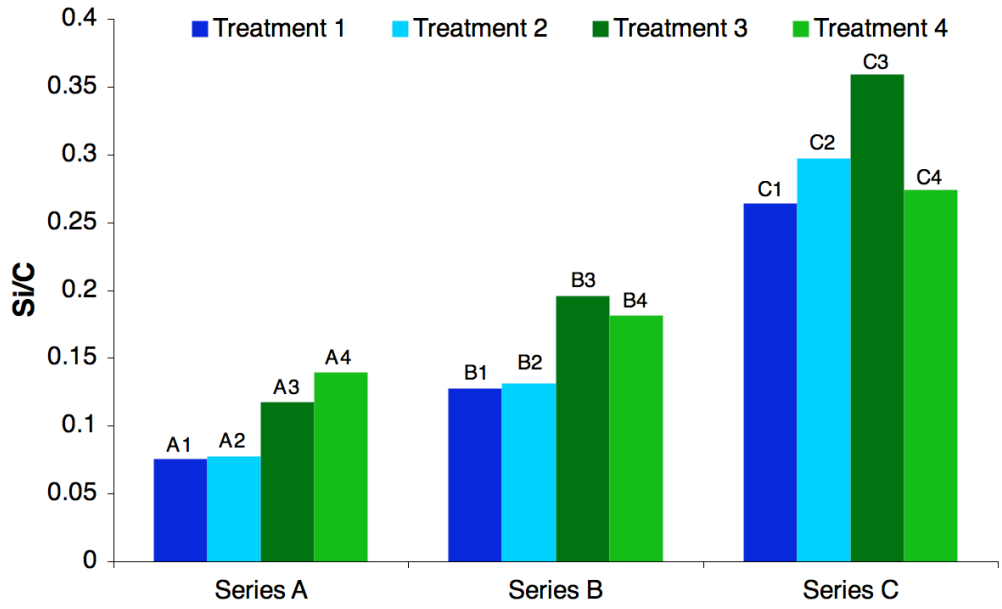

Figure 46. Comparison of Si/C ratio in the different cellulose hybrids.

In the case of nitrogen, as depicted in Figure 47, it was observed that within the same sample series, its amount was very similar for samples obtained from the treatments 1 to 3, whereas samples obtained after acid hydrolysis in the presence of PFDTEOS (treatment 4) possessed lower amounts of this element (Table 18). Similarly to what was discussed above, this behavior was attributed to the important contribution of fluorine to the total weight of the samples, which consequently decreased the percentage of the other elements, including silicon and nitrogen. As in the case of silicon content, when comparing samples from different series, the amount of N increased from series A<series B<series C, according to the OH:ICPTEOS ratio used to modify them (Figure 47 and Table 18), a trend which is tune with the FTIR-ATR results.

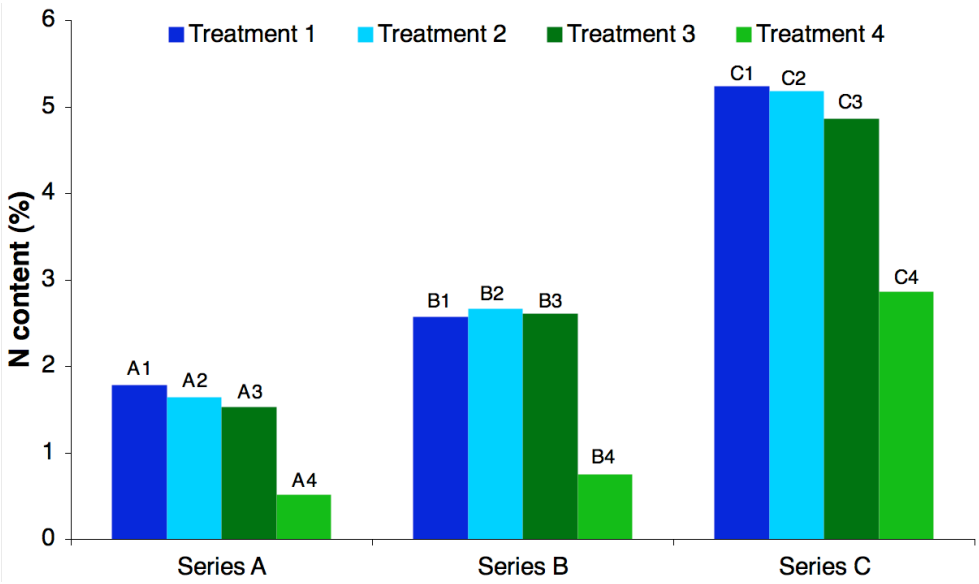

Figure 47. Comparison of N content in the different cellulose hybrids.

As it is possible to visualize in Table 18 and Figure 48, the Si/N ratio was about 2 for the cellulose derivatives obtained from treatment 1 (A1, B1 and C1) and treatment 2 (A2, B2 and C2), which is coherent with the proportion of Si to N in the ICPTEOS moieties and the atomic weight of these elements. In other words, each ICPTEOS moiety, which was the only source of Si and N in both treatments, comprise one atom of each element (silicon and nitrogen) (Figure 42), and as the atomic weight of silicon [Ar(Si)=28] is twice that of nitrogen [Ar(N)=14], their ratio is equal to 2. As expected, after acid hydrolysis in the presence of the siloxanes (TEOS and PFDTEOS) the Si/N ratio increased, due to the addition of other sources of silicon.

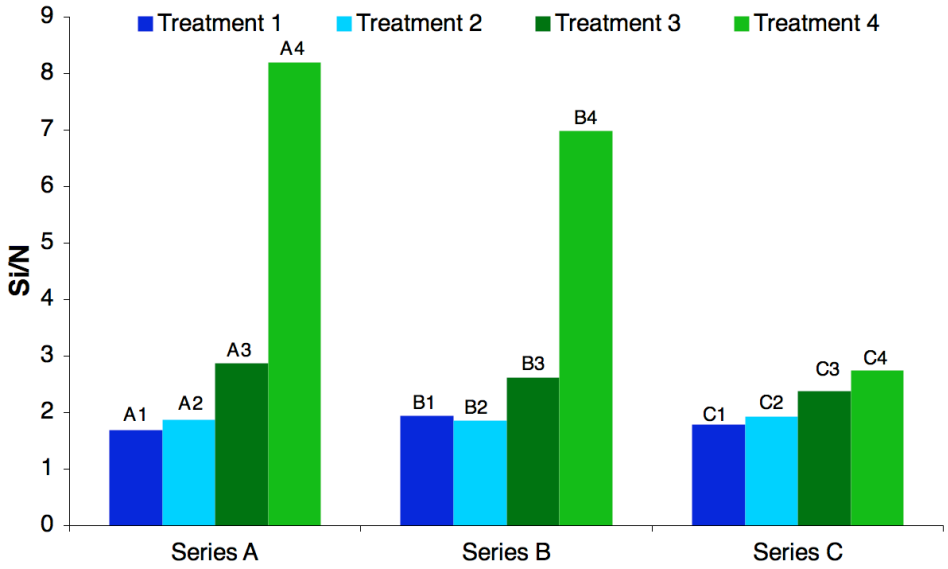

Figure 48. Comparison of Si/N ratio in the different cellulose hybrids.

Interestingly, it was verified that similarly to what was discussed above for the Si content, the contribution of Si from TEOS (A3, B3 and C3) and PFDTEOS (A4, B4 and C4) residues to the Si/N ratio was less pronounced for the samples possessing correspondingly higher extent of modification, thus C3<B3<A3 and C4<B4<A4 (Table 18 and Figure 48).

This behavior was also verified with respect to the fluorine content in the samples obtained from treatment 4. Therefore, in A4 and B4 samples the percentage of fluorine was very similar, but decreased considerably in C4 sample (Table 18), due to the smaller contribution of the PFDTEOS moieties to the F content in samples with higher total weight, *i.e.*, with a higher extent of modification. Similarly, the F/C and F/N ratios (Table 18) also reflected this trend, tending to decrease from A4 to C4 samples.

In conclusion, it was verified that the increase in the extent of modification of the cellulose fibers with ICPTEOS (treatment 1) from series A to series C samples, as suggested by the FTIR-ATR results, was confirmed here by the EA results, mainly in terms of the corresponding increase in the Si and N content. Furthermore, the EA values for the samples obtained in the subsequent acid hydrolysis treatments reflected what was expected, specifically the amount of Si and N in samples from treatment 2 was similar to those from treatment 1, samples from treatment 3 possessed a much higher amount of Si than the others, and, finally, samples from treatment 4 owned a further contribution of F.

As opposed to the cellulose perfluorinated derivatives presented in the previous section, for these organic-inorganic hybrid derivatives, it was not possible to determine the

DS because, as verified by the FTIR-ATR and ^{29}Si CP-MAS results (presented below), after treatment 1, part of the Si-OCH_2H_3 groups already started to hydrolyze to Si-OH and subsequently condensate to Si-O-Si moieties, a feature that prevented the quantitative determination of each moiety, and hence a reliable calculation of the DS.

2.1.3. Solid-State ^{29}Si CP-MAS NMR Spectroscopy

Solid-state ^{29}Si CP-MAS NMR spectroscopy is particularly suitable for the inspection of the structure of silicon-type hybrid materials [290], and was therefore used to analyze the cellulose hybrid materials prepared here.

The silicon sites were labeled according to the conventional T^n notation, corresponding to silicon moieties of the type $CH_2Si(OSi)_n(OCH_2CH_3)_{a-n'}(OH)_{b-n''}$ (where n = 1–3, n' + n'' = *n* and a + b = 3). In general terms *n* is associated to the number of Si-O-Si bridges formed by certain silicon site, as illustrated in Figure 49.

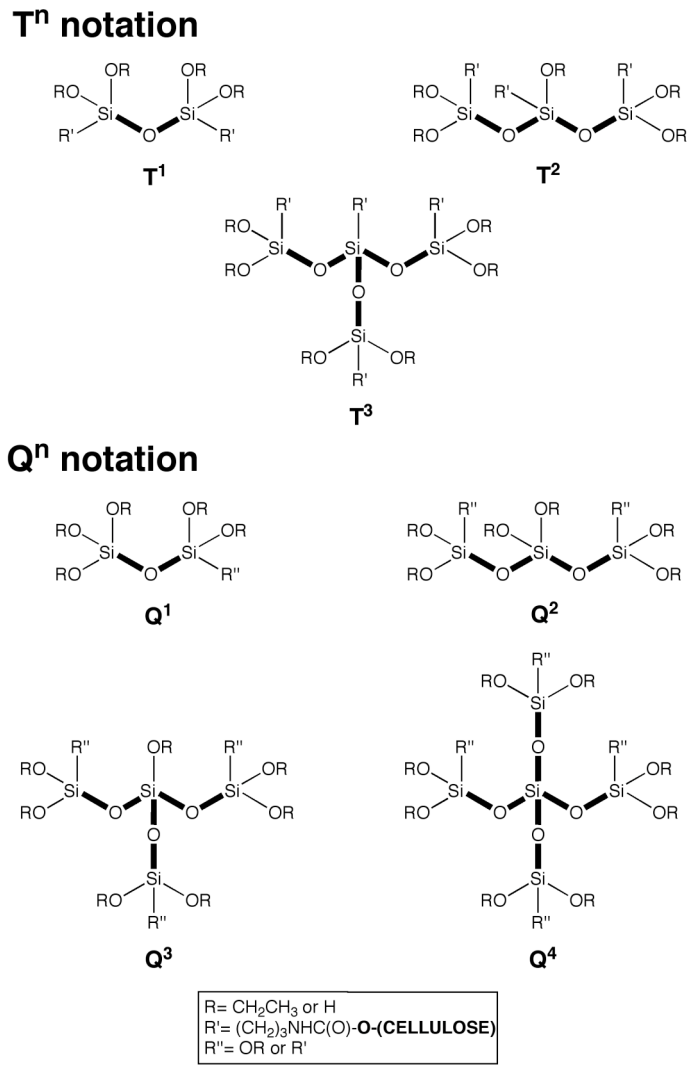

Figure 49. Schematic representation of T^n and Q^n notations with the associated silicon sites.

Figure 50 displays the ^{29}Si CP-MAS NMR spectra of the cellulose fibers modified with 1 equiv. of ICPTEOS and subsequent acid hydrolysis treatments (series C). After modification of the cellulose fibers with different proportions of ICPTEOS, the spectra of the ensuing derivatives exhibited signals in four different regions, specifically at *ca.* -45 (only for the B1 sample), -49, -57 to -58 and -67 ppm (only for the C1 sample), assigned to T^0, T^1, T^2 and T^3 environments, respectively [287]. For the derivatives obtained with just 0.4 equiv. of ICPTEOS (series A), it was difficult to detect any signal due to the background noise, which suggested that in these hybrids the amount of Si present was very small. The presence of T^1 and T^2 peaks in the B1 sample and of an additional T^3 signal in the C1 sample, indicated that the residual moisture present in the system had already started the hydrolysis of some ethoxysilane groups, leading to the formation of Si–O–Si or Si–OH moieties, a deduction that is in agreement with the previously discussed

low intensity of the CH_3 peaks in the FTIR-ATR spectra of C1 sample and with its elemental analysis, especially the Si/C ratio. In these samples, T^2 peaks were predominant, followed by T^1 signals, suggesting that partial condensation favored the formation of linear segments and ‘‘dimeric” structures, rather than the more branched architectures associated with the T^3 peaks.

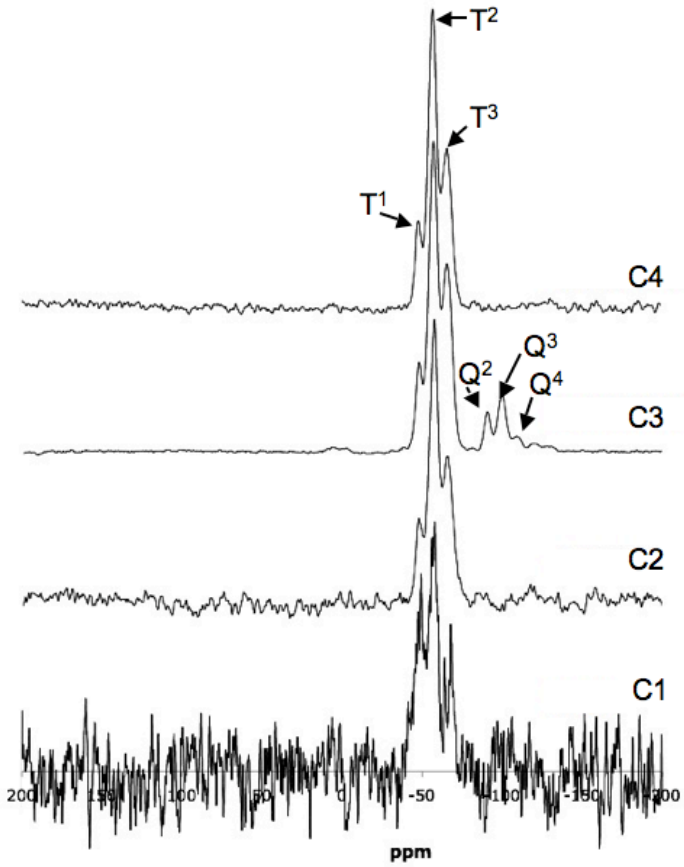

Figure 50. ^{29}Si CP-MAS NMR spectra of cellulose fibers after modification with 1 equiv. of ICPTEOS and subsequent acid hydrolysis treatments (series C).

The samples obtained after acid hydrolysis, with or without PFDTEOS (treatments 4 and 2, respectively), exhibited the same T^1, T^2 and T^3 signals, but with an increase in the relative intensities of T^2 and particularly of T^3 signals when compared to T^1. This observation confirms a dominance of linear and branched silicon based structures, following the mentioned hydrolysis treatments.

After acid hydrolysis in the presence of TEOS (treatment 3), in addition to the three T^n environments, peaks at *ca.* -92, -101 and -112 ppm were also detected in the spectra of the cellulose fiber hybrids, namely in the B3 and C3 (Figure 50) samples. These new signals were labeled according to the Q^n notation, corresponding to silicon moieties of the

type $Si(OSi)_n(OCH_2CH_3)_{a-n'}(OH)_{b-n''}$ (where n = 1–4, n' + n'' = n and a + b = 4), and assigned to Q^2, Q^3 and Q^4 structures, respectively (Figure 49).

The new Si environments resulted from the hydrolysis of the TEOS ethoxy groups and the subsequent formation of novel Si–O–Si or Si–OH moieties. As can be observed in Figure 50, the Q^3 sites were predominant in the C3 sample, and the same was observed for B3, which indicates that the presence of TEOS favored the formation of three-dimensional silicon constructs, although, as can be seen in Figure 50, these Q^n domains are still less important than the T^n counterparts.

In the case of the hybrids obtained after hydrolysis, with or without PFDTEOS, no Q^n moieties were observed, since in these cases all silicon-based structures bore a Si–CH_2 linkage.

It can be concluded that in all these hybrids, the cellulose fibers were surrounded by an inorganic layer involving predominantly linear Si–O–Si networks, together with smaller contributions from more branched networks as well as ‘‘dimeric” structures.

The predominantly linear structure of this layer, in conjunction with the absence of the characteristic CH_3 moieties from the ethoxy groups, indicated that upon hydrolysis, in addition to the formation of Si–O–Si bridges, part of the Si–OCH_2CH_3 groups were also converted into Si–OH groups, which will inevitably influence the surface properties of the corresponding hybrids. In the case of the hydrolysis in the presence of PFDTEOS, the perfluorinated moieties introduced additional peculiarities to the properties of the ensuing hybrids, as is discussed below.

2.1.4. X-Ray Diffraction Analysis

As can be observed in Figure 51A, the samples obtained from the series A and B maintained the characteristic XRD pattern of cellulose I mentioned above, which indicated that the modification had not affected to a great extent the crystalline regions of the inner layers of the fibers. Additionally, the samples obtained after acid hydrolysis in the presence of PFDTEOS exhibited three new diffraction signals at 2θ values of 6º, 9º and 18º (Figure 51B), which were attributed to the self-assembly of the perfluorinated aliphatic chains grafted onto the fibers [214].

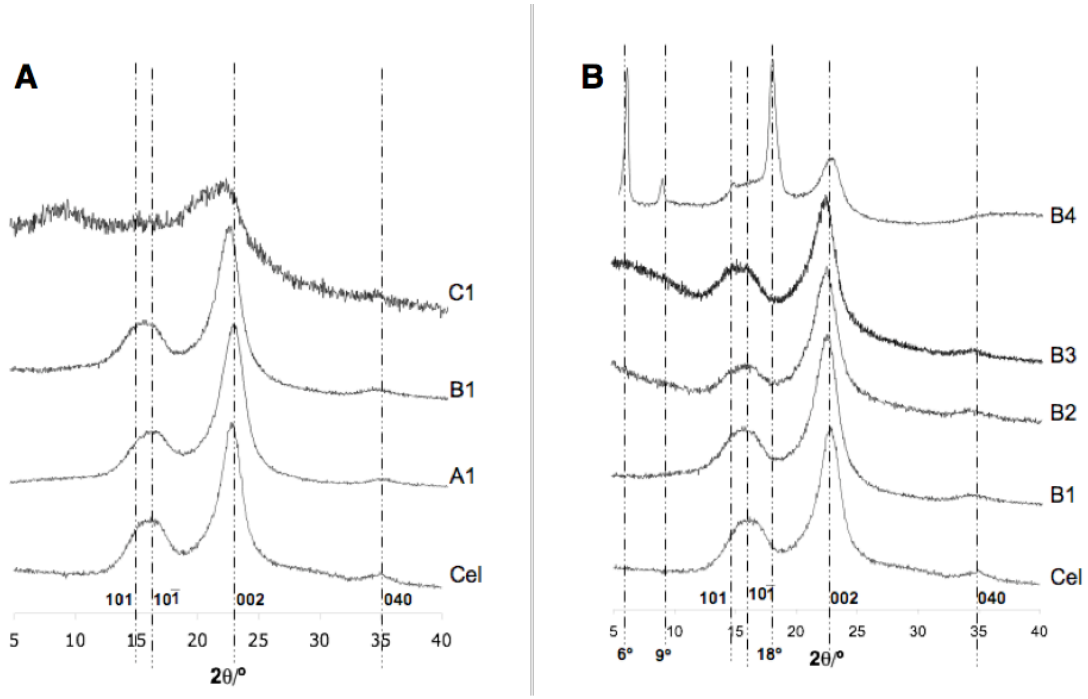

Figure 51. XRD diffractograms of cellulose fibers before and after modification with ICPTEOS at different ratios (A) and of cellulose fibers before and after modification with 0.6 equiv. of ICPTEOS for 5 h and subsequent treatments (B).

Conversely, the cellulose pattern vanished in the XRD diffractograms of the samples from series C (Figure 51A), suggesting that the crystalline structure of the fibers had been affected as a consequence of a deeper modification. This was probably due to the fact that the reaction was carried out in a cellulose swelling solvent (DMF), which, associated with the severity of the treatment in terms of both the amount of reagent and the reaction time, facilitated the interaction between the ICPTEOS molecules and the hydroxyl groups initially belonging to the crystalline regions of the fiber inner layers. The depth of this modification could also have produced the partial cellulose degradation thus explaining the difference in morphology exhibited by the differently modified fibers, as discussed below (SEM results), since the milder treatments left their appearance virtually unchanged, whereas with the 1:1 ratio, they acquired a powdery consistence. This partial degradation is probably the consequence of an excessive fiber stiffening induced by the inorganic coating (SEM results) that led to fiber embrittlement and consequent fracture.

2.1.5. Thermogravimetric Analysis

The thermogravimetric profiles of the hybrid cellulose fibers were evaluated and Figure 52 shows the behavior from the samples from series C, which were found to be less stable than the pristine cellulose fibers (Cel), since they started degrading at lower temperatures, *i.e.* possessed lower T_{di}, and also exhibited lower T_d (Table 19). Nevertheless, they presented a less abrupt decay (Figure 52), certainly assigned to a lower heat transfer to cellulose due to the presence of the inorganic phase around the fiber, and additional degradation steps compared with the pristine fibers, attributed to the decomposition of the organic moieties of the groups appended to the cellulose fibers after the different treatments.

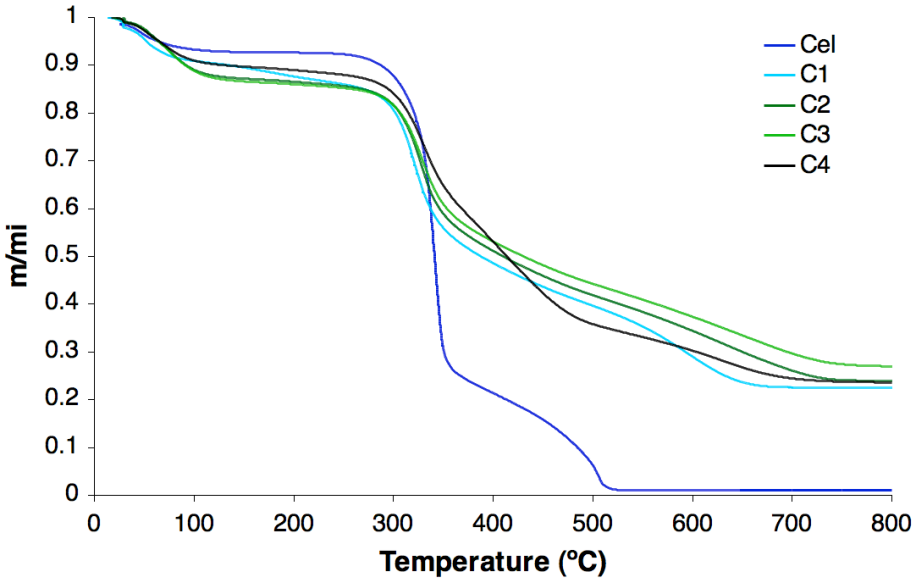

Figure 52. TGA tracings of cellulose fibers before and after modification with 1 equiv. of ICPTEOS for 24 h and subsequent hydrolysis treatments (series C).

Table 19. Thermogravimetric data of pristine and hybrid cellulose fibers from series C.

Sample	T_{di} (ºC)	T_d (ºC)	Weight loss at 800 ºC (%)
Cel	260	343	98.9
C1	125	323	77.0
C2	165	329	76.1
C3	171	331	72.2
C4	185	333	76.4

The absence of total weight loss at *ca.* 800 ºC, corroborated the presence of an inorganic environment around the cellulose fibers. As expected, samples obtained after acid hydrolysis in the presence of TEOS (treatment 3), exhibited lower weight loss at 800 ºC (Table 19) compared with those of the pristine cellulose fibers and of the other derivatives, indicating the presence of a correspondingly higher amount of inorganic components, which is in tune with the EA results.

The derivatives obtained after acid hydrolysis in the presence of PFDTEOS (C4 in Figure 52) showed a more pronounced second degradation step, with a maximum decomposition rate around 420 ºC, attributed to the degradation of the perfluorinated aliphatic chains. The lower proportion of inorganic residue than in the derivatives obtained after hydrolysis in the presence of TEOS (C3 in Figure 52 and Table 19), was here the consequence of the higher initial fraction of organic structures associated with the long PFDTEOS chains, as also indicated by the Si/C ratios in the EA results.

The thermal degradation behavior of the samples prepared by the reactions with 0.4 and 0.6 equiv. of ICPTEOS during 5 h (series A and B, respectively) showed similar profiles but with a lower final residue, in agreement with the results discussed above, including the EA data.

2.1.6. Surface Morphology Characterization by Scanning Electron Microscopy

All the hybrid materials prepared were analyzed by SEM in order to assess the effect of the modifications on their surface morphology.

The SEM micrographs of the cellulose fibers before and after modification with different amounts of ICPTEOS (Figure 53A) indicated that, for samples from series A and B (illustrated only by series A) the fiber structure was largely preserved, whereas for samples from series C the fibers appeared fragmented. These observations are in tune with the XRD results discussed above, being related, not only to the decrease in crystallinity, but also by the already discussed partial degradation of cellulose.

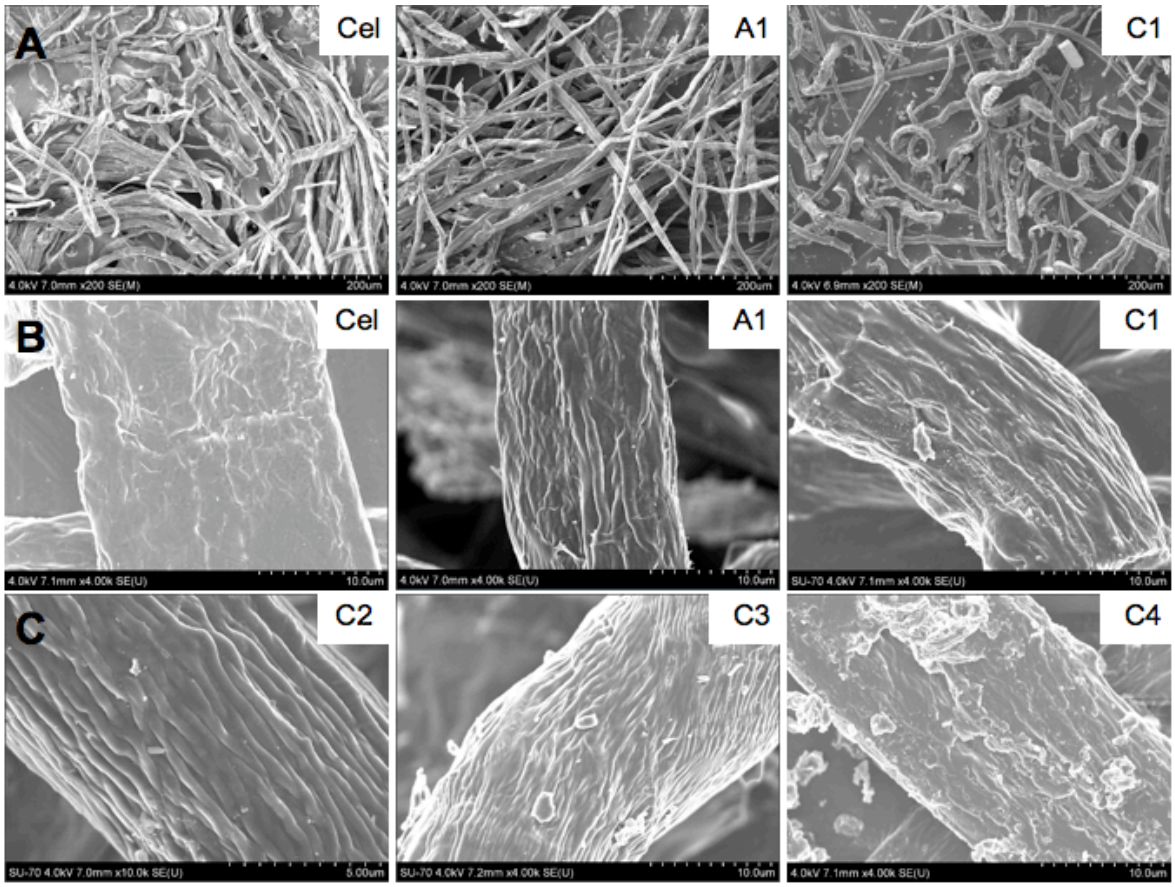

Figure 53. Scanning electron micrographs of unmodified fibers and of fibers modified with 0.4 and 1 equiv. of ICPTEOS (series A and C) at 200x (A) and 4000x (B) magnifications and for some hydrolyzed samples (C).

With an increased magnification, a coating around the fibers became apparent, as shown in Figure 53B, probably arising from the formation of the Si–O–Si bridges, as

clearly indicated by the predominance of the T^2 sites in the ^{29}Si CP-MAS NMR spectra discussed above.

This ‘‘sleeve” appeared to have arisen as a consequence of the increasing [OH]:[ICPTEOS] ratio, and can be associated to the formation of an increasing number of surface Si–O–Si bridges. Similar morphologies were observed in the SEM images of the hybrids obtained after simple acid hydrolysis (Figure 53C). Furthermore, in the samples obtained after acid hydrolysis in the presence of PFDTEOS (Figure 53C), a second coating appeared, which was much more heterogeneous and took the shape of irregular flakes. With an even higher magnification (Figure 54), it was possible to observe that the inorganic surface was coated with nanoscale rugosities. Both the latter morphologies are in principle conducive of the reduced wettability of the corresponding surfaces, as discussed below.

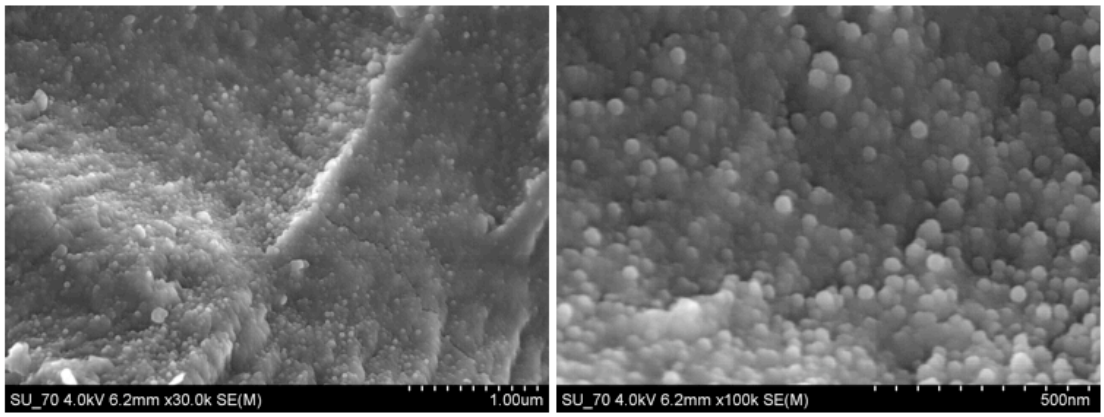

Figure 54. Scanning electron micrographs of C4 samples at 30.000x and 100.000x magnifications.

2.1.7. Contact angle measurements

The contact angles with polar (water) and non-polar (diiodomethane) liquids, measured on the surface of the cellulose hybrid derivatives prepared, are presented in Table 20. All the measurable contact angles did not vary appreciably with time over 30 min, irrespective of the liquid used. This suggests that the hydrophobic, and in some cases even omniphobic, character displayed by the modified surfaces, which is discussed below, was a permanent feature.

Table 20. Contact angles with water and diiodomethane on cellulose fiber pellets before and after modification.

Sample	Contact angles (º)	
	Water	Diiodomethane
Cel	64	37
A1	112	—[a]
B1	103	—[a]
C1	129	—[a]
A4	137	111
B4	132	114
C4	140	134

[a]Droplet was absorbed within 2 s.

As can be observed in Table 20, the modification of cellulose fibers with ICPTEOS (treatment 1) changed their surface properties, since the contact angle with water increase by 40–60º, depending on the conditions. This feature is probably due to the presence of small amounts of -OCH_2CH_3 moieties at the surface of the cellulose fibers (in agreement with the FTIR-ATR results and with the dominant T^2, followed by T^1 domains, in the ^{29}Si CP-MAS NMR spectra), which are known to confer water-repellency to polar substrates, by lowering their surface free energy [291].

It was interesting to verify that even for the fibers modified with a 1:0.4 ratio (A1 sample), for which the extent of reaction was modest, a significant increase in hydrophobicity was detected, which implies that, similarly to what was observed for the perfluorinated cellulose derivatives discussed in the previous section, it was not necessary to push the modification to a large extent in order to reach high contact angles. However, conversely to those perfluorinated cellulose derivatives, the surface of these hybrid cellulose materials showed a high affinity toward diiodomethane (non-polar liquid) (Table 20), which means that they possessed simultaneously a hydrophobic and lipophilic behavior.

After the acid hydrolysis of the ethoxy groups present at the surface of the modified fibers, the ensuing silanol groups (Si-OH) and Si–O–Si bridges, formed by their self-condensation, increased the surface energy of these hybrid materials through their polar contributions, and the contact angles on the surface of the A2, B2 and C2 samples were impossible to measure, as the water drops spread immediately and were absorbed

by the fibers within a couple of seconds. A similar behavior was observed with the samples obtained after acid hydrolysis in the presence of TEOS, since Si-OH groups and Si–O–Si bridges were also formed after this treatment.

Conversely, as expected, after the hydrolysis in the presence of PFDTEOS, the fibers became even more hydrophobic and also lipophobic, as the contact angles reached 140º and 134º with water and diiodomethane, respectively (Table 20). These results are intimately related to the already mentioned properties of the perfluorinated compounds [214]. Furthermore, this highly omniphobic character was displayed even though some OH functions, resulting from ethoxy groups hydrolysis, were also present at the surface of the cellulose derivatives. This observation is in tune with the results presented in *Section 1* for the perfluorinated cellulose derivatives, for which it was observed that, even at very low levels of cellulose fibers' surface functionalization with perfluorinated reagents, hence with most of the OH groups untouched, the materials became nevertheless highly omniphobic. Similarly, the high contact angles observed were not affected by the reaction conditions, namely the [OH]:[ICPTEOS] ratio and the reaction time. Therefore, if the aim of the transformation is the modification of the surface properties of the fibers, preserving their morphology and mechanical properties, the less severe reaction conditions should be used.

It is also important to emphasize that these contact angles were higher than those obtained for the perfluorinated cellulose derivatives reported for the previous system (see *Section 1*), which only reached, at best, 130º and 100º with water and diiodomethane, respectively. Likewise, using another substrate, namely glass, Jeong *et al.* (2001) [292] measured water contact angles only up to 118º after coating it with films containing different proportions of PFDTEOS and TEOS.

In another recent study on this topic performed in our group, but related to class-I hybrid cellulose materials [141], the combination of surface roughness induced by the deposition of silica nanospheres on the fibers' surface and the presence of perfluoro moieties, gave rise to contact angles as high as those measured in the present investigation. These results corroborate the concept that a very high hydrophobicity, as well as lipophobicity, is better achieved by combining the presence of perfluorinated moieties with a rough surface morphology, preferably at the nanoscale level [162].

2.2. Conclusions

The modification of cellulose fibers with ICPTEOS showed to be a promising strategy for preparing new cellulose-based class-II hybrid materials with interesting properties.

Globally, one can conclude that for samples from series A and B, the reaction should have been limited to the amorphous and outermost regions of the fibers since, on the one hand, ^{29}Si could hardly be detected by solid-state CP-MAS NMR and the final residue in the TGA was quite small, and, on the other hand, XRD and SEM confirmed the preservation of the crystallinity and morphology of the fibers, respectively. Conversely, in the case of the samples from series C, both XRD and SEM confirmed that, in addition to the increasing ‘‘sleeve” effect corroborated by solid-state ^{29}Si CP-MAS NMR and TGA results, the reaction also went deeply into the fiber structure, affecting its crystallinity and morphology, respectively.

The modification with ICPTEOS (treatment 1) gave rise to hydrophobic cellulose fibers, as assessed by water contact angles measurements, due to the insertion of -OCH_2CH_3 functions at their surface.

Moreover, depending on the subsequent treatment (hydrolysis/condensation) and on the nature of the functionalities appended when the alkoxysilanes were added during this step, new materials with a broad range of properties and, therefore, potential applications could be designed. Accordingly, after simple acid hydrolysis (treatment 2) or acid hydrolysis in the presence of TEOS (treatment 3), one can obtain highly hydrophilic organic-inorganic hybrid cellulose derivatives, and, on the contrary, by acid hydrolysis in the presence of PFDTEOS (treatment 4), derivatives with remarkable omniphobic surface properties are attained. Furthermore, similarly to the perfluorinated cellulose derivatives presented in *Section 1*, these new surface features of the fibers, achieved with a limited extension of the modification, open the possibility of preserving their morphology and mechanical properties.

Potential applications envisaged to this kind of cellulose derivatives comprise, for instance, fillers in composite materials, or application in packaging, special papers, textiles and paints.

Finally, it is worth mentioning that this work can potentially open the way to the preparation of many other novel class-II organic-inorganic cellulose hybrids with attractive properties, following well-designed expansions of this approach to other reactions, which

can include the use of other inorganic reagents, like other silane-coupling agents or new inorganic moieties in the second step of the process.

3. Vapor-Phase Modification of Cellulose with Chlorosilanes

In pursuit of our research dealing with the surface modification of cellulose fibers to attain highly hydrophobic and lipophobic surfaces, and aiming at the development of a process simpler and greener than those discussed above, it was decided to develop a system capable of inducing such modifications by the interaction of chlorosilane vapors with the solid fibers substrate. The reagent selected for these experiments was the rather volatile trichloromethylsilane (TCMS), which had already been employed to generate branched structures onto the surface of several OH-bearing substrates [110, 160, 224] in order to increase their surface hydrophobicity. Recently, moreover, the effect of TCMS vapors on cellulose fibers had also been reported [109, 110], but in one instance [109] the process called upon four steps involving the dipping of the treated fibers in pyridine as the second step, *i.e.*, under rather environment-unfriendly conditions, whereas the other study [110] involved very long reaction times, dealt essentially with glass substrates and only mentioned the use of cellulose in generic terms, together with other solid surfaces.

3.1. Controlled Heterogeneous Modification of Cellulose with Vapor-Phase Trichloromethylsilane

TCMS was adopted for this investigation because it is a stable and volatile reagent capable in principle of modifying the cellulose fibers' surface under mild conditions and without the use of a solvent, through a process involving only a gas–solid reaction conducted at room temperature and atmospheric pressure.

The presence of moisture is an indispensable feature of the present system, whose aim is to build the siloxane morphologies illustrated in Figure 55, adapted from a previous scheme proposed by Fadeev and McCarthy in a different context [229].

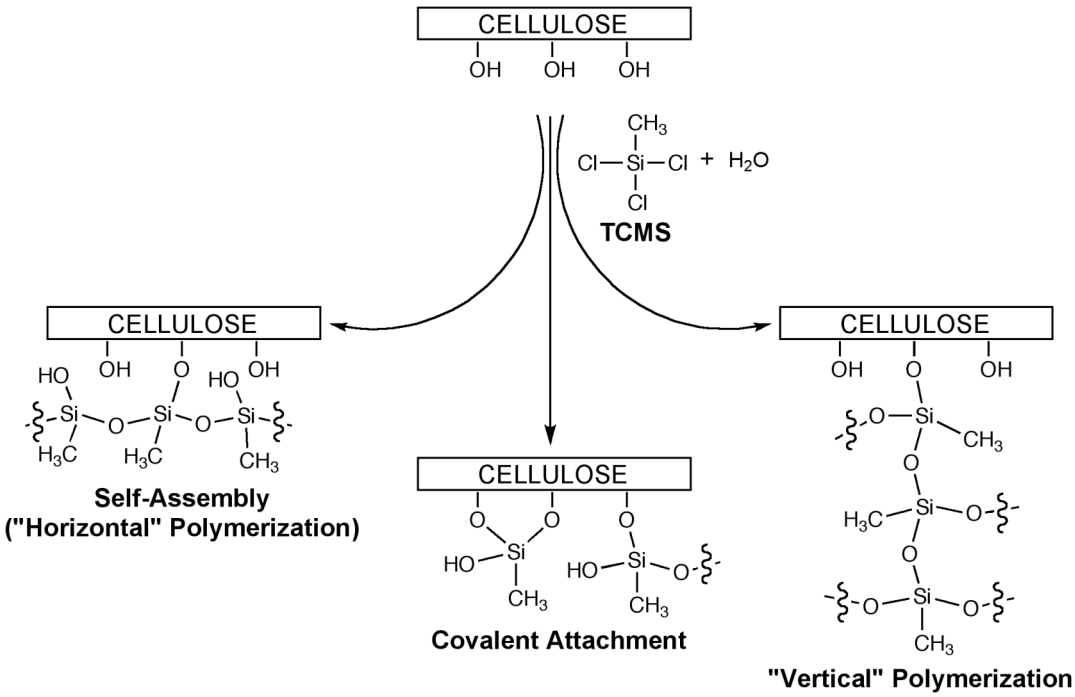

Figure 55. Schematic representation of the possible products of the reaction of TCMS with a cellulose substrate in the presence of controlled humidity (adapted from [229]).

Together with the chemical surface modification associated with the replacement of some cellulose –OH groups by $–OSiCH_3$ moieties (Figure 55), a further contribution to hydrophobicity was expected from the microrugosity generated by these surface condensation reactions.

The feasibility of the condensation reaction between the surface –OH groups of cellulose and the Si–Cl moiety is clearly established in the literature [293, 294], albeit in systems involving the suspension of the fibers in dry toluene and the use of alkyldimethylchlorosilanes as silylating agents. Therefore, the gas–solid system studied in the present work was expected to lead to the same chemical interactions, considering furthermore that the $-Si(Cl)_3$ moiety is more reactive than the $-Si(CH_3)_2Cl$ counterpart, because of the presence of three Si–Cl bonds and the smaller steric hindrance. Notwithstanding these indications, complementary essays were performed to gain clear evidence of this coupling reaction in the present context, particularly since the system employed also involved the presence of water vapor, which, as referred above, reacts very rapidly with TCMS and, thus, could hinder its condensation with cellulose. These complementary essays consisted in conducting a series of experiments using cellulose samples, which were preliminary dried in a vacuum oven at 60 ºC for 24 h. Whereas a

treatment of 30 s under the same TCMS flow conditions as for “dry” and pre-humidified samples (see below) suggested that the reaction time was too short for any detectable reaction (no increase in the water contact angle and no new peaks in the FTIR-ATR spectrum), progressively longer treatments produced correspondingly higher increases in the surface hydrophobicity of the fibers’ surface (water contact angles reaching 130º), accompanied by a similar trend in the intensity of the Si-CH_3 FTIR-ATR peaks (see discussion below) as shown in Figure 56. These results clearly confirmed that with the present setup TCMS reacts directly with the surface hydroxyl groups of cellulose fibers. Any trace of residual moisture could not have been held responsible for the evidence of a growing reaction yield with time, because it would have been rapidly consumed during the initial phase of the treatment, given the well-known pronounced reactivity associating these two compounds.

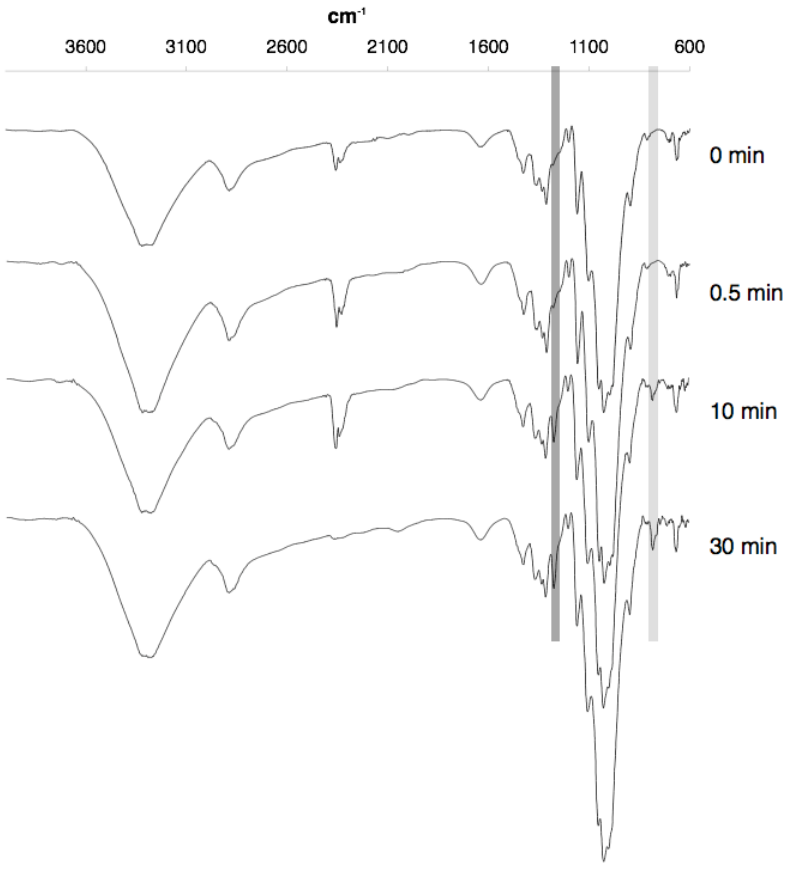

Figure 56. FTIR-ATR spectra of the pre-dried cellulose samples treated with TCMS for 0.5, 10 and 30 min (gas-mixture flow of 0.1L/min).

The fact of having corroborated the occurrence of direct interaction between cellulose OH groups and TCMS does not constitute the aim of the present actual working hypothesis, which calls upon instead on the concomitant occurrence of a series of reactions involving three actors, namely the cellulose OH groups, water molecules and TCMS, both in the vapor-phase. Succinctly, a fraction of the TCMS molecules is hydrolyzed before reaching the cellulose substrate, the extent of this consumption being a function of the relative amount of moisture in the gas flow. Upon reaching the cellulose surface, both the Si-Cl and the newly formed Si-OH moieties react with the cellulose OH groups, whilst two Si-OH moieties can also condense in a classical sol-gel interaction. The net result of this state of affairs is schematically illustrated in Figure 55, *i.e.*, a number of hybrid molecular architectures generated in parallel and responsible for a complex surface micromorphology.

After the necessary model experiments involving the virtual absence of moisture discussed above, the real system was tackled by varying a number of parameters in order to gain an adequate insight into its complex behavior, as described below.

3.1.1. FTIR-ATR Spectroscopic Analysis

The occurrence of the cellulose fibers modification with TCMS was assessed by FTIR-ATR analysis, through the monitoring of two new bands at *ca.* 1270 and 780 cm^{-1}, attributed to the $Si-CH_3$ group symmetric bending and stretching modes [276], respectively, as represented in Figure 57 and as already reported in previous studies dealing with the treatment of cellulose substrates with chloromethylsilanes or derivatives [109, 232].

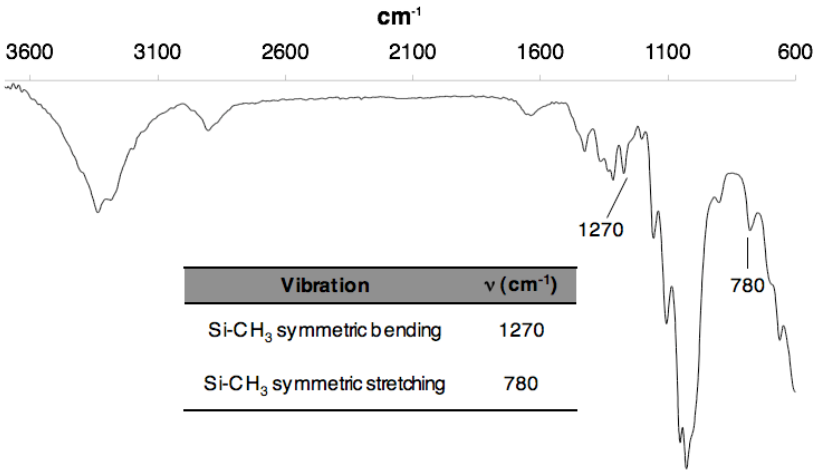

Figure 57. FTIR-ATR spectrum of cellulose fibers modified with TCMS with the assignment of new peaks.

Similarly to what was mentioned above for the organic-inorganic hybrid cellulose derivatives, the presence of Si-OH and Si-O-Si bridges, formed after the moisture-induced hydrolysis of the Si-Cl groups and partial self-condensation of the ensuing Si-OH groups (^{29}Si CP-MAS NMR results), respectively, could not be detected by FTIR-ATR for the same reason, *i.e.*, their vibration frequency around 950 and 1100 cm^{-1}, respectively [276], overlaps with the broad cellulose C-O stretching band centered at *ca.* 1026 cm^{-1} (Figure 57).

The progress of the cellulose fiber treatment with TCMS, with respect to both the gas-mixture (TCMS/N_2) flow and the treatment time, was also monitored by FTIR-ATR spectroscopy, through the evolution of the intensity of the Si-CH_3 peaks referred above (Figure 58).

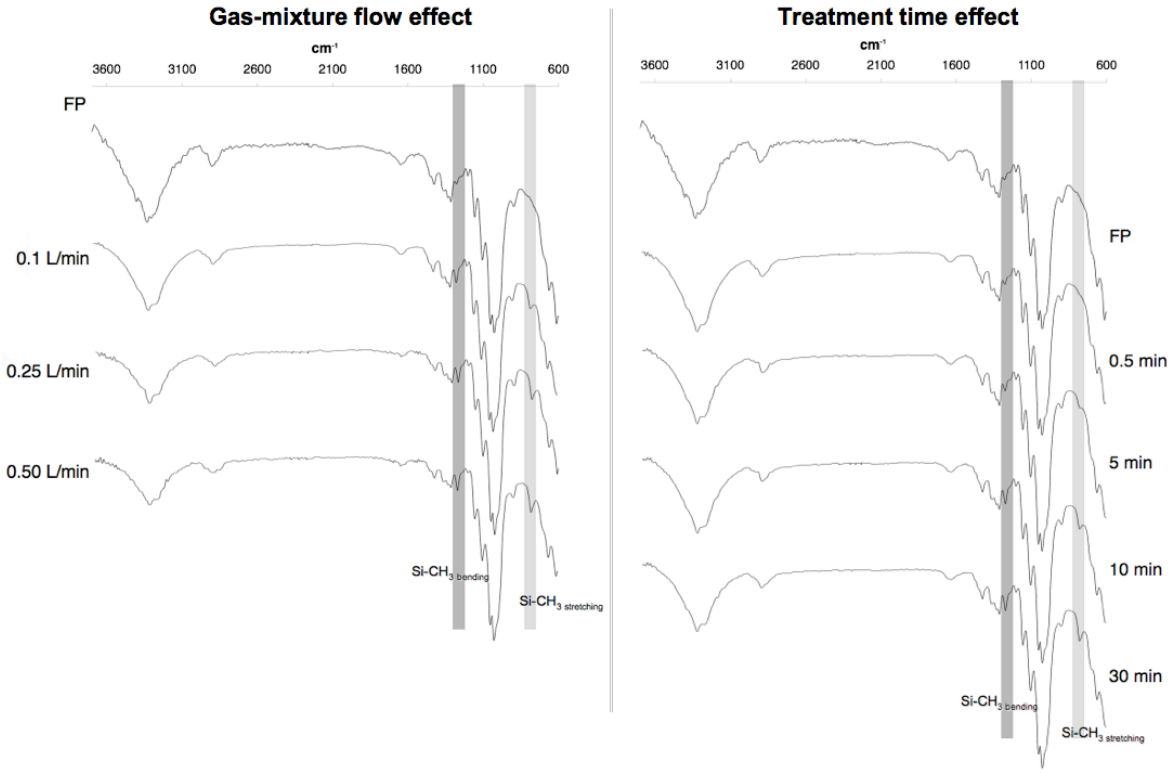

Figure 58. Progress of the TCMS-modification of cellulose fibers with gas-mixture flow (30 min of treatment) and time (gas-mixture flow of 0.1 L/min) as followed by FTIR-ATR.

The gas-mixture flows tested, *viz.* 0.1, 0.25 and 0.50 L/min, did not seem to play a significant role on the extent of the surface modification of the cellulose samples treated for the same period of time (30 min), as clearly visible in the left side of Figure 58, where the intensity of the peaks related to the Si-CH_3 vibrations is very similar in all instances. For this reason, the subsequent TCMS treatments were conducted using always a gas-mixture flow of 0.1 L/min. Conversely, the treatment time, which ranged from 0.5 to 30 min, implying correspondingly growing amounts of TCMS flowed through the samples, showed to influence the yield of cellulose modification (Figure 58), especially above a 0.5 min treatment period. Nonetheless, from 10 to 30 min of treatment, the corresponding raise in the cellulose fiber surface modification, as monitored by this technique, was very modest.

The role of the pre-humidification procedure was equally evaluated by FTIR-ATR spectroscopy. In this sense, it was verified that in the pre-humidified samples, the presence of additional moisture at their surface served as a “physicochemical barrier”, allowing the reactions involving TCMS to take place to a larger extent at that location, and hence made the Si-CH_3 vibrations easily detectable in the FTIR-ATR spectra, as shown in Figure 59, in which they are present as very intense and sharp peaks. In these instances,

an almost spontaneous hydrolysis/condensation of TCMS molecules took place even before their diffusion into the cellulose samples, as was readily confirmed by other spectroscopic techniques described below. However, for the actual occurrence of chemical linkage between cellulose and TCMS molecules, treatment periods above 0.5 min were required, because when they were conducted during only that time, TCMS molecules reacted exclusively with the added moisture, without interacting with the cellulose -OH groups, thus giving rise to self-condensation products that were then extracted with ethanol during the soxhlet extraction procedure. Consequently, no new peaks were observed in the FTIR-ATR spectra of the corresponding samples.

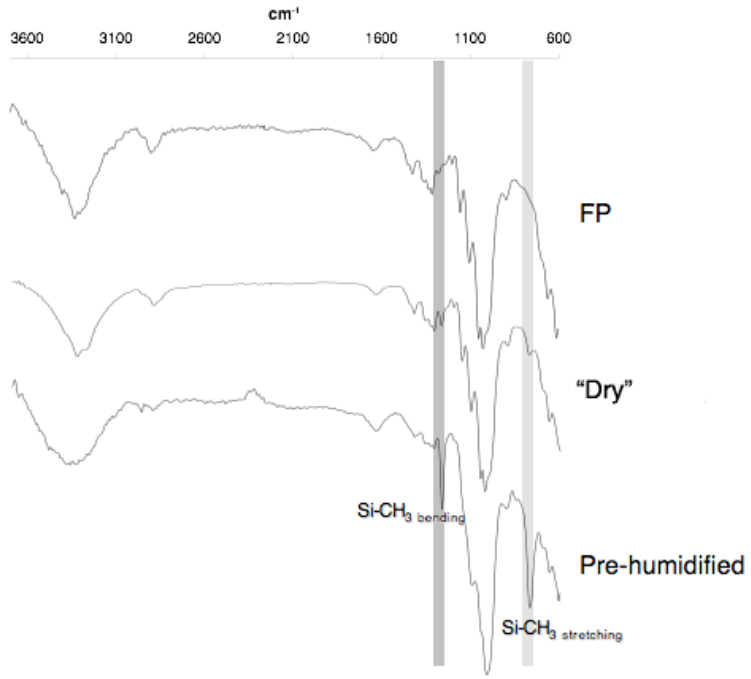

Figure 59. Effect of the pre-humidification in the cellulose samples treated for 30 min with TCMS.

Conversely, for the "dry" samples, the lack of the "physicochemical barrier" enabled the effortless diffusion of TCMS through the cellulose fibers, and the ensuing Si-CH_3 vibration peaks were correspondingly less intense (Figure 59).

Furthermore, in the FTIR-ATR spectra showed in Figure 59, another important difference appeared in the range 3000-3600 cm^{-1} associated with the OH stretching band [276]. Whereas the "dry" samples displayed a shape similar to that of pristine cellulose, the pre-humidified counterparts exhibited a significant widening. This was attributed to the presence of additional intermolecular hydrogen bonds, both between i) the water molecules and the –OH groups of the cellulose samples, including those from the

additional -Si-OH at their surface, and ii) the water molecules on their own [276]. Moreover, the intensity of the band at about 1650 cm^{-1}, related to the bending vibrations of –OH groups in absorbed water [276], increased in the spectra of the pre-humidified samples, corroborating the presence of this additional amount of water.

Following the first results and having verified the reproducibility of experiments conducted under the same conditions, four specific samples were selected, in which the two relevant parameters, namely the moisture content and the reaction time, were varied within a maximum range. These limiting reaction conditions are summarized in Table 21, together with the corresponding sample identification. All the chosen samples, including the pristine cellulose fibers, were fully characterized by different techniques, as discussed below.

Table 21. Conditions used to modify the cellulose samples and their respective identification.

Sample identification	Reaction conditions		
	Pre-humidification	Reaction time (min)	TCMS amount (μL)
FP	No	—	—
FP1	No	0.5	10
FP2	No	30	600
FPh1	Yes	0.5	10
FPh2	Yes	30	600

3.1.2. Solid-State ^{29}Si CP-MAS NMR Spectroscopy

Solid-state ^{29}Si CP-MAS NMR spectroscopy was used in order to understand what type of Si-construction was formed after hydrolysis and condensation of the TCMS residues during the treatment of the cellulose samples with TCMS. Figure 60 illustrates the ^{29}Si CP-MAS NMR spectra of the cellulose samples treated for 30 min. Considering that the Si-Cl bonds of TCMS are easily converted into Si-OH groups in contact with moisture, which, in turn, rapidly self-condense into Si-O-Si linkages [295], in these spectra, the silicon sites were labeled according to the conventional T^n notation, corresponding to silicon moieties of the type $CH_3Si(OSi)_n(OR)_{3-n}$ (where n = 1–3 and R= H or cellulose)

[296]. As in the case of the organic-inorganic hybrid cellulose derivatives discussed above, *n* is associated with the number of Si-O-Si bridges formed by certain silicon site (Figure 49). The modification of these cellulose samples gave rise to spectra with signals in two different regions, *viz. ca.* -57 and -66 ppm, assigned to T^2 and T^3 environments (Figure 49), respectively [287, 296], confirming the occurrence of both the hydrolysis and the condensation of TCMS molecules.

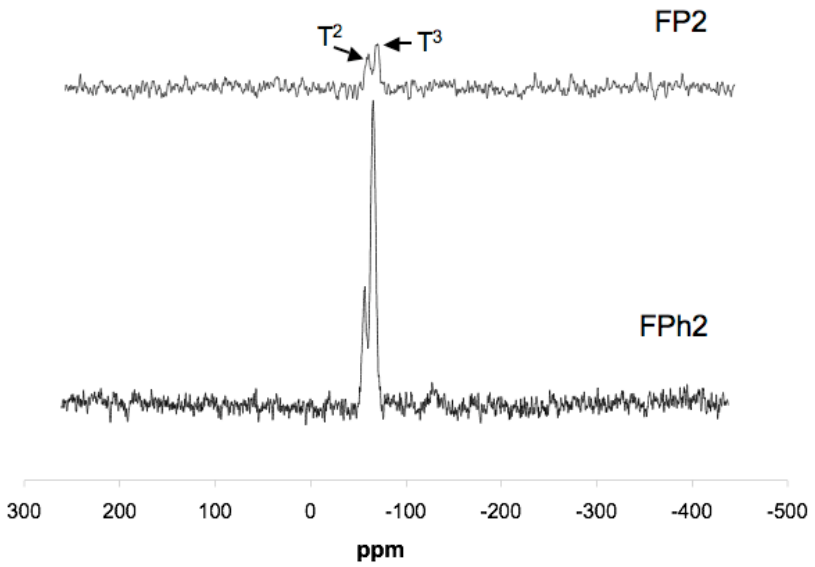

Figure 60. ^{29}Si CP-MAS NMR spectra of the cellulose samples treated with TCMS for 30 min.

The predominance of T^3 environments compared with the T^2 counterparts, suggested that the condensation of TCMS-derived moieties favored the formation of three-dimensional silica constructs together with a lesser contribution of bidimensional geometries, which reflect both covalent attachments to the cellulose and “horizontal” or “vertical” polymerizations, as sketched in Figure 55. The ensuing Si–O–Si branched networks gave rise to a surface inorganic coverage of the fibers, particularly in the case of the FPh2 sample, in which the ^{29}Si CP-MAS NMR signals were more intense (Figure 60), as clearly visible in the SEM images discussed below. Once again, the difference in the intensity of the ^{29}Si resonances for the pre-humidified (FPh2) and “dry” (FP2) samples was attributed to the higher extent of reaction in the former case.

In agreement with the FTIR-ATR results related to the FPh1 sample, no ^{29}Si resonances were detected, confirming that for 0.5 min reaction, the modest amount of TCMS involved (10 μL) reacted exclusively with the added moisture and did not chemically bound to the cellulose fibers.

3.1.3. Elemental Analysis

The elemental composition of the TCMS-treated cellulose samples was determined and the results shown in Table 22.

Table 22. Elemental content of pristine and TCMS-treated cellulose samples.

Sample	Elemental content (%)			
	C	H	O	Si
FP	42.2	6.6	50.2	—
FP1	42.6	6.5	50.6	0.1
FP2	42.4	6.5	50.4	0.3
FPh1	42.2	6.6	50.2	—
FPh2	37.0	6.2	47.0	9.3

Apart from carbon, hydrogen, and oxygen, the treated samples, except for FPh1, also contained silicon. The Si amount in the samples varied considerably with respect to two major parameters, namely i) the pre-humidification treatment and ii) the treatment time. Thus, in the absence of added moisture, FP1 and FP2 samples, the TCMS-treatment led to a low Si amount, which, moreover, showed a modest sensitivity to the reaction time. In contrast, when the pre-humidification process was applied, FPh1 and FPh2 samples, depending on the reaction time, a high content of silicon was attained. In other words, while for a 0.5 min treatment no Si was detected in the pre-humidified sample (FPh1), an increase to 30 min, all other conditions being the same, more than 9% of this element was present in the treated sample (FPh2).

These results corroborated the hypothesis that in the absence of added moisture, most of the TCMS molecules passed through the cellulose sample without reacting with its -OH groups, as previously discussed for the FTIR-ATR results. In other words, after a certain amount of direct condensation of TCMS with the most readily available cellulose OH groups, the excess of it flowed through the sample.

Interestingly, FP2 (30 min reaction) contained only a slightly higher amount of silicon than FP1 (0.5 min reaction), in contrast with both FTIR-ATR and XPS (presented

below) data, which privileged the former. This can be explained considering that whereas the elemental analysis reflects bulk contents, the other two methods are associated with surface composition. It follows that the reactions in the case of FP2 were protracted mostly at the surface of the sample, probably favored by the initial modification, thus showing a higher surface silicon content compared with FP1, as opposed to similar global values. The apparent anomaly associated with the absence of Si in the FPh1 sample is rationalized on the basis of the arguments put forward previously when discussing the corresponding FTIR-ATR and ^{29}Si NMR negative results.

As in the case of the organic-inorganic hybrid cellulose derivatives, it was not possible to determine the DS of the TCMS-treated samples, due to the same reasons discussed in that context.

3.1.4. Thermogravimetric Analysis

As can be seen in Figure 61, the modified cellulose substrates, here represented by the samples treated for 30 min with TCMS, displayed thermograms similar to that of the neat cellulose fibers, with a two-step degradation profile. Moreover, the thermal stability of the TCMS-treated samples was also very similar to that of the pristine substrate, *i.e.*, with very close T_{di} values, although the former, except for FPh1, showed a non-negligible increment in T_d, of about 15 ºC (Table 23), attributed to the presence of an inorganic environment around the fibers.

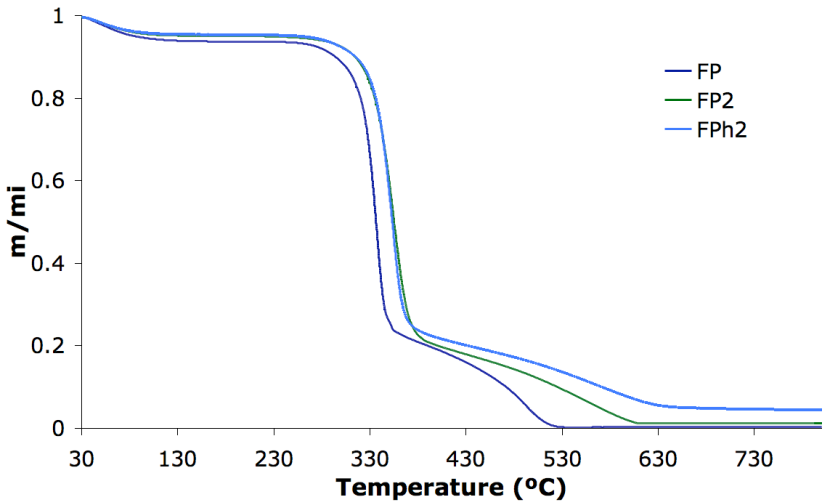

Figure 61. TGA tracings of cellulose samples before and after treatment with TCMS for 30 min (FP2 and FPh2).

Table 23. Thermogravimetric data of pristine and TCMS-treated cellulose samples.

Sample	T_{di} (ºC)	T_d (ºC)	Weight loss at 800 ºC (%)
FP	258	338	99.7
FP1	263	353	98.9
FP2	261	356	98.8
FPh1	259	339	99.6
FPh2	260	354	95.4

Additionally, the absence of total weight loss at 800 ºC in the TCMS-treated cellulose fibers (except for FPh1), or more specifically, a weight loss lower than in the pristine cellulose sample (0.8-4.3% lower), corroborated the presence of silica-related residues (Table 23). Even though that contribution was small due to, one the one hand, the corresponding small quantity of TCMS used in the treatments and, on the other, the diffuse of the excess unreacted TCMS through the substrates. As a result, while the "dry" filter papers treated with TCMS for 0.5 and 30 min (FP1 and FP2, respectively) presented identical total weight loss at 800 ºC (*viz.* about 99%), the FPh2 sample displayed the highest residual weight at that temperature, indicating the presence of a correspondingly higher amount of inorganic components, as already suggested by the FTIR-ATR, elemental analysis and ^{29}Si CP-MAS NMR results discussed above.

3.1.5. Surface Characterization by X-Ray Photoelectron Spectroscopy

The XPS analysis was carried out on both neat and TCMS-treated cellulose samples and provided their surface chemical composition (1.5-10 nm depth). The low-resolution XPS data is summarized in Table 24. As it can be noted, further than carbon and oxygen, the modified samples clearly showed the additional presence of silicon, with contributions of electrons emitted from its 2s and 2p atomic orbitals (binding energies around 150 and 100 eV [297], respectively) (Figure 62). These results clearly confirmed the occurrence of the modification reaction of the cellulose substrates with TCMS. Moreover, as already discussed for the FTIR-ATR and ^{29}Si NMR spectroscopy results, the FPh1 sample did not exhibit the presence of silicon (Table 24), which confirmed once again the absence of modification in this sample for the reasons mentioned above.

Table 24. Low-resolution XPS results of pristine and TCMS-treated filter papers.

Sample	Low-resolution XPS				
	[O]/%	[C]/%	[Si]/%	Si/O	Si/C
FP	42.0	58.0	—	—	—
FP1	43.7	48.9	7.4	0.17	0.15
FP2	43.9	38.6	17.5	0.40	0.45
FPh1	42.3	55.0	—	—	—
FPh2	44.0	38.3	17.7	0.40	0.46

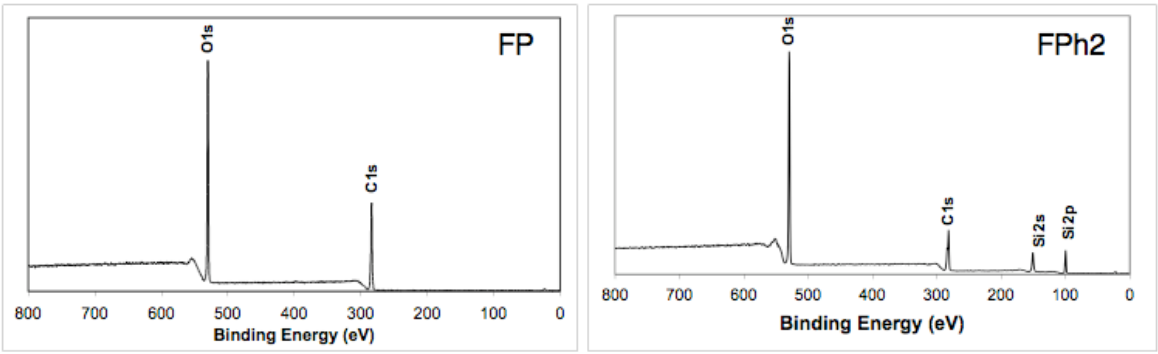

Figure 62. Low-resolution XPS spectra of pristine cellulose (left) and FPh2 (right) samples.

Interestingly, the low-resolution XPS also showed, based on the Si percentage and the Si/O and Si/C ratios (Table 24), that the surface coverage by silicon species, as opposed to the bulk Si content obtained by elemental analysis, seemed to be predominantly affected by the reaction time and not by the pre-humidification of the samples, since a similar surface coverage was obtained for samples treated for the same period of time, *i.e.*, presence of about 18% of silicon for both FP2 and FPh2. Nevertheless, it is important to emphasize here that the term ‘‘surface” refers to 1.5-10 nm, which is the scanning depth of XPS, but this does not imply that the FPh2 sample had indeed a much thicker layer of modified material, as suggested by the elemental analysis showed above and depicted by the Si mapping discussed below.

Additionally, the high-resolution deconvolution of the C*1s* peak (Table 25) revealed the expected increase in the contribution of the C1 carbon atoms (C-H), due to the presence of the Si-CH_3 moieties at the surface of the modified samples, compared with that of the pristine cellulose fibers, and a much higher increment for the longer reactions, reflecting a correspondingly higher surface coverage by siloxane moieties.

Table 25. High-resolution deconvolution of C*1s* signals of pristine and TCMS-treated cellulose samples.

Sample	High-resolution XPS (Area/%)		
	C1	C2	C3
FP	8.8	71.4	17.7
FP1	23.3	60.9	14.6
FP2	57.6	34.9	7.5
FPh1	6.6	73.1	18.2
FPh2	61.7	31.6	6.7

3.1.6. C and Si Mapping

Figure 63 depicts the C and Si distribution at the surface and through the thickness of the samples treated for 30 min. The presence of silicon (blue label) throughout both samples clearly indicated that the reaction of TCMS was not limited to their surface, although in the

case of FPh2 the concentration of silicon was much higher within the first 50 μm (Figure 63C), in contrast with the relative homogeneity of its distribution in the FP2 sample (Figure 63A). The latter observation strongly suggests that the presence of the added moisture at the surface of FPh2 provoked an important contribution of hydrolysis/condensation reactions of the TCMS molecules, as already suggested, thus giving rise to the observed Si gradient, contrary to its more regular distribution throughout the thickness of the FP2 "dry" sample (Figure 63A).

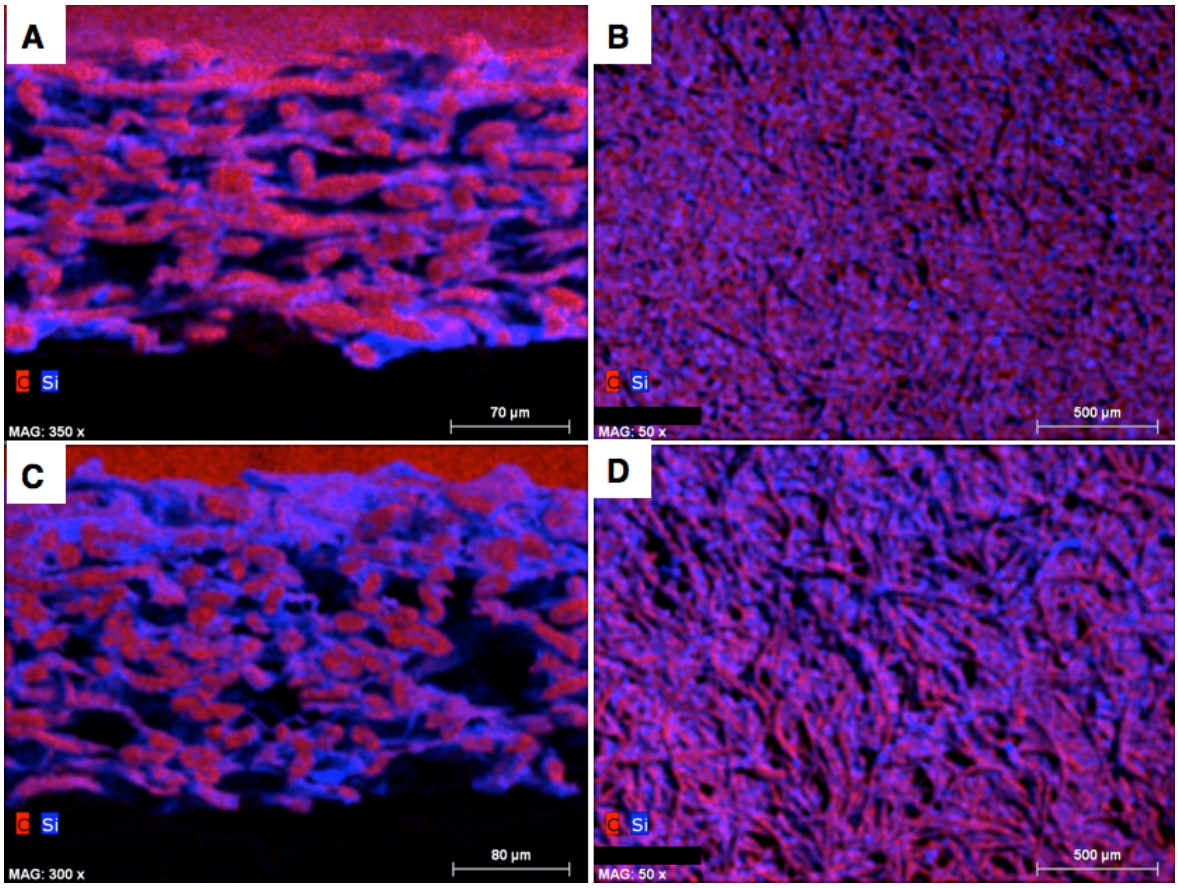

Figure 63. C (red) and Si (blue) mapping of FP2 [(A) cross-section, (B) surface] and FPh2 [(C) cross-section, (D) surface].

Additionally, these observations corroborate the interpretation proposed above as to the apparent contradiction between similar values of silicon detected by XPS, as opposed to a much higher Si content in the former, based on its elemental analysis. The FTIR-ATR spectra shown in Figure 59 further confirmed this hypothesis, with more intense peaks associated with the pre-humidified samples compared with those of the "dry" counterparts, because the depth of analysis is here of the order of a few micrometers (1-2 μm), *i.e.*, some thousand times higher than with XPS. The other important point

associated with these observations is that the availability of TCMS over a sufficiently long period of time resulted in the modification of the cellulose fibers within the bulk of the filter paper instead of a reaction limited to its surface. The mapping of FP1, shown in Figure 64, revealed a cartography similar to that of FP2, except for the fact that the silicon was even more homogeneous throughout the sample thickness. Once again FPh1 did not reveal the a detectable presence of silicon, in tune with all previous observations on this sample. Not surprisingly, the surface distribution of Si and C relative to the inlet side was quite even in the three modified filter papers, as shown in Figure 63B, Figure 63D and Figure 64.

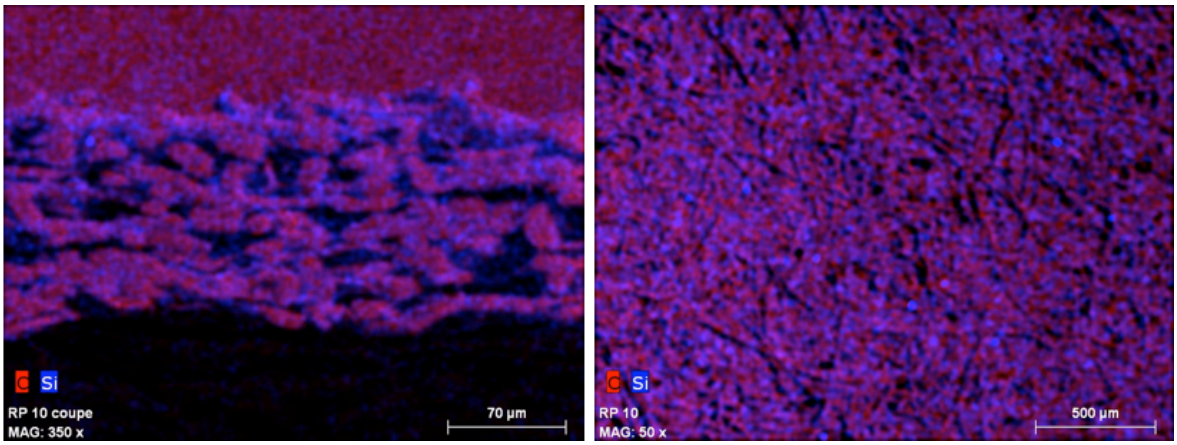

Figure 64. C (red) and Si (blue) mapping of FP1: cross-section (left) and surface (right).

3.1.7. Surface Morphology Characterization by Scanning Electron Microscopy

The SEM micrographs of the pristine cellulose sample (Figure 65) showed the typical features of a refined commercial pure cellulose, characterized by the presence of microfibrils both at the surface (Figure 65A) and within the cross-section (Figure 65B), resulting from the mechanical method associated with the refining process [249]. This type of morphology was maintained in all the modified samples (Figure 65).

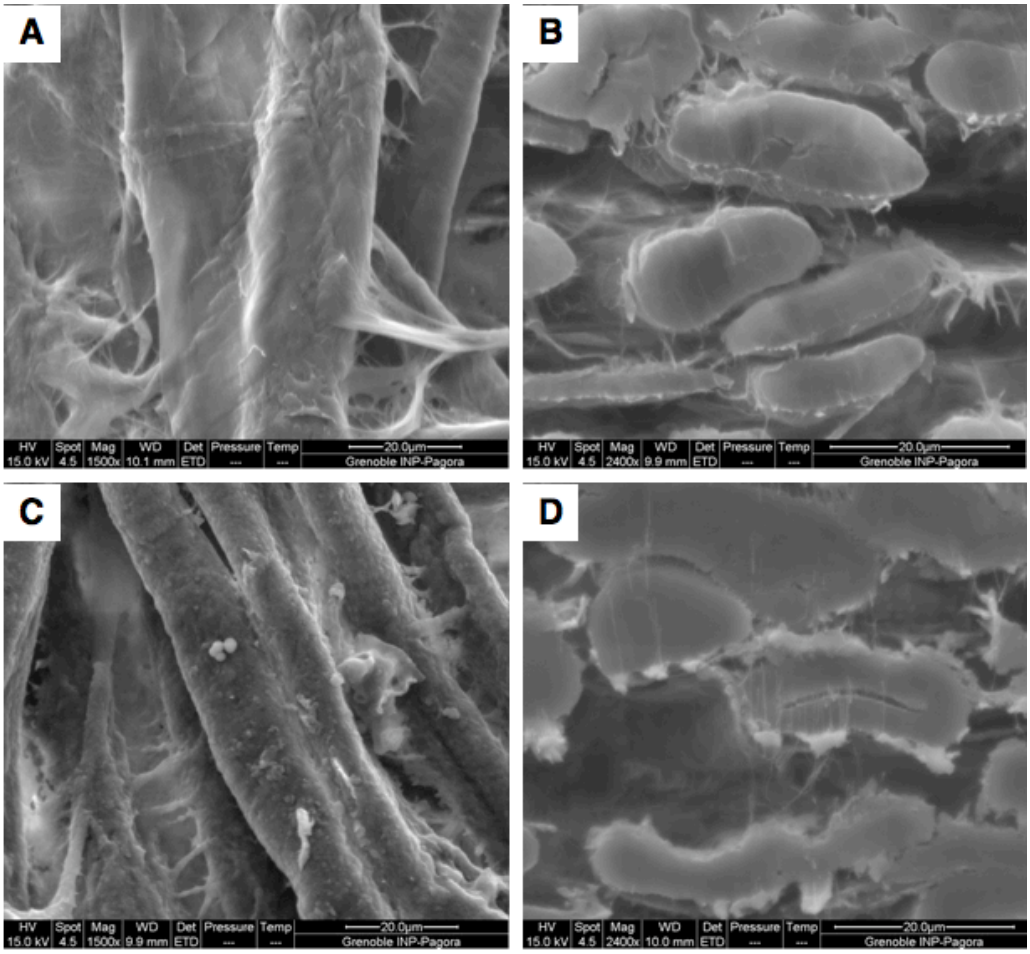

Figure 65. Scanning electron micrographs of pristine filter paper surface [(A) cross-section, (B) surface] and FPh2 sample [(C) cross-section, (D) surface] (surface and cross-sectional images with 1500x and 2400x magnification, respectively).

Additionally, and more importantly, the SEM images of the FP2 and FPh2 samples displayed a characteristic ‘‘coating sleeve” surrounding the cellulose fibers, a feature that was much more pronounced in the latter sample (Figure 65C). This added morphology was made up of an assembly of small particles, probably the result of the formation of Si-O-Si three-dimensional networks, which was again more prominent in the FPh2 sample (Figure 66), probably because of the more pronounced hydrolysis/condensation reactions of TCMS, as already discussed.

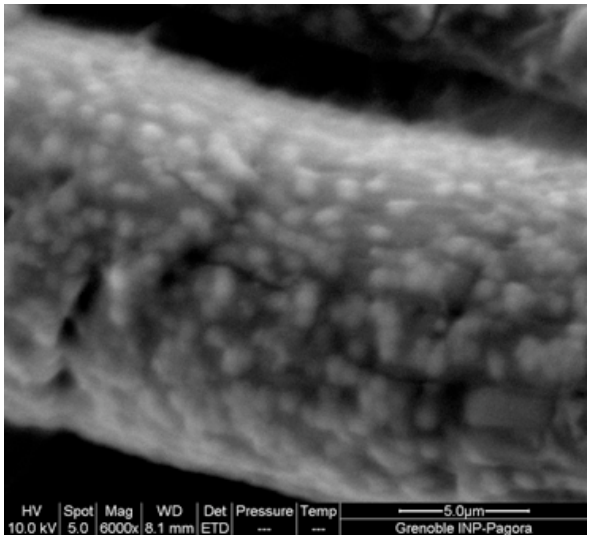

Figure 66. Scanning electron micrograph of FPh2 sample at 6000x magnification.

3.1.8. Contact Angle Measurements and Determination of the Surface Energy

Table 26 gives the average contact angles measured with drops of liquids of different polarities deposited on the inlet surface of the treated samples, compared with those related to the surface of the pristine substrate.

Table 26. Contact angles of different liquids onto the surface of the cellulose samples before and after modification with TCMS.

Sample	Contact angles (º)			
	Water	Glycerol	Diiodomethane	1-Bromonaphthalene
FP	36	41	37	23
FP1	134	98	106	62
FP2	136	127	109	71
FPh1	40	43	39	25
FPh2	125	121	106	82

The large increase in the contact angles with both polar (water and glycerol) and non-polar (diiodomethane and 1-bromonaphthalene) liquids, except for FPh1, gave a clear indication that the character of the modified cellulose surface had been drastically turned into both a high hydrophobicity and a high lipophobicity.

The corresponding polar and dispersive contributions to the surface energy shown in Figure 67 indicate that, again except for FPh1, the major change was associated with an almost total elimination of the former contribution, although the dispersive counterpart was also critically reduced.

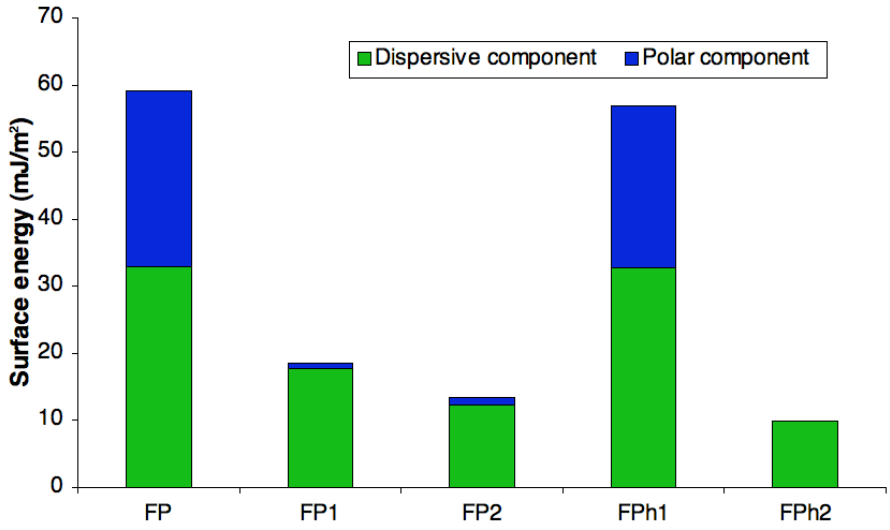

Figure 67. Surface energy, and its respective dispersive and polar components, of pristine and TCMS-treated samples.

This radical modification in the surface properties of cellulose can be rationalized in terms of both the presence of Si–CH_3 moieties at the surface of the modified fibers, which are known to confer water repellency to polar substrates [291], and the novel siloxane micro-morphology generated at the surface of the fibers treated for the longer reaction time, *i.e.*, the joint action of the chemical reduction in the surface polarity (replacement of some -OH groups by -CH_3 moieties) and the increase in its rugosity (presence of the hybrid particles). It is notable that this highly omniphobic behavior was observed even in samples that were treated for short times, as exemplified here in the case of the FP1 sample. Indeed, the use of higher amounts of TCMS did not lead to any appreciable increase in the contact angle values, which corroborates the C and Si mapping observations, *i.e.*, that TCMS also diffused into the samples and reacted therein, but that most of it was left unreacted. This feature was readily verified by a series of runs

in which a growing number of "dry" filter papers, up to six, were piled up in the holder and exposed to the TCMS/N_2 flow for 30 min. Under these conditions, the modifications described above took place in *all of them*.

The fact that the somewhat lower water contact angle value obtained for the FPh2 sample, with respect to those of the FP1 and FP2 samples, was not followed by a corresponding increment in its surface energy (Figure 67), might be related to the empirical character of the Owens-Wendt approach, as discussed in *Chapter 1*, which has, of course, an associated uncertainty.

Finally, the exceptional inhert behavior of the FPh1 sample rejoins all previous observations in that the fibers' surface after extraction displayed contact angles and hence surface energies very close to those of the pristine substrate (Table 26 and Figure 67).

3.2. Conclusions

The approach adopted in this study enabled to induce a substantial increase in the hydrophobic as well as lipophobic character of cellulose fibers through a particularly simple, fast and "green" process, simpler, faster and greener than the previous approaches studied here. Indeed, these positive features were not reported previously within this research area. More specifically it was possible to prepare highly omniphobic cellulose samples using very low amounts of TCMS and treatment times as low as 0.5 min in a gas-solid system, which did not require the use of solvents or catalysts. In these reactions, the moisture content of the substrates played, as expected, a very important role in directing the alternative mechanisms and hence the structure and morphology of the end product. It is therefore imperative to attach the highest importance to the fine-tuning of this parameter in order to be able to tailor the desired final properties.

This kind of omniphobic cellulose derivatives could be applied in different areas such as packaging, special papers and textiles.

At last, it is worth noting that the system developed in this work can be easily applied to other OH-bearing substrates, both natural and synthetic, like starch and polyvinyl alcohol (PVA), respectively. Additionally, this approach can be extended to other chlorosilanes or even chlorosilane mixtures, in order to optimize the applications of the

ensuing materials and enhance their omniphobic effects, while maintaining its original simplicity and sustainability.

Chapter 4

Concluding Remarks and Future Perspectives

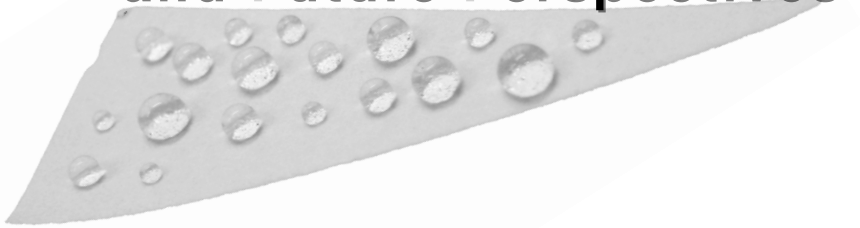

Chapter 4 – Concluding Remarks and Future Perspectives

This thesis offered new approaches for the controlled heterogeneous modification of cellulose fibers and the preparation of innovative cellulose-based materials with tailored surface features.

Thus, the modification of the cellulose fibers with the perfluorinated reagents gave rise to highly hydrophobic and lipophobic cellulose derivatives, without the need of an extensive surface coverage with perfluorinated moieties.

The hydrolytic stability of the perfluorinated cellulose derivatives constituted an interesting characteristic, since they presented different behaviors. Whereas the TFAA-derivatives showed to be highly labile, being readily hydrolyzed in neutral medium, the PFBz- and TFP-derivatives exhibited considerably higher hydrolytic stability in both neutral and acid media, being, however, hydrolyzed in high alkaline pH. This feature constitutes a crucial factor for delineating the potential applications for these cellulose derivatives.

The modification of the cellulose fibers with ICPTEOS and subsequent acid hydrolysis treatment of the ensuing modified fibers, as such or in the presence of TEOS or PFDTEOS, permitted to prepare class-II organic-inorganic hybrid cellulose derivatives with distinct surface features. On the one hand, highly hydrophilic cellulose hybrids were obtained after acid hydrolysis treatment of the ICPTEOS-modified samples, as such or in the presence of TEOS, and on the other, highly hydrophobic, or even bi-phobic cellulose-based hybrid materials were obtained after simple modifications with ICPTEOS or acid hydrolysis in the presence of PFDTEOS, respectively. These new surface features, similarly to those of the perfluorinated cellulose derivatives, can be achieved with a limited extent of surface modification, which represents a positive aspect regarding potential applications for these cellulose-based hybrid materials.

Finally, the heterogeneous modification of the cellulose fibers with vapor-phase TCMS constituted a “greener” strategy for the preparation of highly hydrophobic and lipophobic cellulose-based materials compared with the other two approaches. Moreover, the bi-phobic behavior was attained even for very short treatment times (corresponding to very low amounts of TCMS flowed through the cellulose samples), which represents an additional positive feature of this system.

It is worth mentioning that all the possible applications suggested in *Chapter 3* for all the obtained cellulose derivatives are merely speculative, since, as referred, all the investigations discussed constitute more likely fundamental studies rather than applied studies.

Nonetheless, not devaluing the materials produced, for their actual application several improvements in the methodologies discussed here have to be considered in the future. Specifically, the replacement of the organic solvents employed, *i.e.*, toluene and DMF, by "greener" solvents, *e.g.*, ionic liquids (without capacity to dissolve cellulose), would be desirable. Moreover, eco-friendly catalysts should be chosen instead of pyridine or DBTL, such as solid acids or enzymes.

The considerably high price typically associated with the perfluorinated reagents employed, for instance, could constitute an additional drawback, although it was shown that even a low amount of these would be able to confer highly bi-phobic properties to large quantities of cellulose fibers, thus minimizing this drawback.

Additionally, and as already mentioned, at the end of the perfluorinated cellulose derivatives life-cycle, their recycling or degradation would imply the release of perfluorinated substances that could constitute an environmental threat, especially the pentafluorobenzoic and trifluoropropanoic acids and/or their salts. However, their elimination would be possible, particularly considering that their amount would be very low. On the other hand, if one could design an adequate system for recovering the perfluorinated substances, they could be re-utilized as such or by conversion into other compounds.

In another vein, a further improvement of the vapor-phase system developed, maintaining its initial simplicity, would be the possibility of controlling the relative humidity, since, as discussed, moisture plays a very important role in this process, and also try to recover and re-utilize the TCMS that passes through the samples without reacting. Furthermore, the possibility of using moisture-controlled air instead of nitrogen as carrier gas, constitutes another positive feature of the system, which was already verified experimentally.

In this context, future perspectives include:

(i) Prepare composite materials reinforced by either the perfluorinated cellulose fibers (PFBz- or TFP-derivatives) or the cellulose-based

hybrids, by choosing adequate polymeric matrices, and study their performance;

(ii) Prepare class-II organic-inorganic hybrid cellulose materials by using other silane-coupling agents or siloxanes during the acid hydrolysis treatments, for further tailoring of the surface properties of the ensuing products;

(iii) Test the vapor-phase modification of cellulose fibers with other chlorosilanes or chlorosilanes mixtures, to widen the range of their surface features;

(iv) Modify the cellulose fibers using other reagents under “greener” conditions, for the preparation of cellulose derivatives with interesting and innovative surface features, especially pointing to superhydrophobic properties;

(v) Extend the modifications to other polysaccharides/substrates, for instance starch (thermoplastic or powder) and chitosan (films or powder);

(vi) Perform applied studies with the most promising cellulose derivatives prepared up to now, as well as with the other materials that will be prepared in the future, including derivatives from other substrates.

References

References

1. Gandini, A. and Belgacem, M.N. (**2008**) The state of the art. In M.N. Belgacem and A. Gandini (Eds.), Monomers, polymers and composites from renewable resources (1st ed., 1-16). Amsterdam: Elsevier.
2. Klemm, D., Heublein, B., Fink, H-.P., Bohn, A. (**2005**) Cellulose: Fascinating biopolymer and sustainable raw material. Angew. Chem. Int. Ed., 44(22), 3358-3393.
3. Klemm, D., Philipp, B., Heinze, T., Heinze, U., Wagenknecht, W. (**1998**) Comprehensive cellulose chemistry: Fundamentals and analytical methods. (1st ed., vol. 1). Weinheim: Wiley-VCH.
4. Klemm, D., Philipp, B., Heinze, T., Heinze, U., Wagenknecht, W. (**1998**) Comprehensive cellulose chemistry: Functionalization of cellulose. (1st ed., vol. 2). Weinheim: Wiley-VCH.
5. Ramesh, H.P. and Tharanathan, R.N. (**2003**) Carbohydrates - The renewable raw materials of high biotechnological value. Crit. Rev. Biotechnol., 23(2), 149-173.
6. Gandini, A. (**2008**) Polymers from renewable resources: A challenge for the future of macromolecular materials. Macromolecules, 41(24), 9491-9504.
7. Freire, C.S.R., Silvestre, A.J.D., Neto, C.P., Belgacem, M.N., Gandini, A. (**2006**) Controlled heterogeneous modification of cellulose fibers with fatty acids: Effect of reaction conditions on the extent of esterification and fiber properties. J. Appl. Polym. Sci., 100(2), 1093-1102.
8. Sequeira, S., Evtuguin, D.V., Portugal, I., Esculcas, A.P. (**2007**) Synthesis and characterisation of cellulose/silica hybrids obtained by heteropoly acid catalysed sol-gel process. Mater. Sci. Eng. C, 27, 172-179.
9. French, A.D., Bertoniere, N., Brown, R.M., Chanzy, H., Gray, D., Hattori, K., Glasser, W. (**2007**) Cellulose. In R.E. Kirk and D.F. Othmer (Eds.), Kirk-Othmer encyclopedia of chemical technology (5th ed., vol. 5, 360-393). Hoboken (NJ): John Wiley & Sons.
10. Klemm, D., Schmauder, H-.P., Heinze, T. (**2002**) Cellulose. In E.J. Vandamme, S.D. Baets and A. Steinbüchel (Eds.), Biopolymers (1st ed., vol. 6, 275-312). Weinheim: Wiley–VCH.
11. Krässig, H.A. (**1993**) Cellulose: Structure, accessibility and reactivity (1st ed). Amsterdam: Gordon and Breach Science Publishers.
12. Atalla, R.H. (**1999**) Celluloses. In S.D. Barton, K. Nakanishi, O.M-. Cohn and B.M. Pinto (Eds.), Comprehensive natural products chemistry: Carbohydrates and their derivatives including tannins, cellulose and related lignins (1st ed., vol. 3, 529-598). New York: Elsevier Science..
13. Atalla, R.H., Brady, J.W., Matthews, J.F., Ding, S-.Y., Himmel, M.E. (**2008**) Structures of plant cell wall celluloses. In M.E. Himmel (Ed.), Biomass recalcitrance: Deconstructing the plant cell wall for bioenergy (1st ed., 188-212). Chichester: Wiley-Blackwell.
14. Belgacem, M.N. and Gandini, A. (**2008**) Surface modification of cellulose fibres. In M.N. Belgacem and A. Gandini (Eds.), Monomers, polymers and composites from renewable resources (1st ed., 385-400). Amsterdam: Elsevier.
15. Delmer, D.P. (**1999**) Cellulose biosynthesis: Exciting times for a difficult field of study. Annu. Rev. Plant Physiol. Plant Mol. Biol., 50, 245-276.

16. Brown Jr., R.M. and Saxena I.M. (**2000**) Cellulose biosynthesis: A model for understanding the assembly of biopolymers. Plant Physiol. Biochem., 38(1-2), 57-67.

17. Brown Jr., R.M. (**2004**) Cellulose structure and biosynthesis: What is in store for the 21st century? J. Polym. Sci. Pol. Chem., 42(3), 487-495.

18. Somerville, C. (**2006**) Cellulose synthesis in higher plants. Annu. Rev. Cell. Dev. Bi., 22, 53-78.

19. Chawla, P.R., Bajaj, I.B., Survase, S.A., Singhal, R.S. (**2009**) Microbial cellulose: fermentative production and applications. Food Technol. Biotech., 47(2), 107-124.

20. Shoda, M. and Sugano, Y. (**2005**) Recent advances in bacterial cellulose production. Biotechnol. Bioproc. Eng., 10(1), 1-8.

21. Kobayashi, S., Sakamoto, J., Kimura S. (**2001**) In vitro synthesis of cellulose and related polysaccharides. Prog. Polym. Sci., 26, 1525-1560.

22. Dammstrom, S., Glasser, W., Gatenholm, P. (**2006**) Preparation and properties of cellulose/xylan nanocomposites. In D. Stokke and L.H. Groom (Eds.), Characterization of the cellulosic cell wall (1st, 53-63). Iowa: Wiley-Blackwell.

23. Pecoraro, É., Manzani, D., Messaddeq, Y., Ribeiro, S.J.L. (**2008**) Bacterial cellulose from *Glucanacetobacter xylinus*: Preparation, properties and applications. In M.N. Belgacem and A. Gandini (Eds.), Monomers, polymers and composites from renewable resources (1st ed., 369-384). Amsterdam: Elsevier.

24. Habibi, Y., Lucia, L.A., Rojas, O.J. (**2010**) Cellulose nanocrystals: Chemistry, self-assembly, and applications. Chem. Rev., 110(6), 3479-3500.

25. Atalla, R.H. and Vanderhart, D.L. (**1984**) Native cellulose: A composite of two distinct crystalline forms. Science, 223, 283-285.

26. Vanderhart, D.L. and Atalla R.H. (**1984**) Studies of microstructure in native celluloses using solid-state ^{13}C NMR. Macromolecules, 17(8),1465-1472.

27. Sugiyama, J., Okano, T., Yamamoto, H., Horii, F. (**1990**) Transformation of Valonia cellulose crystals by an alkaline hydrothermal treatment. Macromolecules, 23(12), 3196-3198.

28. Wada, M., Heux, L., Nishiyama, Y., Langan, P. (**2009**) X-ray crystallographic, scanning microprobe X-ray diffraction, and cross-polarized/magic angle spinning ^{13}C NMR studies of the structure of cellulose III_{II}. Biomacromolecules, 10(2), 302-309.

29. Gardiner, E.S. and Sarko, A. (**1985**) Packing analysis of carbohydrates and polysaccharides. 16. The crystal structures of celluloses IV_I and IV_{II}. Can. J. Chem., 63(1), 173-180.

30. Heinze, T. and Liebert, T. (**2001**) Unconventional methods in cellulose functionalization. Prog. Polym. Sci., 26, 1689-1762.

31. Edgar, K.J., Buchanan, C.M, Debenham, P.A.R., Seiler, B.D., Shelton, M.C., Tindall, D. (**2001**) Advances in cellulose ester performance and application. Prog. Polym. Sci., 26, 1605-1688.

32. Liebert, T. (**2010**) Cellulose solvents – Remarkable history, bright future. In T. Liebert, T. Heinze and K.J. Edgar (Eds.), ACS symposium series - Cellulose solvents: analysis, shaping, and chemical modification (vol. 1033, 3-54). Washington, D.C.: American Chemical Society.

33. Heinze, T. and Petzold, K. (**2008**) Cellulose chemistry: Novel products and synthesis paths. In M.N. Belgacem and A. Gandini (Eds.), Monomers, polymers and composites from renewable resources (1st ed., 343-368). Amsterdam: Elsevier.

34. Heinze, T. and Koschella, A. (**2005**) Solvents applied in the field of cellulose chemistry: A mini review. Polímeros, 15(2), 84-90.

35. Pinkert, A., Marsh, K.N., Pang, s., Staiger, M.P. (**2009**) Ionic liquids and their interaction with cellulose. Chem. Rev., 109(12), 6712-6728.

36. El Seoud, O.A. and Heinze, T. (**2005**) Organic esters of cellulose: New perspectives for old polymers. Adv. Polym. Sci., 186, 103-149.

37. Shelton, M.C. and Edgar, K.J. (**2004**) Cellulose esters. In H.F. Mark (Ed.), Encyclopedia of polymer science and technology (3rd ed., vol. 9). Hoboken (NJ): John Wiley & Sons.

38. Majewicz, T.G., Majewicz, P.E.E-., Podlas, T.J (**2004**) Cellulose ethers. In H.F. Mark (Ed.), Encyclopedia of polymer science and technology (3rd ed., vol. 5). Hoboken (NJ): John Wiley & Sons.

39. Edgar, K.J., Pecorini, T.J., Glasser, W.G. (**1998**) Long-chain cellulose esters: preparation, properties, and perspective. In T.J. Heinze and W.G. Glasser (Eds.), Cellulose derivatives: Modification, characterizaion, and nanostructures (1st ed., vol. 688, 38-60). ACS Symposium Series.

40. El Seoud, O.A., Marson, G.A., Ciacco, G.T., Frollini, E. (**2000**) An efficient, one-pot acylation of cellulose under homogeneous reaction conditions. Macromol. Chem. Phys., 201(8), 882-889.

41. Rahn, K., Diamantoglou, M., Klemm, D., Berghmans, H., Heinze, T. (**1996**) Homogeneous synthesis of cellulose p-toluenesulfonates in N,N-dimethylacetamide/LiCl solvent system. Die Angew. Makromol. Chem., 238(1), 143-163.

42. Belgacem, M.N. and Gandini, A. (**2005**) Surface modification of cellulose fibres. Polímeros, 15(2), 114-121.

43. Freire, C.S.R. and Gandini, A. (**2006**) Recent advances in the controlled heterogeneous modification of cellulose for the development of novel materials. Cell. Chem. Technol., 40(9-10), 691-698.

44. Gandini, A. and Belgacem, M.N. (**2007**) Surface and In-Depth Modification of Cellulose Fibers. In D.S. Argyropoulos (Ed.), ACS symposium series – Materials, chemicals, and energy from forest biomass (1st ed., vol. 954, 93-106). Washington, D.C.: Oxford University Press.

45. Hua, L., Flodin, P., Rönnhult, T. (**1987**) Cellulose fiber-polyester composites with reduced water sensitivity. 2. Surface analysis. Polym. Compos., 8(3), 203-207.

46. Taj, S., Munawar, M.A., Khan, S. (**2007**) Natural fiber-reinforced polymer composites. Proc. Pakistan Acad. Sci., 44(2), 129-144.

47. Mohanty, A.K., Misra, M., Drzal, L.T. (**2005**) Natural fibers, biopolymers, and biocomposites (1st ed.). Boca Raton: CRC Press.

48. Bledzki, A.K. and Gassan, J. (**1999**) Composites reinforced with cellulose based fibres. Prog. Polym. Sci., 24(2), 221-274.

49. Gauthier, R., Joly, C., Coupas, A.C., Gauthier, H., Escoubes, M. (**1998**) Interfaces in polyolefin/cellulosic fiber composites: Chemical coupling, morphology, correlation with adhesion and aging in moisture. Polym. Compos., 19(3), 287-300.

50. Gaceva, G.B-., Avella, M., Malinconico, M., Buzarovska, A., Grozdanov, A., Gentile, G., Errico, M.E. (**2007**) Natural fiber eco-composites. Polym. Compos., 28(1), 98-107.

51. Plackett, D., Andersen, T.L., Pedersen, W.B., Nielsen, L. (**2003**) Biodegradable composites based on L-polylactide and jute fibres. Compos. Sci. Technol., 63(9): 1287-1296.

52. Mohanty, A.K., Misra, M., Hinrichsen, G. (**2000**) Biofibres, biodegradable polymers and biocomposites: An overview. Macromol. Mater. Eng., 276/277, 1-24.

53. Herrmann, A.S., Nickel, J., Riedel, U. (**1998**) Construction materials based upon biologically renewable resources-from components to finished parts. Polym. Degrad. Stabil., 59(1), 251-261.

54. Riedel, U. and Nickel, J. (**1999**) Natural fibre-reinforced biopolymers as construction materials - new discoveries. Angew. Makromol. Chem., 272(1), 34-40.

55. Satyanarayana, K.G., Arizaga, G.G.C., Wypych, F. (**2009**) Biodegradable composites based on lignocellulosic fibers - An overview. Prog. Polym. Sci., 34(9), 982-1021.

56. Lau, K-.t., Ho, M-.p., Yeung, C-.t.A-., Cheung, H-.y. (**2010**) Biocomposites: Their multifunctionality. Int. J. Smart Nano Mat., 1(1), 13 - 27.

57. John, M.J. and Thomas, S. (**2008**) Biofibres and biocomposites. Carbohyd. Polym., 71(3), 343-364.

58. Yu, L., Dean, K., Li, L. (**2006**) Polymer blends and composites from renewable resources. Prog. Polym. Sci., 31(6), 576-602.

59. Matsumura, H., Sugiyama, J., Glasser, W.G. (**2000**) Cellulosic nanocomposites. I. Thermally deformable cellulose hexanoates from heterogeneous reaction. J. Appl. Polym. Sci., 78(13), 2242-2253.

60. Matsumura, H. and Glasser, W.G. (**2000**) Cellulosic nanocomposites. II. Studies by atomic force microscopy. J. Appl. Polym. Sci., 78(13), 2254-2261.

61. Freire, C.S.R., Silvestre, A.J.D., Neto, C.P., Gandini, A., Fardim, P., Holmbom, B. (**2006**) Surface characterization by XPS, contact angle measurements and ToF-SIMS of cellulose fibers partially esterified with fatty acids. J. Colloid Interf. Sci., 301(1), 205-209.

62. Lu, X., Zhang, M.Q., Rong, M.Z., Shi, G., Yang, G.C. (**2002**) All-Plant fiber composites. I: Unidirectional sisal fiber reinforced benzylated wood. Polym. Compos., 23(4), 624-633.

63. Lu, X., Zhang, M.Q., Rong, M.Z., Shi, G., Yang, G.C. (**2003**) All-plant fiber composites. II: Water absorption behavior and biodegradability of unidirectional sisal fiber reinforced benzylated wood. Polym. Compos., 24(3), 367-379.

64. Lu, X., Zhang, M.Q., Rong, M.Z., Shi, G., Yang, G.C. (**2003**) Self-reinforced melt processable composites of sisal. Compos. Sci. Technol., 63(2), 177-186.

65. Gandini, A., Curvelo, A.A.S., Pasquini, D., Menezes, A.J. (**2005**) Direct transformation of cellulose fibres into self-reinforced composites by partial oxypropylation. Polymer, 46(24), 10611-10613.

66. Nishino, T., Matsuda, I., Hirao, K. (**2004**) All-cellulose composite. Macromolecules, 37(20), 7683-7687.

67. Nishino, T. and Arimoto, N. (**2007**) All-cellulose composite prepared by selective dissolving of fiber surface. Biomacromolecules, 8, 2712-2716.

68. Duchemin, B.J.C., Newman, R.H., Staiger, M.P. (**2009**) Structure-property relationship of all-cellulose composites. Compos. Sci. Technol., 69(7-8), 1225-1230.

69. Gindl, W., Schöberl, T., Keckes, J. (**2006**) Structure and properties of a pulp fibre-reinforced composite with regenerated cellulose matrix. Appl. Phys. A, 83(1), 19-22.

70. de Menezes, A.J., Pasquini, D., Curvelo, A.A.S., Gandini, A. (**2009**) Self-reinforced composites obtained by the partial oxypropylation of cellulose fibers. 1. Characterization of the materials obtained with different types of fibers. Carboh. Polym., 76(3), 437-442.

71. Erasmus, E. and Barkhuysen, F.A. (**2009**) Superhydrophobic cotton by fluorosilane modification. Indian J. Fibre Text. Res., 34, 377-379.

72. Bayer, I.S., Steele, A., Martorana, P.J., Loth, E., Miller, L. (**2009**) Superhydrophobic cellulose-based bionanocomposite films from Pickering emulsions. Appl. Phys. Lett., 94(16), 163902(3).

73. Nyström, D., Lindqvist, J., Östmark, E., Hult, A., Malmström, E. (**2006**) Superhydrophobic bio-fibre surfaces *via* tailored grafting architecture. Chem. Commun., 34, 3594-3596.

74. Nyström, D., Lindqvist, J., Östmark, E., Antoni, P., Carlmark, A., Hult, A., Malmström, E. (**2009**) Superhydrophobic and self-cleaning bio-fiber surfaces *via* ATRP and subsequent postfunctionalization. ACS Appl. Mater. Interfaces, 1(4), 816-823.

75. Werner, O., Quan, C., Turner, C., Petterson, B., Wågberg, L. (**2010**) Properties of superhydrophobic paper treated with rapid expansion of supercritical CO_2 containing a crystallizing wax. Cellulose, 17(1), 187-198.

76. Balu, B., Breedveld, V., Hess, D.W. (**2008**) Fabrication of "roll-off" and "sticky" superhydrophobic cellulose surfaces via plasma processing. Langmuir, 24(9), 4785-4790.

77. Li, G., Wang, H., Zheng, H., Bai, R. (**2010**) A Facile approach for the fabrication of highly stable superhydrophobic cotton fabric with multi-walled carbon nanotubes–azide polymer composites. Langmuir, 26(10), 7529-7534.

78. Rowell, R. (**1990**) Chemical modification of lignocellulosic fibers to produce high-performance composites. In J.E. Glass and G. Swift (Eds.), ACS symposium series - Agricultural and synthetic polymers: biodegradability and utilization (vol. 433, 242-258). Washington, D.C.: American Chemical Science.

79. Quillin, D.T., Caulfield, D.F. and Koutsky, J.A. (**1993**) Surface energy compatibilities of cellulose and polypropylene. Mat. Res. Soc. Symp. Proc., 266, 113-126.

80. Klason, C., Kubát, J., Gatenholm, P. (**1992**) Wood fiber reinforced composites. In W.G. Glasser and H. Hatakeyama (Eds.), ACS symposium series - Viscoelasticity of Biomaterials (vol. 489, 82-98). Washington, D.C.: American Chemical Society.

81. Garnier, G. and Glasser, W.G. (**1996**) Measuring the surface energies of spherical cellulose beads by inverse gas chromatography. Polym. Eng. Sci., 36(6), 885-894.

82. Pasquini, D., Belgacem, M.N., Gandini, A., Curvelo, A.AS. (**2006**) Surface esterification of cellulose fibers: Characterization by DRIFT and contact angle measurements. J. Colloid Interf. Sci., 295(1), 79-83.

83. Jandura, P., Kokta, B.V., Riedl, B. (**2000**) Fibrous long-chain organic acid cellulose esters and their characterization by diffuse reflectance FTIR spectroscopy, solid-state CP/MAS ^{13}C-NMR, and X-ray diffraction. J. Appl. Polym. Sci., 78(7), 1354-1365.

84. Gandini, A. and Belgacem, M.N. (**2007**) Recent contributions to the realm of polymers from renewable resources. In D.S. Argyropoulos (Ed.), ACS symposium series – Materials, chemicals, and energy from forest biomass (1st ed., vol. 954, 48-60). Washington, D.C.: Oxford University Press.

85. Frisoni, G., Baiardo, M., Scandola, M. (**2001**) Natural cellulose fibers: Heterogeneous acetylation kinetics and biodegradation behavior. Biomacromolecules, 2(2), 476-482.

86. Yuan, H., Nishiyama, Y., Kuga, S. (**2005**) Surface esterification of cellulose by vapor-phase treatment with trifluoroacetic anhydride. Cellulose, 12, 543-549.

87. Östenson, M., Järund, H., Toriz, G., Gatenholm, P. (**2006**) Determination of surface functional groups in lignocellulosic materials by chemical derivatization and ESCA analysis. Cellulose, 13(2), 157-170.

88. Buchholz, V., Adler, P., Bäcker, M., Hölle, W., Simon, A., Wegner, G. (**1997**) Regeneration and hydroxyl accessibility of cellulose in ultrathin films. Langmuir, 13(12), 3206-3209.

89. Peydecastaing, J., Girardeau, C., Garcia, C.V-., Borredon, M.E. (**2006**) Long chain cellulose esters with very low DS obtained with non-acidic catalysts. Cellulose, 13(1), 95-103.

90. Boufi, S. and Belgacem, M.N. (**2006**) Modified cellulose fibres for adsorption of dissolved organic solutes. Cellulose, 13(1), 81-94.

91. Dankovich, T.A. and Hsieh, Y-.L. (**2007**) Surface modification of cellulose with plant triglycerides for hydrophobicity. Cellulose, 14(5):, 469-480.

92. Antova, G., Vasvasova, P., Zlatanov, M. (**2004**) Studies upon the synthesis of cellulose stearate under microwave heating. Carbohyd. Polym., 57(2), 131-134.

93. Gandini, A., Botaro, V., Zeno, e., Bach, S. (**2001**) Activation of solid polymer surfaces with bifunctional reagents. Polym. Int., 50(1), 7-9.

94. Ly, B., Thielemans, W., Dufresne, A., Chaussy, D., Belgacem, M.N. (**2008**) Surface functionalization of cellulose fibres and their incorporation in renewable polymeric matrices. Compos. Sci. Technol., 68(15-16), 3193-3201.

95. Sreekala, M. and Thomas, S. (**2003**) Effect of fibre surface modification on water-sorption characteristics of oil palm fibres. Compos. Sci. Technol., 63(6), 861-869.

96. Botaro, V.R. and Gandini, A. (**1998**) Chemical modification of the surface of cellulosic fibres. 2. Introduction of alkenyl moieties via condensation reactions involving isocyanate functions. Cellulose, 5(2), 65-78.

97. Botaro, V.R., Gandini, A., Belgacem, M.N. (**2005**) Heterogeneous chemical modification of cellulose for composite materials. J. Thermoplast. Compos. Mater., 18(2), 107-117.

98. Belgacem, M.N. and Gandini, A. (**2005**) The surface modification of cellulose fibres for use as reinforcing elements in composite materials. Compos. Interf., 12(1-2), 41-75.

99. Pothan, L.A., Bellman, C., Kailas, L., Thomas, S. (**2002**) Influence of chemical treatments on the electrokinetic properties of cellulose fibres. J. Adhes. Sci. Technol., 16(2), 157-178.

100. Matuana, L.M., Balatinecz, J.J., Park, C.B., Sodhi, R.N.S. (**1999**) X-ray photoelectron spectroscopy study of silane-treated newsprint-fibers. Wood Sci. Technol., 33(4), 259-270.

101. Redondo, S.U.A., Radovanovic, E., Gonçalves, M.C., Yoshida, I.V.P. (**2002**) Eucalyptus kraft pulp fibers as an alternative reinforcement of silicone composites. I. Characterization and chemical modification of Eucalyptus fibers with organosilane coupling agent. J. Appl. Polym. Sci., 85(12), 2573-2579.

102. Abdelmouleh, M., Boufi, S., Belgacem, M.N., Duarte, A.P., Salah, A.B., Gandini, A. (**2004**) Modification of cellulosic fibres with functionalised silanes: Development of surface properties. Int. J. Adhes. Adhes., 24(1), 43-54.

103. Pickering, K.L., Abdalla, A., Ji, c., McDonald, A.G., Franich, R.A. (**2003**) The effect of silane coupling agents on radiata pine fibre for use in thermoplastic matrix composites. Composites Part A, 34(10), 915-926.

104. Abdelmouleh, M., Boufi, S., Salah, A.b., Belgacem, M.N., Gandini, A. (**2002**) Interaction of silane coupling agents with cellulose. Langmuir, 18(8), 3203-3208.

105. Castellano, M., Gandini, A., Fabbri, P., Belgacem, M.N. (**2004**) Modification of cellulose fibres with organosilanes: Under what conditions does coupling occur? J. Colloid Interf. Sci., 273(2), 505-511.

106. Gaiolas, C., Costa, A.P., Nunes, M., Silva, M.J.S., Belgacem, M.N. (**2008**) Grafting of paper by silane coupling agents using cold-plasma discharge. Plasma Process. Polym., **5**, 444-452.

107. Ly, B., Belgacem, M.N., Bras, J., Salon, M.C.B. (**2009**) Grafting of cellulose by fluorine-bearing silane coupling agents. Mater. Sci. Eng. C, 30(3), 343-347.

108. Tomšič, B., Simončič, B., Orel, B., Černe, L., Tavčer, P.F., Zorko, M., Jerman, I., Vilčnik, A., Kovač, J. (**2008**) Sol-gel coating of cellulose fibres with antimicrobial and repellent properties. J. Sol-Gel Sci. Techn., 47(1), 44-57.

109. Li, S., Xie, H., Zhang, S., Wang, X. (**2007**) Facile transformation of hydrophilic cellulose into superhydrophobic cellulose. Chem. Commun., 46, 4857-4859.

110. Zimmermann, J., Seeger, S., Artus, G., Jung, S. (**2004**) Superhydrophobic coating. Patent WO/2004/113456.

111. Hebeish, A. and Guthrie, J.T. (**1981**) The chemistry and technology of cellulosic copolymers (1st ed.). New York: Springer-Verlag.

112. Samal, R.K., Sahoo, P.K., Samantaray, H.S. (**1986**) Graft copolymerization of cellulose, cellulose derivatives, and lignocellulose. Polym. Rev., 26(1), 81-141.

113. Stannett, V.T. (**1989**), Some recent developments in cellulose science and technology in North America. In J.F. Kennedy, G.O. Phillips and P.A. Williams (Eds.), Cellulose: Structural and functional aspects (19-31). Chichester: Ellis Horwood Ltd.

114. Carlmark, A. and Malmstrom, E. (**2003**) ATRP grafting from cellulose fibers to create block-copolymer grafts. Biomacromolecules, 4(6), 1740-1745.

115. Carlmark, A. and Malmstrom, E. (**2002**) Atom transfer radical polymerization from cellulose fibers at ambient temperature. J. Am. Chem. Soc., 124(6), 900-901.

116. Coskun, M. and Temüz, M.M. (**2005**) Grafting studies onto cellulose by atom-transfer radical polymerization. Polym. Int., 54(2), 342-347.

117. Zhou, Q., Greffe, L., Baumann, M.J., Malmström, E., Teeri, T.T., Brumer III, H. (**2005**) Use of xyloglucan as a molecular anchor for the elaboration of polymers from cellulose

surfaces: A general route for the design of biocomposites. Macromolecules, 38(9), 3547-3549.

118. Roy, D., Guthrie, J.T., Perrier, S. (**2005**) Graft polymerization: Grafting poly(styrene) from cellulose via reversible addition– fragmentation chain transfer (RAFT) polymerization. Macromolecules, 38, 10363-10372.

119. Margutti, S., Vicini, S., Proietti, N., Capitani, D., Conio, G., Pedemonte, E., Segre, A.L. (**2002**) Physical-chemical characterisation of acrylic polymers grafted on cellulose. Polymer, 43, 6183-6194.

120. Princi, E., Vicini, S., Proietti, N., Capitani, D. (**2005**) Grafting polymerization on cellulose based textiles: A ^{13}C solid state NMR characterization. Eur. Polym. J., 41, 1196-1203.

121. Princi, E., Vicini, S., Pedemonte, E., Gentile, G., Cocca, M., Martuscelli, E. (**2006**) Synthesis and mechanical characterisation of cellulose based textiles grafted with acrylic monomers. Eur. Polym. J., 42, 51-60.

122. Lee, S.B., Koepsel, R.R., Morley, S.W., Matyjaszewski, K., Sun, Y., Russel, J. (**2004**) Permanent, nonleaching antibacterial surfaces. 1. Synthesis by atom transfer radical polymerization. Biomacromolecules, 5(3), 877-882.

123. Hafrén, J. and Córdova, A. (**2005**) Direct organocatalytic polymerization from cellulose fibers. Macromol. Rapid. Comm., 26(2), 82-86.

124. Lönnberg, H., Zhou, Q., Brumer III, H., Teeri, T.T., Malmström, E., Hult, A. (**2006**) Grafting of cellulose fibers with poly(ε-caprolactone) and poly(L-lactic acid) via ring-opening polymerization. Biomacromolecules, 7, 2178-2185.

125. Belgacem, M.N., Czeremuszkin, G., Sapieha, S. (**1995**) Surface characterization of cellulose fibres by XPS and inverse gas chromatography. Cellulose, 2(3), 145-157.

126. Wielen, L.C.V., Osteson, M., Gatenholm, P., Ragauskas, A.J. (**2006**) Surface modification of cellulosic fibers using dielectric-barrier discharge. Carbohyd. Polym., 65(2), 179-184.

127. Sahin, H.T., Manolache, S., Young, R.A., Denes, F. (**2002**) Surface fluorination of paper in CF_4-RF plasma environments. Cellulose, 9(2), 171-181.

128. Sahin, H.T. (**2007**) RF-CF_4 plasma surface modification of paper: Chemical evaluation of two sidedness with XPS/ATR-FTIR. Appl. Surf. Sci., 253(9), 4367-4373.

129. Strlič, M., Kolar, J., Šelih, V-.S., Marinček, M. (**2003**) Surface modification during Nd:YAG (1064 nm) pulsed laser cleaning of organic fibrous materials. Appl. Surf. Sci., 207, 236-245.

130. Kato, K., Vasilets, V.N., Fursa, M.N., Meguro, M., Ikada, Y., Nakamae, K. (**1999**) Surface oxidation of cellulose fibers by vacuum ultraviolet irradiation. J. Polym. Sci. Polym. Chem., 37(3), 357-361.

131. Boufi, S. and Gandini, A. (**2002**) Formation of polymeric films on cellulosic surfaces by admicellar polymerization. Cellulose, 8(4), 303-312.

132. Aloulou, F., Boufi, S., Belgacem, N., Gandini, A. (**2004**) Adsorption of cationic surfactants and subsequent adsolubilization of organic compounds onto cellulose fibers. Colloid. Polym. Sci., 283(3), 344-350.

133. Aloulou, F., Boufi, S., Chakchouk, M. (**2004**) Adsorption of octadecyltrimethylammonium chloride and adsolubilization on to cellulosic fibers. Colloid. Polym. Sci., 282(7), 699-707.

134. Aloulou, F., Boufi, S., Beneventi, D. (**2004**) Adsorption of organic compounds onto polyelectrolyte immobilized-surfactant aggregates on cellulosic fibers. J. Colloid Interf. Sci., 280(2), 350-358..

135. Alila, S., Boufi, S., Belgacem, M.N., Beneventi, D. (**2005**) Adsorption of a cationic surfactant onto cellulosic fibers. I. Surface charge effects. Langmuir, 21(18), 8106-8113.

136. O'Reilly, J-.A.T-., Cavaille, J-.Y., Gandini, A. (**1997**) The surface chemical modification of cellulosic fibres in view of their use in composite materials. Cellulose, 4(4), 305-320.

137. Gupta, K.C. and Khandekar, K. (**2003**) Temperature-responsive cellulose by ceric(IV) ion-initiated graft copolymerization of N-isopropylacrylamide. Biomacromolecules, 4(3), 758-765.

138. Chauhan, G.S., Guleria, L., Sharma, R. (**2005**) Synthesis, characterization and metal ion sorption studies of graft copolymers of cellulose with glycidyl methacrylate and some comonomers. Cellulose, 12(1), 97-110.

139. Waly, A., Mohdy, F.A.A-., Aly, A.S., Hebeish, A. (**1998**) Synthesis and characterization of cellulose ion exchanger. II. Pilot scale and utilization in dye-heavy metal removal. J. Appl. Polym. Sci., 68, 2151-2157.

140. Sanchez, C., Julián, B., Belleville, P., Popall, M. (**2005**) Applications of hybrid organic–inorganic nanocomposites. J. Mater. Chem., 15, 3559-3592.

141. Gonçalves, G., Marques, P.A.A.P., Trindade, T., Neto, C.P., Gandini, A. (**2008**) Superhydrophobic cellulose nanocomposites. J. Colloid Interf. Sci., 324(1-2), 42-46.

142. Gonçalves, G., Marques, P.A.A.P., Pinto, R.J.B., Trindade, T., Neto, C.P. (**2009**) Surface modification of cellulosic fibres for multi-purpose TiO_2 based nanocomposites. Compos. Sci. Technol., 69(7-8), 1051-1056.

143. Barud, H.S., Assunção, R.M.N., Martines, M.A.U., Dexpert-Ghys, J., Marques, R.F.C., Messaddeq, Y., Ribeiro, S.J.L. (**2008**) Bacterial cellulose–silica organic–inorganic hybrids. J. Sol-Gel Sci. Technol., 46(3), 363-367.

144. Maeda, H., Nakajima, M., Hagiwara, T., Sawaguchi, T., Yano, S. (**2006**) Bacterial cellulose/silica hybrid fabricated by mimicking biocomposites. J. Mater. Sci., 41(17), 5646-5656.

145. O'Kelly, J., Crockett, R., Martin, H., Calvert, P. (**1997**) Biomimetic processing of gel glasses and organic-inorganic hybrids. J. Sol-Gel Sci. Technol., 8(1-3), 641-644.

146. Sequeira, S., Evtuguin, D.V., Portugal, I. (**2007**) Cellulose-silica hybrid materials obtained by heteropolyacid catalyzed sol-gel synthesis. In D.S. Argyropoulos (Ed.), Materials, chemicals, and energy from forest biomass, ACS symposium series (1 ed., vol. 954, ch. 8, 121-136). Washington DC: American Chemical Society.

147. Pinto, R.J.B., Marques, P.A.A.P., Barros-Timmons, A.M., Trindade, T., Pascoal Neto, C. (**2008**) Novel SiO_2/cellulose nanocomposites obtained by *in situ* synthesis and via polyelectrolytes assembly. Compos. Sci. Technol., 68(3-4), 1088-1093.

148. Hou, A., Shi, Y., Yu, Y. (**2009**) Preparation of the cellulose/silica hybrid containing cationic group by sol–gel crosslinking process and its dyeing properties. Carbohyd. Polym., 77(2), 201-205.

149. Buršíková, V., Stahel, P., Navrátil, Z., Buršík, J., Janča, J. (**2004**) Surface energy evaluation of plasma treated materials by contact angle measurement (1st ed.). Brno: Masaryk University Publishing.

150. Feng, L., Li, S., Li, Y., Li, H., Zhang, L., Zhai, J., Song, Y., Liu, B., Jiang, L., Zhu, D. (**2002**) Super-hydrophobic surfaces: From natural to artificial. Adv. Mater., 14(24), 1857-1860.

151. Shirtcliffe, N.J., McHale, G., Atherton, S., Newton, M.I. (**2009**) An introduction to superhydrophobicity. Adv. Colloid Interf. Sci., 161(1-2), 124-138.

152. Zhang, X., Shi, F., Niu, J., Jiang, Y., Wang, Z. (**2008**) Superhydrophobic surfaces: From structural control to functional application. J. Mater. Chem., 18(6), 621-633.

153. Marmur, A. (**2006**) Super-hydrophobicity fundamentals: Implications to biofouling prevention. Biofouling, 22(2), 107-115.

154. Guo, Z., Liu, W., Su, B-.L. (**2011**) Superhydrophobic surfaces: From natural to biomimetic to functional. J. Colloid Interf. Sci., 353(2), 335-355.

155. Dorrer, C. and Rüehe, J. (**2009**) Some thoughts on superhydrophobic wetting. Soft Matter, 5(1), 51-61.

156. Bhushan, B. and Jung, Y.C. (**2010**) Natural and biomimetic artificial surfaces for superhydrophobicity, self-cleaning, low adhesion, and drag reduction. Prog. Mater. Sci., 56(1), 1-108.

157. Neinhuis, C. and Barthlott, W. (**1997**) Characterization and distribution of water-repellent, self-cleaning plant surfaces. Ann. Bot., 79(6), 667-677.

158. Genzer, J. and Efimenko, K. (**2006**) Recent developments in superhydrophobic surfaces and their relevance to marine fouling: A review. Biofouling, 22(5), 339-360.

159. Koch, K. and Barthlott, W. (**2009**) Superhydrophobic and superhydrophilic plant surfaces: An inspiration for biomimetic materials. Phil. Trans. R. Soc. A, 367(1893), 1487-1509.

160. Gao, L. and McCarthy, T.J. (**2009**) Wetting 101 degrees. Langmuir, 25(24), 14105-14115.

161. Feng, X. and Jiang, L. (**2006**) Design and creation of superwetting/antiwetting surfaces. Adv. Mater., 18(23), 3063-3078.

162. Roach, P., Shirtcliffe, N.J., Newton, M.I. (**2008**) Progess in superhydrophobic surface development. Soft Matter, 4, 224-240.

163. Quéré, D. (**2008**) Wetting and roughness. Annu. Rev. Mater. Res., 38, 71-99.

164. Marmur, A. (**2004**) The lotus effect: Superhydrophobicity and metastability. Langmuir, 20, 3517-3519.

165. Erbil, H.Y., Demirel, A.L., Avci, Y., Mert, O. (**2003**) Transformation of a simple plastic into a superhydrophobic surface. Science, 299(5611), 1377-1380.

166. Marmur, A. (**2003**) Wetting on hydrophobic rough surfaces: To be heterogeneous or not to be? Langmuir, 19, 8343-8348.

167. Feng, L., Song, Y., Zhai, J., Liu, B., Xu, J., Jiang, L., Zhu, D. (**2003**) Creation of a superhydrophobic surface from an amphiphilic polymer. Angew. Chem. Int. Edit., 42(7), 800-802.

168. Sun, T., Feng, L., Gao, X., Jiang, L. (**2005**) Bioinspired surfaces with special wettability. Acc. Chem. Res., 38(8), 644-652.

169. Park, S-.G., Moon, J.H., Lee, S-.K., Shim, J., Yang, S-.M. (**2009**) Bioinspired holographically featured superhydrophobic and supersticky nanostructured materials. Langmuir, 26(3), 1468-1472.

170. Gao, L. and McCarthy, T.J. (**2006**) “Artificial lotus leaf” prepared using a 1945 patent and a commercial textile. Langmuir, 22, 5998-6000.

171. Li, X-.M., Reinhoudt, D., Calama, M.C-. (**2007**) What do we need for a superhydrophobic surface? A review on the recent progress in the preparation of superhydrophobic surfaces. Chem. Soc. Rev., 36, 1350-1368.

172. Kim, D., Kim, J., Park, H.C., Lee, K.H., Hwang, W. (**2008**) A superhydrophobic dual-scale engineered lotus leaf. J. Micromech. Microeng., 18, 015019(5).

173. Xi, J. and Jiang, L. (**2008**) Biomimic superhydrophobic surface with high adhesive forces. Ind. Eng. Chem. Res., 47, 6354-6357.

174. Genzer, J. and Marmur, A. (**2008**) Biological and synthetic self-cleaning surfaces. MRS Bull., 33, 742-746.

175. Lim, H., Jung, D-.H., Noh, J-.H., Choi, G-.R., Kim, W-.D. (**2009**) Simple nanofabrication of a superhydrophobic and transparent biomimetic surface. Chin. Sci. Bull., 54(19), 3613-3616.

176. Mao, C., Liang, C., Luo, W., Bao, J., Shen, J., Hou, X., Zhao, W. (**2009**) Preparation of lotus-leaf-like polystyrene micro- and nanostructure films and its blood compatibility. J. Mater. Chem., 19(47), 9025-9029.

177. Crick, C.R. and Parkin, I.P. (**2009**) A single step route to superhydrophobic surfaces through aerosol assisted deposition of rough polymer surfaces: duplicating the lotus effect. J. Mater. Chem., 19(8), 1074-1076.

178. Liu, M., Zheng, Y., Zhai, J., Jiang, L. (**2009**) Bioinspired super-antiwetting interfaces with special liquid-solid adhesion. Acc. Chem. Res., 43(3), 368-377.

179. Wu, D., Chen, Q-.D., Xia, H., Jiao, J., Xu, B-.B., Lin, X-.F., Xu, Y., Sun, H-.B. (**2010**) A facile approach for artificial biomimetic surfaces with both superhydrophobicity and iridescence. Soft Matter, 6, 263-267.

180. Hsu, S-.H. and Sigmund, W.M. (**2010**) Artificial hairy surfaces with a nearly perfect hydrophobic response. Langmuir, 26(3),1504-1506.

181. Crick, C.R. and Parkin, I.P. (**2010**) Superhydrophobic polymer films via aerosol assisted deposition - Taking a leaf out of nature's book. Thin Solid Films, 518, 4328-4335.

182. Rothstein, J. (**2010**) Slip on superhydrophobic surfaces. Ann. Rev. Fluid Mech., 42, 89-109.

183. Chen, W., Fadeev, A.Y., Hsieh, M.C., Öner, D., Youngblood, J., McCarthy, T.J. (**1999**) Ultrahydrophobic and ultralyophobic surfaces: Some comments and examples. Langmuir, 15(10), 3395-3399.

184. Jiang, L., Wang, R., Yang, B., Li, T.J., Tryk, D.A., Fujishima, A., Hashimoto, K., Zhu, D.B. (**2000**) Binary cooperative complementary nanoscale interfacial materials. Pure Appl. Chem., 72(1-2), 73-81.

185. Li, H., Wang, X., Song, Y., Liu, Y., Li, Q., Jiang, L., Zhu, D. (**2001**) Super-"amphiphobic" aligned carbon nanotube films. Angew. Chem. Int. Edit., 40(9), 1743-1746.

186. Tuteja, A., Choi, W., Mabry, J.M., McKinley, G.H., Cohen, R.E. (**2008**) Robust omniphobic surfaces. Proc. Nat. Acad. Sci. U.S.A., 105(47), 18200-18205.

187. Darmanin, T., Nicolas, M., Guittard, F. (**2008**) Electrodeposited polymer films with both superhydrophobicity and superoleophilicity. Phys. Chem. Chem. Phys., 10(29), 4322-4326.

188. Xi, J., Feng, L., Jiang, L. (**2008**) A general approach for fabrication of superhydrophobic and superamphiphobic surfaces. Appl. Phys. Lett., 92, 053102 (3).

189. Sheen, Y-.C., Chang, W-.H., Chen, W-.C., Chang, Y-.H., Huang, Y-.C., Chang, F-.C. (**2009**) Non-fluorinated superamphiphobic surfaces through sol-gel processing of methyltriethoxysilane and tetraethoxysilane. Mater. Chem. Phys., 114(1), 63-68.

190. Darmanin, T. and Guittard, F. (**2009**) Super oil-repellent surfaces from conductive polymers. J. Mater. Chem., 19(38), 7130-7136.

191. Im, M., Im, H., Lee, J-.H., Yoon, J-.B., Choi, Y-.K. (**2010**) A robust superhydrophobic and superoleophobic surface with inverse-trapezoidal microstructures on a large transparent flexible substrate. Soft Matter, 6(7), 1401-1404.

192. Choi, W., Tuteja, A., Chhatre, S., Mabry, J.M., Cohen, R.E., McKinley, G. (**2009**) Fabrics with Tunable Oleophobicity. Adv. Mater.21(21), 2190-2195.

193. Zhang, J., Huang, W., Han, Y. (**2006**) A composite polymer film with both superhydrophobicity and superoleophilicity. Macromol. Rapid. Comm., 27(10), 804-808.

194. Chhatre, S.S., Tuteja, A., Choi, W., Revaux, A., Smith, D., Mabry, J.M., McKinley, G.H., Cohen, R.E. (**2009**) Thermal annealing treatment to achieve switchable and reversible oleophobicity on fabrics. Langmuir, 25(23), 13625-13632.

195. Darmanin, T. and Guittard, F. (**2009**) One methylene unit to control super oil-repellency properties of conducting polymers. Chem. Commun., 16, 2210-2211.

196. Fang, J., Kelarakis, A., Estevez, L., Wang, Y., Rodriguez, R., Giannelis, E.P. (**2010**) Superhydrophilic and solvent resistant coatings on polypropylene fabrics by a simple deposition process. J. Mater. Chem., 20(9), 1651-1653.

197. Xia, F., Zhu, Y., Feng, L., Jiang, L. (**2009**) Smart responsive surfaces switching reversibly between super-hydrophobicity and super-hydrophilicity. Soft Matter, 5(2), 275-281.

198. Guo, Y., Xia, F., Xu, L., Li, J., Yang, W., Jiang, L. (**2010**) Switchable wettability on cooperative dual-responsive poly-L-lysine surface. Langmuir, 26(2), 1024-1028.

199. Wang, S., Song, Y., Jiang, L. (**2007**) Photoresponsive surfaces with controllable wettability. J. Photochem. Photobiol. C, 8(1), 18-29.

200. Wang, D., Liu, Y., Zhou, F., Liu, W., Xue, Q. (**2009**) Towards a tunable and switchable water adhesion on a TiO_2 nanotube film with patterned wettability. Chem. Commun., 45, 7018-7020.

201. Xin, B. and Hao, J. (**2010**) Reversibly switchable wettability. Chem. Soc. Rev., 39(2), 769-782.

202. Sun, T., Wang, G., Feng, L., Liu, B., Ma, Y., Jiang, L., Zhu, D. (**2004**) Reversible switching between superhydrophilicity and superhydrophobicity. Angew. Chem. Int. Edit., 43(3), 357-360.

203. Minko, S., Müller, M., Motornov, M., Nitschke, M., Grundke, K., Stamm, M. (**2003**) Two-level structured self-adaptive surfaces with reversibly tunable properties. J. Am. Chem. Soc., 125(13), 3896-3900.

204. Öner, D. and McCarthy, T.J. (**2000**) Ultrahydrophobic surfaces. Effects of topography length scales on wettability. Langmuir, 16(20), 7777-7782.

205. Jeong, H-.J., Kim, D-.K., Lee, S-.B., Kwon, S-.H., Kadono, K. (**2001**) Preparation of water-repellent glass by sol–gel process using perfluoroalkylsilane and tetraethoxysilane. J. Colloid Interf. Sci., 235(1), 130-134.

206. Tada, H. and Nagayama, H. (**1994**) Chemical vapor surface modification of porous glass with fluoroalkyl-functional silanes. 1. Characterization of the molecular layer. Langmuir, 10(5), 1472-1476.

207. Tada, H. and Nagayama, H. (**1995**) Chemical vapor surface modification of porous glass with fluoroalkyl-functional silanes. 2. Resistance to water. Langmuir, 11(1), 136-142.

208. Amigoni, S., de Givenchy, E.T., Dufay, M., Guittard, F. (**2009**) Covalent layer-by-layer assembled superhydrophobic organic-inorganic hybrid films. Langmuir, 25(18), 11073-11077.

209. Shibuichi, S., Yamamoto, T., Onda, T., Tsuji, K. (**1998**) Super water- and oil-repellent surfaces resulting from fractal structure. J. Colloid Interf. Sci., 208(1), 287-294.

210. Wang, S., Feng, L., Liu, H., Sun, T., Zhang, X., iang, L. Zhu, D. (**2005**) Manipulation of surface wettability between superhydrophobicity and superhydrophilicity on copper films. ChemPhysChem., 6(8), 1475-1478.

211. Bae, G.Y., Jang, J., Jeong, Y.G., Lyoo, W.S., Min, B.G. (**2010**) Superhydrophobic PLA fabrics prepared by UV photo-grafting of hydrophobic silica particles possessing vinyl groups. J. Colloid Interf. Sci., 344(2), 584-587.

212. Song, W., Gaware, V.S., Rúnarsson, Ö.V., Másson, M., Mano, J.F. (**2010**) Functionalized superhydrophobic biomimetic chitosan-based films. Carbohyd. Polym., 81(1), 140-144.

213. Carvalho, A.J.F., Curvelo, A.A.S., Gandini, A. (**2005**) Surface chemical modification of thermoplastic starch: Reactions with isocyanates, epoxy functions and stearoyl chloride. Ind. Crop. Prod., 21, 331-336.

214. Pagliaro, M. and Ciriminna, R. (**2005**) New fluorinated functional materials. J. Mater. Chem., 15(47), 4981-4991.

215. Cunha, A.G. and Gandini, A. (**2010**) Turning polysaccharides into hydrophobic materials: a critical review. Part 1. Cellulose, 17(5), 875-889.

216. Cunha, A.G. and Gandini, A. (**2010**) Turning polysaccharides into hydrophobic materials: a critical review. Part 2. Hemicelluloses, chitin/chitosan, starch, pectin and alginates. Cellulose, 17(6), 1045-1065.

217. Gau, H., Hermimghaus, S., Lenz, P., Lipowsky, R. (**1999**) Liquid morphologies on structured surfaces: from microchannels to microchips. Science, 283(5398), 46-49.

218. Lenz, P. (**1999**) Wetting phenomena on structured surfaces. Adv. Mater., 11(18), 1531-1534.

219. Shull, K.R. and Karis, T.E. (**1994**) Dewetting dynamics for large equilibrium contact angels. Langmuir, 10, 334-339.

220. Hui, M-.H. and Blunt, M.J. (**2000**) Effects of wettability on three-phase flow in porous media. J. Phys. Chem. B, 104(16), 3833-3845.

221. Abbott, S., Ralston, J. Reynolds, G., Hayes, R. (**1999**) Reversible wettability of photoresponsive pyrimidine-coated surfaces. Langmuir, 15(26), 8923-8928.

222. Yoo, D., Shiratori, S.S., Rubner, M.F. (**1998**) Controlling bilayer composition and surface wettability of sequentially adsorbed multilayers of weak polyelectrolytes. Macromolecules, 31(13), 4309-4318.

223. Abbott, N.L., Folkers, J.P., Whitesides, G.M. (**1992**) Manipulation of the wettability of surfaces on the 0.1- to 1-micrometer scale through micromachining and molecular self-assembly. Science, 257(5075), 1380-1382.

224. Gao, L., McCarthy, T.J., Zhang, X. (**2009**) Wetting and Superhydrophobicity. Langmuir, 25(24), 14100-14104.

225. de Mongeot, F.B., Chiappe, D., Gagliardi, F., Toma, A., Felici, R., Garibbo, A., Boragno, C. (**2010**) Wetting process in superhydrophobic disordered surfaces. Soft Matter, 6(7), 1409-1412.

226. Krasowska, M., Zawala, J., Malysa, K. (**2009**) Air at hydrophobic surfaces and kinetics of three phase contact formation. Adv. Colloid Interf. Sci., 147-48, 155-169.

227. Nosonovsky, M. and Bhushan, B. (**2007**) Hierarchical roughness makes superhydrophobic states stable. Microelectron. Eng., 84(3), 382-386.

228. Plueddemann, E.P. (**1991**) Silane coupling agents. (2nd ed.). New York: Plenum Press.

229. Fadeev, A. and McCarthy, T. (**2000**) Self-assembly is not the only reaction possible between alkyltrichlorosilanes and surfaces: monomolecular and oligomeric covalently attached layers of dichloro- and trichloroalkylsilanes on silicon. Langmuir, 16(18), 7268-7274.

230. Artus, G.R.J., Jung, S., Zimmerman, J., Gautschi, H-.P., Marquardt, K., Seeger, S. (**2006**) Silicone nanofilaments and their application as superhydrophobic coating. Adv. Mater., 18(20), 2758-2762.

231. Daoud, W.A., Xin, J.H., Tao, X. (**2004**) Superhydrophobic silica nanocomposite coating by a low-temperature process. J. Am. Ceram. Soc., 87(9), 1782-1784.

232. Li, S., Zhang, S., Wang, X. (**2008**) Fabrication of superhydrophobic cellulose-based materials through a solution-immersion process, Langmuir, 24, 5585-5590.

233. Li, S., Wei, Y., Huang, J. (**2010**) Facile fabrication of superhydrophobic cellulose materials by a nanocoating approach. Chem. Lett., 39(1), 20-21.

234. Tang, W., Huang, Y., Meng, W., Qing, F-.L. (**2010**) Synthesis of fluorinated hyperbranched polymers capable as highly hydrophobic and oleophobic coating materials. Eur. Polym. J., 46(3), 506-518.

235. Vilčnik, A., Jerman, I., Vuk, A.Š., Koželj, M., Orel, B., Tomšič, B., Simončič, B., Kovač, J. (**2009**) Structural properties and antibacterial effects of hydrophobic and oleophobic sol-gel coatings for cotton fabrics. Langmuir, 25(10), 5869-5880.

236. Vince, J., Orel, B., Vilčnik, A., Fir, M., Vuk, A. Š., Jovanovski, V., Simončič, B. (**2006**) Structural and water-repellent properties of a urea/poly(dimethylsiloxane) sol-gel hybrid and its bonding to cotton fabric. Langmuir, 22(15), 6489-6497.

237. Xu, B., Cai, Z., Wang, W., Ge, F. (**2010**) Preparation of superhydrophobic cotton fabrics based on SiO_2 nanoparticles and ZnO nanorod arrays with subsequent hydrophobic modification. Surf. Coat. Tech., 204(9-10), 1556-1561.

238. Yang, H. and Deng, Y. (**2008**) Preparation and physical properties of superhydrophobic papers. J. Colloid Interf. Sci., 325(2), 588-593.

239. Daoud, W.A., Xin, J.H., Zhang, Y.H., Mak, C.L. (**2006**) Pulsed laser deposition of superhydrophobic thin Teflon films on cellulosic fibers. Thin Solid Films, 515, 835-837.

240. Navarro, F., Dávalos, F., Denes, F., Cruz, L.E., Young, R.A., Ramos, J. (**2003**) Highly hydrophobic sisal chemithermomechanical pulp (CTMP) paper by fluorotrimethylsilane plasma treatment. Cellulose, 10(4), 411-424.

241. Mukhopadhyay, S.M., Joshi, P., Datta, S., Zhao, J.G., France, P. (**2002**) Plasma assisted hydrophobic coatings on porous materials: Influence of plasma parameters. J. Phys. D: Appl. Phys., 35, 1927-1933.

242. Barni, R., Zanini, S., Beretta, D., Riccardi, C. (**2007**) Experimental study of hydrophobic/hydrophilic transition in SF_6 plasma interaction with polymer surfaces. Eur. Phys. J. Appl. Phys., 38(3), 263-268.

243. Berlioz, S., Boisseau, S.M-., Nishiyama, Y., Heux, L. (**2009**) Gas-phase surface esterification of cellulose microfibrils and whiskers. Biomacromolecules, 10, 2144-2151.

244. Bras, J., Garcia, C.V-., Borredon, M-.E., Glasser, W. (**2007**) Oxygen and water vapor permeability of fully substituted long chain cellulose esters (LCCE). Cellulose, 14(4), 367-374.

245. Crépy, L., Chaveriat, L., Banoub, J., Martin, P., Joly, N. (**2009**) Synthesis of cellulose fatty esters as plastics - Influence of the degree of substitution and the fatty chain length on mechanical properties. ChemSusChem, 2(2), 165-170.

246. Gaiolas, C., Belgacem, M.N., Silva, L., Thielemans, Costa, A.P., Nunes, M., Silva, M.J.S. (**2009**) Green chemicals and process to graft cellulose fibers. J. Colloid Interf. Sci., 330(2), 298-302.

247. Ly, E.h.B., Bras, J., Sadocco, P., Belgacem, M.N., Dufresne, A., Thielemans, W. (**2010**) Surface functionalization of cellulose by grafting oligoether chains. Mater. Chem. Phys., 120(2-3), 438-445.

248. Paquet, O., Krouit, M., Bras, J., Thielemans, W., Belgacem, M.N. (**2010**) Surface modification of cellulose by PCL grafts. Acta Mater., 58(3), 792-801.

249. Roberts, J.C. (**1996**) Paper chemistry (2nd ed.). London: Chapman & Hall.

250. Gess, J. and Rende, D. (**2005**) Alkenyl succinic anhydride (ASA). Tappi J., 4(9), 25-30.

251. Lindstrom, T. and Larsson, P.T. (**2008**) Alkyl ketene dimer (AKD) sizing - A review. Nord. Pulp Pap. Res. J., 23(2), 202-209.

252. Bourbonnais, R. and Marchessault, R.H. (**2010**) Application of polyhydroxyalkanoate granules for sizing of paper. Biomacromolecules, 11(4), 989-993.

253. Zhang, H., Kannangara, D., Hilder, M., Ettl, R., Shen, W. (**2007**) The role of vapour deposition in the hydrophobization treatment of cellulose fibres using alkyl ketene dimers and alkenyl succinic acid anhydrides. Colloid Surf. A, 297(1-3), 203-210.

254. Butler, L. (**1975**) Enzyme immobilization by adsorption on hydrophobic derivatives of cellulose and other hydrophilic materials. Arch. Biochem. Biophys., 171(2), 645-650.

255. Dixon, J. and Butler, L. (**1977**) Utilization of hydrophobic esters of cellulose for enzyme immobilization. Fed. Proc., 36(3), 864-864.

256. Dixon, J., Andrews, P., Butler, L. (**1979**) Hydrophobic esters of cellulose – Properties and applications in biochemical technology. Biotechnol. Bioeng., 21(11), 2113-2123.

257. Lamba, N.M.K., Woodhouse, K.A., Cooper, S.L. (**1998**) Polyurethanes in biomedical applications. Boca Raton: CRC Press.

258. Barr, T.L (**1994**) Modern ESCA: The principles and practice of X-ray photoelectron spectroscopy. Boca Raton: CRC Press.

259. Nefedov, V.I (**1988**) X-ray photoelectron spectroscopy of solid surfaces. Utrecht: VSP BV.

260. Watts, J. F. and Wolstenholme, J. (**2003**) An introduction to surface analysis by XPS and AES (2nd ed.). Chichester: John Wiley & Sons.

261. Grams, J. (**2007**) New trends and potentialities of ToF-SIMS in surface studies. New York: Nova Science Publishers Inc.

262. Rivière, J. and Myhra, S. (**1998**) Handbook of surface and interface analysis: Methods for problem-solving (2nd ed.). Boca Raton: CRC Press.

263. Ishikawa, N. and Taniguchi, H. (**1984**) Fluorine-containing cellulose derivatives. U.S. Patent 4487926.

264. Matsui H. and Shiraishi, N. (**1993**) Graft-copolymerization of 2-(perfluorooctyl)ethyl acrylate onto cellulose. Mokuzai Gakkaishi, 39(10), 1188-1193.

265. Liebert, T., Schnabelrauch, M., Klemm, D., Erler, U. (**1994**) Readily hydrolysable cellulose esters as intermediates for the regioselective derivatization of cellulose; II. Soluble, highly substituted cellulose trifluoroacetates. Cellulose, 1, 249-258.

266. Sealey, J.E., Frazier, C.E., Samaranayake, G., Glasser, W.G. (**2000**) Novel cellulose derivatives. V. Synthesis and thermal properties of esters with trifluoroethoxy acetic acid. J. Polym. Sci. Pol. Phys., 38, 486-494..

267. Glasser, W.G., Becker, U., Todd, J.G. (**2000**) Novel cellulose derivatives. Part VI. Preparation and thermal analysis of two novel cellulose esters with fluorine-containing substituents. Carbohyd. Polym., 42, 393-400.

268. Fabbri, P., Champon, G., Castellano, M., Belgacem, M.N., Gandini, A. (**2004**) Reactions of cellulose and wood superficial hydroxy groups with organometallic compounds. Polym. Int., 53, 7-11.

269. Selli, E., Mazzone, G., Oliva, C., Martini, F., Riccardi, C., Barni, R., Marcandalli, B., Massafra, M.R. (**2001**) Characterisation of poly(ethylene terephthalate) and cotton fibres after cold SF_6 plasma treatment. J. Mater. Chem., 11(8), 1985-1991.

270. Barba, L.E.C-., Manolache, S., Denes, F. (**2003**) Generation of Teflon-like layers on cellophane surfaces under atmospheric pressure non-equilibrium SF_6-plasma environments. Polym. Bull., 50(5-6), 381-387.

271. Bora, U., Kannan, K., Nahar, P. (**2005**) A simple method for functionalization of cellulose membrane for covalent immobilization of biomolecules. J. Membrane Sci., 250(1-2), 215-222.

272. Yasuda, T., Okuno, T., Tsuji, K., Yasuda, H. (**1996**) Surface-configuration change of CF_4 plasma treated cellulose and cellulose acetate by interaction of water with surfaces. Langmuir, 12(5), 1391-1394.

273. Koschella, A. and Heinze, T. (**2003**) Unconventional cellulose products by fluorination of tosyl cellulose. Macromol. Symp., 197, 243-254.

274. Yamaguchi, F. and Sakamoto, E. (**2001**) Process for fluorinating cellulosic materials and fluorinated cellulosic materials. U.S. Patent 6293972.

275. Reisinger, J.J. and Hillmyer, M.A. (**2002**) Synthesis of fluorinated polymers by chemical modification. Prog. Polym. Sci., 27(5), 971-1005.

276. Bellamy, L.J. (**1975**) The infrared spectra of complex molecules (3rd ed.). London: Chapman and Hall.

277. Hon, D.N-.S. (**1996**) Chemical modification of lignocellulosic materials. New York: Marcel Dekker, Inc.

278. Arseneau, D.F. (**1971**) Competitive reactions in the thermal decomposition of cellulose. Can. J. Chem., 49, 632-638.

279. Fardim, P. and Durán, N. (**2003**) Modification of fibre surfaces during pulping and refining as analysed by SEM, XPS and ToF-SIMS. Colloid. Surface A, 223(1-3), 263-276.

280. Briggs, D. and Beamson, G. (**1992**) Primary and secondary oxygen-induced C1s binding energy shifts in X-ray photoelectron spectroscopy of polymers. Anal. Chem., 64(15), 1729-1736.

281. Bernett, M.K. (**1974**) Surface chemical properties of highly fluorinated ethylenic polymers. Macromolecules, 7(6), 917-920.

282. Winter, J.G. and Scott, J.M.W. (**1968**) Studies in solvolysis. Part I. The neutral hydrolysis of some alkyl trifluoroacetates in water and deuterium oxide. Can. J. Chem., 46, 2887-2894.

283. Curran, D.P. (**2006**) Organic synthesis with light-fluorous reagents, reactants, catalysts, and scavengers. Aldrichimica Acta, 39, 3-9.

284. Freire, C.S.R., Silvestre, A.J.D., Pascoal Neto, C., Rocha, R.M.A. (**2005**) An efficient method for determination of the degree of substitution of cellulose esters of long chain aliphatic acids. Cellulose, 12(5), 449-458.

285. Boutonnet, J.C., Bingham, P., Calamari, D., de Rooij, C., Franklin, J., Kawano, T., Libre, J-.M., Ioch, A.M-., Malinverno, G., Odom, J.M., Rusch, G.M., Smythe, K., Sobolev, I., Thompson, R., Tiedje, J.M. (**1999**) Environmental risk assessment of trifluoroacetic acid. Hum. Ecol. Risk Assess., 5(1), 59-124.

286. Berends, A.G., Boutonnet, J.C., de Rooij, C.G., Thompson, R.S. (**1999**) Toxicity of trifluoroacetate to aquatic organisms. Environ. Toxicol. Chem., 18(5), 1053–1059.

287. Silva, S.S., Ferreira, R.A.S., Fu, L., Carlos, L.D., Mano, J.F., Reis, R.L., Rocha, J. (**2005**) Functional nanostructured chitosan–siloxane hybrids. J. Mater. Chem., 15, 3952-3961.

288. Chen, X., Liu, Y., Qin, F., Kong, L., Zou, H. (**2003**) Synthesis of covalently bonded cellulose derivative chiral stationary phases with a bifunctional reagent of 3-(triethoxysilyl) propyl isocyanate. J. Chromatogr. A, 1010(2), 185-194.

289. Tingting, Y., Hui, P., Shiyuan, C., Park, I.J. (**2005**) Surface immobilization of perfluorinated acrylate copolymers by self-crosslinking. J. Fluorine Chem., 126(11-12), 1570-1577.

290. Takayama, T. (**1998**) Inorganic polymers. In T. Asakura and I. Ando (Eds.), Solid-state NMR of polymers (1 ed., 613-666). Amsterdam: Elsevier.

291. Bogdan, A. and Kulmala, M. (**2006**) Pyrogenic silica and alumina. In P. Somasundaran (Ed.). Encyclopedia of Surface and Colloid Science (2nd ed., vol. 7, 5314-5328). New York: Taylor & Francis.

292. Jeong, H-.J., Kim, D-.K., Lee, S-.B., Kwon, S-.H., Kadono, K. (**2001**) Preparation of water-repellent glass by sol-gel process using perfluoroalkylsilane and tetraethoxysilane. J. Colloid Interf. Sci., 235(1), 130-134.

293. Gousse, C., Chanzy, H., Excoffier, G., Soubeyrand, L., Fleury, E. (**2002**) Stable suspensions of partially silylated cellulose whiskers dispersed in organic solvents. Polymer, 43(9), 2645-2651.

294. Gousse, C., Chanzy, H., Cerrada, M.L., Fleury, E. (**2004**) Surface silylation of cellulose microfibrils: preparation and rheological properties. Polymer, 45(5), 1569-1575.

295. Schubert, U. and Hüsing, N. (**2005**) Synthesis of inorganic materials (2nd ed.). Weinheim: Wiley-VCH

296. Senani, S.M-., Bonhomme, C., Ribot, F., Babonneau, F. (**2009**) Covalent grafting of organoalkoxysilanes on silica surfaces in water-rich medium as evidenced by ^{29}Si NMR. J. Sol-Gel Sci. Technol., 50(2), 152-157.

297. Vickerman, J.C. (**2003**) Surface analysis - The principal techniques (6th ed.). Chichester: John Wiley & Sons.

Annexes

Annex 1

Study of the effect of different reaction conditions on the progress of the pentafluorobenzoylation and trifluoropropanoylation of the cellulose fibers as assessed by FTIR-ATR spectroscopy.

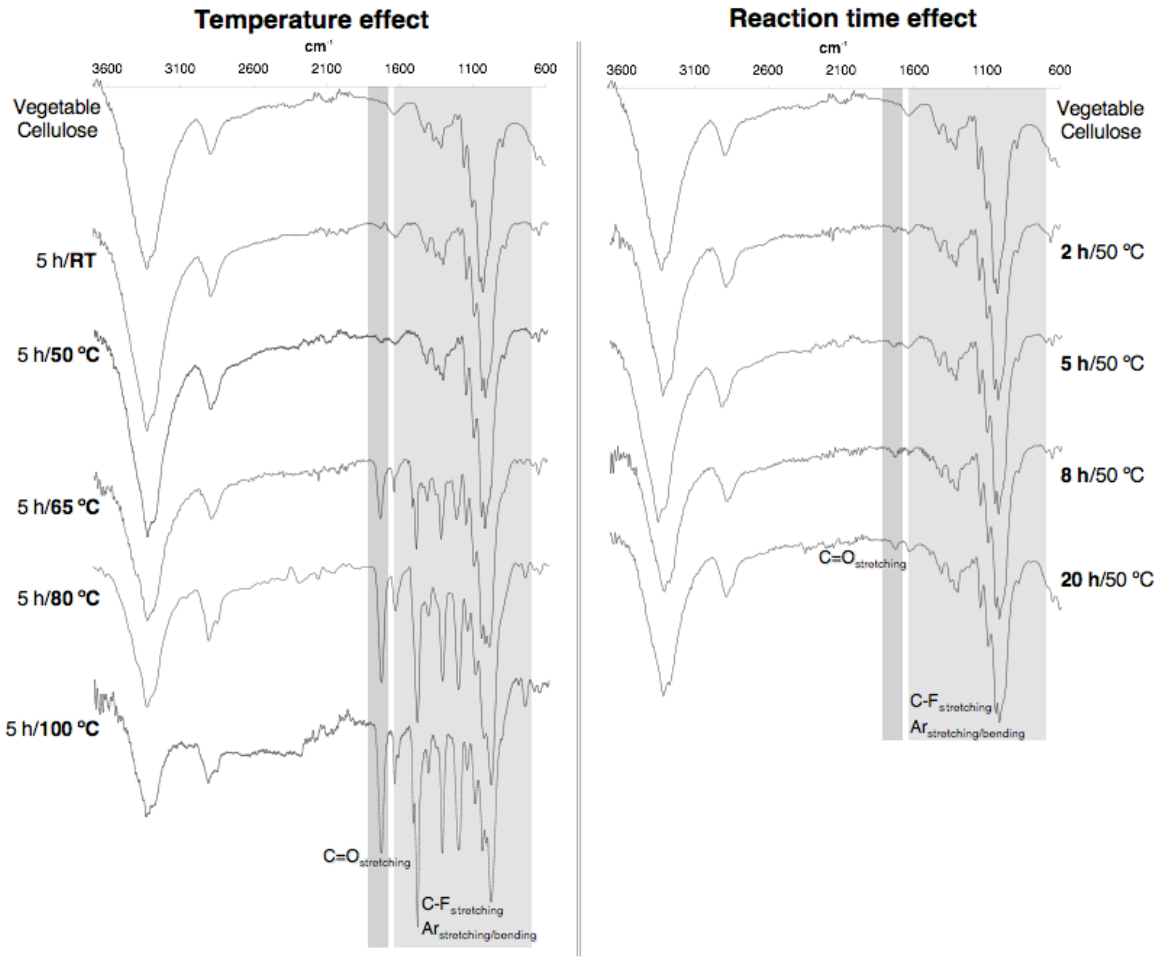

Figure A1-1. Progress of the pentafluorobenzoylation of the vegetable cellulose fibers with different temperatures and reaction times.

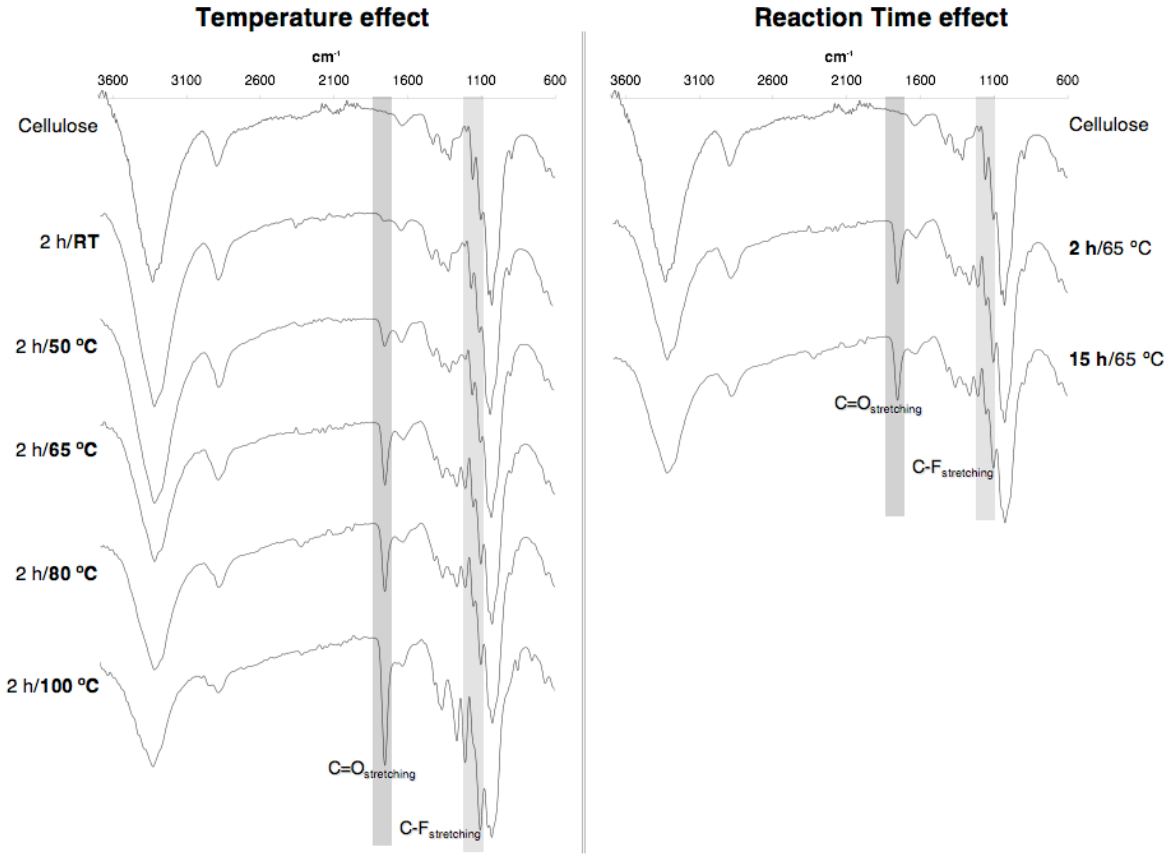

Figure A1-2. Progress of the trifluoropropanoylation of the cellulose fibers with different temperatures and reaction times.

Annex 2

Thermogravimetric results of the pentafluorobenzoylated and trifluoropropanoylated cellulose fibers.

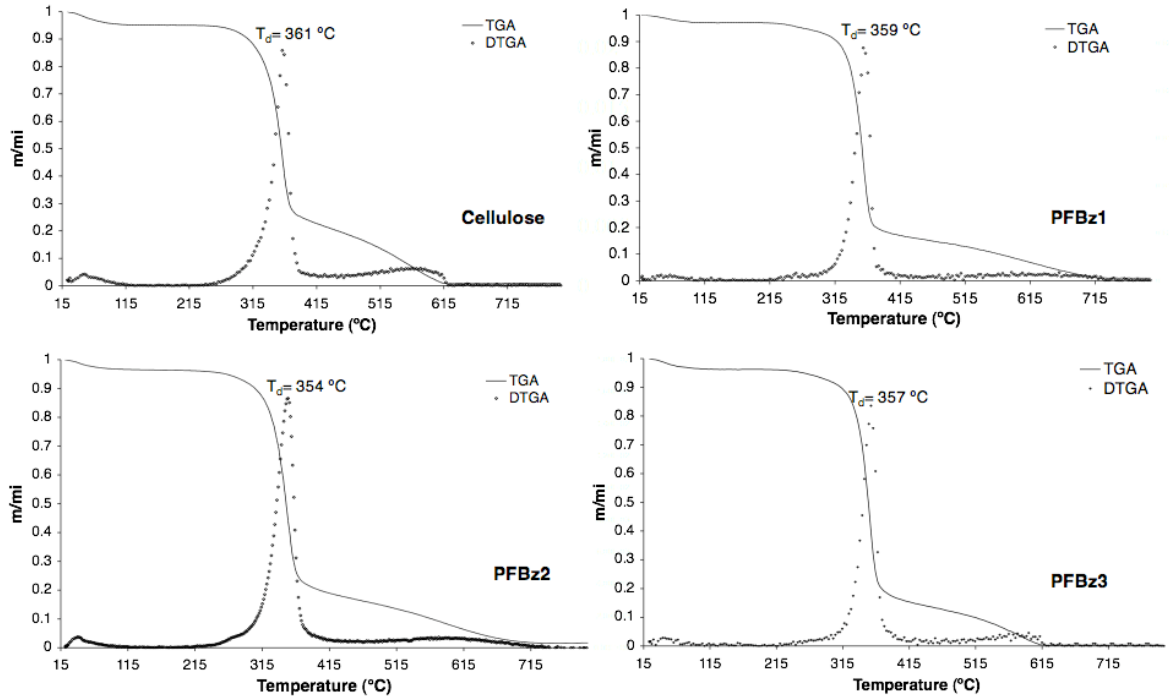

Figure A2-1. Thermograms of the unmodified and pentafluorobenzoylated vegetable cellulose fibers.

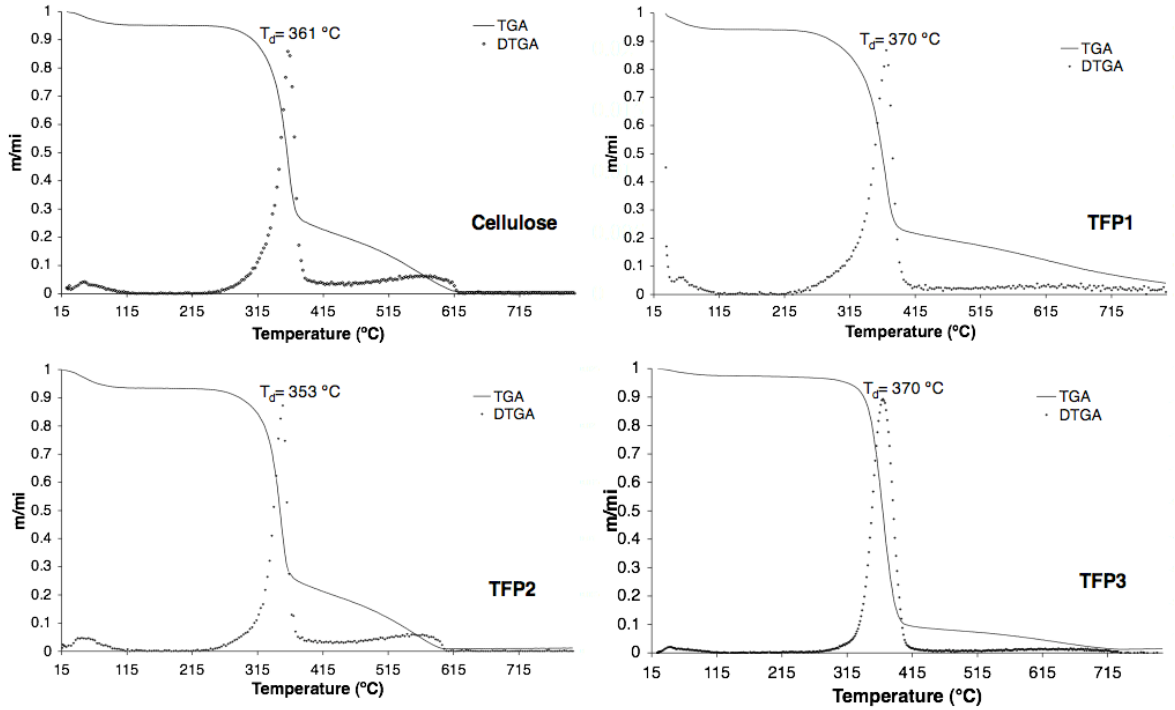

Figure A2-2. Thermograms of the unmodified and trifluoropropanoylated cellulose fibers.